Synthetic Approaches to PNA-Containing Acridine Threading Intercalators as Potential Novel HIV-1 Integrase Inhibitors

Koenraad M P Collart

A dissertation submitted for the degree of Doctor of Philosophy

Heriot-Watt University

School of Engineering and Physical Sciences

March 2010

Abstract

The overall objectives of this research were to devise a viable synthetic route to conjugates, in which 9-aminoacridine 4-carboxamide was tethered through its 4-position to peptide nucleic acids (PNAs), and to evaluate their abilities to act as novel inhibitors of HIV-1 integrase (IN). It was reasoned that such compounds could inhibit the process catalysed by IN either directly by binding to the enzyme or indirectly by binding to the proviral DNA substrate through threading intercalation.

The first route to these conjugates investigated involved synthesis of the intermediates 9-oxoacridan-4-carboxylic acid and the thyminyl-PNA monomer ethyl ester. Both these compounds were successfully prepared following established literature procedures. In order to explore the conditions required for coupling 9-oxoacridan-4-carboxylic acid and the thyminyl-PNA monomer ethyl ester, a model study was undertaken involving preparation of the known threading intercalator, 9-amino-DACA. Following literature precedence, 9-oxoacridan-4-carboxylic acid was treated first with excess thionyl chloride to yield 9-chloroacridine-4-carboxyl chloride. Subsequently, this was reacted selectively with *N*,*N*-dimethylethylenediamine to give 9-chloro-DACA. Finally, treatment of a phenolic solution of 9-chloro-DACA with gaseous ammonia successfully afforded 9-amino-DACA in a 26% over-all yield. Unfortunately, on applying a similar approach for synthesis of the 9-aminoacridine-4-carboxamide PNA conjugate, none of the desired compound could be identified.

In a second alternative strategy a number of alkyl-9-oxoacridan-4-carboxylate precursors (methyl, *iso*-propyl and *t*-butyl) were synthesised and subsequently activated, via 9-triazolylation, to allow for substitution in the 9 position with benzyl amine. This resulted in the successful synthesis of the *iso*-propyl- and *t*-butyl-9-benzylaminoacridine-4-carboxylate intermediates. Subsequent attempts to generate the 4-carboxyl group in both intermediates, via alkyl-ester cleavage, were only successful via a basic hydrolysis of the *iso*-propyl ester. Unfortunately, attempts to activate the 4-carboxyl group of the resulting 9-benzylaminoacridine-4carboxylic acid via 4-*N*-hydroxysuccinimide (NHS) ester formation, to enable subsequent substitution in the 4 position with a PNA monomer, were unsuccessful. The nature of the 9-amino substituent was found to be of importance as it was shown that for 9-anilinoacridine-4-carboxylic acid, NHS activation of the 4-carboxyl was successful and led to synthesis

of a 9-anilinoacridine-4-carboxamide PNA conjugate. This result prompted us to revise our strategy and led to the synthesis of 9-*t*-Boc- and 9-Alloc-aminoacridine-4-NHS esters that subsequently both were coupled successfully to a thyminyl-PNA monomer. Subsequent deprotection steps for the 9-Alloc protected PNA-acridine conjugate proved to be cumbersome but fortunately, for the *t*-Boc protected PNA-acridine conjugate *t*-Boc cleavage with TFA followed by an aqueous basic ethyl ester hydrolysis of the PNA monomer's C-terminus resulted in completion of a 9-step synthetic route (4% over-all yield) towards the target 9-amino-4-PNA-acridine conjugate, 2-(*N*-(2-(9-aminoacridine-4-carboxamido)ethyl)-2-(thymin-1-yl)acetamido) acetic acid.

The IN inhibitory activities of 9-amino-DACA and one intermediate 9-aminoacridine-containing compound were evaluated in a cell based antiviral assay. Although their absolute potencies of inhibition were in the micromolar range, their novel scaffold warrants their further investigation as potential anti-IN inhibitors

Acknowledgements

I wish to thank Dr. Allan S.F. Boyd for his suggestions and guidance regarding NMR experiments and spectra interpretation, Mrs Christina Graham for performing elemental analysis and giving general technical support but also for her heart-warming kindness and friendship, Professor David R. Adams for his kind permission for the use of illustrations and for his support and general advice given on scientific issues, Dr. Georgina M. Rosair for her help with crystal structure determinations, Dr. Robert W. Allcock for his advice and guidance on numerous chemical issues, Dr. Michael Thomas for his general support and advice, Ms Lia Tazioli for her scientific contribution to the project and her support and friendship and, last but not least, the numerous staff and fellow students in the chemistry department I had the pleasure to work with.

I also wish to express special gratitude to my supervisor, Dr. Nicola M. Howarth, for her continuing support throughout the project and to my wife Ping who never stopped encouraging me during difficult times.

Finally, I also would like to thank Dr. Jean-François Mouscadet for bioactivity testing, the EPSRC Mass Spectrometry Service Centre, Swansea for LRMS and HRMS data and the European Commission Framework 6 Programme (project ref.: LSHB-CT-2003-503480) for funding.

Table of Contents

Glossary

AIDS: Acquired immune deficiency syndrome

Alloc: Allyloxycarbonyl

AZT: 3'-azidothymidine

BAF: Barrier-to-autointegration factor

BSA: N,O-Bis(trimethylsilyl)acetamide

cDNA: Complementary DNA

CDI: Carbonyldiimidazole

CCD: Catalytic core domain

CTD: C-terminal domain

CC_{50}: Half maximal cytotoxic concentration

DNA: Deoxyribonucleic acid

ds: double stranded

DKA: Diketo acid

DAPY: Diarylpyrimidine

DACA: *N*-[2-(dimethylamino)ethyl]-acridine-4-carboxamide

DMF: Dimethylformamide

DCM: Dichloromethane

DMSO: Dimethylsulfoxide

DTT: Dithiothreitol

DPIC: Diphenyliodonium carboxylate

EI: Entry inhibitors

EED: Embryonic ectoderm development

EC_{50}: Half maximal effective concentration

ERA: European Research Area

FISH: Fluorescent *in situ* hybridisation

FDA: Food and drug administration

Fab: Fragment antigen binding

gp: glycoprotein

HEPES: 4-(2-hydroxyethyl)-1-piperazineethanesulfonic acid

HMBC: Hetero-nuclear multiple bond correlation

HIV: Human immunodeficiency virus

HMGA1: High mobility group protein A1

HBTU: 2-(1H-Benzotriazol-1-yl)-1,1,3,3-tetramethyluronium hexafluorophosphate

HSQC: Hetero-nuclear single quantum coherence

HDAC: Histone deacetylase

HRP2: Hepatoma-derived growth factor related protein 2

HSP: Heat shock protein

HAART: Highly active anti-retroviral therapy

IR: Infrared

IC_{50}: Half maximal inhibitory concentration

IN: Integrase

INBI: Integrase binding inhibitors

INI1: Integrase interactor 1 protein

LTR: Long terminal repeats

LEDGF: Lens epithelium derived growth factor

LVG: Leaving group

MA: Matrix

NHS: *N*-hydroxysuccinimide

NRTI: Nucleoside (and nucleotide) reverse transcriptase inhibitors

NNRTI: Non-nucleoside reverse transcriptase inhibitors

NNIBP: Non-nucleoside inhibitor binding pocket

NTD: N-terminal domain

NADPH: Nicotinamide adenine dinucleotide phosphate

NC: Nucleocapsid

NOESY: Nuclear Overhauser effect spectroscopy

NMR: Nuclear magnetic resonance

PBS: Phosphate buffered saline

PI: Protease inhibitors

PIC: Pre-integration complex

PPE: Poly-phosphoric ethyl ester

PNA: Polyamide nucleic acids

RNA: Ribonucleic acid

RT: Reverse transcriptase

RER: Rough endoplasmic reticulum

RT: Reverse transcriptase

ROESY: Rotational Overhauser effect spectroscopy

ss: single stranded

TRIoH: Targeting replication and integration of HIV

TLC: Thin layer chromatography

THF: Tetrahydrofuran

TopPipU: 2-(2-Oxo-1(2H)-pyridyl)-1,1,3,3-bis-pentamethyleneuroniumtetrafluoroborate

TFA: Trifluoroacetic acid

***t*-Boc**: *t*-Butyloxycarbonyl

UNG: Uracil-N-glycosylase

Vpr: Viral protein R

Z: Carboxybenzyl

Chapter 1: Introduction

1.1 Preamble

AIDS or Acquired Immunodeficiency Syndrome is caused by HIV or Human Immunodeficiency Virus and was discovered in 1983 by Luc Montagnier from the Pasteur Institute in Paris, France. Since the early eighties the disease has taken on pandemic proportions and worldwide over 33 million people are thought to carry the virus. AIDS is one of the ten main causes of death in the world and has an immense socio-economic impact, particularly in certain hard-hit sub-Saharan countries with adult HIV prevalence of over 15%.

This forms a huge challenge for those wishing to contribute scientifically to the solution of the AIDS problem and continuing efforts are made on a European political level to join multidisciplinary scientific forces in order to tackle this growing global health threat.

In 2003 different partners from business and academic backgrounds, of which Dr. Howarth's Nucleic Acids Lab was one, joined efforts in a European Commission '6th Framework Programme' integrated project known as TRIoH (Targeting Replication and Integration of HIV: Project number: LSHB-CT-2003-503480). The main objective of the 6th Framework Programme was to further accommodate the creation of a European Research Area (ERA) by improving integration and co-ordination of so far largely fragmented research. Under this European umbrella TRIoH focused on the integration of different research efforts from different European partners to develop novel anti-HIV molecules targeting viral replication and integration.

This dissertation is a record of my contribution to Dr. Howarth's partnership in the TRIoH consortium. It comprises general background information on HIV/AIDS, the current therapeutic approach and the existing collection of HIV antiretroviral drugs and their mechanisms of action. I take a more in-depth look at HIV's integrase enzyme, its structure and function as well as the development of integrase inhibitors and their mode of action. As an introduction to a new approach we took in the development of novel potential HIV-Integrase inhibitors, referred to as PNA-Acridine threading intercalators, I discuss the properties and therapeutic potential of DNA intercalators and Polypeptide Nucleic Acids (PNA) and how a conjugation of PNA with a DNA intercalator like acridine holds the potential to inhibit HIV integrase through binding to the enzyme

donor substrate (viral DNA) and/or the actual enzyme. Finally, a comprehensive discussion of the followed synthetic strategies towards the development of PNA-acridine conjugates and the chemistry involved is reported.

1.2 Acquired Immune Deficiency Syndrome or AIDS

1.2.1 Key facts about AIDS

AIDS, or Acquired Immune Deficiency Syndrome, is caused by HIV, the Human Immunodeficiency Virus. It is characterized by a gradual deterioration of the immune function. HIV causes the destruction of lymph nodes and related immunologic organs and disables a specific type of immune cell, called CD4+ T cells, during the course of the infection.[1] These T-helper cells, as they are also called, are crucial to the function of the immune system because they send activating signals to other immune cells that take part in the complex immune response following infection. Therefore, the immune system's failure, understandably, has devastating effects on the human body, leaving it open to attack from even the most harmless of infections.

The term AIDS applies to the most advanced stage of HIV infection in which patients have less than 200 CD4+ T cells per mm^3 of blood (a healthy person has between 800 and 1200 CD4+ T cells per mm^3 of blood).[1] Early symptoms of HIV infection include fever, headache, tiredness and the presence of enlarged lymph nodes. Often these are mistaken for other viral infections. It can take between 3 months to over 10 years after contracting HIV infection before the actual onset of AIDS occurs. This is accompanied by a gradual increase in the severity of the above symptoms, going from a lack of energy, severe weight loss and persistent yeast infections to mental problems such as confusion and forgetfulness, severe and persistent diarrhoea and development of cancers such as Kaposi's sarcoma and certain types of lymphomas.

HIV is transmitted through unsafe sex with an infected partner, during which the virus enters the body through the lining of the vagina, vulva, penis, rectum or mouth.[1] Transmission can also occur through contact with infected blood, for example through sharing of contaminated needles or syringes among drug users. Between 25 to 33% of untreated HIV positive pregnant women will transmit HIV to their babies during birth or pregnancy. This risk is strongly reduced when the anti-AIDS drug 3'-

azidothymidine (AZT) is taken by the mother during pregnancy and by the baby for the first 6 months after birth. There is no evidence that HIV can be spread through sweat, tears, urine or faeces. In addition, although HIV has been found in the saliva of infected people, there is no evidence supporting transmission via this route, neither can HIV be contracted through casual contacts, such as sharing of food, utensils, towels, bedding, swimming pools, telephones and toilet seats or from biting insects.

1.2.2 Epidemiology

At the end of 2007, it was estimated that 33.2 (30.6-36.1) million people in the world were living with HIV/AIDS; 28.2-33.6 million adults (with a 50/50 distribution between the genders) and between 2.2 and 2.6 million children below the age of 15 years.[2] More than 67 percent of these people (i.e. 20.9-24.3 million) live in Sub-Saharan Africa and another 12 percent (3.3-5.1 million) live in South and South-East Asia. Western and Central Europe and North America combined represent just over 6 percent (1.1-3.0 million) of the worldwide prevalence. In 2007, it was reported, between 1.9 and 2.4 million people died of HIV/AIDS related illnesses. Furthermore it has been estimated that 1.8 to 4.1 million people became newly infected with HIV during 2007. More than 80 percent of newly diagnosed adult HIV infections resulted from heterosexual intercourse whereas more than 90 percent of HIV infections in infants and children were a result of mother-to child (vertical) transmission.

1.2.3 HIV's viral structure, replication cycle and genome structure

(i) HIV structure

HIV is an enveloped RNA virus and a retrovirus, which means its genetic material, RNA, needs to be 'transcribed' into DNA for the virus to be able to replicate.[3] HIV is also a lentivirus (a genus within the retrovirus family). The members of this family are characterized by a long incubation period ('lenti' is Latin for slow). The HIV virus acquires its phospholipid envelope while budding out of the host cell (e.g. a helper-T cell) during replication. The spherical virus has a diameter of about 100 nm (**Figure 1.1** illustrates the HIV structure). 72 peg-like structures (peplomers), viral RNA encoded, protrude from the viral envelope. Each peg consists of two types of

glycoprotein (gp 41 and gp 120): trimeric gp 41 molecules constitute the stem of the peg while trimeric gp 120 molecules form the cap. Inside the envelope there is a matrix made up of p17 protein molecules. The matrix surrounds a hollow, cone shaped capsid (composed of p24 protein and human cyclophilin A protein molecules), harbouring two (+)-sense single RNA strands and copies of three important enzymes in HIV's lifecycle i.e.: HIV reverse transcriptase, HIV protease and HIV integrase. P9 protein molecules form a nucleocapsid sheath in complex with the RNA strands.

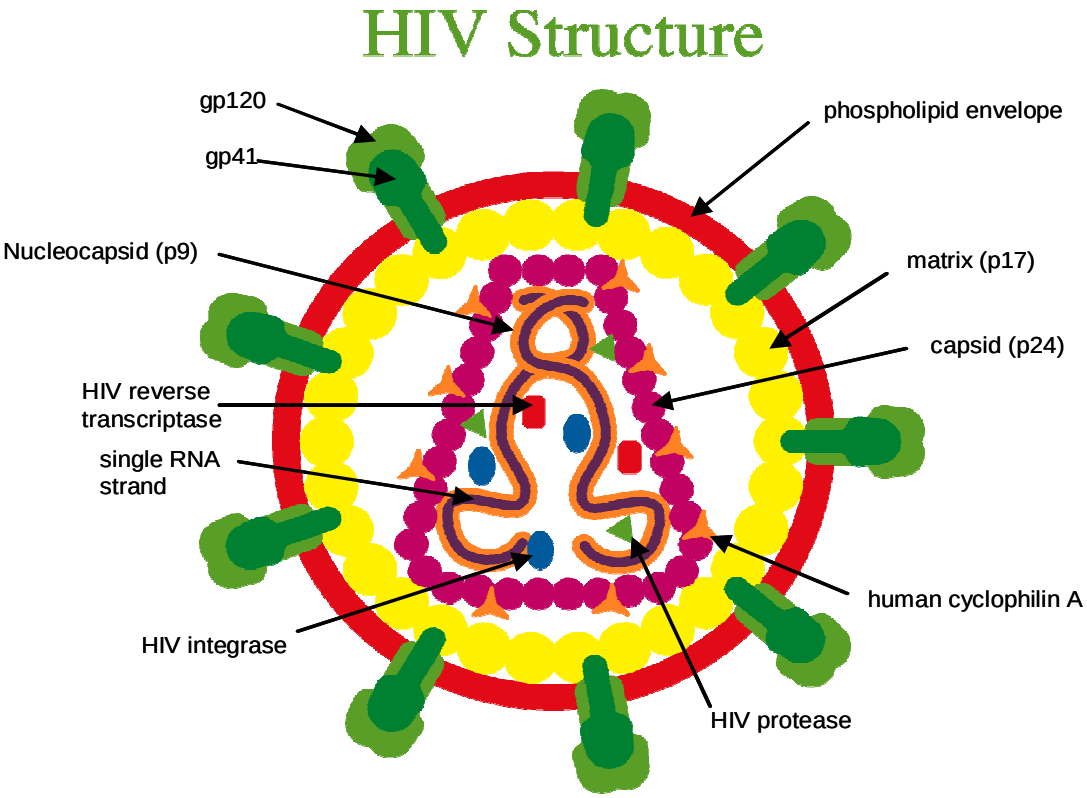

Figure 1.1: HIV structure (D.R. Adams: used by permission)

(ii) HIV replication cycle

The main target for HIV in the human immune system seems to be the helper T cell (T-lymphocyte) but other cells, like macrophages and monocytes, can become infected as well and all can harbour large numbers of viruses.[3] HIV's entry into the T cell requires the binding of gp 120, on the HIV surface, to the CD4 receptor molecules and to a co-receptor, both on the host cell's surface. (Step 1 in **Figure 1.2**: the HIV replication cycle; co-receptors are not shown in Figure 1.2).

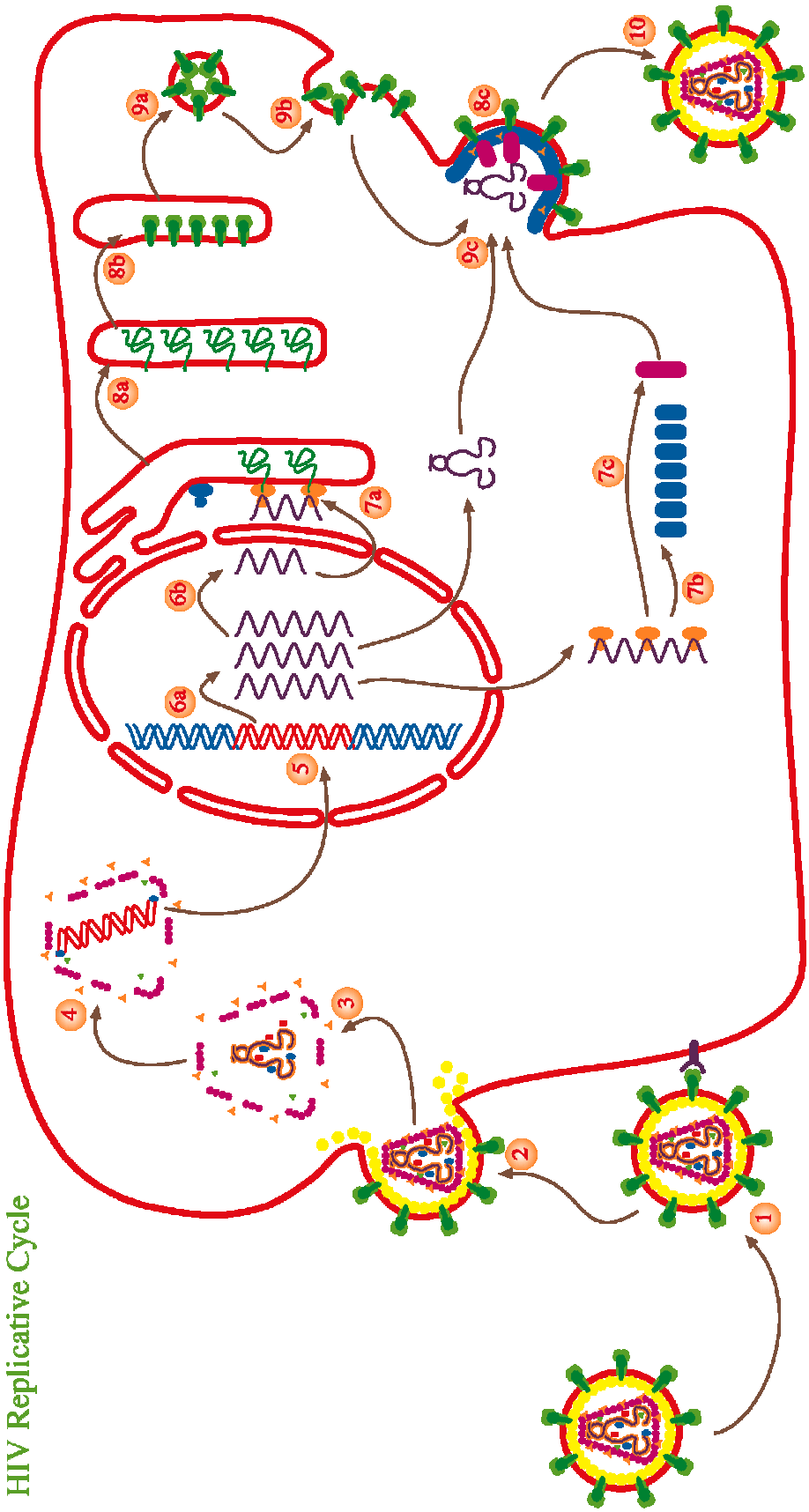

Figure 1.2: HIV replication cycle (D.R. Adams: used by permission)

Two different co-receptors, CCR5 and CXCR4 have been found to be involved. They are involved early in the infection, during the asymptomatic phase or late in the infection, during the symptomatic phase respectively. Viruses isolated from individuals early in the infection have been shown to typically infect macrophages in the laboratory, rather than T cells. However, the latter can be infected by viruses taken from patients in late infection stage. Once HIV has bound to the host cell (e.g. a T-lymphocyte), its viral envelope fuses with the host's cell membrane and the viral RNA and enzymes are released into the host's cytoplasm (i.e. the fusion process: step 2 in **Figure 1.2**). During this process the viral matrix disintegrates and the cyclophilin A molecules, part of the viral capsid, dislocate the latter (the uncoating process: step 3 in **Figure 1.2**). In turn this opens up the capsid core to the host cell's cytoplasm. The viral enzyme reverse transcriptase (RT) now has access to the host cell's nucleotide building blocks and transcribes the viral RNA into its Watson-Crick complementary single-stranded DNA (ss-DNA). DNA synthesis and RNA hydrolysis are co-ordinated so that RNA is removed only after it has served as a template. The resulting viral ss-DNA forms the template for viral double-stranded DNA (ds-DNA) synthesis which is also effected by RT. Thus, RT carries out three kinds of reactions: 1) RNA-directed DNA synthesis, 2) Hydrolysis of RNA, 3) DNA-directed DNA synthesis. DNA synthesis is carried out by the polymerase moiety of RT whereas RNA hydrolysis is performed by the RNAse H moiety. All this occurs inside an expanded capsid structure and is generally referred to as reverse transcription (step 4 in **Figure 1.2**). The next step in the HIV lifecycle involves the viral enzyme integrase. HIV integrase catalyses the integration of the viral ds-DNA into the host's cellular chromosome (splicing) after which the viral DNA is referred to as the provirus (a state in which infection becomes irreversible) (integration: step 5 in **Figure 1.2**). The "blending in" allows the virus to be latent and effectively evade host responses. Transcription of the provirus by hijacking the host's cellular synthesis machinery leads to the generation of viral RNA (steps 6a and 6b in **Figure 1.2**). Initially viral mRNA coding for viral accessory proteins and the *env* gene is produced (step 6b). In a later stage genomic viral RNA and mRNA for expression of the viral *gag* and *pol* genes is generated (step 6a). In the subsequent translation processes (steps 7 in **Figure 1.2**) the first viral proteins to be synthesised are Rev and Tat (regulatory proteins with names similar to their associated genes). Rev protein facilitates RNA export to the cytoplasm and by doing so prevents splicing of longer viral RNA transcripts, which in turn allows for production of

structural proteins and RNA genome. Tat protein increases transcription of all the HIV genes. The *env* gene transcript is translated by ribosomes on the rough endoplasmic reticulum (RER) thereby producing, inside the RER, the gp160 precursor of gp41 and gp120 (step 7a). In the cytoplasm the *gag* gene transcript is translated into Gag protein, the precursor to viral matrix protein (p17), capsid protein (p24) and nucleocapsid protein (p9) (step 7b). Also cytoplasmatic, the *pol* gene transcript is translated into Gag-Pol protein, the precursor to the viral enzymes reverse transcriptase, integrase and protease (step 7c). In a first maturation step the Env protein (gp 160) progresses from the endoplasmic reticulum to the Golgi apparatus, in which glycosylation and subsequent formation of the mature gp41-gp120 complex takes place (steps 8a and 8b **in Figure 1.2**). The subsequent virion assembly (steps 9 **in Figure 1.2**) initially involves expression of the viral glycoprotein spikes (gp41-gp120) on the host cell membrane via fusion of the latter with Golgi generated, peplomer carrying vesicles (steps 9a and 9b). The generated patch of 'spiked' host cell membrane allows for localised cytoplasmatic recruitment of the immature viral components: Gag and Gag-Pol, cyclophilin A and two copies of full-length RNA (step 9c). This organised assembly causes the viral particles to bud from the host cell membrane, thereby making use of the latter to function as viral envelope (the release process: step 10 in **Figure 1.2**). A final maturation (step 8c) takes place, during or soon after budding, by the action of HIV protease, which processes Gag and Gag-Pol to produce their functional forms. This maturation step is required for the virus to become fully infective.

The HIV replication cycle, comprising viral entry into the host cell, replication, assembly, subsequent release of new viral particles and infection of other cells, can take as little as 36 hours.[4]

(iii) HIV genome structure

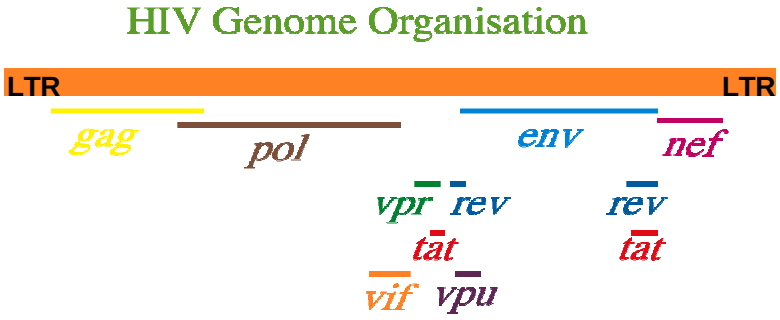

Figure 1.3: organisation of the HIV genome (D.R. Adams: used by permission)

The above representation of the HIV genome (top orange strip) contains a total of 9 genes (thinner, labelled strips), some of which are fragmented and/or overlapping with other genes. The total coding region in the HIV genome takes up about 9.2 kb.[3] The two regions at both ends of the genome flanking the functional genes are referred to as long terminal repeats (LTR) (see **Figure 1.3**). LTR are non-coding regions that play a role in integration of viral ds-DNA into the host genome and in regulation of transcription initiation. The 9 genes are known as ***gag***, ***pol***, ***env***, ***nef***, ***vpr***, ***rev***, ***tat***, ***vif*** and ***vpu***.

gag: holds the information for core and structural proteins i.e. matrix protein (p17), capsid protein (p24) and nucleocapsid protein.

pol: holds the information for the viral enzymes reverse transcriptase, integrase and protease (both ***gag*** and ***pol*** products are processed by viral protease to generate the functional protein forms).

env: holds the information for the glycoprotein spikes (the gp120-gp41 complex). The ***env*** product gp160 is split into the gp120-gp41 complex by a host cell protease.

The remaining genes, ***nef***, ***vpr***, ***rev***, ***tat***, ***vif*** and ***vpu***, are single genes that code for similarly named proteins (**Nef**, **Vpr**, **Rev**, **Tat**, **Vif** and **Vpu**). They are regulatory, non-structural genes controlling different parts of the viral life-cycle.

1.2.4 Current Treatment

There are a total of 32 FDA approved medications (single drug + co-formulations) for anti-HIV treatment which target a number of different processes in the HIV life-cycle.[5] These anti-HIV drugs are divided into five different classes: (i) fusion or entry inhibitors (EIs); (ii) nucleoside (and nucleotide) reverse transcriptase inhibitors (NRTIs); (iii) non-nucleoside reverse transcriptase inhibitors (NNRTIs); (iv) protease inhibitors (PIs) and (v) integrase inhibitors.[5]

(i) Entry and fusion inhibitors:

These inhibitors function by blocking the HIV virus entry into human cells. The first FDA approved and marketed fusion inhibitor was enfuvirtide (**Figure 1.4**). Enfuvirtide is a synthetic peptide of 36 natural amino acids (with an acylated N-terminus and a carboxamide C-terminus) that binds to HIV-1's glycoprotein 41, thereby interfering with its capacity to combine viral and cellular membranes, thus effectively blocking

membrane fusion.[6] Another peptide-based candidate in clinical trials is known as TRI-1144 (**Figure 1.4**), a 38 amino acid peptide that partially overlaps with the enfuvirtide sequence but appears to have better potency and pharmacokinetic properties and is less prone to resistance development.[7]

Ac-Tyr-Thr-Ser-Leu-Ile-His-Ser-Leu-Ile-Glu-Glu-Ser-Gln-Asn-Gln-Gln-Glu-Lys-Asn-Glu-Gln-Glu-Leu-Leu-Glu-Leu-Asp-Lys-Trp-Ala-Ser-Leu-Trp-Asn-Trp-Phe-NH_2

Enfuvirtide

Thr-Thr-Trp-Glu-Ala-Trp-Asp-Arg-Ala-Ile-Ala-Glu-Tyr-Ala-Ala-Arg-Ile-Glu-Ala-Leu-Leu-Arg-Ala-Leu-Gln-Glu-Gln-Gln-Glu-Lys-Asn-Glu-Ala-Ala-Leu-Arg-Glu-Leu

TRI-1144

Figure 1.4: 1° structure of TRI-1144 (in clinical trials) and Enfuvirtide (FDA approved)

A second FDA approved and marketed entry inhibitor is known as Maraviroc (**Figure 1.5**), which is an antagonist of the chemokine co-receptor CCR5 on the CD4+ T cell membrane.[8] Maraviroc thereby prevents binding of HIV's gp 120 to CCR5 and blocks subsequent membrane fusion events required for viral entry.

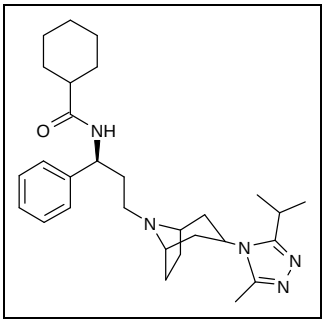

Figure 1.5: entry inhibitor Maraviroc

Furthermore, a number of potential new fusion/entry inhibitors are currently in development, targeting either HIV's gp 41 and gp120 or helper T cells' CD4 receptor and CCR5 and CXCR4 co-receptors.

(ii) Nucleoside (and nucleotide) reverse transcriptase inhibitors (NRTIs)

There are currently 13 FDA approved medications containing nucleoside (and nucleotide) reverse transcriptase inhibitors (NRTIs) available, as single drug (nine) or as a co-formulation (four). NRTIs are nucleoside (or nucleotide) analogues that

suppress replication of retroviruses by interfering with the HIV reverse transcriptase enzyme.

Approved single drug NRTIs are zidovudine (AZT), stavudine (d4T), lamivudine (3TC), emtricitabine (FTC), didanosine (ddI), zalcitabine (ddC), abacavir (ABC) and tenofovir D (TDF) [5] (**Figure 1.6**). During reverse transcription, by HIV reverse transcriptase, these nucleoside/nucleotide analogues (also referred to as chain terminators) are incorporated into the viral DNA, but because they lack the 3'-OH of a natural nucleoside/nucleotide unit, which is required to make the phospho-ester linkage with the incoming deoxynucleoside triphosphate, DNA synthesis is prematurely terminated.

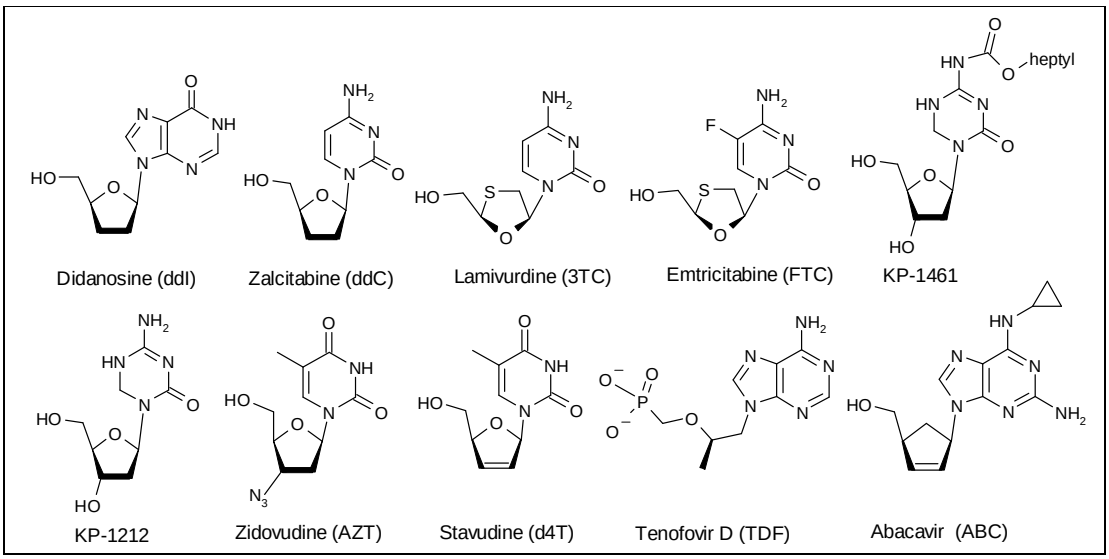

Figure 1.6: Nucleoside (and nucleotide) reverse transcriptase inhibitors (NRTIs)

Currently, there are 4 new NRTIs undergoing clinical trials.[5] An intriguing NRTI known as KP-1212 (the prodrug of which is KP-1461) (**Figure 1.6**) works by a mechanism new to the nucleoside analogues. It is a non-chain terminating mutagen. Due to its capacity to randomly incorporate itself in the viral DNA and pair with multiple bases it generates multiple mutations, thereby rapidly rendering the virus unviable.[9] However, recently clinical trials for KP-1461 have been terminated.

(iii) Non-nucleoside reverse transcriptase inhibitors (NNRTIs)

Non-nucleoside reverse transcriptase inhibitors or NNRTIs, like NRTIs suppress HIV replication by interfering with HIV's reverse transcriptase enzyme.[10] NNRTIs are

non-competitive inhibitors of RT, i.e. they do not compete with RT natural substrates but exert their effect by binding to reverse transcriptase at a site different form the catalytic binding site. This induces a conformational change that disrupts the catalytic site which in turn renders the enzyme incapable of normal interaction with the viral RNA, slowing down or blocking DNA-dependant and RNA dependant polymerase activities.

FDA approved NNRTIs are nevirapine, efavirenz, delavirdine and etravirine (**Figure 1.7**).[5] Etravirine was approved early in 2008 (10 years after the last NNRTI, efavirenz, had been approved).[5] Etravirine, a diarylpyrimidine (DAPY), is a second generation NNRTI and was developed after studies on first generation NNRTIs revealed that increased inhibitor flexibility could induce binding to the so-called non-nucleoside inhibitor binding pocket (NNIBP) in a number of different conformations.[11] Most importantly this increased conformational freedom meant the NNRTIs could intrinsically adapt to mutation induced changes to the binding pocket, making them very potent inhibitors of key drug-resistant HIV-1 strains.[12], [13] Another not yet approved diarylpyrimidine, rilpivirine (**Figure 1.7**), also shows potent activity against NNRTI resistant HIV and is currently undergoing clinical trials [14].

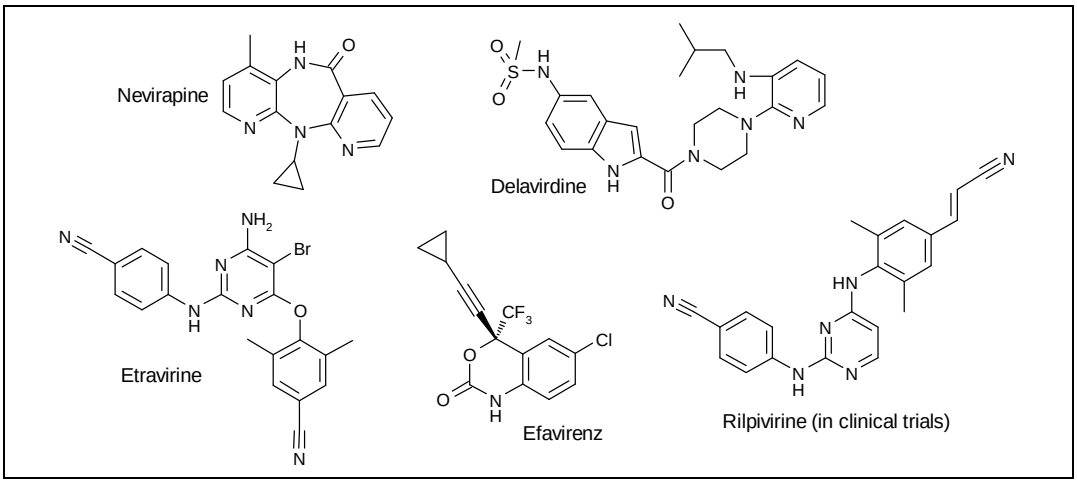

Figure 1.7: Non-nucleoside reverse transcriptase inhibitors (NNRTIs)

(iv) protease inhibitors (PIs)

PI's target the HIV's protease enzyme. This enzyme is responsible for proteolytic cleavage of HIV's polypeptide precursors into mature enzymes and structural proteins.

Generally this means, by binding to this enzyme, these PIs render the HIV's protease incapable of performing its catalytic function. Thus, upon budding, the liberated immature viral particles containing catalytically inactive protease are unable to undergo maturation to produce an infective form.[15]

HIV protease is an aspartate protease (which belongs to one of two mechanistically different protease classes) in which a water molecule, activated/deprotonated by the two aspartyl β-carboxy groups at the protease's active site, nucleophilically attacks the carbonyl of the scissile peptide bond. As a result of this proteolytic process a tetrahedral transition state is generated.[16] (see **Figure 1.8a** for a protease mechanism suggested by Suguna *et al.*[17]) This knowledge led to the development of 'natural substrate-like' protease inhibitors carrying non-cleavable *iso*-steres mimicking the tetrahedral transition state of this hydrolysis step.

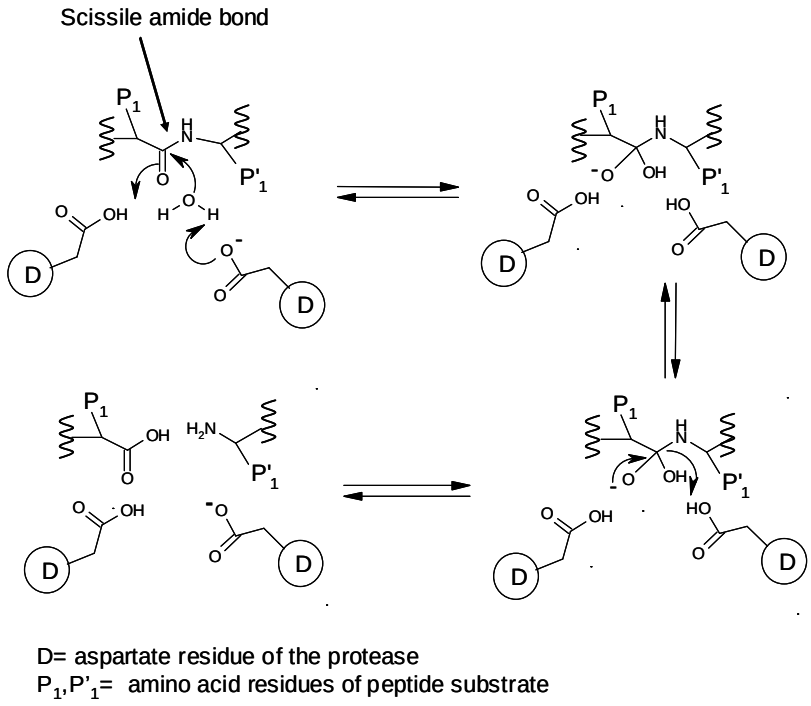

Figure 1.8a: aspartate protease mechanism (as suggested by Suguna *et al.*[17])

Currently there are 10 FDA approved and marketed PIs: saquinavir mesylate, ritonavir, indinavir, nelfinavir, amprenavir, lopinavir, atazanavir, fosamprenavir, darunavir and tipranavir (**Fig. 1.8b**).[5]

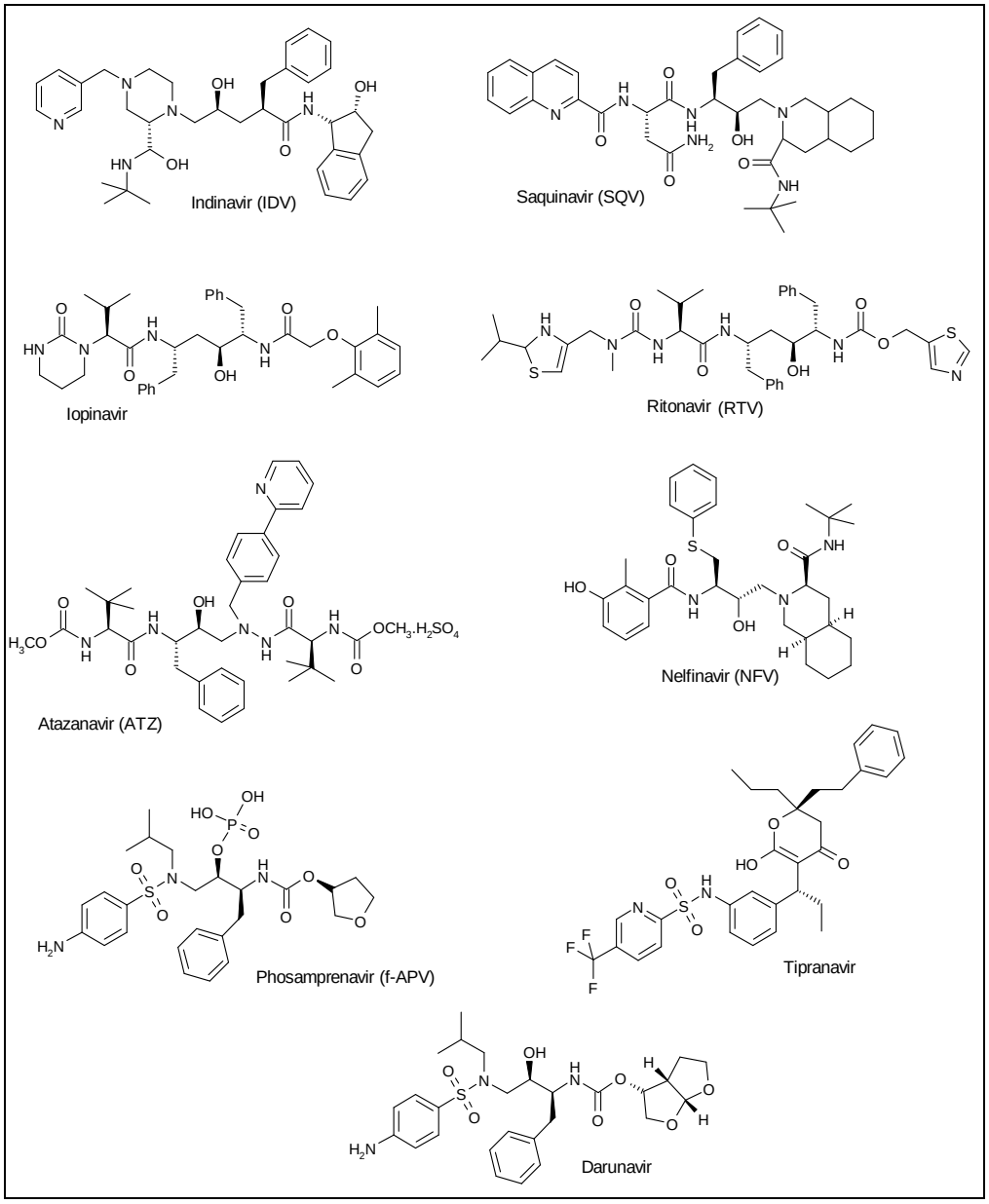

Figure 1.8b: FDA approved HIV-protease inhibitors (PI's)

Saquinavir (mesylate) was the first PI to be granted FDA approval and is a selective, competitive, reversible inhibitor of HIV-protease.[18] It has a non-hydrolysable hydroxyethylamine group in place of the natural substrate's hydrolysable peptide bond (linking phenylalanine and proline residues in the natural substrate).[16] The same hydroxyethylamine *iso*-steric moiety is also present in atazanavir, nelfinavir, darunavir and phosamprenavir.

Another occurring non-hydrolysable *iso*-steric moiety is hydroxyethylene (indinavir, ritonavir, lopinavir).

Tipranavir is a non-peptide, more recently developed PI (FDA approved in 2005).[5] Ritonavir was initially thought of/used as an HIV PI but turned out to have the beneficial effect of inhibiting the metabolism of other PI's by the host liver enzyme cytochrome P450-3A4, hence it is now also increasingly used in co-formulations as a booster for other HIV PI's.[19]

(v) Integrase inhibitors

Currently only one integrase inhibitor (raltegravir) has obtained FDA approval [5]. Hence, in the range of HIV-antivirals currently available integrase inhibitors are somewhat under-represented. The two main reasons for this are, early assay conditions that never adequately distinguished between authentic and false leads (due to insufficient specificity), but also an under-representation of the integrase inhibitor pharmacophore in existing compound libraries.[20] The current state of affairs regarding these inhibitors will be discussed later in this chapter in a separate section 1.2, together with the integrase enzyme, its structure and its mechanism.

Other investigational anti HIV drugs

Besides the targets and their inhibitors described above a number of new targets have emerged for which potential new inhibitors are currently undergoing clinical trials. Three examples of investigational drugs are: Bevirimat, Poly(I)-Poly(C12U) (aka Ampligen) and Valproic Acid. (**Figure 1.8c**)

Bevirimat, a maturation inhibitor first-in-its-class, has shown strong activity against wild-type HIV-1 but more importantly, also against certain antiretroviral-resistant strains.[5] During maturation a newly translated HIV polyprotein precursor, encoded by the viral *gag* gene, is processed by the HIV protease (*gag* codes for the basic structural viral proteins). This processing comes down to a cutting up of the *gag* into separate units that can only then obtain their final conformations to become (mature) viral enzymes or structural proteins. Unlike protease inhibitors, bevirimat targets the gag protein and by doing this prevents protease from making a critical cleavage that would result in the generation of the mature capsid protein p24. The subsequently formed viral particles are non-infectious, hence viral replication is no longer possible.[21]

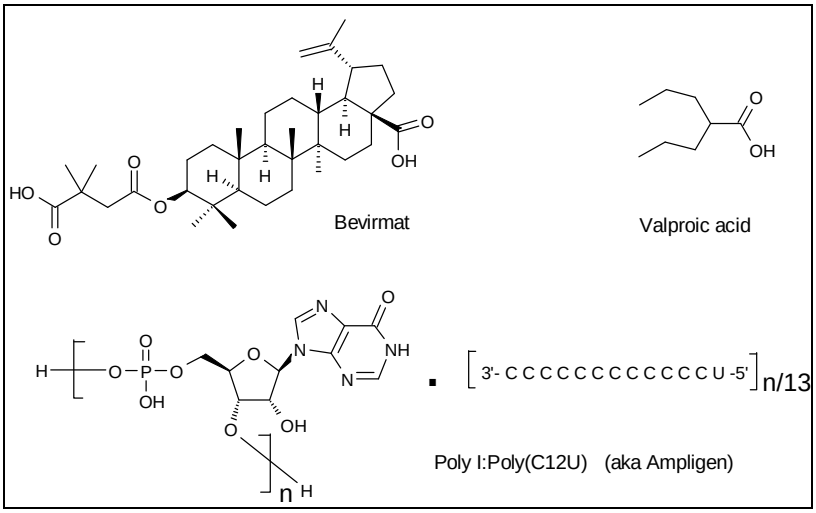

Figure 1.8c: Investigational anti-HIV drug Bevirimat, Valproic acid and Ampligen

A second investigational drug is Poly(I)-Poly(C12U), also know as ampligen (5'-Inosinic acid, homopolymer, complex with 5'-cytidylic acid polymer with 5'-uridylic acid (1:1)). Ampligen is a (synthetic) biological response modifier with widespread anti-viral activity, including HIV.[5] Biological response modifiers (BRM's), natural or synthetic, can actuate the body's natural response to different infections. Ampligen is a double-stranded RNA (dsRNA) capable of activating dormant cellular defences against tumours and viruses.[5]

The third example of a potential anti-HIV drug in clinical trials is Valproic Acid. It is a histone deacetylase (HDAC)-1 inhibitor, which has the downstream effect of stimulating latent T cells to release HIV. In turn this allows for circulating antiretrovirals to attack the re-emerged virus.[5] The normal function of histone deacetylase is to increase the binding affinity (by deacetylating the amines of histones) between histones and the DNA backbone, which condenses DNA structure and prevents transcription.

Highly Active Anti-Retroviral Therapy (HAART)

The current strategy in the treatment of HIV infection consists of patient tailored combinations of antiretrovirals (usually three or four antiretrovirals from different drug classes). This is referred to as **H**ighly **A**ctive **A**nti-**R**etroviral **T**herapy (HAART). Usual combinations (referred to as a triple cocktail) consist of two nucleoside (and

nucleotide) reverse transcriptase inhibitors (NRTIs) and one non-nucleoside reverse transcriptase inhibitor (NNRTIs) or protease inhibitor (PI).[22], [23] When HAART treatment started in 1996 initial drug regimens (for newly infected patients showing signs of immuno deficiency) consisted of over twenty tablets daily (1996), after which treatment slowly evolved to three tablets daily (2003), to two tablets daily of a combined fixed dose of anti-retrovirals (2004) and finally in 2006, one tablet daily containing three different classes of anti-HIV drugs.[24]

The logic behind the HAART (drug combination) strategy is founded in the viral biosynthetic characteristics. It has been shown that a high level of genetic heterogeneity characterises the human immunodeficiency virus.[25] Frameshift and point mutations generated during reverse transcription are believed to generate most of this genetic variability. The short replication cycle and high rate of biosynthetic errors generates a very rapidly mutating virus. HIV reverse transcriptase mismatches approximately 1 in every 7500 bases when synthesising (-)DNA from an RNA template. Similar biosynthetic errors occur naturally in all living organisms but in most cases are subsequently corrected by proofreading enzymes. This safeguard system leads to an error rate of 1 in a million to 1 in 10 billion for DNA replication in eukaryotes.[26] However, when HIV reverse transcriptase converts viral RNA into viral DNA no proofreading enzymes are recruited and errors are left uncorrected. It is this apparent biosynthetic flaw that makes the HIV virus (as it does for other viruses) so resilient against antiviral drugs. Most mutations do not convey any advantage to the virus, if not a disadvantage (by weakening them and/or rendering them incapable of reproducing). However, due to the high mutation rate and short life-cycle there are sufficient opportunities for the virus to acquire a true advantage once infection of the host organism has taken place. This can e.g. be a single point mutation leading to a different amino acid in the 1° structure (and hence part of the higher 3° or 4° structure) of one of the viral protein components against which a particular drug might be acting. Due to the presence of a different amino acid, the interaction of the drug with the viral protein component is changed and the drug's therapeutic effect might no longer be present. In this case the virus has become resistant against that particular drug and the number of virions with this particular trait will rapidly increase in the host organism. If however a patient is taking a combination of antiretrovirals, when resistance against one of the drugs arises, the other drugs will still suppress proliferation of that mutation.

Because no single antiretroviral has been shown to suppress HIV for long, combinations of antiretrovirals need to be taken for a lasting effect, which is referred to as the Highly Active Anti-Retroviral Therapy (HAART).

HAART has significantly improved conditions for patients in terms of suppressing AIDS-related diseases and increasing life expectancies.[27] Although the advantages of HAART are clear, there are some disadvantages as well. Not all potential combinations of the above mentioned drug classes are possible (e.g. certain drugs reduce each others activity), side-effects of particular cocktails can be severe and dosing schedules can be complicated. The latter two complications are important factors in adherence failure which, together with low level residual replication of the virus, is currently leading to the emergence of multiple drug-resistant HIV strains. This is set to jeopardize the benefits of these potent drug cocktails [27] and is one of the reasons why it is of great importance to keep searching for new anti-HIV drugs, preferably targeting alternative steps in the HIV life-cycle. Hopefully, increasing numbers of useful combinations of new antiretrovirals will increase inhibition potency and reduce the risk of cross-resistance emergence (i.e. resistance against drugs that are related in their mechanism of action because of chemical similarities or similar modes of binding).

1.3 Integrase

1.3.1 Integrase as a target in anti-HIV drug development

Integrase was identified as a valid drug target based on the following observations: specific inhibitors of HIV-1 integrase inhibited HIV infection *in vitro* and this was related to a significant reduction of integrated provirus in host cell DNA, [28] mutations in the enzyme's active site given the opportunity to proliferate during treatment with integrase inhibitors rendered the enzyme significantly less susceptible to those inhibitors, and in human clinical trials the use of specific integrase inhibitors has shown that integrase inhibition leads to a reduced viral load.[29]

Integrase has gradually gained more interest as a biological target that used to be underrepresented among targets of the existing drug collection. At present there is only one approved integrase inhibitor on the market which makes this enzyme an appealing

biological target for further drug development. As already mentioned, integrase is required for the integration of the viral ds-DNA into the host's chromosome. Research into the function, mechanism and possible inhibition of integrase has been ongoing now for over 12 years.

Besides the obvious merits of inhibiting an additional viral target (circumventing drug resistance because it would require multiple viral mutations), the absence of a human version of integrase means that integrase inhibitors would potentially be highly selective and should be of low toxicity.[30] These properties, however, cannot exclude possible interactions that integrase inhibitors may have with mechanistically related human enzymes. During the early stages of diketo acid development (a class of integrase inhibitors) these compounds were found to inhibit the human enzyme RAG 1/2 recombinase (this enzyme is involved in somatic recombination in developing lymphocytes, which enables the generation of antibody diversity), although at concentrations 20-fold higher than needed for integrase inhibition.[31] Although initially considered unlikely to be successful, sustained research into these diketoacid compounds has now produced the first approved HIV-integrase inhibitor on the market, known as raltegravir.[5]

Generally, integration of the viral DNA is interesting as a drug target because this can be seen as a point of no return.[32] However, the fact that it is an all-or-none event can also be considered a drawback, since it occurs only once in the HIV life-cycle. Integrase drug development needs to take into account the multiple DNA-protein interactions in the pre-integration complex (PIC), which may obstruct inhibitors from reaching the catalytically active sites [27] (or other potential activity-impairing sites). On the other hand this also means more potential targets to interfere with as more interactions are required for functionality. The window in time just after infection, during which PIC formation can be prevented, is however limited.[27]

Finally, another factor that needs to be taken into account is that integrase is known to alter its conformation upon DNA binding.[33] Hence, co-crystallisation data of the complete integrase-DNA complex would be useful to provide information which can be utilised for enzyme structure based drug design.[27]

1.3.2 Integrase Structure

Integrase (of HIV-1) is a 32 kDa enzyme and consists of a single polypeptide chain with 288 amino acid residues.[30] It is released from a larger viral polypeptide,

encoded by the *pol* gene (which also codes for protease and reverse transcriptase), by viral protease during maturation.[34] Integrase is folded into three distinct functional domains: The zinc binding *N*-terminal domain (NTD) (residues 1-50), the catalytic core domain (CCD) (residues 50-212) and the non-specific DNA binding *C*-terminal domain (CTD) (residues 212-288) (**Figure 1.9a**).[34] For a long time obtaining a crystal structure for the full length integrase was problematic due to low solubility of the enzyme and to date no structure has been reported for the complete integrase molecule nor for its complex with DNA. It was not until the discovery of a F185K mutant (obtained via site-directed mutagenesis), for which solubility of the catalytic core domain (CCD) increased significantly, that the crystal structure of the CCD (of the F185K mutant) was obtained.[35]

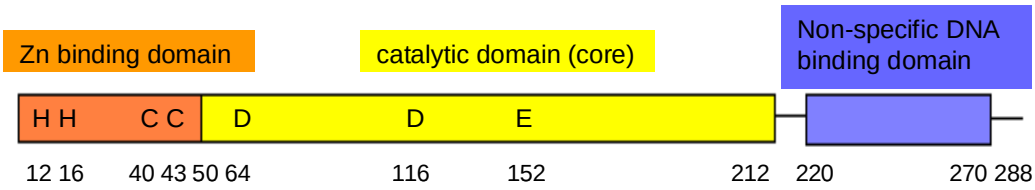

Figure 1.9a: the three functional domains of HIV integrase

Since then more X-ray structures have been determined for the CCD, as well as for the combined *N*-terminal-core catalytic domains and for the combined core catalytic-*C*-terminal domains.[33],[40]

The structure of the separate NTD was elucidated through 2 and 3-dimensional NMR spectroscopy experiments on NTD dimers in solution. (See **Figure 1.9b** for the solution structure of the HIV-2 integrase NTD). The N-terminal domain of HIV-1 integrase contains a conserved (DNA-binding) Zinc finger motif (i.e. the conserved HHCC motif composed of two histidine residues at position 12 and 16 and two cysteine residues at 40 and 43).[34] The NTD monomer consists of four α-helices stabilised by hydrophobic interactions and one Zn^{2+} cation tetrahedrally coordinated to the two conserved histidine (H12 and H16) and two cysteine residues (C40 and C43). In its dimeric form (in solution) HIV's NTD takes on two interconverting folded states (in which reversal of the relative positions of H12 and H16 is one important difference). The NTD dimers are stabilised by hydrophobic forces. The four helices of the

monomer are part of a helix-turn-helix motif common to DNA recognition. The Zn^{2+} cation is essential for the enzyme's highly ordered α-helix secondary structure and point mutations of the conserved His or Cys residues (and subsequent loss of order due to the cation absence) significantly reduce 3'-processing and strand-transfer reactions (the two main catalytic steps of IN) but doesn't interfere with disintegration capacity. The latter observations suggest that NTD is not the only DNA binding moiety and the IN active site is not part of the NTD.[36],[37]

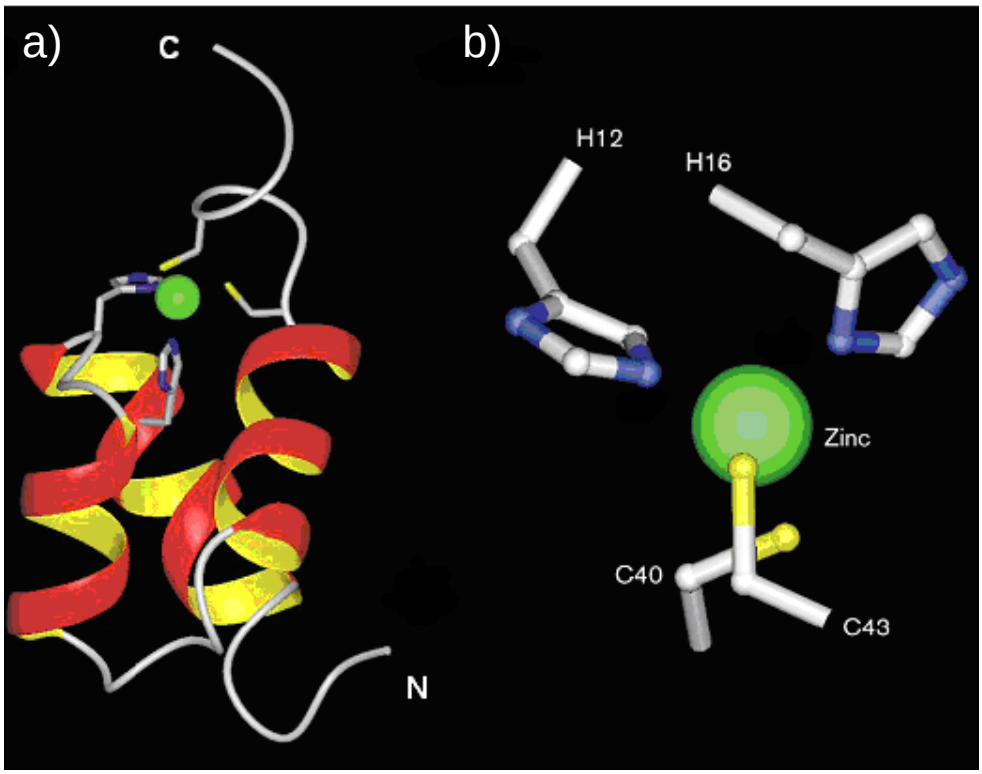

Figure1.9b: a) ribbon diagram of the HIV-2 integrase N-terminal domain monomer b) coordination topology of the Zinc centre. (Source: Eijkelenboom, A.P. *et al*., 1997, [38])

Experiments with chimeric (HIV-1 and visna virus) integrase suggest non-specific DNA binding for the NTD.[39] Multimerization of the full length integrase and 3'-processing and strand-transfer steps (*in vitro*) are all enhanced in the presence of Zn^{2+}. Hence the general consensus is that this is due to essential interactions between the N-terminal domain and the catalytic core domain.[40] The N-terminal domain also binds with two more cellular transcription factors (INI1 and LEDGF/p75) in the PIC.[34]

Initial crystal structure elucidations of the catalytic core domain (CCD) were not as useful as hoped for. The first CCD crystal structure (for the F185K mutant) was solved by Dyda *et al.* but showed disrupted *in vivo* virion assembly.[35] For later crystal structures this problem was resolved by using a F185H mutant (that also retained full integrase activity). A number of structures exist for the core domain, differing mostly in detail but in particular regarding the conformation of a loop (residues 140-152) adjacent to the active site. This loop is thought to be flexible, only adopting a relevant conformation in the presence of DNA substrate.[46] The loop's flexibility is believed to be essential for integration because replacement of the loop's conformational hinges (residues G140 and G149) with alanine leads to loss of catalytic activity while DNA binding capacity is retained. The general consensus is that the loop's involvement in the catalytic process occurs after DNA binding.[41]

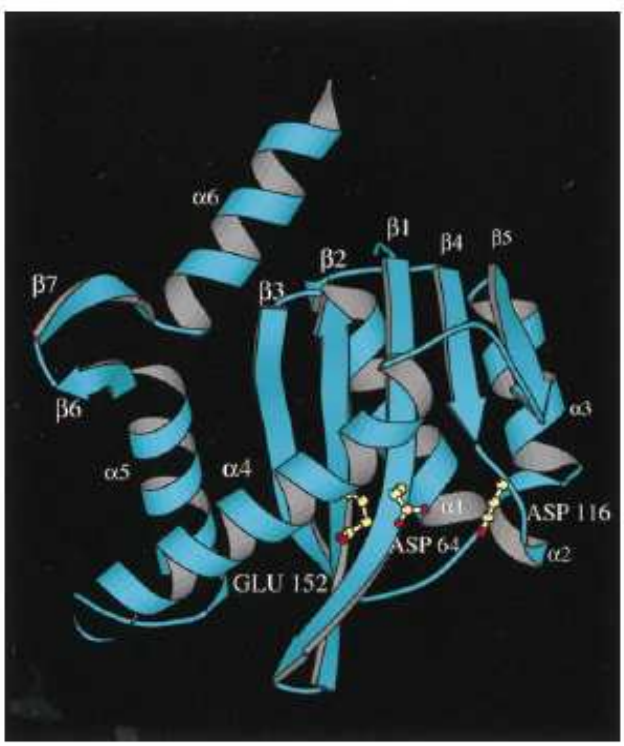

Figure 1.9c: Ribbon diagram of a monomer of the HIV-IN CCD double mutant F185K, W131E showing the seven β-strands, six α-helices and the catalytic triad residues Asp 64, Asp 116 and Glu 152. (Source: Goldgur, Y. *et al.*, 1998, [51])

In a crystal structure of a double CCD mutant (F185K + W131E) the core domain was shown to consist of an α/β structure containing a seven strand β-sheet together with six α-helices.[51] (See **Figure 1.9c** above for a ribbon diagram of HIV-IN CCD double mutant F185K, W131E)

In all the crystal structures two core domains will associate to form a two-fold axis related dimer with a 1400 Å^2 solvent excluded interface.[46] The catalytic core domain has three conserved residues known as the catalytic triad motif DDE, made up of two aspartate residues at positions 64 and 116 and a glutamate at 152 (**Figure 1.9c**).[34] These three acidic amino acid residues, conserved generally among integrases, make up the enzyme's active site and form a shallow cavity on the protein's surface. Mutation of any of these residues confers complete loss of activity and infectivity of the virus.[42],[43],[44],[45] It is presumed that in the active site the catalytic triad coordinates to Mg^{2+} (or Mn^{2+}), in complex with viral and host DNA.[46] Although only one metal has been observed so far in HIV-IN crystal structures, involvement of two metal ions has been suggested in a catalytic mechanism where they act to activate hydroxy nucleophiles.[47],[48] The metal ions' positions in the active site were postulated based on the DNA polymerase I mechanism. One Mg^{2+} was observed between D64 and D116, the other Mg^{2+} is believed to be positioned between D116 and E152 and to bind only in the presence of DNA.[49],[50],[51] In the full IN enzyme the CCD is believed to play a crucial role in 3'-processing and strand-transfer reactions and in recognizing target and viral DNA.[52],[53],[54]

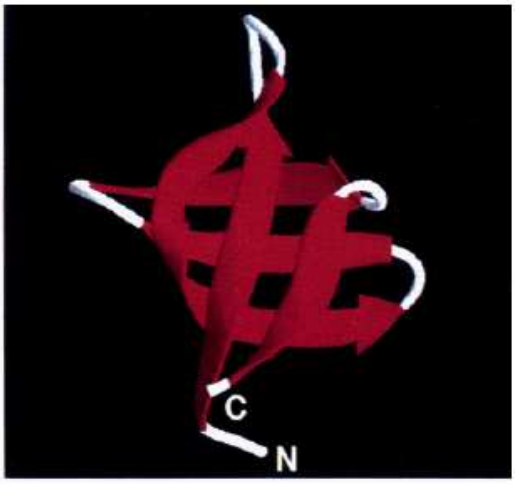

Figure 1.9d: Ribbon diagram of a monomer of Int$^{220\text{-}270}$ (the CTD) showing 5 anitparallel β-sheets (Source: Lodi, P.J. *et al.*, 1995, [55])

A large part of the structure of the *C*-terminal domain (residues 220-270) has been elucidated by NMR spectroscopy. In solution the CTD forms a dimer in which the individual monomers are arranged antiparallel. Each CTD monomer consists predominantly of five antiparallel β-sheets (see **Figure 1.9d** above). The CTD binds

DNA non-specifically [46] and has a high number of positively charged lysine and arginine residues, consistent with DNA binding.[56],[57],[58],[59] It is also the least conserved part of IN. Besides its requirement for 3'-processing and strand-transfer reactions, CTD's role in multimerization and DNA binding was identified after mutational analyses revealed CTD residues crucial to these interactions.[60],[61],[62],[63] Further experiments have shown interactions of the CTD with viral DNA adjacent to the CAGT sequence (at the LTR termini). Recent research clarified that all three domains (NTD, CCD and CTD) bind target (chromosomal) DNA. [50],[64] The CTD also interacts with the viral reverse transcriptase and a cellular protein (EED) in the PIC. [34]

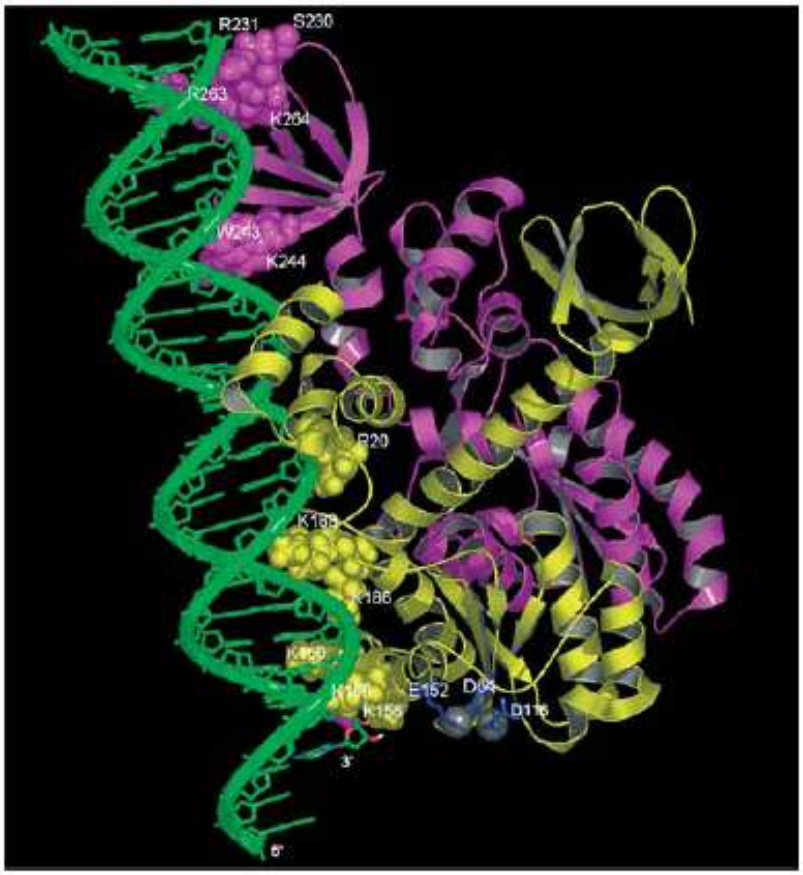

Figure 1.9e: model of the viral DNA (green) docked to an Integrase dimer (made up of a yellow and purple monomer).(Source: De Luca, L. *et al*., 2003, [66]) Amino acids in direct contact with the DNA are shown as spheres (for the yellow IN monomer: residues K156, K159, K160, K186 and K188 in the catalytic core domain and R20 in the N–terminal domain; for the purple IN monomer: S230, R231, W243, K244, K263 and K264 in the C-terminal domain). The catalytic triad D64, D116 and E152 (in the yellow IN monomer) are shown in blue, the bound Mg^{2+} metal ions are grey spheres. The 3'-OH of the conserved viral adenosine is pointing towards the acid catalytic residues.

Crystal structures were elucidated for the combined CCD-CTD (a five-fold mutant) and combined NTD-CCD (a triple mutant) showing CCD dimeric structures similar to the single CCD domain dimers. Both CTD and NTD structures, linked to CCD, differed however from their single domain dimer structure.[65] Structures of both IN^{1-212} (NTD-CCD) and IN^{52-288} (CDD-CTD) allowed for a model for the full length integrase to be proposed.[66] In viral DNA docking studies with the proposed IN model DNA-IN interactions were observed between CCD and NTD of one monomer and the CTD of another monomer.(see **Figure 1.9e** above) In the same study the conserved CA dinucleotide (at the LTR termini) was positioned near the catalytic triad DDE.

1.3.3 Integrase Mechanism

After reverse transcription of the viral RNA in the host's cytoplasm, integrase dimers tightly bind to each of the two conserved sequences 5'-GCAGT-3' found at the ends of the viral ds-DNA long terminal repeats (LTR).[67] Long terminal repeats flank the centrally located HIV genes. Retroviral LTR are non-coding, direct repeats with almost identical sequences, between 500 and 1000 nucleotides in length, and contain regions important for regulation of transcription initiation and polyadenylation.[27],[68].

In order to enable incorporation of the viral ds-DNA into the host's DNA, integrase first removes (by endonucleolytic cleavage) from the conserved CAGT sequence at the 3' ends of the viral LTR the two terminal conserved pGpT dinucleotides (adjacent to the conserved 3'-CA sequences). This step is known as 3'-processing and it takes place in the host's cytoplasm (**Figure 1.10a**) The reaction is a single-step hydrolysis of the phosphodiester bond (linking the adenosine and guanosine nucleotides) and requires a divalent metal ion and a nucleophile.[69] The nucleophile, which can be a H_2O molecule or even small alcohols or amino acids, is activated *in vitro* by Mg^{2+} or Mn^{2+}, although *in vivo* Mg^{2+} is believed to be the active cation.[70],[71],[72] The 3'-phosphodiester of the conserved adenosine (in the CAGT sequence) is attacked by an activated hydroxy group, which results in the release of the terminal 5'-GT-3' dinucleotides. This produces recessed 3'-CA-OH ends on the viral ds-DNA and is the start of the formation of a larger nucleoprotein complex known as the pre-integration complex (PIC).[27] After this first (3'-processing) catalytic step, integrase remains associated with the retroviral DNA in the PIC and this entire complex is translocated across the host's nuclear membrane. The microtubule network is thought to play a role in translocation of the PIC toward the nucleus but there is no full understanding yet of

the nuclear import mechanism.[73] Once in the host's nucleus it is thought the two DNA-bound integrase dimers form a tetramer which allows the PIC to associate with the host DNA (**Figure 1.10a**).[74] Although the latter view is widely accepted it has also been suggested that not a dimer but a tetramer is the minimal integrase molecule present in human HIV-infected cells and an integrase octamer is involved in the nuclear strand-transfer step.[75] Subsequently in the strand-transfer step, the integrase tetramer (or octamer) cleaves the target host DNA with a 5 base-pair stagger and the viral DNA's 3'-CA OH-ends are ligated to the (newly generated) 5'-O-phosphate ends of the host DNA. This is known as the strand-transfer or joining step (**Figure 1.10a and Figure 1.10b**).[76] Integration of the viral DNA has been shown to occur in transcribed genes, albeit randomly.[34]

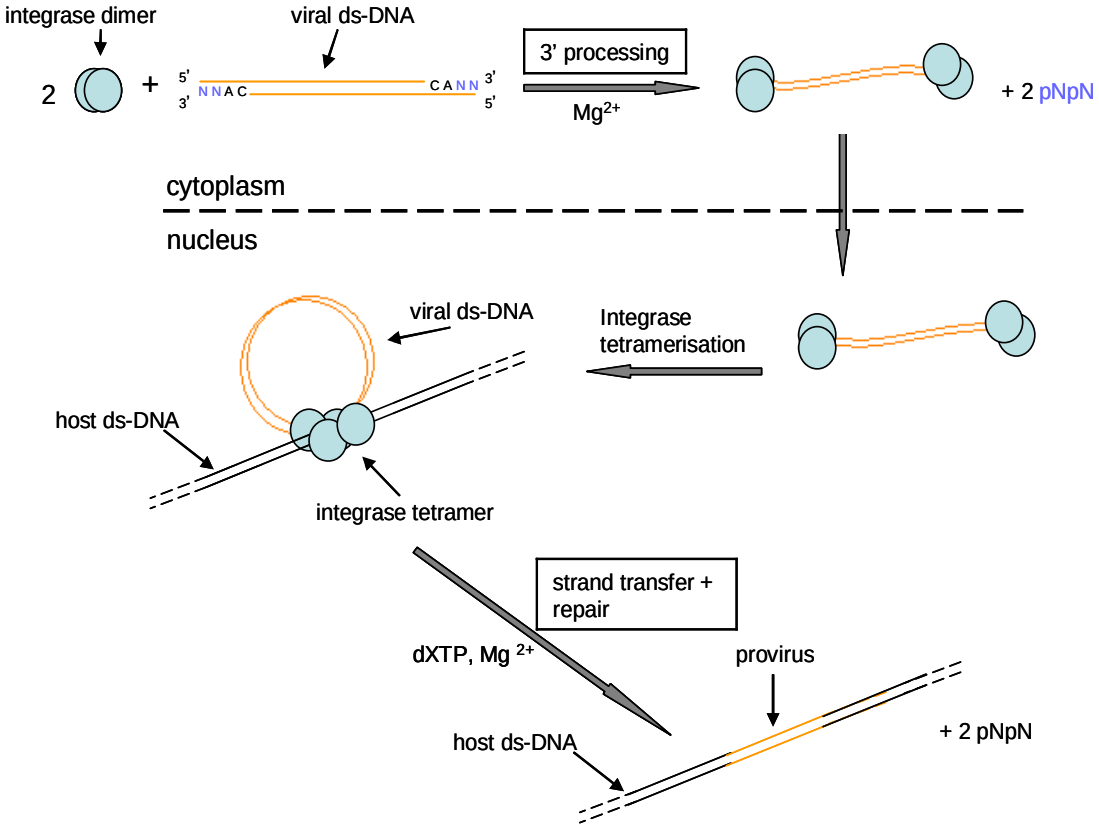

Figure 1.10a: Illustration of proposed integrase mechanism(s) (only the integrase component of the PIC is shown) (dXTP = any natural deoxynucleosidetriphosphate)

In the final step, the retroviral dinucleotides at the 5' ends of the LTR termini are removed, the 5 base-pair gaps in the chromosomal DNA are filled and the 5'-retroviral DNA termini are ligated to the 3'-ends of the host's chromosomal DNA.[77] All this is

referred to as 'repair' (**Figure 1.10a** and **Figure 1.10b**) and is accomplished by host DNA repair enzymes and HIV integrase. HIV is also capable of catalysing the reverse reaction or disintegration but this has only been observed in vitro and the physiological significance remains unclear. Remarkably, disintegration is the only reaction catalysed by recombinant molecules carrying only the integrase catalytic core domain, the significance of which is that only a complete integrase enzyme (as part of the PIC) will catalyse the diversity of reactions involved in integration.[70]

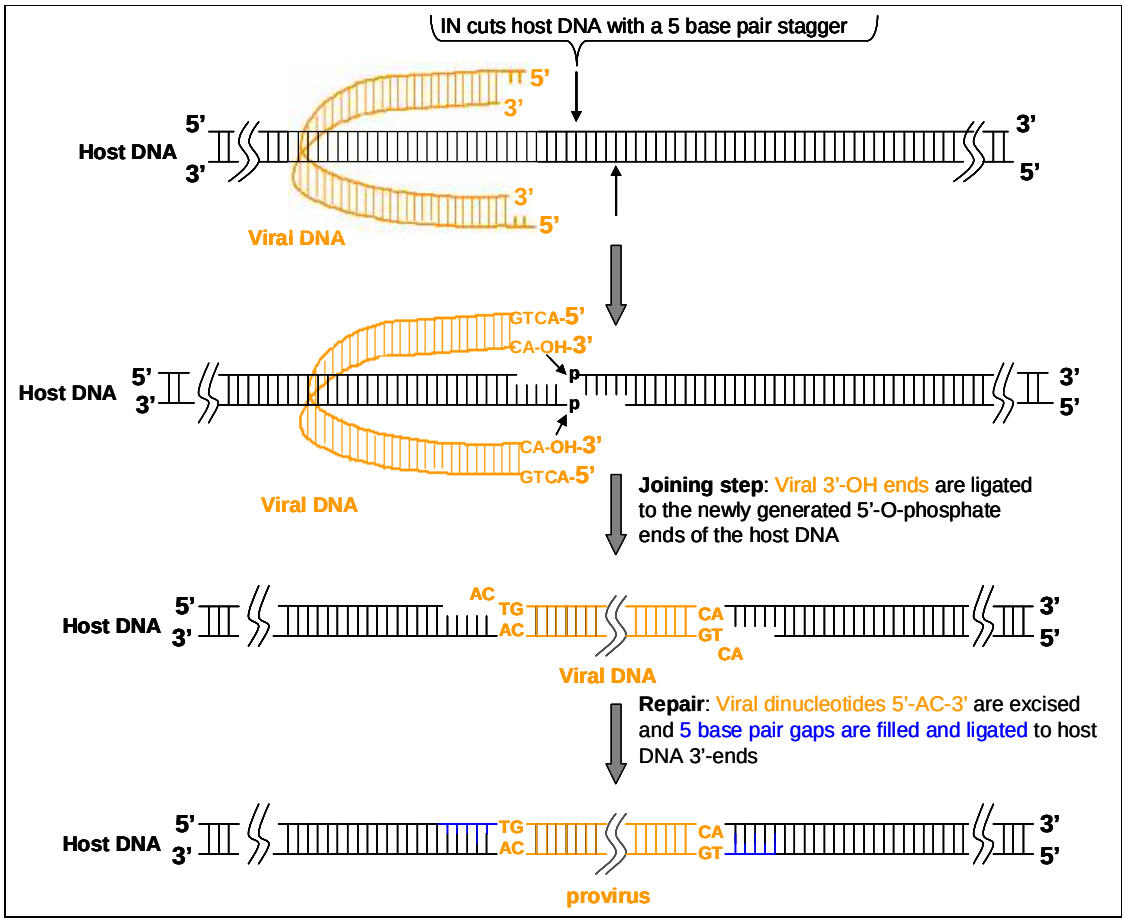

Figure 1.10b: illustration of the strand-transfer step in the integrase mechanism

The current consensus is that there are two PIC DNA binding sites; a donor site (binding viral DNA) and an acceptor site (binding the host chromosome).[34] It is believed the 3'-processing allows for a conformational change in the integrase that enables the host chromosome to bind and allows for the subsequent strand-transfer reaction to take place.[34] It is the latter step that is inhibited by raltegravir, currently the only marketed integrase inhibitor.

1.4 Integrase inhibitors

Compared to NRTI's, NNRTI's and PI's, the development of integrase inhibitors has taken a long time and has been particularly arduous. Besides the lack of specificity in early assays and the lack of a lead compound, other reasons for the slow progress were the lack of a crystal structure for the full length protein complexed with the viral and host DNA, and a misplaced confidence in the potential of prolonged HAART to eradicate HIV. Nevertheless, when monotherapy turned out to be insufficient in significantly prolonging the life of HIV-1 infected individuals, inhibition of integrase was very early on considered as a possible strategy to tackle HIV. Early research focused on biochemical studies in order to shed light on the complex biology of the provirus. Preliminary approaches in searching for integrase inhibitors involved the use of ribozymes designed to cleave the integrase gene [78] and small DNA binding molecules.[79] One of the first molecules to target the enzyme rather than its DNA substrate was aurintricarboxylic acid (see **Figure 1.11**), one of a number of tested polyhydroxylated aromatics which inhibited integrase at micromolar levels but lacked activity in cell-based assays.[80],[81] Further research involved development of screening assays for specific integrase inhibitors and the discovery of new valuable sources for compounds, which pushed forwards early integrase inhibitor development. For some time the focus remained on targeting the viral DNA substrate of integrase, resulting in the discovery of one of the first integrase inhibitors, a G-quartet oligonucleotide referred to as AR177, which made it as far as human clinical trials.[82] AR177 (or 5'-GTGGTGGGTGGGTGGGT-3') is made up of deoxyguanosine and thymidine and contains single phosphorothioate linkages at its 5' and 3' ends for stability. AR177 showed potent activity against integrase at nanomolar concentrations.[83] Somewhat ambiguously no significant mutations were found in the integrase coding region but rather in the region coding for gp120, suggesting interference at the point of viral entry rather than integration.[84] Also, more polyhydroxylated aromatic compounds were tested and found to inhibit integrase. Examples were β-conidendrol, cucurmin and the dicaffeoylquinic acids 3,5-dicaffeoylquinic acid and 1-methoxyoxalyl-3,5-dicaffeoylquinic acid (see **Figure 1.11**).[85],[86] The latter two compounds, derived from medicinal plants, were among the first to show both integrase inhibition and inhibition of HIV-replication *in vitro*.[87] Although the hydroxylated aromatics at this stage never fulfilled the expectations, they

would serve as lead compounds for studies in the following years. In 1994 an important (as it would turn out later) discovery was made by Merck researchers when they found a number of naturally occurring fungal compounds that had integrase inhibitory activity.[88],[89] The first fungal compound showing inhibition of integrase was discovered in an extract of *Fusarium heterosporum* (isolated from marine sources).[88], [90] This compound had long been known as a mycotoxin and derived its name, equisetin (**Figure 1.11**), from *F. equiseti*, one of many *Fusarium* species that produced it.[91] Strand-transfer inhibition IC_{50} value for equisetin was 7 µM and the compound was patented as an integrase inhibitor in 1996.[92] Related compounds like phomasetin (from the terrestrial fungus *Phoma* spp.) (**Figure 1.11**) and its tetrahydroderivative had similar integrase inhibitory activities.[90] The presence of a β-hydroxyketo group in these fungal compounds would later turn out to be an essential structural requirement for integrase inhibitory potency.[88] From 1996 onwards a period followed of intense research into more fungal compounds. One particular compound referred to as an integracide (isolated from *Fusarium* spp. extracts) (**Figure 1.11**) showed inhibition of HIV-1 replication *in vitro* with a EC_{95} value of 25 µM but unfortunately also showed unacceptable levels of cytotoxicity.[88] A different strain of *Fusarium* spp. contained chaetochromins (**Figure 1.11**), a class of compounds for which certain semi-synthetic derivatives showed EC_{50} values of less than 10 µM (for HIV-1 replication *in vitro*). Also, promising IC_{50} values (for integrase inhibition) were found for certain lichen acids (IC_{50}~5µM) (**Figure 1.11)**,[79] and for some synthetic acids like styrylquinolines (IC_{50}~1µM) (**Figure 1.11**), although the latter turned out not to be true integrase inhibitors (but acting somewhere between reverse transcription and integration).[93] At Merck insights grew into integrase inhibition by (equally potent) fungal sesquiterpenoids like equisetin, phomasetin, oteromycin and integric acid (**Figure 1.11**). Innovative experiments in which equisetin and integric acid inhibited integrase, in assays mimicking for the first time conditions in HIV-1 infected cells closer to reality, led Merck researchers to identify the crucial structural elements characterizing a new class of integrase inhibitors. Compounds in this class consist of a sesquiterpenoid backbone linked to a (2,4-pyrrolidinedione) tetramic acid-like moiety bearing a coplanar β-hydroxyketo group (in equisetin and phomasetin) or diketo group (in oteromycin), or in the case of integric acid a carboxylate group thought (by Merck) to functionally replace the tetramic acid like moiety.

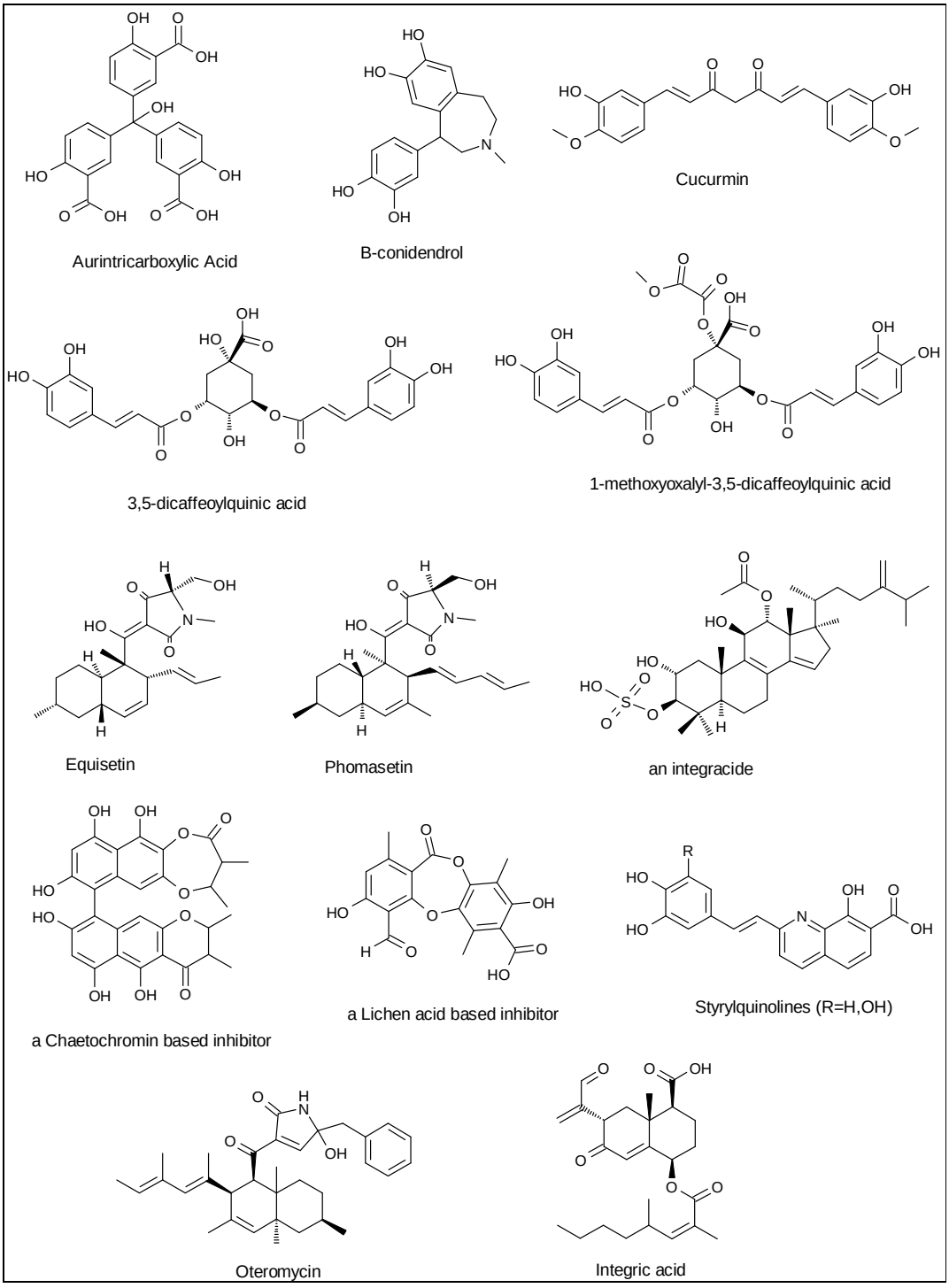

Figure 1.11: Early integrase inhibitors

The most successful class of compounds carrying some of these structural elements is currently referred to as diketo acids (DKA, see **Figure 1.13** for the structure of a generic diketo acid), although the name 'γ-keto α-enol acids' more accurately reflects their biologically active form. Diketo acids were independently discovered by Merck and Shionogi Company. An essential compound developed by Shionogi was 5-CITEP (**Figure 1.12**), a DKA analogue bearing a chloro-substituted indole and a tetrazole as an isosteric replacement for the carboxyl group (compared to the generic DKA structure in **Figure 1.13**). 5-CITEP showed a selective inhibition of the strand-transfer step (IC_{50}: 0.65-3 μM) with a 3'-processing IC_{50} value of 35 μM.[94],[95]. 5-CITEP was the first strand-transfer inhibitor for which a crystal structure of the compound bound to the integrase CCD was elucidated.[94] From the electron density map it was clear that 5-CITEP was positioned in the active site between the catalytic acidic residues D64, D166 and E152. This observation suggested 5-CITEP could be competing with the DNA substrate and in doing so prevented the natural substrate to bind to the active site. 5-CITEP, in complex with the integrase CCD, assumed a planar conformation, indicating the keto-enol form was the biologically active tautomer.[94] It was also noted that 5-CITEP's enolic hydroxy group was in hydrogen-bonding distance from the catalytic triad residue E152. A structurally related compound S-1360 (**Figure 1.12**), developed by Shionogi Company and GlaxoSmithKline, with a furan moiety in place of the indole group, was the first strand-transfer inhibitor to reach clinical trials. [78] This diketo acid bioisostere S-1360 (**Figure 1.12**) inhibits the strand-transfer reaction with an IC_{50} value of 0.02 μM.[30] The EC_{50} value is 0.2 μM and the CC_{50} value is 12 μM (the drug concentration cytotoxic to 50% of the cells used in the *in vitro* assay).[30] After a review of the trials data, development of S-1360 (**Figure 1.12**) was ended because low efficacy emerged due the compound being rapidly cleared from the body after being metabolised and rendered inactive by human liver enzymes known as aldo-keto reductases (carbonyl reducing, NADPH-dependant and cytosolic).[96] S-1360 (**Figure 1.12**) remained useful in experiments investigating mutations responsible for generation of strand-transfer inhibitor resistance.[97] Two more DKA bioisosteres, developed by Merck and Shionogi, showed potent and specific inhibition of the strand-transfer step. They are referred to as L-731,988 and L-708,906 (**Figure 1.12**), and have IC_{50} values for strand-transfer inhibition around 80 nM. Mutants resistant to the latter inhibitors showed mutations clustered around the active site in the integrase CCD.[98] Dependence, for L-731,988 (**Figure 1.12**), of inhibition capacity on target DNA

concentration confirmed the presumed competitive binding to the active site, initially observed in the crystal structure of 5-CITEP in complex with the integrase CCD.[33]

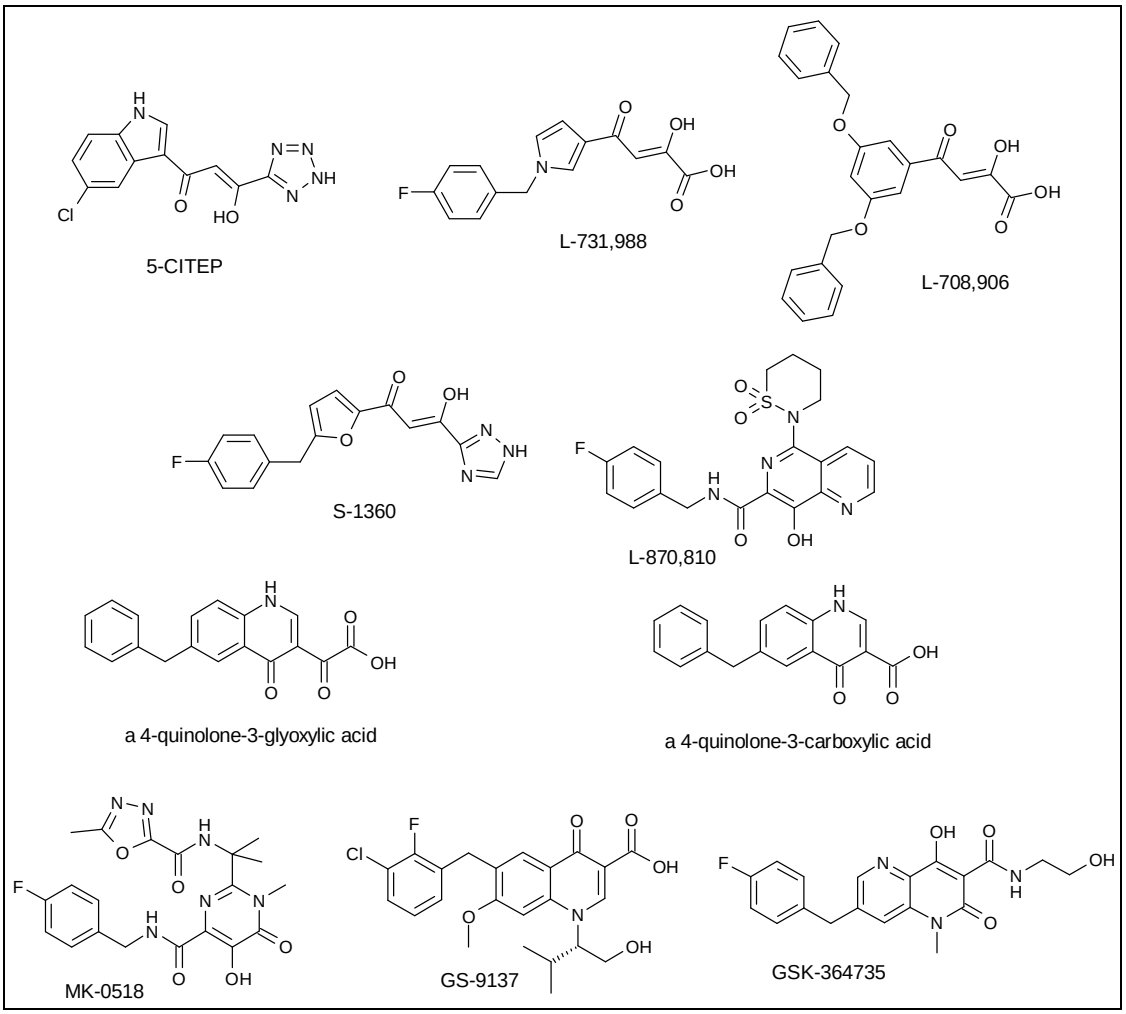

Figure 1.12: Diketoacid-based integrase inhibitors.

Calculations on the latter crystal structure also confirmed the importance of the keto-enol group in the sense that the observed interactions of 5-CITEP were consistent with predictions of how a keto-enol moiety would be positioned when coordinated to the metal ions also presumed to bind the acidic catalytic residues D64, D166 and E152.[99] Structure-activity relationship studies, using wild type HIV, revealed potent strand-transfer inhibition was maintained when replacing the carboxylate (as in the generic DKA structure, **Figure 1.13**) with a tetrazole moiety, but only in the presence of Mn^{2+} (not for the other possible Mg^{2+}cofactor).[100] Presence of an indole (in the hydrophobic moiety of the generic DKA structure) was associated with increased metal

dependency of inhibitory capacity, a condition absent for inhibitors with a substituted phenyl moiety (as in L-708,906, **Figure 1.12**). The SAR studies concluded that regarding inhibitor activity/structure conditions, Mg^{2+} imposes stricter limitations than Mn^{2+}. Continued attempts to improve established inhibitory capacities of DKA-based compounds, by Merck researchers, led to a number of new molecules of which the most potent was L-870,812 (**Figure 1.12**). Compared to the generic DKA structure, in L-870,812 an 8-hydroxy-1,6-naphthyridine moiety replaces both the carboxylate and the α-enol moiety with respectively heterocyclic nitrogen and a phenolic –OH, the γ-ketone is replaced with a benzyl amide and a cyclic sulphonamide on the naphthyridine moiety optimises its oral bioavailability, pharmacokinetic parameters and cardiac safety. The retained coplanarity of the essential structural features confirmed the earlier hypothetical condition for biological activity. [101] [102] L-870,810 (**Figure 1.12**), inhibits integrase activity, *in vitro*, with an IC_{50} of 0.01 μM and gave an EC_{95} of 0.019 μM (inhibition of viral replication) and a CC_{50} >5 μM in a cell culture assay.[30] These assay values indicated a favourable (high) therapeutic index (ratio of toxic drug dose to therapeutic drug dose, CC_{50}/EC_{50}). However, after long term dosing in dogs, an unacceptable level of toxicity was revealed and so further clinical development of L-870,810 was put on hold.[103] In 2006, researchers from Japan Tobacco Company came up with a newly designed scaffold, as present in a 4-quinolone-3-glyoxylic acid (**Figure 1.12**), that respected the coplanarity condition (of γ-keto, α-enol and carboxylic acid in DKAs) presumed essential for strand-transfer inhibition specificity.[104] Surprisingly, it turned out that the 4-quinolone-3-glyoxylic acid scaffold showed no activity, but a 4-quinolone-3-carboxylic acid (**Figure 1.12**) with a coplanar monoketo acid motif did! This was a quite dramatic discovery and provided new insights into the binding properties of these specific strand-transfer inhibitors. Of note, the α-ketone of 4-quinolone-3-glyoxylic acid cannot tautomerise, suggesting this leads to loss of activity regardless of the coplanarity of the involved functionalities.

It can be concluded that so far the DKAs and their bioisosteres have been the most successful compounds in the quest for integrase inhibitors and the (potential) associated inhibition of HIV replication. Currently, one DKA-derived integrase inhibitor is in early clinical trials and two are undergoing advanced clinical trials. They are respectively known as GSK364735, GS-9137 (Elvitegravir) and MK-0518 (**Figure 1.12**), the latter of which has obtained FDA approval in October 2007 and is commercially known as Raltegravir (or Isentress), effectively the first and so far only

integrase inhibitor marketed. MK-0158 (**Figure 1.12**) was developed by Merck and is structurally related to one of its less successful predecessors L-870,810 (**Figure 1.12**). MK-0518 (Raltegravir) (**Figure 1.12**) has an IC_{95} of 33 nM.[105] Further clinical trials to assess different long-term effects are ongoing. GS-9137 (**Figure 1.12**) was developed by Japan Tobacco Company and Gilead Sciences and has the 4-quinolone-3-carboxylic acid scaffold with the monoketo acid motif. GS-9137 (**Figure 1.12**) has an EC_{50} value of 0.9 mM in an acute HIV infection assay. The final inhibitor in clinical trials, GSK364735 (**Figure 1.12**), developed by GlaxoSmithKline and Shionogi inhibits the integrase strand-transfer reaction with an IC_{50} of 9 nM.[106], [107]

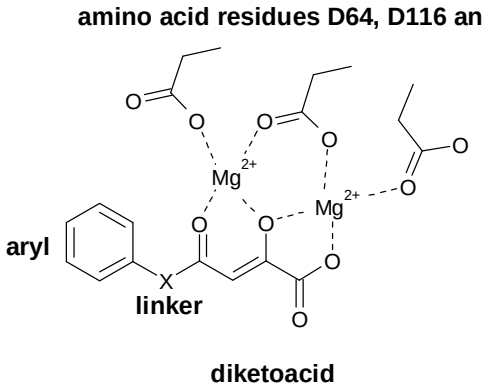

Figure 1.13: Essential pharmacophore elements of the generic diketo acid template involved in coordination to Mg^{2+} in the integrase active site.[20]

Regarding the possible mechanism of DKA-based integrase strand-transfer inhibition, a interesting suggestion was made by Pommier *et al.*[108] It was suggested integrase has two different DNA binding sites, one for the viral (donor) DNA and one for the host (acceptor) DNA. Binding of the viral (donor) DNA and the subsequent 3'-processing reaction induces a conformational change in the PIC due to which the binding site for the acceptor DNA becomes accessible to the latter. At this point, binding of a DKA-based inhibitor at the interface between the catalytic triad and the acceptor DNA, by chelating to the metal cations (Mg^{2+} or Mn^{2+}) in complex with the catalytic acid residues (as in **Figure 1.13**), prevents proper binding of the host DNA and subsequent integration. This hypothetical inhibitory mechanism is referred to as interfacial inhibition.[108]

A different class of integrase inhibitors is referred to as the pyrano-dipyrimidines, the most potent member of which is known as V-165 (**Figure 1.14**). V-165 inhibits viral replication at micromolar concentrations and has a favourable therapeutic index of 14. SAR Studies conclude the sulfhydryl and p-nitro moieties are crucial for activity. Time of addition experiments suggest V-165 (**Figure 1.14**) inhibits integration as well as reverse transcription but V-165's major target was shown to be the 3'-processing reaction.[109] Currently, also a number of older compounds are being re-evaluated, among them the coumarins (**Figure 1.14**) which are a class of hydroxylated aromatics with potent IN-inhibitory activity that do not contain a catechol moiety previously shown to be highly cytotoxic.[110] It was shown in a recent study these coumarin inhibitors inhibit integrase in a non-competitive way by binding to specific α-helices of the integrase CCD, thereby preventing formation of functional integrase multimeric complexes.[110]

Peptides and antibodies have also, for over ten years, been subject to investigations into their integrase inhibitory potential. In 1995, screening of a synthetic peptide combinatorial library led to the discovery of the first peptide (with sequence HCKFWW) to show inhibitory activity, at micromolar concentrations, for both 3'-processing and strand-transfer reactions.[111] More recently, peptides were developed based on the sequence of α-helices at the dimerization interface of the CCD. Two such peptide inhibitors, INH1 (ATGQETAYFLLKLAGKA-$CONH_2$) and INH5 (DQAEHLKTAVQMAVFIHNYKA-$CONH_2$), consisting of part of the sequence of respectively helix α1 and helix α5 (both part of the dimerization interface of CCD) were each shown to prevent formation of functional IN oligomers (IC_{50} values for integrase inhibition were 80 nM and 280 nM for INH5 and INH1 respectively).[112] A study of the inhibitory mechanism pointed out that INH5 interacts with helix α1 and could serve as a lead in the development of new integrase inhibitors. A number of natural peptides also have been shown to have integrase inhibitory activity. Examples are the complestatins [113] (isolated from *Streptomyces* bacterial extracts) and the integramides [114] (isolated from fungal extracts of *Dendrodochium* sp.) (**Figure 1.14**) with good IC_{50} values in the micromolar range but unfortunately cytotoxic in the relevant assays.

A number of IN-specific antibodies (identified after screening a library of monoclonal antibodies raised against purified IN) were shown to have IN-inhibitory capacity.[115] Different IN-inhibiting antibodies were found that separately bound to each of the three

IN domains, NTD, CCD and CTD. For one antibody, mAB17, the epitope was determined as part of the helix-turn-helix motif of the NTD domain of IN.

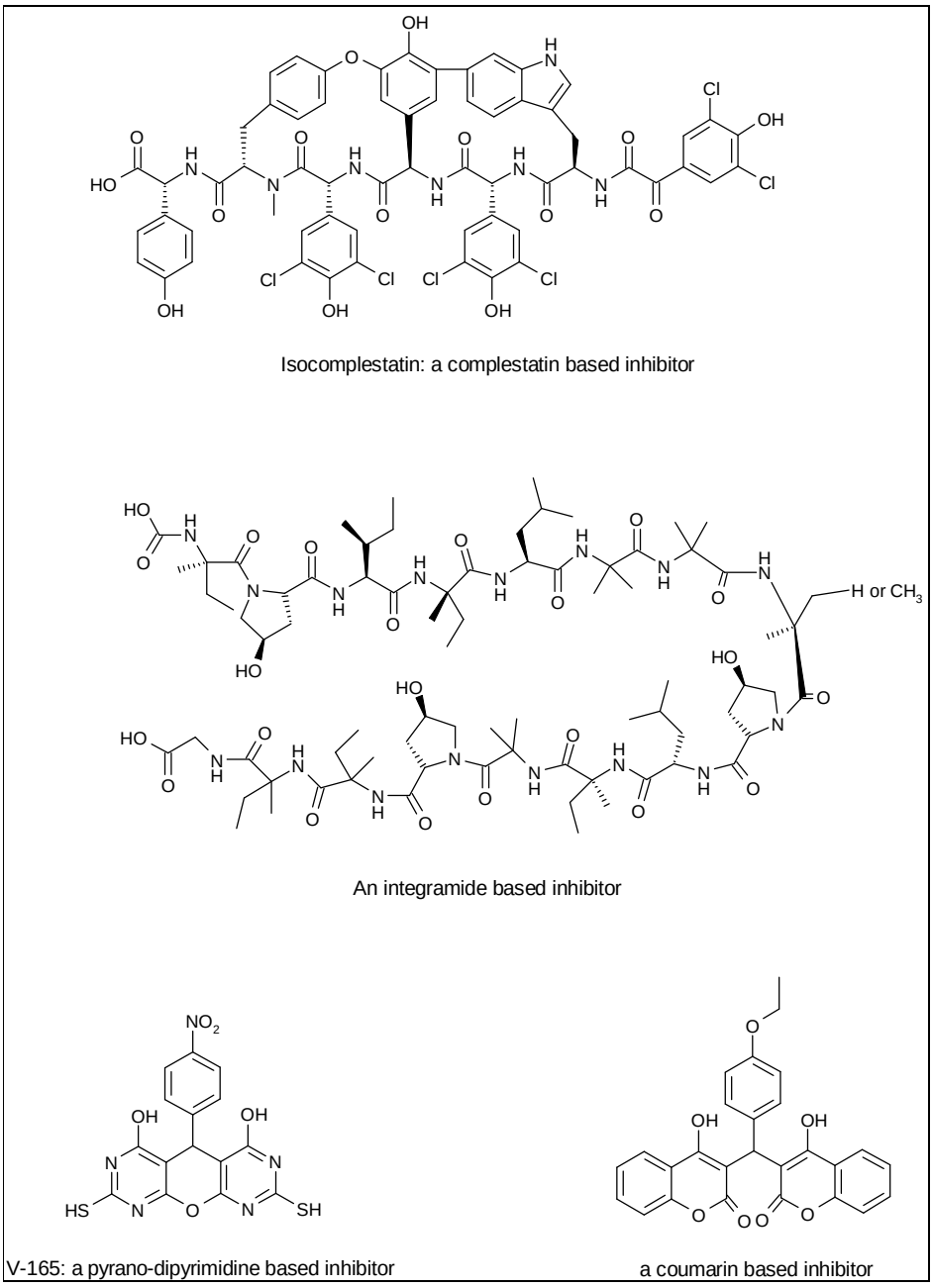

Figure 1.14: Integrase inhibitors

Destabilization of the terminal helix, due to antibody binding, was believed to contribute to the inhibition. Both mAB17 and its Fab fragment inhibited the 3'-processing step, although the Fab fragment was 10 times less potent (IC_{50} of 4.5 and 0.4 µM for mAB17 and its Fab respectively). The epitope region within the conserved

sequence Asp^{25}-Glu^{35} forms a potential target for the development of new small molecule IN inhibitors.

Currently, also a lot of effort is being made to potentially inhibit integration by targeting the numerous viral and cellular cofactors, and their mutual interfaces, involved in the PIC and contributing to the overall integration process.[20],[34]

The most important of these cofactors are:

1) BAF or barrier-to-autointegration factor, believed to stimulate chromosomal integration and preventing autointegration of the viral cDNA. As part of the PIC it bridges and condenses viral cDNA. BAF is a host cellular protein, under normal conditions involved in chromatin organization. It is hypothesized that interference with BAF in HIV infected cells would stimulate autointegration and in doing so inhibit viral replication. One suggested strategic targets for this interference would be the interface of BAF with MA (matrix) protein, with which BAF also associates in the functional PIC. [116], [34]

2) HMGA1 or high mobility group protein A1 is believed to enable a concerted integration (into the host DNA) of the viral cDNA by bridging and condensing the cDNA in the PIC. HMGA1 is a host protein, under normal conditions binding DNA and involved in chromosomal organization. Targeting the HMGA1 interface with DNA could potentially inhibit chromosomal integration due to the lack of a functional PIC. [34]

3) INI1/hSNF5 or integrase interactor 1 protein (the human homologue of yeast SNF5) is also thought to interact with IN in the PIC. INI1/hSNF5 is believed to become part of the PIC after it is exported out of the cell nucleus and/or it is brought into the cell by the virus. Under normal conditions INI1/hSNF5 is a transcriptional activator and part of a chromatin remodelling complex. Targeting the interfaces in which this cofactor is involved in the PIC could potentially lead to inhibition of chromosomal integration and viral replication.[34]

4) LEDGF/p75 or lens epithelium derived growth factor interacts with IN in the PIC. This host nuclear protein is thought to be involved in nuclear import of the PIC and attachment of the latter to the host chromosome.[50] Under normal conditions LEDGF is involved in regulation of gene expression and cellular stress response. Of the four co-factors mentioned above only LEDGF/p75 has been shown to function not only *in vitro* but also *in vivo* as a cellular co-factor for integration.[117] It was recently shown that certain LEDGF/p75 derived peptides inhibit the DNA-binding of IN due to a shift

in the IN oligomerization equilibrium rendering the enzyme incapable of 3'-end processing, the first 'part' of IN catalytic activity. Two peptides, LEDGF/p75 361–370 (WNSLKIDNLDV) and LEDGF/p75 402–411 (WKKIRRFVSQVIM) showed inhibition of HIV-1 replication in cultured cells with EC_{90} values below 2.5 µM.[118]

Recently, four more host (human) proteins have been implicated to function as cellular co-factors to the integration process (they have all been shown to interact with IN) and hence could be contributing to PIC formation and functionality.[34] They are: 1) the Polycomb group embryonic ectoderm development (EED) protein (normally involved in repressing gene translation), 2) Hepatoma-derived growth factor related protein 2 (HRP2), 3) HSP60 (a heat shock protein), and 4) the p300 acetyltransferase (involved in acylation of histone lysine residues, regulating DNA transcription rates). Each of these human protein interfaces with IN, or other PIC components, is being considered a target for inhibition of the integration process.

Additionally, a number of viral proteins are believed to be part of the PIC.[34] They are: 1) Matrix (MA) protein p17 (shown to interact with IN and BAF and to be involved in PIC nuclear import).[119] The obvious targets are the MA/IN and the MA/BAF interface, interference with which could lead to inhibition of PIC nuclear import. 2) Vpr or viral protein R: involved in PIC nuclear import, responsible for apoptosis in proliferating cells and induction of viral replication in non-dividing cells like macrophages, capable of reducing viral mutations by interacting with uracil-N-glycosylase (UNG) which excises mismatched uracil from DNA.[120] Vpr interaction with UNG is one of the proposed targets for potential inhibition of viral replication, 3) NC and RT: the final stages of reverse transcription and the start of the integration process are believed to coincide and the consensus is that HIV-reverse transcriptase, after reverse transcription, remains associated with integrase and nucleocapsid (NC) in the PIC.[27],[121],[122] Nucleocapsid is a nucleic acid chaperone and a viral co-factor of reverse transcriptase, involved in stimulation of integration. A recent study, investigating the IN-inhibitory capacity of HIV-RT, led to the discovery of RT derived peptides capable of IN inhibition.[123] Because full-length HIV-RT showed inhibitory capacity under *in vitro* circumstances without the presence of other cofactors (that are normally part of the PIC) it was suggested this might represent an alternative way to prevent autointegration. This might be the function of RT in the PIC as well, since there is a considerable time-span between PIC formation and actual integration, and all components for autointegration are present in the PIC. Following this discovery a

library of HIV-RT derived peptides were tested for IN-inhibitory activity. The two most potent inhibitors are known as Peptide 4286 (KILEPFRKQNPDIVIYQYMD) and Peptide 4321 (NQIIEQLIKKEKVY), respectively originating from the RT DNA polymerase domain and from the RT ribonuclease H domain. They inhibited 3'-processing with respective EC_{50} values of 4.8 and 6.9 µM, and strand-transfer reactions with respective EC_{50} values of 4.5 and 5 µM.[123] It was concluded for Peptide 4286, based on computer aided molecular docking experiments, IN-inhibition was the result of steric hindrance of the active site of IN.

Research interest into the potential of PIC related cofactors and/or interfaces as new targets towards development of anti-HIV drugs has significantly increased over the last years. Hopefully this effort will lead to the successful development of long anticipated new anti-HIV drugs and in doing so complement the current range of antivirals.

In the next sections aspects of both PNA and acridines, two classes of compounds that, structurally, are part of the potential new integrase inhibitors we intended to develop in this research project, are introduced; i.e. what are they made of, what are their properties and how can they potentially inhibit integrase.

1.5 PNA-acridine conjugates: DNA threading intercalators and potential new integrase inhibitors?

In what follows a new approach is introduced in the development of potential new integrase-inhibiting antivirals. The strategy involved the use of a known DNA intercalator, a 9-aminoacridine-4-carboxamide, substituted with a polyamide nucleic acid or PNA. DNA intercalators and PNA are separately introduced and their current therapeutic values and usages are discussed. Subsequently, it is explained why combining these two classes of compounds, in the form of PNA-acridine conjugates, holds the potential to indirectly inhibit IN catalytic functions by targeting the LTR sequences at the termini of the viral DNA and in doing so obstructing interactions between viral DNA and IN in the PIC.

1.5.1 DNA intercalators: definition, properties and examples.

DNA intercalators are flat, aromatic compounds generally consisting of two or more fused 6-membered rings (heterocycles and/or aryl rings) that bind DNA by insertion

between successive base-pairs. The nature of the DNA-intercalator interaction was clarified by Lerman as a result of X-ray fibre diffraction and hydrodynamic studies of the proflavine-DNA complex (proflavine is a flat, aromatic acridine derivative) (**Figure 1.15**).[130] The X-ray fibre diffraction pattern revealed retention of the regular base-pair stacking in the DNA, perpendicular to the helix axis, but loss of the long range helix regularity. Also, it was found that intercalation increased viscosity and lowered the sedimentation coefficient of the complex.[130] These observations were rationalized by proposing that the planar proflavine molecule (**Figure 1.15**) became inserted between the base-pairs of DNA.[130]

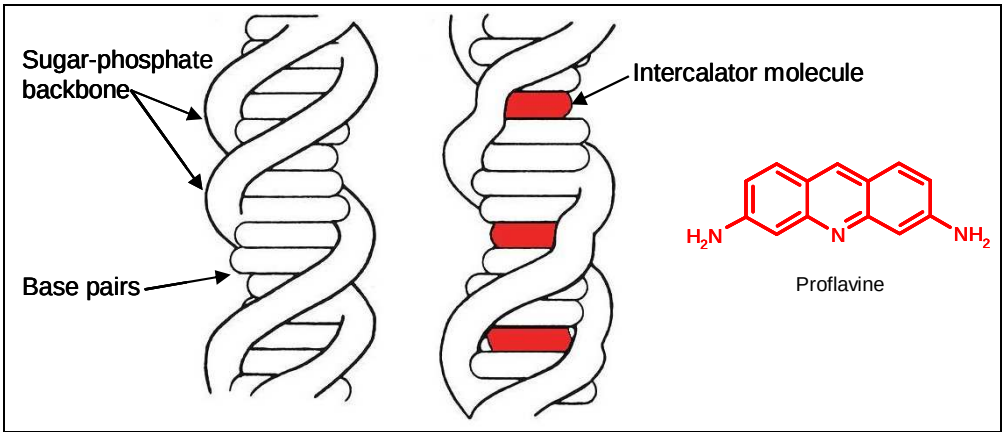

Figure 1.15: model of intercalation of three proflavine (acridine-3,6-diamine) molecules between different successive base-pairs of B-type DNA.

A major structural distortion occuring during intercalation is a local unwinding of the helix at the site of intercalation, ranging from 10 to 26°. Helix unwinding is caused by rotation about torsional bonds in the phosphodiester backbone necessary to accommodate for the intercalators aromatic ring system, the consequence of which is a length increase of approximately 3.4Å (the thickness of an aromatic ring) (see **Figure 1.15** for a model of intercalation) [130] The amount of helix unwinding is very much dependant on the type of intercalator, e.g. proflavine and related acridines typically cause an unwinding of about 17°, whereas ethidium bromide (**Figure 1.16**) unwinds the helix by 26° (Ethidium bromide is commonly used as a fluorescent nucleic acid stain e.g. in gel electrophoresis experiments). Intercalation and the associated DNA-intercalator complex formation, is driven by a combination of electrostatic, entropic, hydrogen-bonding, van der Waals and hydrophobic interactions, and usually is reversible.[124] The strongest driving force undoubtedly is the energetically favourable

transfer of a predominantly nonpolar molecule from an aqueous solution into the predominantly nonpolar environment in between successive base-pairs. This goes hand in hand with the entropically favourable release of H_2O molecules from the intercalator's hydration layer, into the bulk solution. Although the helix conformational changes (unwinding, length increase) are unfavourable, this is countered by a favourable decrease in localized charge density due to the moving apart of charged backbone phosphate groups. Furthermore, due to the polyanionic character of the helix, and the consequent presence of a sheath of counter-cations (e.g. Na^+) to provide neutrality and stability of the helix in aqueous solution, expulsion of one of the latter single cations into the solvent due to binding of a cationic intercalator, is entropically favoured and at its maximum for the largest difference in salt concentration between the condensation sheath (~1 M) and the solvent. Interactions that contribute favourably to the enthalpy part of the free energy (associated with intercalation) are the non-covalent interactions between the intercalator and the helix, like van der Waals interactions, H-bonding, electrostatic and hydrophobic interactions.

For different non-threading acridine intercalators experiments have shown intercalation occurs via different mechanisms.[124] The mechanism for proflavine intercalation, for example, consists of a fast initial bimolecular attachment to the helix surface and one or two more, slower intercalation steps.[125] Experiments on ethidium bromide revealed a distinctly different mechanism in which intercalation occurs in a single step i.e. without externally bound intermediate stages.[126] Investigations into base-sequence specificity of non-threading intercalators like ethidium and proflavine, show a preference for mixed and alternating pyrimidine-purine sequences, and relative exclusion from stretches of A and T (most likely due to the latter's more rigid structure).[127],[128] Furthermore it has been shown, for ethidium, propidium, proflavine and 9-aminoacridine (**Figure 1.15** and **Figure 1.16**), that within the former pyrimidine-purine stretches there is a preference to intercalate between pyrimidine-3',5'-purine successive base-pairs rather than between purine-3',5'-pyrimidine sequences; according to molecular orbital calculations the result of an energetically more favourable unwinding process.[129] It can be generally concluded that the sequence preference of the above mentioned intercalators is not determined by a capacity to recognize a 'long range' base-pair sequence, but by the ability to differentiate between different 'short range' polynucleotide structures.[128]

Since the discovery of DNA intercalators, threading and non-threading, in the early years of the search for chemotherapeutic agents, a large number of planar, aromatic ligands have been shown to bind to DNA in an identical manner, although the mechanistic link between biological activity of compounds and DNA intercalation was not realized from the start.[130] Intercalating agents have the capacity to inhibit the template functions (i.e. DNA and RNA synthesis) of DNA both *in vivo* and *in vitro*, and are poisons of the enzyme topoisomerase, which carry out the essential function of relieving tension built up in the duplex due to the active template functions (hence intercalators are potentially cytotoxic).[130] DNA is thus the natural target for these intercalating compounds with the potential to kill cells, be it prokaryotic (as in bacteria) or eukaryotic (as in certain parasites or as in cancer cells) [124].

Historically important examples of therapeutic intercalators belong to the acridine compound class; proflavine (**Figure 1.15**) and 9-aminoacridine (**Figure 1.16**) were both used in wound asepsis before the era of antibiotics and are currently still used for topical antibacterial purposes, quinacrine (**Figure 1.16**) was used as antihelminthic and both quinacrine and the related chloroquine (**Figure 1.16**) played an important role in malaria treatment. Actinomycin (**Figure 1.16**), the first antibiotic isolated in 1940 by Waksman and Woodruff, is an intercalator and has proven its value in treatment of a particular childhood kidney cancer known as Wilm's tumour. Subsequent research into and development of intercalating antitumour agents delivered more acridine-based compounds with therapeutic value. Important examples are: amsacrine (**Figure 1.16**) (used for treatment of leukaemia), nitracrine (**Figure 1.16**) (used for treatment of mammary and ovarian tumours), and the anthracycline antibiotic adriamycin (**Figure 1.16**) and analogues (used in treatment of a variety of cancers).

Due to additional interactions with DNA, threading intercalators are DNA-intercalating agents that show increased stability of the associated DNA-threading intercalator complex and hence will have a longer residence time at particular DNA sites (with consequent relevance to potential biological activity).[131] Besides the usual π-stacking, extra stabilization of the complex occurs through favourable interactions (a combination of possible ionic, hydrogen-bonding and van der Waals interactions) between the intercalator substituents and DNA major and/or minor groove functionalities [124], which often confers some base-sequence binding preference to the complex, as exemplified (see next section 1.4.2) by nogalamycin and 9-amino-DACA (respectively a natural and a synthetic threading intercalator).

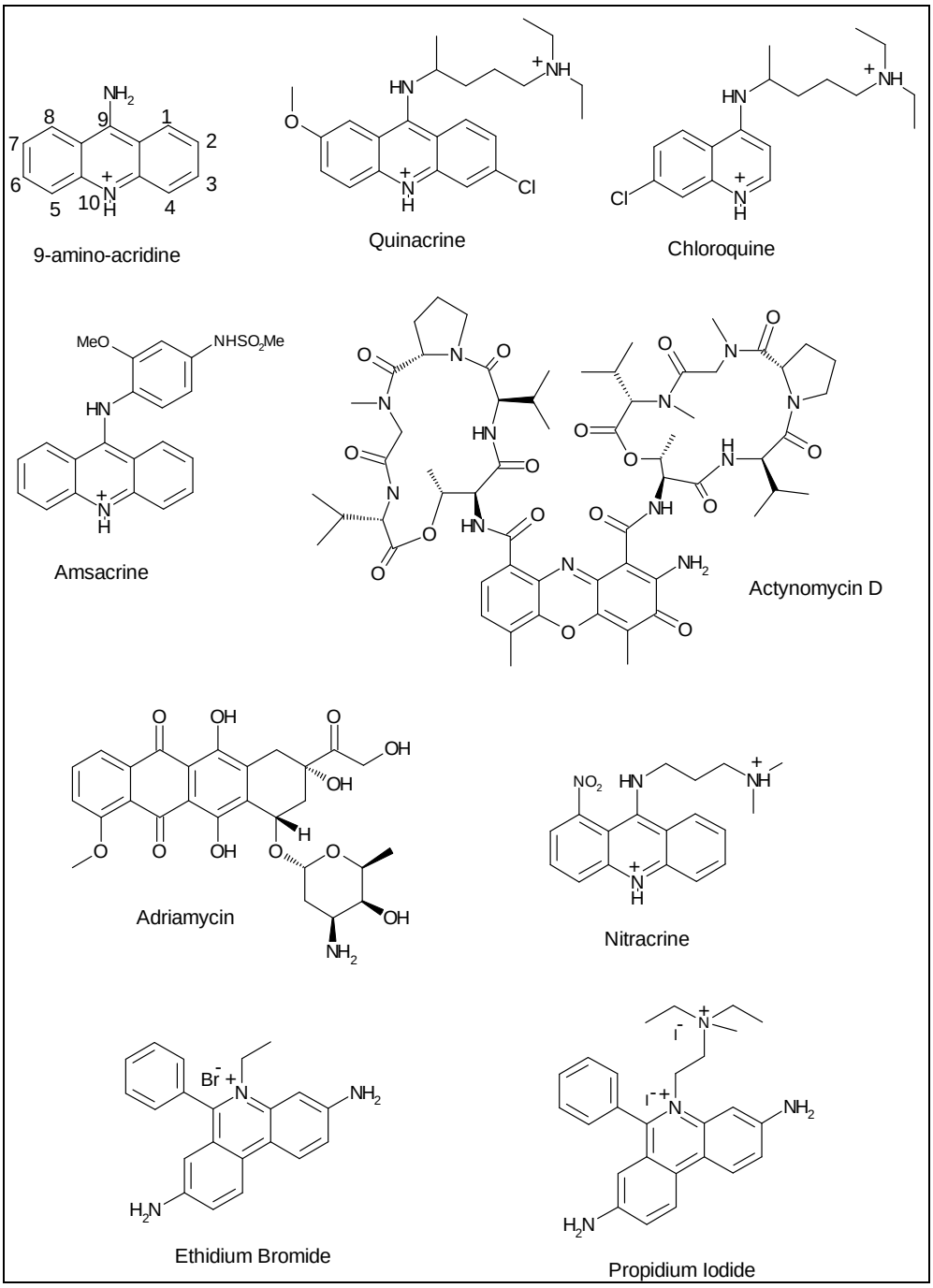

Figure 1.16: Nucleic Acid Intercalators

Studies of intercalators binding kinetics have shown a clear association between longer drug/DNA residence times and cytotoxicity/antitumour activity.[132] Threading intercalation is a binding mode in which the intercalating moiety simultaneously directs substituents into both grooves of a duplex. This requires one of the side-chains to thread through the base-pairs during the complex formation, a process facilitated by

'breathing' of the DNA duplex. The bulkiness of the penetrating substituent slows down the process but will lead to increased post–threading stabilisation of the complex. [132]

1.5.2 Examples of threading intercalators: Nogalamycin and 9-amino-DACA

Synthetic threading intercalators are often based on natural products like nogalamycin (**Figure 1.17**), an anthracycline antibiotic (isolated from extracts of *Streptomyces nogalator* var. *nogalator*) with activity against certain tumours and Gram-positive bacteria.[133] Nogalamycin consist of an aglycone chromophore (rings A, B, C and D) with at each end a bulky sugar substituent: a nogalose sugar moiety (and a methyl ester group) attached to the A ring and a bicyclic amino sugar linked to the D ring (**Figure 1.17**).

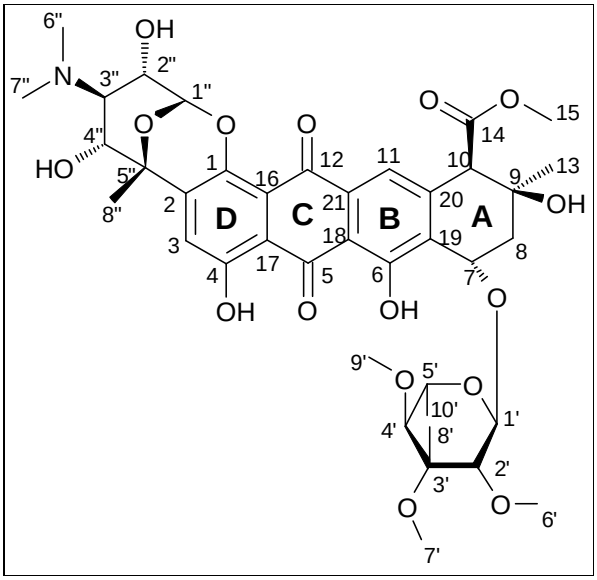

Figure 1.17: Nogalamycin

It was shown that nogalamycin forms a stable intercalation complex in which association and dissociation with/from the helix is a relatively slow process, compared to non-threading intercalators, due to the unusual dumbbell shape of the antibiotic.[134] For the bulky nogalamycin to intercalate the DNA helix, the latter has to transiently open up (breathing), a process for which two different mechanisms were suggested. A first mechanism suggests transient melting of several base-pairs, which would create an opening large enough to accommodate for insertion of the bulky side-chains.[135] In a

second mechanism transient unstacking of base-pairs (without disruption of base-pairing), in combination with extension of the helix and buckling of base-pairs should allow for a large enough opening to facilitate large side-chain moieties to pass between the helix strands.[136] Intercalation occurs preferentially between dinucleotides GpT and TpG in stretches composed of alternating purine-pyrimidine sequences, GpCpA being the most preferred combination.[137] Furthermore, H-NMR experiments also revealed the orientation of nogalamycin in which the aglycon is intercalated, the nogalose sugar moiety directed into the minor groove and the fused bicyclic aminosugar positioned in the major groove of the DNA hexamer $d(GCATGC)_2$.[138]

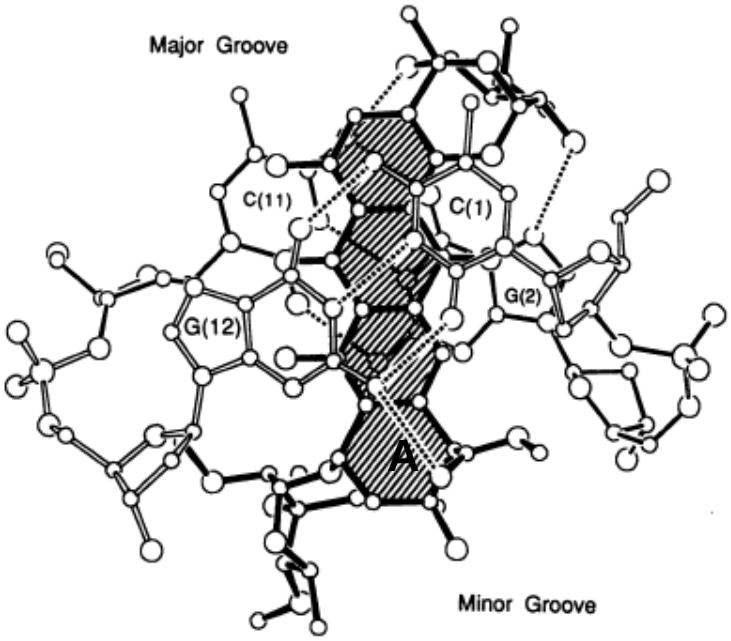

Figure 1.18: Nogalamycin intercalated between the terminal C(1)-G(12) base-pair (drawn with thick hollow bonds) and the lower base-pair G(2)-C(11) (drawn with thin bonds) of a DNA hexamer $d(^{m5}CGTsA^{m5}CG)_2$. (Nogalamycin is drawn with thick solid bonds and is shaded) (Source: Williams *et al.*, **1990**, [136])

The latter experiment also suggests that the long axis of the aglycone is almost perpendicular to the long axis of the adjacent base-pairs, a conclusion that was confirmed in the crystal structure of nogalamycin in complex with the DNA hexamer $d(^{m5}CGTsA^{m5}CG)_2$ (see **Figure 1.18**).[136] From the latter crystal structure the following interaction could be observed: the aglycon rings B, C and D (as in **Figure 1.17**) are stacked with the A ring protruding into the minor groove; in the major groove two base-pair bridging H-bonds are formed between the drug's 2"-OH (donor) and N7 of G(uanosine)2 and between the drug's 4"-OH (acceptor) and N4 of C(ytidine)11

(**Figure 1.18**); also in the major groove there is an indirect H-bond (via a H_2O molecule) interaction between the charged N3" of nogalamycin and N6 of A(denosine)10 (not shown in **Figure 1.18**); in the minor groove the carbonyl oxygen of the drug's A ring accepts an H-bond from N2 of G(uanosine)12 (**Figure 1.18**); also in the minor groove the nogalose sugar O4' (see **Figure 1.17**) indirectly (via a H_2O molecule) is H-bonded to the O3' of T(hymidine)3 and the sugar ring C7' shows van der Waals contact with the O4' of ribose of A(denosine)10 (not shown in **Figure 1.18**). In solution, it was shown interaction of the nogalose ring with the helix minor groove is weak enough for the sugar ring to flip between several isoenergetic conformational states. [136]

The acridine derivative *N*-[2-(dimethylamino)ethyl]-9-aminoacridine-4-carboxamide, or 9-amino-DACA (**Figure 1.19**), is a synthetic threading intercalator and an established anti-cancer drug (antileukaemic) that preferentially intercalates at GC-rich areas.[139] The 9-amino-DACA carboxamide side-chain threads through the DNA-duplex, entering from the minor groove, after which the chromophore settles between the base-pairs and the threader gets lodged in the major groove, stabilized by hydrogen bonding involving the threader's NH-groups and major groove functionalities.[140]

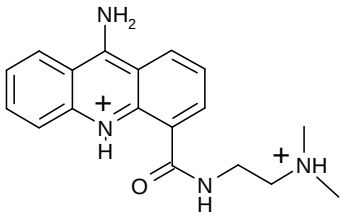

Figure 1.19: 9-amino-DACA

In the crystal structure of the related 9-amino-6-bromo-DACA with the DNA hexamer d(CG(5-BrU)ACG)$_2$ two molecules of 9-amino-6-bromo-DACA each intercalate between separate d(CG)$_2$ base-pairs.[141] No distortion of the base-pair hydrogen bonds was observed. The long axis of the drug is aligned with the long axis of the base-pairs and there is an optimal overlap/stacking interaction between the side-chain-bearing ring of the drug and the guanine and cytosine six-membered ring on either site of the intercalator (**Figure 1.20**). Each intercalated molecule causes a helix unwinding of 12°.

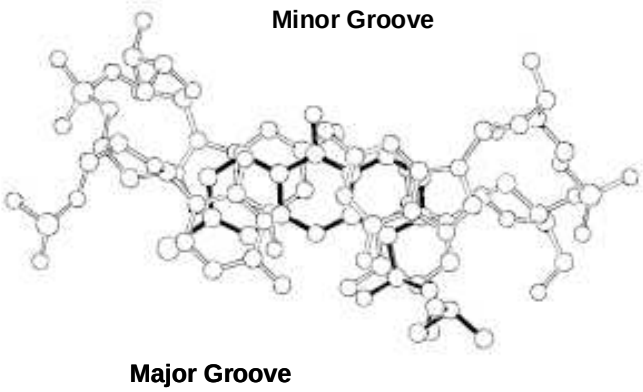

Figure 1.20: Overlap between 9-amino-6-bromo-DACA and the adjacent GC base-pairs of the DNA hexamer d(CG(5-BrU)ACG)$_2$. (Source: Todd, A.K. *et al.*, **1999**) [141]

The intercalator-helix interactions observed in the crystal structure of 9-amino-6-bromo-DACA in complex with the DNA hexamer d(CG(5-BrU)ACG)$_2$ revealed a so-called 'DNA-induced' side-chain orientation established through a conserved bound H_2O molecule and a negative charge (from a backbone phosphate group) at the site of intercalation (**Figure 1.21**), facilitated by the near coplanarity of the carboxamide moiety with the acridine plane.[141]

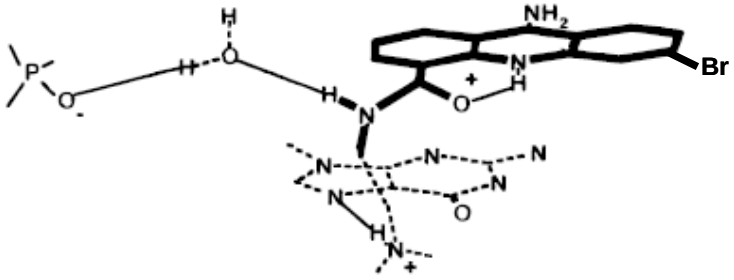

Figure 1.21: The major interactions of 9-amino-6-bromo-DACA in its complex with a DNA hexamer d(CG(5-BrU)ACG)$_2$. (Source: Todd, A.K. *et al.*, **1999**) [141]

One should acknowledge the importance of the 9-amino functionality in stabilizing this 'DNA-induced' anchoring of the compound's carboxamide side-chain. The 9-amino group significantly increases the basicity of the ring N10 (pKa 8.3 compared to pKa 3.5 in the 9-deamino analogue), causing the latter to be protonated which in turn allows formation of the N(10)H hydrogen bond to the carboxamide oxygen and the

involvement of the conserved water molecule in bridging the carboxamide NH to a backbone phosphate group. Of note, comparative DNA binding studies revealed a binding affinity, for the 9-amino compound, six times greater than for the 9-deamino analogue.[142] A single hydrogen bond is also formed between the -$NH(CH_3)_2^+$ group of the side-chain and the N7 of one of the guanine bases of the intercalation site (see **Figure 1.21**). The two side-chain nitrogen atoms are held in a *gauche* conformation. The delocalized charge on the acridine's (protonated) N10 is further spread out over the carboxamide moiety via a hydrogen bond with the latter's carbonyl oxygen (acceptor). Subsequently, the crystal structure of 9-amino-DACA in complex with the DNA hexamer $d(CGTACG)_2$ was solved at a slightly lower resolution of 1.6Å (compared to 1.3 Å) and revealed an almost identical conformation/interaction of the intercalator (compared to the above described crystal structure) with the DNA hexamer.[143] The only significant difference was the presence of a three-centred H-bonding between the -$NH(CH_3)_2^+$ group of the side-chain and the N7 and O6 of the guanine base of the intercalation site (instead of the single H-bond to N7). The described interactions with functionalities in the helix major groove hold the intercalator's side-chain in its depicted unique conformation which is believed to contribute to inhibition of the topoisomerase enzyme by 9-NH_2-DACA by effectively altering the local electrostatic potential and blocking the helix major groove. Structure-activity relationship studies show that both the nature and the position of the substituents (including the 4-carboxamide moiety peri to the ring nitrogen) are critical for 9-NH_2-DACA's potent biological (topoisomerase inhibiting) activity and kinetic stability of the DNA complex.[141]

1.5.3 Polyamide Nucleic Acids (PNA): definition, properties and examples

Polyamide nucleic acids (PNA) (**Figure 1.22**) are nucleic acid analogues in which the sugar-phosphate backbone of the natural nucleic acid has been replaced by a synthetic backbone composed of *N*-(2-aminoethyl)glycine subunits.[144] PNA are achiral and uncharged and were developed in the search for oligonucleotide-based therapeutics exhibiting improved properties, relative to natural phosphodiester oligonucleotides, such as increased nucleic acid-binding affinities, biological stabilities and cellular uptake.[145] PNA is not degraded inside a living cell due to its chemical stability and resistance to hydrolytic (enzymatic) cleavage.[146] PNA is capable of sequence-

specific recognition of single-stranded DNA and RNA targets and the resulting hybrid complexes exhibit extraordinary thermal stability, a property attributed to the lack of electrostatic repulsion between the neutral PNA strand and the anionic nucleic acid backbone.[144]

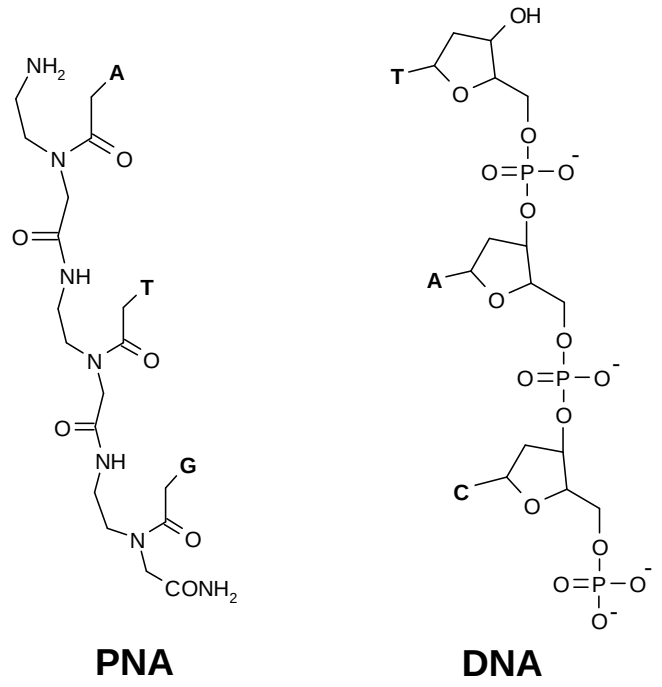

Figure 1.22: Illustration of PNA and DNA fragments (in antiparallel orientation i.e. the PNA N-terminus and C-terminus corresponds with the respective oligonucleotide 5'-terminus and 3'-terminus)

PNA obey the Watson-Crick base-pairing when hybridising with a single complementary nucleic acid strand and can do so in parallel and antiparallel orientation.[146] The resulting PNA:nucleic acid complexes, when in antiparallel orientation, compared to the corresponding DNA-RNA and DNA-DNA duplexes, show increased (hetero)duplex melting temperatures, more so for PNA-RNA (melting temperature T_m increases with ~1.5 K/base) than for PNA-DNA complexes (T_m increases with ~1.0 K/base).[146] For example, T_m measurement experiments involving the PNA oligomer H-TGTACGTCACAACTA-NH_2 gave the following results: the DNA-PNA duplex has a T_m of 70°C for the antiparallel orientation and a T_m of 56°C for the parallel orientation, the corresponding 15-mer DNA-DNA duplex has a T_m of 53°C.[144] Hence, the stability of the (antiparallel) ds-DNA is almost equal to that of the parallel PNA-DNA complex, the latter however forms much slower (several hours) than the much stabler antiparallel PNA-DNA hybrid, which can form in tens of

seconds.[147] Base mismatches destabilise PNA-DNA heteroduplexes to a larger extent than for the corresponding DNA duplexes; in a DNA-DNA duplex a single mismatched base lowers the T_m with 11°C on average while for a DNA-PNA duplex the same mismatch would lower T_m by an average of 15°C.[144]

The above findings reflect the increased stability and sequence-specificity of the PNA heteroduplexes in comparison to the nucleic acid duplexes. PNA are also capable of hybridising with their complementary nucleic acid strands at temperatures and ionic strengths where it is impossible for DNA duplexes to form.[148]. This was clearly illustrated by Tomac *et al.* in an experiment showing a significant increase of T_m for a DNA-DNA hybrid (> 20 K for a 10-mer) when increasing NaCl concentration from 0.01 to 0.5 M.[149] The same salt concentration increase caused the T_m to decrease by 8 K for the corresponding PNA-DNA hybrid, which thereby acquired approximately the same stability as the ds-DNA at 0.5 M NaCl. Again, the PNA neutral backbone is responsible for the difference in heteroduplex T_m dependence of salt concentration, compared to the ds-DNA. Increased counter-ion association for DNA-DNA formation and counter-ion displacement for DNA-PNA formation explain the observed T_m differences. Interestingly, the latter differences can be exploited in PNA-based probing experiments for particular nucleic acid sequences as ionic strength manipulation can eliminate competition of complementary nucleic acid strands or melt undesired secondary structures.[150] In PNA-nucleic acid duplexes the DNA strand closely resembles a B-form structure while RNA conformation is much closer to the A-form, particularly regarding the sugar pucker, which is C3'-endo compared to the B-form C2'-endo sugar pucker.[144]

A number of specific molecular complexes have been observed when certain PNAs bind to single-stranded or double-stranded RNA and DNA targets. Generally, homopyrimidine PNAs form very stable $(PNA)_2$-DNA triplexes (T_m > 70°C) with complementary DNA stretches with stability depending on the PNA length and increasing by about 10°C per base-pair.[144] This was demonstrated with PNA-T_8, which by binding to a single poly(dA) strand forms a right-handed $(PNA)_2$-DNA triplex in which one PNA strand engages in Watson-Crick bonding with the DNA strand (in anti-parallel orientation) while the second PNA strand binds parallel to the DNA strand via Hoogsteen H-bonds (**Figure 1.23**).

For C-rich homopyrimidine PNA and GC-rich DNA duplexes only, a wide helical PNA-$(DNA)_2$ triplex has been reported in which the PNA nucleobases engage in Hoogsteen-hydrogen bonding to the DNA purines.[144] Curiously, this type of triplex (Hoogsteen interaction of ss-PNA bases with ds-DNA) was the type originally intended/expected in the development of PNA (as alternative oligonucleotide-based therapeutics) but is much less stable than the $(PNA)_2$-DNA triplexes and is pH-dependent (optimum between pH 5.0 and 5.5) due to protonation of PNA cytosine (allowing for the second Hoogsteen hydrogen bond involved in the $C.G*C^+$ base triplet, the other base triplet being T.A*T.) (**Figure 1.23**)

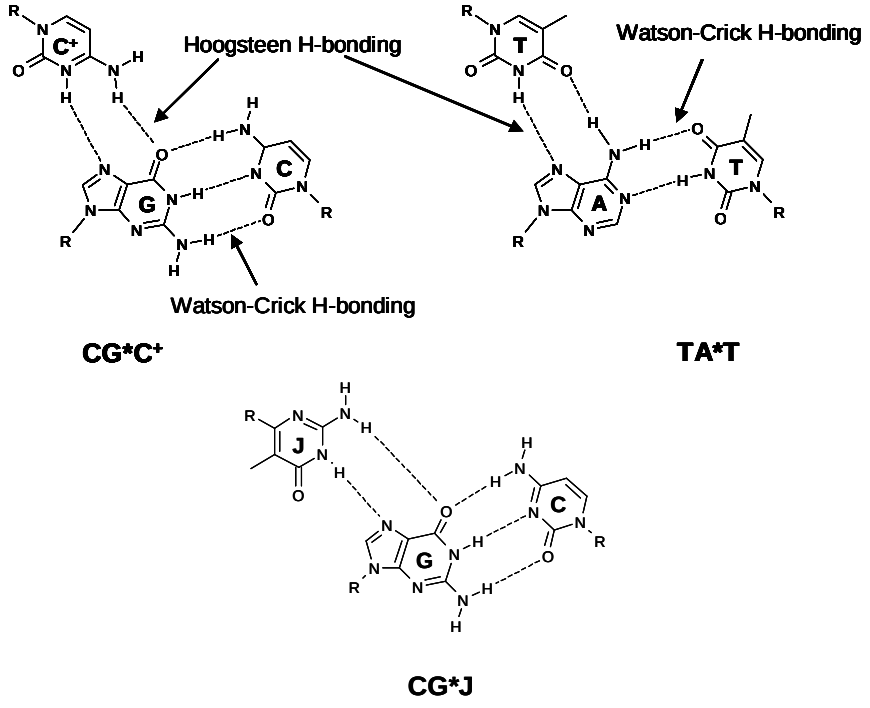

Figure 1.23: CG*C, TA*T and CG*J nucleobase triplets (as in $(PNA)_2$-DNA, $(DNA)_2$-PNA or bis-PNA-DNA triplexes. (* = Hoogsteen H-bonds, J = pseudo-isocytosine)

$(PNA)_2$-RNA triplexes have been observed in biological experiments in which they were found capable of inhibiting CAT-mRNA (Chloramphenicol acetyl transferase mRNA) translation.[144] $(PNA)_2$-RNA triplexes have stabilities comparable to their DNA counterparts [151]

A stable triplex strand-invasion complex has been observed for homopyrimidine PNA binding to a homopurine ds-DNA target.[144] During strand invasion an initial single PNA strand recognizes and binds its complementary sequence in the homopurine DNA strand. Simultaneously the DNA homopyrimidine sequence is displaced and remains a

single-stranded 'looped out' structure (P-loop) while the second PNA strand binds to the PNA-DNA duplex to form the stable PNA-DNA-PNA triplex. (**Figure 1.24**)

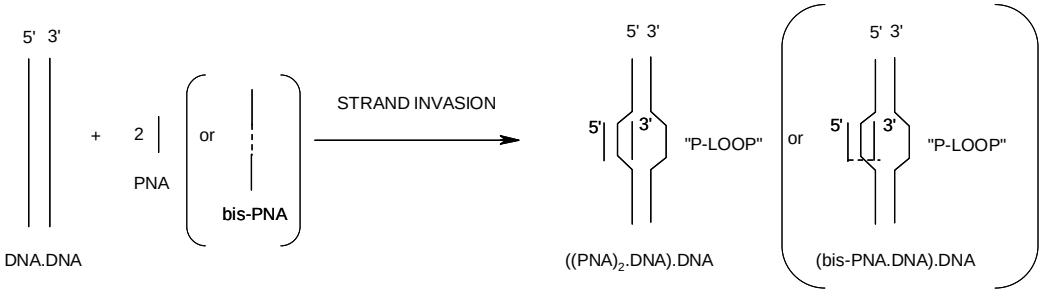

Figure 1.24: PNA and bis-PNA strand invasion leading to PNA_2-DNA and bis-PNA-DNA triplex formation

Strand invasion is favoured by the presence of A-rich stretches and by low ionic strengths (< 50 mM NaCl). The process is also very sequence-specific, with one-base mismatch in a 10-mer PNA (at 20°C) leading to a 100-fold decrease in DNA binding affinity and a two-base mismatch leading to almost complete loss of binding affinity.[152]

An even greater triplex stability (T_m-values of ~100°C for a 10-mer) can be achieved by so-called bis-PNAs, in which the Watson-Crick PNA strand is linked to the Hoogsteen PNA strand via ethylene glycol type linkers.[153] Moreover, bis-PNA-DNA triplexes show a strongly decreased hysteresis in their T_m-curve relative to the unlinked PNA-DNA-PNA triplex (from > 20°C to ~2°C). In current applications, when targeting small homopurine stretches, the preferred constructs are bis-PNAs in which cytosine bases are replaced with pseudo-isocytosine (aka J-bases) in the Hoogsteen strand in order to make the (intended) triplex pH independent (**Figure 1.23**).

Right-handed $(PNA)_2$-DNA triple helices were first observed/discovered through circular and linear dichroism spectroscopic experiments.[154] $(PNA)_2$-DNA crystal structures showed however significant differences with their naturally occurring (albeit seldom) DNA triplex counterparts, the most striking difference being the single strand DNA conformation resembling the A-form (and not its native B-form as in the Watson-Crick duplex part of a DNA triplex or in a PNA-DNA duplex).[155] For reasons believed to be associated with greater torsional freedom of PNAs compared to DNA, PNA rarely forms B-like structures.[144] Because of the greater flexibility of PNAs it

is believed to conformationally adapt to its more rigid complementary nucleic acid structures but in PNA-PNA duplexes it takes on its own preferred conformation referred to as P-form, characterized by a very large pitch (18 base-pairs per turn) and a large diameter of 28 Å (in comparison, B-DNA has 10 base-pairs per turn and a diameter of ~20 Å) [156]

A second type of strand-invasion complex has been reported only for very purine-rich PNA, which are capable of invading a ds-DNA and forming an extremely stable (single) duplex invasion complex (**Figure 1.25a**).[157]
The final type of strand invasion referred to as double duplex invasion (**Figure 1.25a**) involves so-called pseudocomplementary PNA. The latter comprises two pseudocomplementary PNA strands containing the non-standard nucleobases diaminopurine and thiouracil (replacing respectively adenine and thymine), forming virtual base-pairs which are destabilised due to steric hindrance (and hence prevent formation of undesired PNA-PNA duplexes) but are capable of recognizing their AG or GC counterparts in the ds-DNA (**Figure 1.25b**).

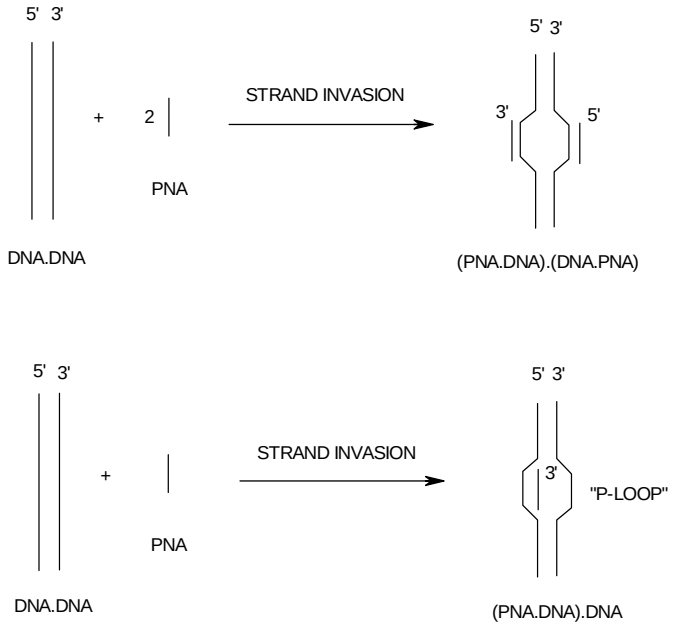

Figure 1.25a: ds-DNA + ss-PNA strand-invasion double duplex (top) and single duplex formation (bottom);

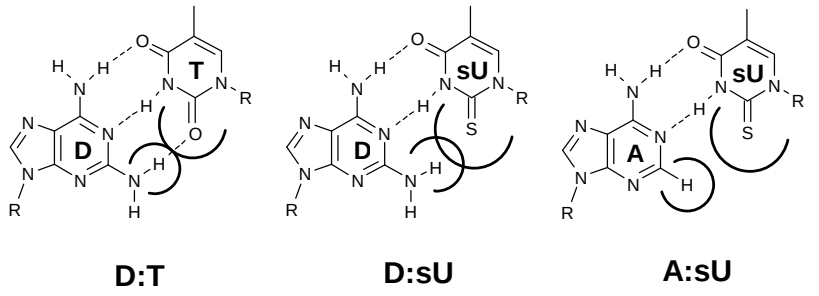

Figure 1.25b: Watson-Crick H-bonding (**:**) in a strand-invasion double duplex (**D:T** and **A:sU**) involving non-standard nucleobases 2,6-diaminopurine (**D**) and thiouracil (**sU**) and the sterically hindered unstable (virtual) base-pair **D:sU** in pseudocomplementary PNA.

Experiments by Lohse *et al*. [158] showed successful and complementary double duplex binding, to the target ds-DNA, of pseudo complementary PNA decamers (GTAGATCACT/AGTGATCTAC) in which adenine and thymine were respectively replaced by non-standard nucleobase 2,6-diaminopurine (D) and 2-thiouracil (sU). It was concluded from T_m measurements on 10-mer PNA that a minimum of 40% AT content in the DNA target was required for a stable double duplex formation to occur. Without the restriction the Hoogsteen homopyrimidine motif imposed (cf. homopyrimidine-based strand-invasion triplex) this means more than 83% of all possible ds-DNA 10-mer sequences can potentially be targeted.[158]

Hence, the lack of sufficient binding free energy of mixed-sequence PNA (containing the standard nucleobases (A,T,G,C) to invade B-DNA can be partially overcome by using non-standard nucleobases.[159] Currently more research is ongoing into how any mixed purine-pyrimidine sequence in ds-DNA could be a target for PNA. An interesting approach dealing with this problem was reported on by Rapireddy *et al*. They constructed so-called conformational preorganized helical dodecameric chiral γ-PNA (**Figure 1.26**) capable of strand-invasion of mixed-sequence B-DNA (via Watson-Crick base-pairing) and showing strong sequence-specificity (i.e. no strand invasion was observed for single base mismatched target ds-DNA).[144] γ-PNA differs from PNA in that it contained chiral (*R*)-*N*-(2-aminopropyl)glycine subunits instead of the usual achiral *N*-(2-aminoethyl)glycine subunits and it (γ-PNA) pre-organises itself into a right-handed helical structure, as was shown by circular dichroism spectra of the dodecameric γ-PNA.[160] Compared to the randomly folded PNA structure for which complex formation with ds-DNA requires an entropy penalized structural

reorganization, the secondary structure of γ-PNA was shown to have improved ds-DNA invasion kinetics and thermodynamics.[161]**,** [162] However, although thermal stability of mixed sequence (dodecameric) (γ)-PNA-DNA hybrids was significantly higher for γ-PNA than for PNA (T_m: 90°C vs. 59°C), invasion of ds-DNA only occurred with γ-PNA dodecamers bearing an acridine moiety linked to the L-lysine side-chain on the C-terminal unit (**Figure 1.26**).[144] This clearly emphasises the importance of the acridine intercalating moiety in stabilising the strand-invasion complex presumably by preventing PNA-DNA end fraying, a conclusion already suggested earlier, by Bentin and Nielsen [163], for acridine-bearing homopyrimidines.[159] Acridine can be even more beneficial as part of PNA-conjugate, as exemplified by the effect on characteristic poor cell-delivery properties of PNAs. The latter has been a drawback associated with PNAs since their early development.[146]

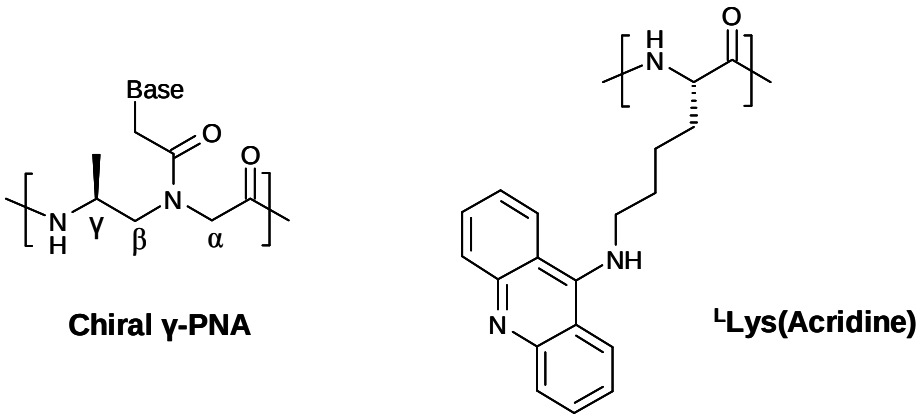

Figure 1.26: Chiral γ-PNA (left) and its link to acridine in the dodecameric PNA-acridine H-^{L}Lys-GACCACAGAT-^{L}Lys(Acr)-^{L}Lys-NH_2 (right) (as reported by Rapireddy *et al.*).[159]

It is well known that high molecular mass compounds (like PNA can be) can pose problems regarding their passage through cell membranes. This problem may be overcome by conjugating PNA to suitable ligand molecules that could enhance cellular uptake. Recent research again has shown the significance of acridine, this time to address cell-delivery problems. *Ex-vivo* experiments showed cationic liposome-mediated cellular delivery (cytoplasm as well as nucleus) of PNA oligomers was significantly improved by attachment of lipophilic poly (hetero) aromatic compounds, acridine in particular (see **Figure 1.27** for the applied linker between the acridine and

the PNA).[164] Other strategies to improve cellular delivery include attachment of short peptide sequences, oligonucleotide sequences, antibodies or steroids.[165],[166]

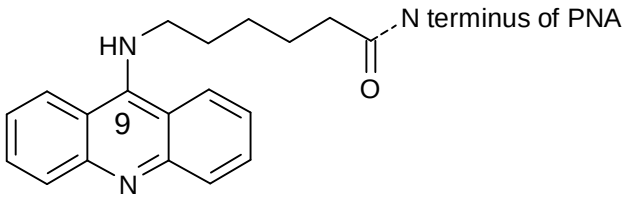

Figure 1.27: 9-aminoacridine attached to a PNA via an aliphatic linker.

An additional limitation with PNAs is that, as they are charge-neutral, they exhibit low water solubility.[146] However, this may be resolved by slight backbone modifications (e.g. introduction of positively charged lysine residues), as exemplified by the earlier mentioned dodecameric γ-PNA developed by Rapireddy *et al.* (**Figure 1.26**)

In vitro and ex vivo studies using PNA oligomers have demonstrated that they have the capacity, by means of their antisense and antigene properties, to interfere with replication, transcription and translation. This is due to the fact that PNA-nucleic acid complexes interfere with or block the enzyme/protein-nucleic acid interactions necessary for the above template-based functions to proceed.[146] In the light of our own project this is an interesting feature with respect to PIC formation in HIV's life-cycle, as PNA-nucleic acid interaction could potentially interfere with this process essential for HIV replication. Although constant progress is being made, the main problem in the successful development of PNA-based therapeutics remains their poor cell-delivery properties. More successful are the practical PNA applications in molecular biology, diagnosis and detection or their use as biosensors for nucleic acids. One example from molecular biology is its use as an artificial restriction system. In this application two (strand-invading) PNA oligomers targeting two adjacent sequences on ds-DNA opposite strands will generate two single displaced strands, which can then subsequently be cleaved by the single-strand-specific nuclease S1.[167] The latter nuclease together with the PNA oligomers hence constitutes a restriction system in which the recognition sequence is determined by the PNA sequences employed. Another example, illustrating the use of PNA as a detection tool, concerns a fluorescent *in situ* hybridisation (FISH) experiment in which a fluorescein-labeled PNA probe

enabled quantitative analysis of vertebrate telomere (something that was not possible quantitatively with oligonucleotides due to inefficient hybridization).[168] The latter PNA-FISH application, established by Lansdorp *et al.*, subsequently resulted in the use of telomeric PNA-probes for *in situ* studies of cancer and ageing. Micro arrays making use of PNA probes instead of DNA probes are an example of its application as nucleic acid biosensors. In the latter application PNA have shown improved selectivity, sensitivity and stability compared to their DNA counterparts.[150]

Generally PNA are considered valuable chemical tools in various fields of biology. PNA remain strong potential candidates in the search for new (alternative) oligonucleotide-based antisense and antigene therapeutics, the realisation of which will be the fruit of successful collaborations at the chemistry/biology interface.

Both the DNA-binding properties of PNA and the intercalating 9-amino-DACA and their capacity to inhibit DNA template functions were the main inspiration to our research project. In it we sought to develop a new potential inhibitor of HIV-integrase by combining (conjugating) the acridine intercalator properties with the characteristics of polyamide nucleic acids (or PNA). The following sections discuss the significance of 9-aminoacridine conjugates in the life sciences and the general synthetic strategies towards them. Subsequently the potential of our novel PNA-(9-amino)-acridine conjugates as HIV-integrase inhibitors and our efforts towards their synthesis will be discussed.

1.5.4 9-Aminoacridine conjugates: significance in the Life Sciences

9-aminoacridines have been of enormous significance in treatment of several diseases since the early 20th century (e.g. quinacrine and amsacrine, used for treatment of respectively malaria and leukaemia, see earlier subsection 1.5.1).

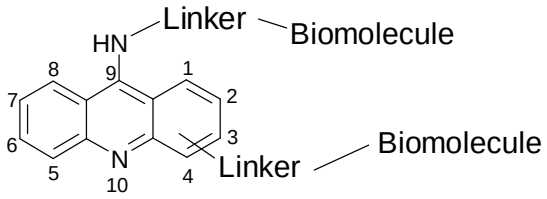

Figure 1.28: general structure of a 9-aminoacridine conjugate

Structure-activity relationship studies of 9-aminoacridines have pinpointed the 9-amino substitution as crucial to its biological activity.[169] Not surprisingly 9-aminoacridines have been conjugated to numerous biomolecules in order to generate agents with altered/improved properties in terms of activity, bioavailability and applicability.[170] A general representation of the 9-aminoacridine conjugates is depicted in **Figure 1.28**.

1.5.5 9-Aminoacridine conjugates: general synthetic strategies and some specific applications

Mid 20th century, the synthesis of 9-aminoacridine was described, starting from the non-substituted acridine, under Chichibabin reaction conditions (amination of pyridine).[171] (see **Scheme 1.1**)

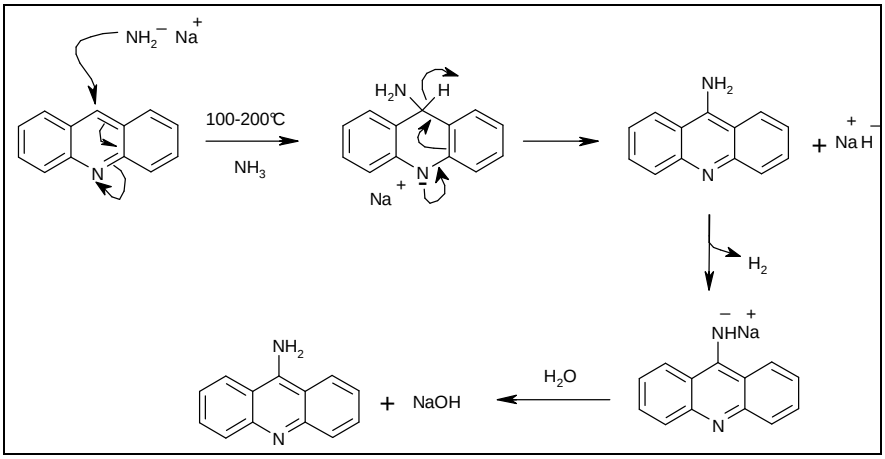

Scheme 1.1: Synthesis of 9-aminoacridine under Chichibabin reaction conditions

Reaction however takes place in liquid NH_3 and these are harsh conditions for numerous functional groups. When other ring substitutions, besides the 9 amino group, are intended, their introduction (or an anchor for them) preferentially occurs before establishing the 3-ring acridine system. One way of accomplishing this is by using substituted N-phenylanthranilic acids and then generating the acridine system by subsequent ring closure via aromatic electrophilic substitution. Depending on reaction conditions, this leads to either substituted 9-chloroacridines, primed in the 9-position for further substitution, or to 9-acridones which require further activation (towards substitution in the 9-position)(see **Scheme 1.2** below).[170] Ring closure can be established with sulphuric acid [172] but, in the presence of acid-labile groups, the

tetraethyl tetrametaphosphate (in chloroform) is the preferred dehydrating agent.[173] Heating the (R,R'-substituted) N-phenylanthranilic acid in phosphorus oxychloride yields the labile 9-chloroacridine derivative [174] which can/should be used directly in a subsequent 9-substitution step.

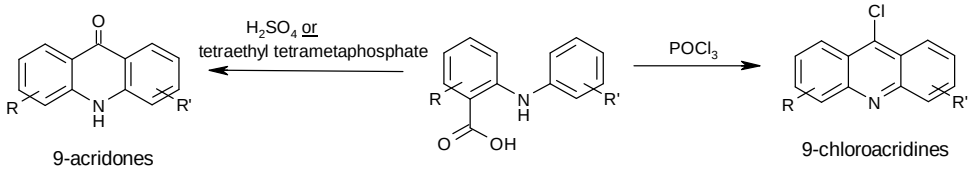

Scheme 1.2: acridine-generating ring-closure reactions of (R,R'-substituted) N-phenylanthranilic acids.

Two commonly used strategies in establishing the 9-amino substituent, using either the 9-acridones or the 9-chloroacridines, are represented in **Scheme 1.3** below

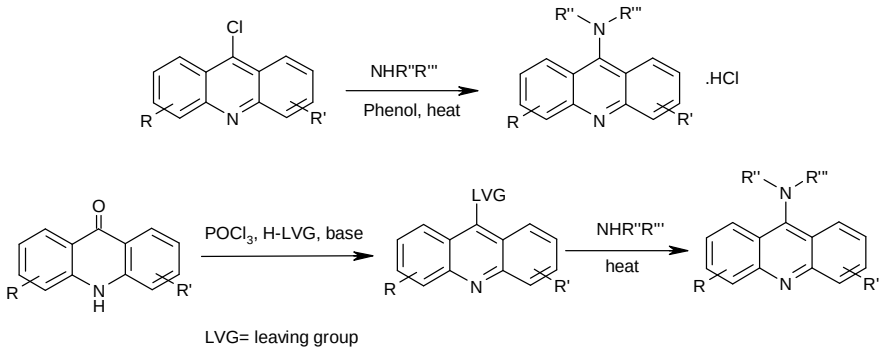

Scheme 1.3: common routes to establishing 9-aminoacridines

The top reaction in **Scheme 1.3** was first described by Dupre and Robinson.[175] It is a nucleophilic substitution of the 9-chloro substituent by the free amine and it is catalysed by phenol (via the reactive 9-phenoxyacridine intermediate).[174] However, other alcohols can be used as catalyst as well, e.g. methanol can be used at lower reaction temperatures, and in some cases gives a better yield and less by-products compared to phenol.[176] The bottom reaction in **Scheme 1.3** involves *in situ* $POCl_3$ activation, which puts a reactive leaving group (LVG) in the 9 position, e.g. 9-imidazol-1-yl [177] or 9-(1H-1,2,4-triazol-1-yl) [180] which subsequently can be substituted with the amine. Due to the relatively ease with which a 9-amino group is established, the majority of conjugates are those in which the (bio)molecule of interest is linked solely

to the 9-amino group. Some relevant examples are, e.g.: 2,6-diaminopurine conjugated to the acridine moiety via different guanidine-carrying linkers (**Figure 1.29**). They showed the ability to potentiate cytotoxicity for alkylating anti-tumour compounds by occupying abasic sites in certain cancer cells (mouse leukaemia and human pulmonary adenocarcinoma) in cell-based assays.[178]

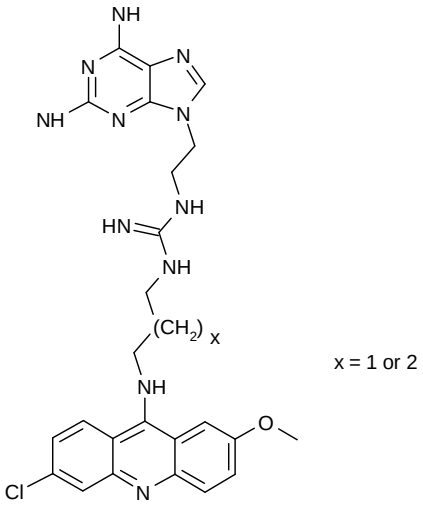

Figure 1.29: two anti-tumour active, diaminopurine-containing 9-aminoacridine conjugates. [178]

In another example, 11-mer oligonucleotide-acridine conjugates (with the oligomers resembling the extremities of the HIV-1 integrase LTR) showed the capability of inhibiting HIV-1 integrase catalytic activity, *in vitro*, in the IC_{50} µmolar range, provided they were conjugated to acridine.[179] E.g. GGTTTTTGTGT-Acr (in which the oligonucleotide is linked to acridine's 9-amino) showed IC_{50} values of 2.5 and 2µM for 3'-processing and strand transfer respectively. These oligonucleotide-acridine conjugates induced the efficient dissociation of preassembled integrase-DNA complexes. Although it was shown that this conjugate binds directly to integrase at a site different from its DNA_binding site, there was also evidence of at least a partial competitive inhibition (i.e. presuming base-sequence recognition). The latter conclusion was based on observed increased inhibitory activity in competitive conditions rather than with preassembled integrase-DNA complexes.[179]

9-Aminoacridine conjugates in which the biomolecule(s) of interest are not (only) attached via the 9-amino group have been much less the subject of research so far. One interesting exception to this is Beal's work on synthesis of a small acridine-peptide conjugate library for the purpose of screening their potential as DNA/RNA binding therapeutics.[180] A combinatorial library of acridine-peptide conjugates (**Figure 1.30**) was synthesised, using solid-phase synthesis in which the appropriately activated 9-anilinoacridine-4-carboxylic acid was linked, via a 4-carboxyl/carboxamide anchor, to the solid support bound peptides.

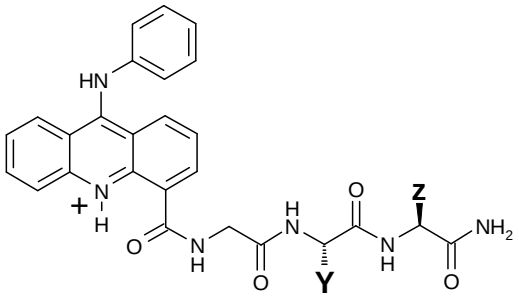

Y, Z= sidechain of glycine, serine, alanine or lysine

Figure 1.30: Acridine-peptide conjugate library synthesised by Beal *et al.*

Although 9-aminoacridine compounds, in spite of their enormous potential in drug development, are currently treated somewhat stepmotherly by the pharmaceutical industry due to their toxicity, colour and fluorescence properties, their merits are undisputed. Currently, clinical trials on 9-aminoacridine derivatives with potential anti-tumour activity,[170] and their therapeutic potential in e.g. treatment of prion diseases [181],[182] and protozoal parasites [183] confirm their continuing importance in drug research.

The premises of this research project firmly acknowledge the value of the acridine moiety and the therapeutic potential of the less prevalent acridine 4,9-substitution pattern in the development of 9-aminoacridine conjugates for anti-retroviral purposes. This is discussed in the next and final part of this introduction.

1.5.6 PNA-acridine conjugates as potential new integrase inhibitors

In the development of novel 9-aminoacridine conjugates, for the purpose of HIV integrase inhibition, our aim was to devise and execute a synthetic route in which a PNA moiety is conjugated to the acridine and to do this in the somewhat less tried but not less meritorious 9-aminoacridine-4-(bio)-molecule substitution pattern, as e.g. was applied by Beal *et al.* [180] in his acridine-peptide conjugate library (see **Figure 1.30** in subsection 1.5.4) and as present in the very potent anti-leukaemia drug, 9-amino-DACA (see **Figure 1.19** in subsection 1.4.2). The 4,9-substitution pattern converts the acridine from a classical intercalator to a potential threading intercalator [184],[185] which is of particular interest if one wishes to increase intercalator residence time. The latter in turn has been shown to be positively correlated to bioactivity (see subsection 1.5.1). Moreover, a 4-carboxamide-linked substituent (of the acridine) exerts control over DNA binding as it allows for specific contacts between the substituent and accessible base functionalities in the major groove.[143],[141] In subsection 1.5.2 these interactions, and the importance of the acridine's 9-amino group in them, were discussed for 9-amino-DACA. In subsection 1.5.3 it was argued that, besides increasing the stability of complexation of PNA with ds-DNA, the acridine moiety in particular has proven to carry the additional benefit of improving cellular delivery of PNA oligomers (cytoplasm as well as nucleus). We now sought to develop the chemistry towards combining the obvious therapeutic potential of this type of intercalator with the DNA binding properties of peptide nucleic acids or PNA**.** PNA, with the appropriate complementary base-sequence, could in this way potentially selectively target the ends of HIV viral ds-DNA long terminal repeats, thereby inhibiting HIV integrase activity by obstructing/interfering with the normal viral DNA-integrase binding interactions. Hence, in the design of the conjugate it was proposed that the acridine moiety would bind to the ds-DNA through intercalation, whilst the PNA would thread through the DNA helix and form hydrogen bonds with the adjacent complementary nucleobase stretches (as in the PNA/ds-DNA interactions discussed in subsection 1.5.3) and this enabled by the threading acridine 4,9-substitution pattern.

Figure 1.31 below depicts the general structure of our primary PNA-acridine targets. **Figure 1.31** also suggests a potential viral DNA binding mode (i.e. major/minor groove preference) of our primary PNA-acridine synthetic targets based on 9-amino DACA's threading mode and illustrates an altered 9-amino substituent which holds the potential

to effect additional recognition/interaction with the viral DNA minor groove functionalities. This can be e.g. an amino acid or a second PNA moiety directly, or via a linker moiety, connected to the acridine.

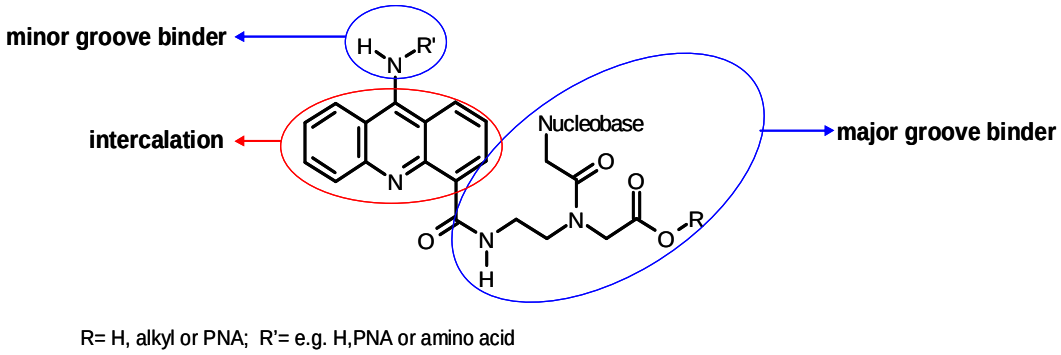

Figure 1.31: General structure of primary PNA-acridine targets.

Although there are limitations (when using 'regular' PNA, depicted in **Figure 1.22** in subsection 1.5.3) to the nature and length of sequences that can be (sequence-specifically) targeted due to the fact that stable PNA-dsDNA complexes have only been observed for homopyrimidine PNA (triplex invasion complex) (see **Figure 1.24** in subsection 1.5.3) or very purine rich PNA (single duplex invasion complex) (see **Figure 1.25a** in subsection 1.5.3), this was not our main concern in the development of a synthetic pathway towards the 9-amino-4-PNA-acridine conjugates. Moreover, modified PNA might resolve these issues of non-compatibility with random ds-DNA by using e.g. pseudocomplementary PNA (see **Figure 1.25b** in subsection 1.5.3) or the pre-organized chiral γ-PNA (see **Figure 1.26** in subsection 1.5.3). As mentioned, the DNA-binding properties of PNA and 9-amino-DACA as well as their capacity to inhibit DNA template functions were the main inspiration for this project. By exchanging 9-amino-DACA's 4-carboxamide side-chain with a PNA oligomer while retaining the 9-amino functionality we were hoping this would further increase drug/ds-DNA complex stability and bioactivity inherent to 9-amino-DACA. This was an obvious desirable trait in the development of potential new anti-retrovirals. Hence, retainment/availability of the primary 9-amino substituent was considered a desirable feature in our conjugates and synthetic routes were devised accordingly. Constructing the PNA-acridine conjugate, with the intended 4,9 substitution pattern, as in **Figure 1.32**, did however raise a number of interesting complications e.g. regarding the acridine ring nitrogen (N10) basicity and the necessity to control this.

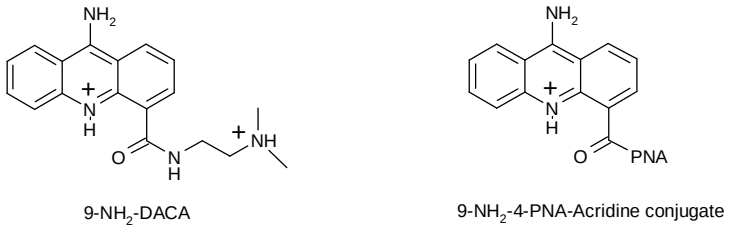

Figure 1.32: 9-amino-DACA compared to the envisaged PNA-acridine conjugates

The bulk of the next chapter, 'Results & Discussion', deals with the challenges and pitfalls encountered in our endeavours to synthesise the envisaged PNA-acridine conjugates. More specifically, the next chapter discusses the chemistry towards the development of new PNA-acridine conjugates and gives a detailed account of a novel 9-step synthetic pathway towards a PNA monomer-acridine conjugate. The applied chemistry is solution-based but we believe it could be applied in a solid-phase synthetic strategy for acridine-PNA libraries for screening of (sequence-specific) IN-inhibitory activity.

In first instance our hope is that the envisaged PNA-acridine conjugates will lead to specific new and potent HIV-integrase inhibitors and in second instance that they will also prove worthy to be considered for other nucleic acid targeting purposes.

The next chapter 'Results and Discussion' deals with the chemical synthetic strategies, encountered problems and subsequent solutions towards the development of the envisaged PNA-acridine conjugates. Each of the synthesised intermediates is discussed separately.

Chapter 2: Results and Discussion

2.1 Objectives

Our objective was to synthesise potentially HIV-integrase inhibiting PNA-acridine conjugates. Our approach was such that we intended to synthesise the acridine moiety and the PNA monomer/oligomers separately and subsequently combine these building blocks thereby making several potential PNA-acridine threading intercalators. We set out to synthesise 9-aminoacridines conjugated to a (pseudo)bio-molecule (PNA) in the acridine's 4-position. In **Scheme 2.1**, a generalised retrosynthetic analysis shows two ways in which the relevant substitutions in the acridine's 4 and 9 position could be established.

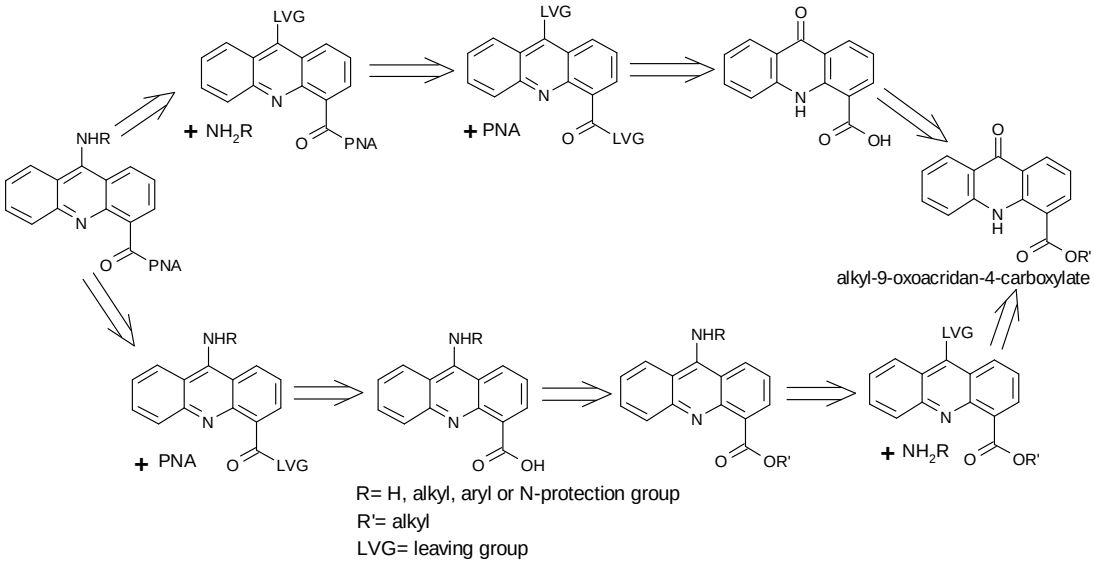

Scheme 2.1: Retrosynthetic analysis of two routes to 9-amino-4-PNA-acridine conjugates

The top route in **Scheme 2.1** has the least steps and establishes the PNA substituent before the 9-amino functionality. In this route, different reactivities of the same leaving group (LVG) in both 4 and 9 position of the acridine allow for chemoselectivity. In the bottom route the order of substitution is reversed (i.e. 9-amino established before 4-PNA) and an extra step is required. Variations on both routes were investigated and are discussed in the following sections. Synthesis of the depicted mutual starting

compound for both routes (alkyl-9-oxoacridan-4-carboxylate on the right) is well established (hence omitted here but discussed later).

2.2 Synthetic strategies towards PNA-acridine conjugates.

When synthesising substituted acridines, more specifically 9-aminoacridines-4-carboxamides, generally the three-ring aromatic acridine moiety is synthesised carrying oxygen-based functionalities in the 4 and 9 positions (e.g. alcohol, carbonyl or carboxyl groups), which can then be appropriately substituted. One of the main issues in our project was to find the order in which the oxygen-based functionalities would ideally be converted and/or protected in order to obtain our 9-aminoacridine conjugates reproducibly and in a reasonable yield. In our attempts to achieve this, three different synthetic strategies were investigated. The three routes were based on literature precedents and are referred to as the 'Denny route', the 'Beal route' and a 'revised Beal route', after the principal authors who reported similar chemical conversions in their work. The 'Denny route' conforms to the top part of **Scheme 2.1**, while the 'Beal route' and 'revised Beal route' conform to the bottom strategy in **Scheme 2.1.** Over the following sections, each of the strategies will be discussed together with our findings.

2.3 The 'Denny route'

In 1984 William Denny reported on the synthesis of 9-aminoacridine-4-carboxamides as a new class of anti-tumour agents, the most promising of which was *N*-[2-(dimethylamino)ethyl]-9-aminoacridine-4-carboxamide, also known as 9-amino-DACA **6** (see **Scheme 2.3** below).[131] As mentioned earlier, 9-amino-DACA, due to its DNA binding properties (discussed in subsection 1.5.2) was one of the inspirations behind this research project. We decided to initially focus on preparing 9-amino-DACA, in order to familiarise ourselves with each of the reactions in this synthetic pathway (we obtained an over-all yield of 23.2% for the HCl salt of 9-amino-DACA, compared to 27.4% for Denny). 9-amino-DACA was also considered to be a good control compound to evaluate for anti-IN activity. To the best of our knowledge anti-IN activity has not been reported for 9-amino-DACA.

The key features of the 'Denny route', with regard to establishing the desired substitutions in the acridine 4 and 9 positions, were conversion of the oxygen carrying functionalities in the acridine 4 and 9 position into respectively an acid chloride and an

aromatic chloride functionality, followed by respectively 4-carboxamide and 9-amino formation (see **Scheme 2.2** below). The chemistry involved in these conversions is discussed in detail for the synthesis of 9-amino-DACA **6** in the following section.

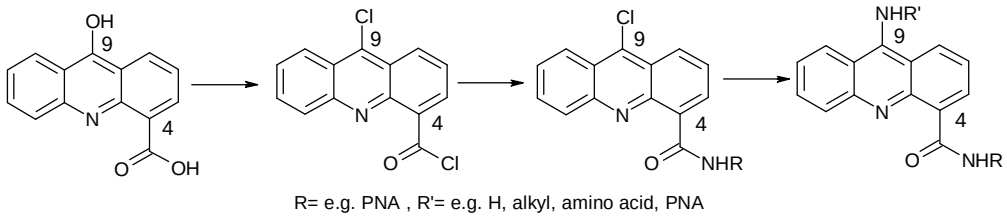

Scheme 2.2: key transformations in the 'Denny route'

2.4 Synthesis of 9-amino-DACA (according to an adapted Denny protocol) [186], [187]

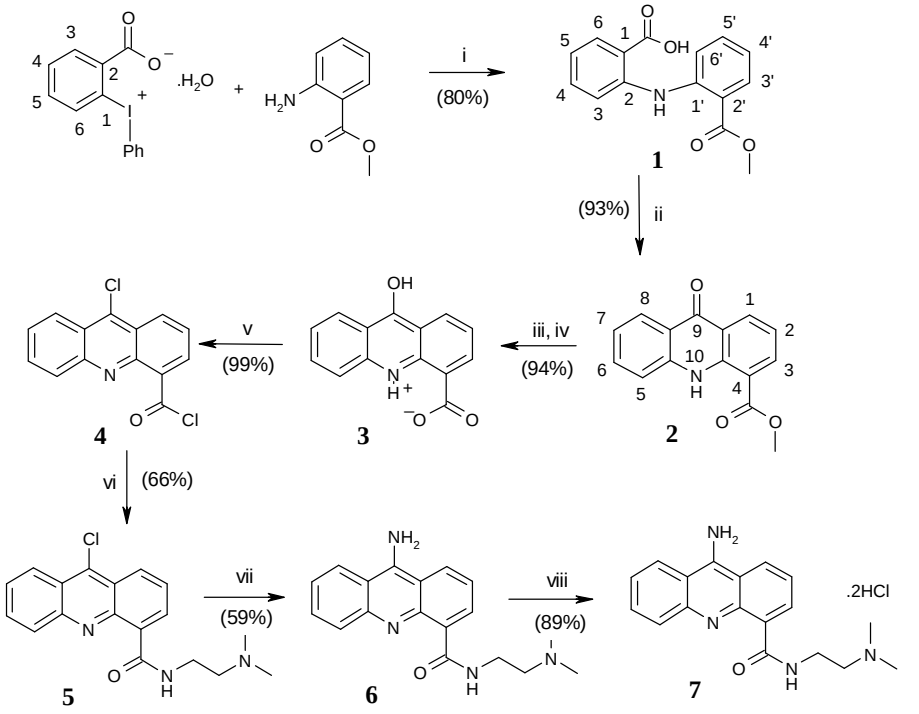

Scheme 2.3: synthetic route to 9-NH_2-DACA

A detailed discussion of each of the steps *i* to *viii* in Denny's route to 9-amino-DACA **7** (see **Scheme 2.3** above), coupled with our observations, now follows.

2.4.1 Step i: generating the first intermediate, 2-(2-Methoxycarbonylphenylamino)-benzoic acid (1)

The first step in the synthetic pathway towards 9-amino-DACA (**7**) involved reaction of diphenyliodonium-2-carboxylate (DPIC) with methyl anthranilate, in the presence of Cu(II)acetate catalyst, to afford **1** (see **Scheme 2.4**).

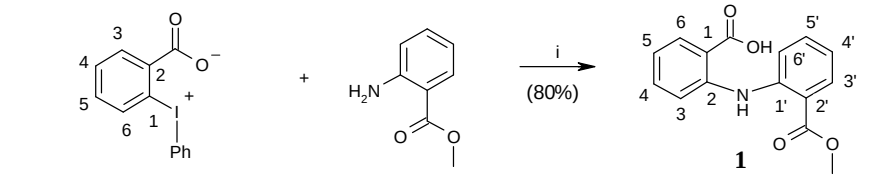

Reagents and Conditions: DMF, Cu-acetate (cat), 90℃

Scheme 2.4

Both DPIC and methyl anthranilate were commercially available. In this reaction, the aromatic primary amino substituent of methyl anthranilate nucleophilically attacked at C1 of diphenyliodonium-2-carboxylate which lead to the displacement of the phenyliodonium substituent**.** This reaction was successfully accomplished in our hands, using a similar procedure to that reported by Denny, to afford **1** in an 80 % yield. This was an improvement compared to Denny's reported yield of 65% for **1**. [187] DPIC was used here because it lead to significantly higher yielding and cleaner reactions than in the classic Ullmann-Goldberg route in which 2-chlorobenzoic acid was used (instead of DPIC) in the preparation of the ortho-substituted benzoic acid **1**. One limitation when using DPIC in the synthesis of **1** was that temperature had to be kept below 130°C (above this temperature DPIC decomposes mainly to phenyl o-iodobenzoate and above 160°C the main decomposition product is benzyne.[188] Some unusual aspects of the DPIC reaction, as depicted in **Scheme 2.4**, were its high specificity for nucleophilic attack on the carboxylate-bearing ring and the fact that the reaction was copper(II) catalyzed, in contrast with the usually copper(I) catalyzed Ar_2I^+-salt reactions (in which the degree of selectivity for which aryl will be substituted is reduced, due to the reduction by copper(I), to the radical species $Ar_2I^{\cdot}$).[189] In this

light the high selectivity in the direction of cleavage (of the copper(II) catalysed DPIC reaction) certainly supported the proposed S_N Ar mechanism rather than a radical mechanism. Although no mechanism had been suggested by which copper(II) catalysis occurs, a possible involvement of the catalyst could be that the ionic interaction between the carboxylate substituent and Cu^{2+} cation increased the electrophilic character of the position ortho to the carboxylate group, which consequently increased the susceptibility of this ortho position to nucleophilic attack. The catalytic requirement for copper(II), not copper(I), could be explained by the fact that an increased negative charge on the carboxylate group (due to its –M effect) would not be stabilised by Cu^{+} to the extent it would be by Cu^{2+}. This difference might be important as an increased (partial) positive charge on the ortho carbon (of the carboxylate bearing ring) was energetically unfavourable (adjacent to $-I^{+}-$) and for this to be countered/stabilized, interaction of the carboxylate with Cu^{2+} was possibly necessary. On the other hand, perhaps it may have been that Cu^{2+} withdrew electron density from both carboxylate and iodonium lone pairs thus enhancing the electrostatic repulsion between the ortho carbon (partial) positive charge and the iodonium charge. Admittedly, these hypotheses do not completely clarify why Cu^{+} would not also, to some extent, be a catalyst for this reaction.

At a later stage in our project the synthesis of the first intermediate (**1**) had to be performed via the lower-yielding Ullmann-Goldberg reaction with commercially available *o*-chlorobenzoic acid as a substitute for the diphenyliodonium-2-carboxylate (due to it being commercially discontinued). This was done according a procedure reported by Palacios and Comdom (see **Scheme 2.5** below) who described this Ullmann-Goldberg reaction with aromatic amines related to our methyl anthranilate, the closest match being anthranilic acid for which they reported a 79% yield of the conjugated product.[190]

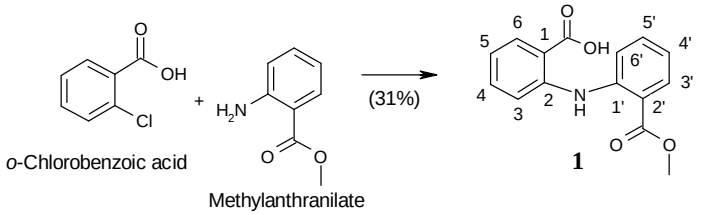

Reagents and Conditions: Water/ DMF, K_2CO_3, Cu (cat), 100℃

Scheme 2.5

In our hands, using methyl anthranilate for the amine, the yield for **1** was only 31%. In this procedure the product (**1**) was deemed sufficiently pure to be used in a next step without further purification. Although the yield was unsatisfactory we decided to stick to this procedure because cost of the starting materials was low and they were easily recoverable and reusable.

Although Cu powder was used as the catalyst source, it was reported the actual catalyst was copper(I) because of the following observations: absence of air strongly reduced the activity of metallic copper and CuI catalysed the reaction in the presence of KI (a condition under which Cu^{2+} cannot exist).[191],[192],[193] Regarding the involvement of the catalyst in the reaction mechanism opinions seemed to be divided. Little support existed for a free-radical course of the reaction.[194] Consensus seemed to lie with an S_N mechanism in which catalysis was believed to occur via intramolecular coordination of the halogen to copper(I), which in turn increased the polarity of the C-Cl bond and activated it toward nucleophilic substitution in the position ortho to the carboxylate group.[195] (See **Figure 2.1** for the partial mechanism suggested in the literature [196])

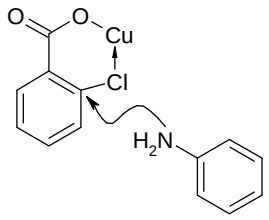

Figure 2.1: Suggested involvement of copper(I) catalyst in a typical Ullmann-Goldberg reaction between *o*-chlorobenzoic acid and aniline. (Source: Gagan, J. M. F., 1973, [196])

2.4.2 Step ii: ring-closure step generating methyl-9-oxoacridan-4-carboxylate (2)

The second step (*ii*) in the synthesis of 9-amino-DACA (**7**) involved cyclization of **1** to yield methyl-9-oxoacridan-4-carboxylate (**2**) (see **Scheme 2.6** below). This was accomplished readily by heating a solution of **1** and an excess of tetraethyl tetrametaphosphate (**2"**) (see **Figure 2.2** below for structure of **2"**) in dry chloroform to reflux. The tetraethyl tetrametaphosphate (**2"**) used in this reaction was first freshly prepared according to the literature method by Pollmann and Schramm.[139]

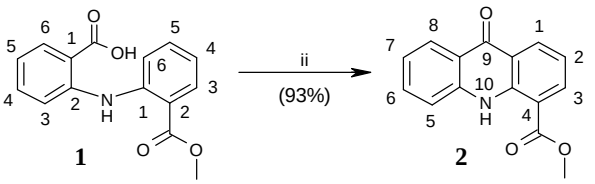

Reagents and Conditions: Tetraethyl tetrametaphosphate (**2"**), $CHCl_3$, reflux

Scheme 2.6

The IR spectrum recorded for the obtained tetraethyl tetrametaphosphate **2"** showed an absorption band at 1310 cm^{-1} which was characteristic of P=O stretching in cyclic phosphate esters [197], and a band at 950-1100 cm^{-1} which was characteristic for P-O-C alkyl stretching. No absorption band was present at 1200-1250 cm^{-1} which indicated the absence of open chained (hydrolysed) polyphosphate esters.[139] The tetraethyl tetrametaphosphate **2"** was obtained in a 94% yield and could directly be used in step *ii*, as suggested by Pollmann and Schramm and based on comparison of reported IR spectra of tetraethyl tetrametaphosphate with our own IR spectrum for **2"**.

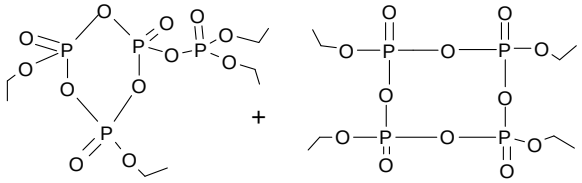

2''

Figure 2.2: The prepared tetraethyl tetrametaphosphate **2"** is a mixture of the depicted compounds.

In step *ii* (**Scheme 2.6**) dry conditions were important as hydrolysis of tetraethyl tetrametaphosphate (**2"**) could jeopardize ring closure of **1**. Pollmann and Schramm had reported splitting of the P-O-P linkage(s) of tetraethyl tetrametaphosphate by hydroxy-containing compounds; examples were H_2O, ethanol and phosphoric acid.[139] In our case, presumably the –OH of the carboxyl group of **1** reacted with tetraethyl tetrametaphosphate, splitting a P-O-P linkage, and formed a mixed acid anhydride between **1** and tetraethyl tetrametaphosphate (**2"**). This was then followed by ring closure of **1** via an S_E Ar step and subsequent loss of the ethyl polyphosphate groups (see **Scheme 2.7** below for our suggested reaction mechanism).

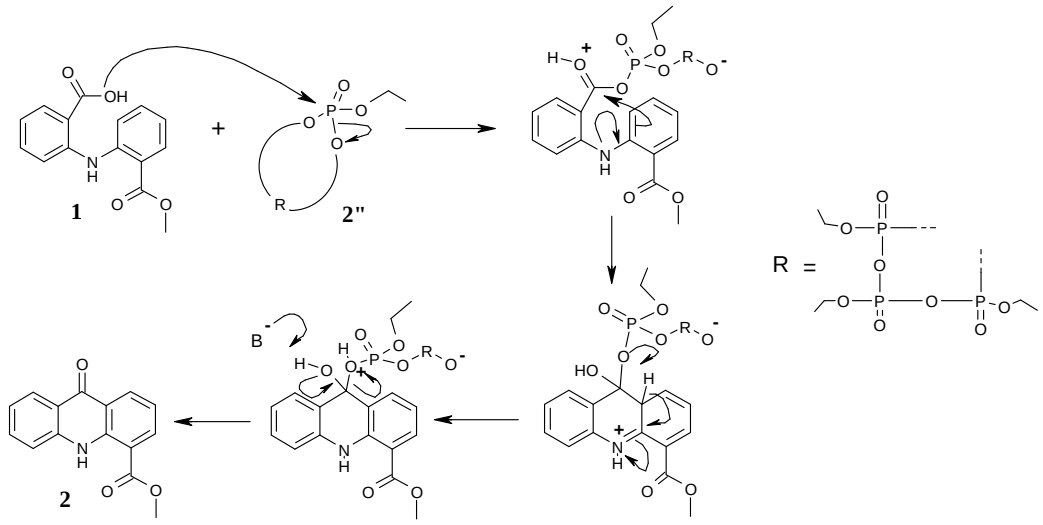

Scheme 2.7: Suggested reaction mechanism for ring closure of 2-(2-methoxycarbonylphenylamino)benzoic acid (**1**) using tetraethyl tetrametaphosphate (**2"**)

After work-up, compound **2** was obtained in a 93 % yield, which was slightly below the yield of 96% reported by Denny *et al.* [187] (no further purification was required). In the ^{1}H-NMR spectrum of **2,** reduction of the number of aromatic protons from 8 (in **1**) to 7 protons indicated successful ring closure. The high value of the most downfield signal at 11.60 ppm (assigned to the NH-proton) was attributed to the NH-proton being engaged in intra-molecular H-bonding with the carbonyl oxygen of the methoxycarbonyl substituent at C4. This presumably would have locked **2** into its tautomeric form, as represented in the left part of **Figure 2.3** (the other tautomer having full aromaticity, and an –OH group at C9). The existence of this intra-molecular H-bonding, where the proton is shared between the side-chain carbonyl oxygen and the acridine ring nitrogen, was also observed in the X-ray crystal structures obtained for similarly substituted acridines, *iso*-propyl-9-oxoacridan-4-carboxylate (**22**) and methyl-9-benzyloxycarbonylaminoacridine-4-carboxylate (**45**). These shall be discussed later in the thesis in subsections 2.10.2 and 2.14.2 respectively.

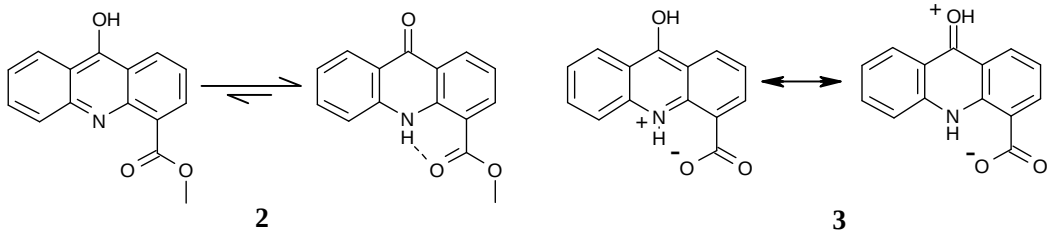

Figure 2.3: Tautomerism, intra-molecular H-bonding and ionic interactions in acridines **2** and **3**.

2.4.3 Steps iii and iv: generating the 9-oxoacridan-4-carboxylic acid (3)

In step *iii* in the synthesis of 9-amino-DACA (**7**)**,** the sodium salt of compound **3** was obtained by basic aqueous hydrolysis of compound **2** (see **Scheme 2.8**).

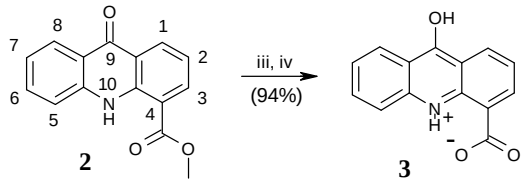

Reagents and Conditions: iii NaOH 2M, reflux
iv Dowex (H^+), EtOH, rt

Scheme 2.8

The work-up (step *iv*) reported by Denny *et al.* [187], involving acidification of the resulting basic solution with glacial acetic acid, proved to be problematic due to a persistent acetic acid contamination in the crude product **3**. In order to overcome this problem, we decided to use Dowex H^+-exchange resin, which had been swollen in absolute ethanol, and was added to the basic reaction mixture instead. This procedure neatly converted the sodium salt into the product **3**. Our modified work-up gave rise to **3** in a slightly enhanced yield (94%) compared to that reported by Denny *et al.* (87%).[187]

A ^{1}H-NMR analysis of the spectrum of **3** verified the disappearance of the methyl protons of **2** and showed an unusually high signal at 13.95 ppm. The latter signal was assigned to N(10)H and its high value attributed to a partial positive charge it carried (see canonical forms of **3** in **Figure 2.3**) because, in **3**, there was ionic interaction between the carboxylate functionality and the protonated ring nitrogen N(10)H. To the best of our knowledge, ^{1}H-NMR analysis of compound **3** has not been reported in the literature. Compound **3** was deemed sufficiently pure to be used in the subsequent step without further purification.

2.4.4 Steps v and vi: activation of the acridine acid (3) towards subsequent carboxamide formation.

The next step (*v*) in the synthesis of 9-amino-DACA involved treatment of **3** with excess thionyl chloride in the presence of a catalytic amount of DMF to afford the

corresponding 4,9-dichloroderivative **4** (99% yield). The DMF catalysis was required here to accommodate, for the (aromatic) 9-oxo/hydroxy→9-chloro conversion, nucleophilic chloride attack on the aromatic system (i.e. on the C(9) of the intermediate $[(aryloxy)HC=N(CH_3)_2]^+$). Since compound **4** could easily undergo hydrolysis, it was used directly in the next step (*vi*) of the synthetic pathway without further purification (see **Scheme 2.9**).

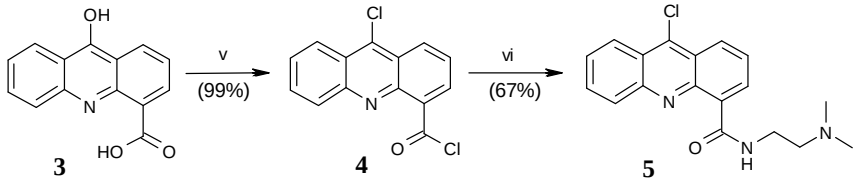

Reagents and Conditions: v $SOCl_2$, DMF (cat.), heat
vi $NH_2CH_2CH_2N(CH_3)_2$, DCM, 0°-30°C

Scheme 2.9

The sensitivity to hydrolysis of **4** involved both the 9-chloro and the (obvious) acid chloride group. It was reported by Raulins that for 9-chloroacridines hydrolysis to 9-oxoacridines is usually effected by boiling with dilute acid but that the ease of hydrolysis is also dependant on the substituents present, with electron-withdrawing groups (like the acid chloride group in **4**) generally enhancing the rate.[198] This was confirmed by the recuperation of small amounts of **3** in the chromatographic purification of crude compound **5**.

Subsequently, in step *vi*, compound **4** was treated with excess dimethylethylenediamine to establish the carboxamide-substituent in the acridine's 4-position, thus generating compound **5**. The carboxamide functionality in **5** was established via an addition/elimination reaction of the primary amine with the acid chloride functionality of **4**. We found the crystallisation procedure reported in the literature [186] for purification of **5** proved to be cumbersome so instead we applied column chromatography which gave rise to **5** in a 67% yield. This was slightly below the yield of 71% reported by Denny *et al.*

Subsequent analysis of the ^{1}H-NMR spectrum of **5** showed the expected signals for the side chain protons ($-CH_3$ at 2.45 ppm and $-(CH_2)_2$ at 2.72 and 3.79 ppm), confirming the reaction had been successful. The high value of the amide proton signal at 11.90 ppm again was an indication of involvement in hydrogen bonding, as mentioned before, with the heterocyclic nitrogen. (See **Figure 2.4** below)

Once again, to the best of our knowledge, ours is the first ^{1}H-NMR analysis of compound **5**.

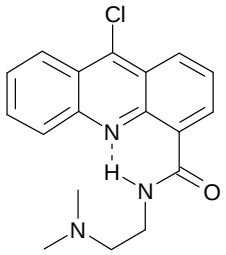

5

Figure 2.4: Intramolecular H-bonding in acridine derivative **5**

2.4.5 Steps vii and viii: generating the 9-amino-DACA free base and its HCl salt

Step *vii* in the synthetic pathway towards 9-amino-DACA (**6**) involved replacing the 9-chloro-substituent of **5** with a primary amino group, via an S_N Ar reaction, using the protocol described by Denny *et al*. [186] in which dry ammonia gas was bubbled through a heated phenolic solution of **5** (see **Scheme 2.10**).

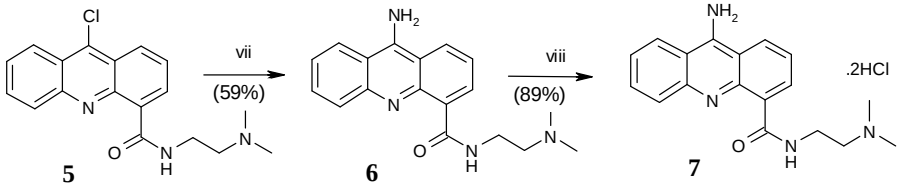

5 **6** **7**

Reagents and Conditions: vii (a) dry phenol, heat, 50℃; (b) NH_3 (g), 115℃
viii HCl(g), MeOH, rt

Scheme 2.10

Again a different approach to that reported in the literature [186] was undertaken for purification of crude **6**. The method reported by Denny involved diluting the reaction mixture with an excess of 40% aqueous solution of sodium hydroxide which, upon cooling, gave the crude solid product that then could be re-crystallized. Following this work-up, Denny *et al*. directly used **6** for a subsequent conversion of **6** into its HCl salt and reported an over-all yield of 72 % (for **7**). However, our attempt to reproduce Denny's crystallisation was unsuccessful so instead we purified the crude oil product by flash column chromatography which afforded **6** in a 59% yield.

A key feature of the ^{1}H-NMR spectrum recorded for **6** was the appearance of a broad singlet at 6.50 ppm which was assigned to the 9-NH_2 protons. The latter signal disappeared upon D_2O addition, indicating the exchangeable nature of the primary amino protons. The high value of the signal at 12.38 ppm was attributed to the amide proton believed to be engaged in hydrogen bonding with the heterocyclic nitrogen, as described for the previous compound **5** in **Figure 2.4**. Once again, we were unable to find any report in the literature which describes NMR data for compound **6** and to the best of our knowledge, ours was the first ^{1}H-NMR analysis of this compound.

Peculiar in this step *vii* was the use of phenol (as solvent and catalyst) and formation of the reaction-facilitating 9-phenoxyacridine intermediate, which allowed for preparation of the 9-amino acridine at temperatures 20-40°C lower than without phenol as solvent.[199]

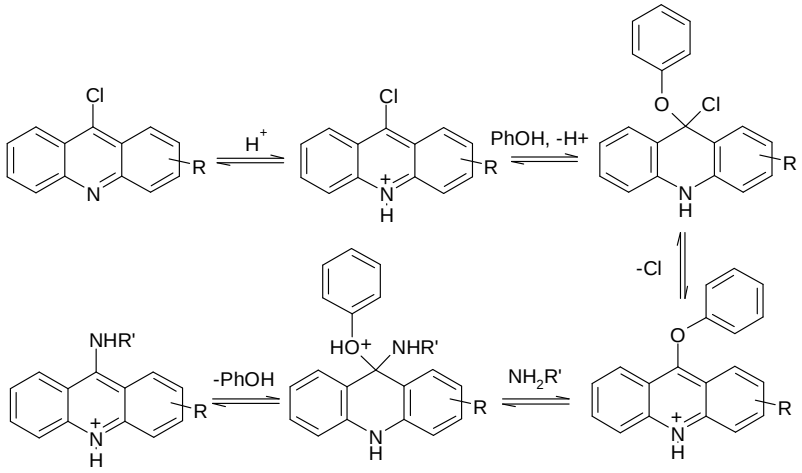

Scheme 2.11: the role of phenol in converting 9-chloroacridines into 9-aminoacridines (as suggested by Adcock,[200])

See **Scheme 2.11** above for the S_N Ar reaction mechanism suggested in the literature. In this mechanism the phenol protonated the heterocyclic nitrogen thereby increasing the electrophilicity of C9 and facilitating nucleophilic attack at C9, initially by phenol or phenoxide which was then substituted by the amine upon addition of the latter to the reaction mixture. It has been reported that aqueous acids can act as catalysts as well [201] but due to the sensitivity of the 9-chloro group to hydrolysis this would presumably lead to lower yields, hence the use of the organic 'acid' phenol. Another possible reason for the established use of phenol (in the discussed substitution

reactions) is that it is good solvent for acridines as both compounds (to a degree) are amphiphilic.

The last step (*viii*) in the synthetic pathway towards 9-amino-DACA involved conversion of the pure base **6** into its di-hydrochloride salt **7** for which we had to develop an alternative protocol to that reported by Denny *et al*. [186] In Denny's approach, a solution of **6** in methanol was treated with a concentrated solution of hydrochloric acid, and the resulting salt **7** was precipitated from the reaction mixture by addition of ethyl acetate and re-crystallised from methanol/ethyl acetate. However, in our hands, compound **7** did not precipitate from the reaction mixture. This was probably due to the fact that **7**, being a di-hydrochloride salt, was quite well solvated in the aqueous, polar, protic environment. In order to obtain **7** from **6**, we decided to treat **6** with dry methanol saturated with HCl which, after work-up, afforded **7** as yellow crystals in an 89 % yield.

Analysis of the ^{1}H-NMR spectrum recorded for **7**, following recrystallisation, suggested it was the di-hydrochloride salt. This conclusion was based on the observation that, compared to the ^{1}H-NMR spectrum recorded for the free base **6**, two extra signals of exchangeable protons were present. To the best of our knowledge no ^{1}H-NMR data has been reported for **7**. Compound **7** was sent off for evaluation of anti-IN activity, the result of which will be discussed later.

In the following sections the 'Denny route' strategy was applied to the synthesis of a PNA-acridine conjugate **16.** A retrosynthetic analysis of the conjugate **16** is given below in **Figure 2.5** to illustrate the steps involved. In what follows we separately discuss synthesis of the PNA monomer backbone (**10**) in section 2.5 and a PNA nucleobase moiety (**11**) in section 2.6, to then discuss how both compounds **10** and **11** were linked to each other and the acridine moiety in section 2.7 (illustrated in **Scheme 2.14**, later)

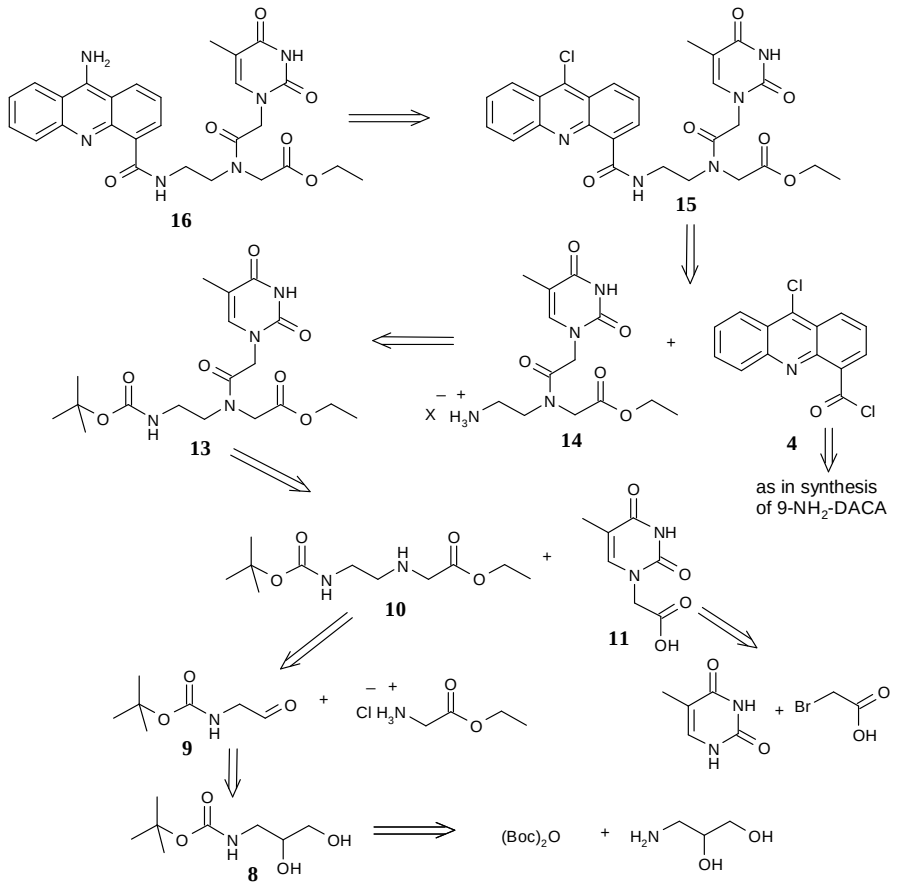

Figure 2.5: Retrosynthetic analysis for the thyminyl-PNA-acridine conjugate **16**

2.5 Synthesis of the *t*-Boc-protected PNA-monomer ethyl ester backbone (10)

The *t*-Boc-protected PNA monomer backbone, or ethyl *N*-(2-*t*-butoxycarbonylamino-ethyl)glycinate (**10**), was prepared from commercially available 3-amino-1,2-propanediol and di-*t*-butyl dicarbonate in three steps, based on well known chemistry described by Finn *et al*.[202] (**Scheme 2.12**).

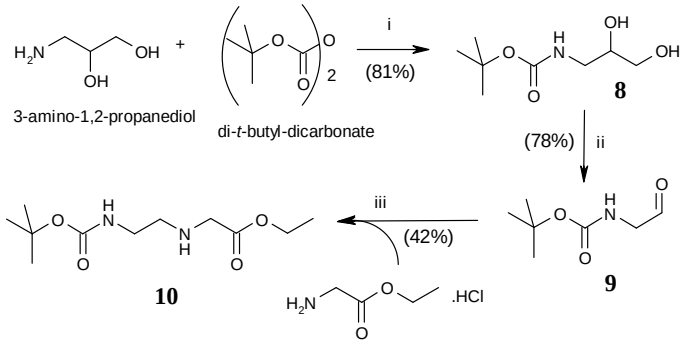

Reagents and Conditions: i a) H_2O/Dioxane, 0℃ ; b) rt, pH 11. ii $NaIO_4$, H_2O, rt. iii $NaBH_3CN$, MeOH, rt

Scheme 2.12: PNA-monomer backbone synthesis

The N-terminal primary amino function and the C-terminal carboxylic acid moiety in **10** were protected with a *t*-Boc and ethyl ester group, respectively. This ensured that the later coupling of thymin-1-yl acetic acid (**11**) to **10** could only occur with the free secondary amino group of **10** (see **Scheme 2.14** later).

Thus, in **Scheme 2.12**, the first step *i* in the synthesis of **10** involved reaction of 3-amino-1,2-propanediol with di-*t*-butyl dicarbonate in which aminolysis of the latter lead to the *t*-Boc-protected intermediate **8**, according to the method described by Finn *et al*. [202] In this procedure the pH of the reaction mixture was maintained above 10 (by addition of aqueous NaOH) in order to prevent the 1°-amino group of aminopropanediol from being protonated by the $(CH_3)_3CHCO_3$ acid generated in this substitution. Compound **8** was obtained in an 81 % yield after work-up (Finn *et al*. reported a yield of 97%).
The ^{1}H-NMR spectrum recorded for the resulting product was consistent with reported data [202] and **8** was deemed to be sufficiently pure for use in the next step of the synthetic pathway.

Step *ii* in the reaction pathway involved oxidation of the diol **8** with sodium periodate to its corresponding aldehyde, t-butyloxycarbonylaminoacetaldehyde **9** (**Scheme 2.12**). In this reaction a cyclic 5-membered periodate ester was rapidly formed which subsequently slowly decomposed to the aldehyde products and the I(V) species HIO_3.[203] (See **Figure 2.6** below)

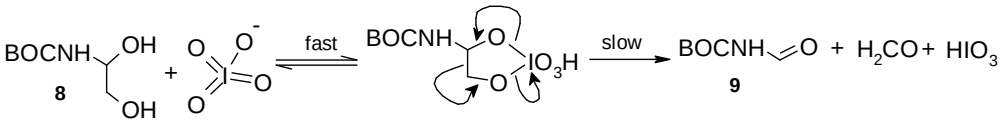

Figure 2.6: oxidation of the vicinal diol groups in **8** with IO_4^- proceeds via a cyclic periodate ester (electron pair movements shown in the intermediate relate to the slow, rate determining step). [222]

Once again, the above reaction was performed according to the method described by Finn *et al.* [202] to yield **9** in a 78 % yield (Finn *et al.* reported a yield of 94%). The ^{1}H-NMR spectrum recorded for **9** was comparable to that reported [202] and **9** was deemed to be sufficiently pure for the next step in the synthetic pathway. A key feature of the ^{1}H-NMR spectrum of **9** was the aldehyde proton signal at 9.65 ppm.

The final step in this synthetic pathway (**Scheme 2.12**) involved reductive amination of the *t*-Boc-protected aldehyde (**9**) in which the latter was treated with a methanol solution of glycine ethyl ester hydrochloride and $NaBH_3CN$. The reaction was performed as described by Finn *et al.*[202] In this reaction the initially formed imine picked up a proton (e.g. from the solvent methanol) to form the iminium which was subsequently rapidly reduced by the mild reducing agent, generating the secondary amine. No stronger reducing agent was required here because the iminium (carbon) was such a good electrophile, in particular compared to aldehydes and ketones with which $NaBH_3CN$ reacts only very slowly.[226] This chemoselectivity was convenient here because of the aldehyde group in the starting material (**9**). The product ethyl N-(2-*t*-butoxycarbonylaminoethyl)glycinate (**10**) was afforded in a 42 % yield (Finn *et al.* reported a yield of 43%). The recorded ^{1}H-NMR spectrum of **10** was comparable to that reported and **10** was deemed to be sufficiently pure to be used in the next coupling step with a nucleobase moiety, the synthesis of which is discussed in the next section 2.6.

2.6 Synthesis of a PNA nucleobase moiety

In PNA, the nucleobase moieties are attached to the secondary amine nitrogen of **10** via a methylenecarbonyl linker. Thus, appropriate acetic acid functionalized nucleobases needed to be prepared. The latter was achieved by reacting the (protected) nucleobase with bromoacetic acid (under strong alkaline conditions), which attached selectively at the nucleobase N(1), via an S_N2 reaction in which the α-bromide was substituted (as in **Scheme 2.13** below). The acid functionalized nucleobase moiety was now ready to undergo peptide-coupling to the PNA monomer backbone (**10**). For the purpose of this project, we focused on only one of the four possible nucleobases; that of thymine. The reason for this was that it was known to be the simplest nucleobase to work with as its heterocyclic ring does not require any protection and it also poses the least problems solubility wise. We envisaged that if the thymine PNA-acridine conjugates proved to be effective anti-IN agents worthy of further investigation, that the analogous conjugates bearing the other three nucleobases could be similarly prepared. Thus, thymin-1-yl acetic acid **11** was prepared in one step, according to the method reported

by Kosinkyna *et al.*, [146] as illustrated below in **Scheme 2.13**, in 93% yield (Kosinkyna *et al.* reported a yield of 80%).

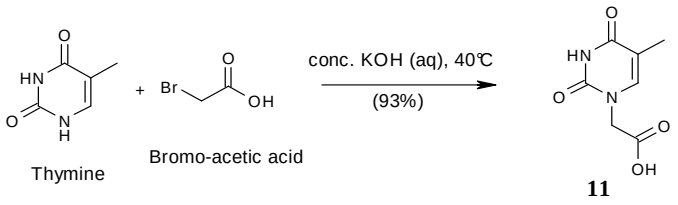

Scheme 2.13: Thymin-1-yl acetic acid synthesis

Selective alkylation at N(1) rather than at N(3) of thymine was possible here due to the significant difference in pKa for thymine N(1) (pKa=9.86) compared to N(3) (pKa=13.96).[204] The recorded ^{1}H-NMR spectrum of **11** was consistent with that reported [146] and **11** was deemed to be sufficiently pure to be coupled to the *t*-Boc-protected PNA monomer backbone **10** in the next step of the synthetic pathway, as will be discussed in the next section 2.7.

2.7 Linking nucleobase moiety, PNA monomer backbone and acridine moiety to generate the PNA-acridine conjugate 16 in the 'Denny route' approach.

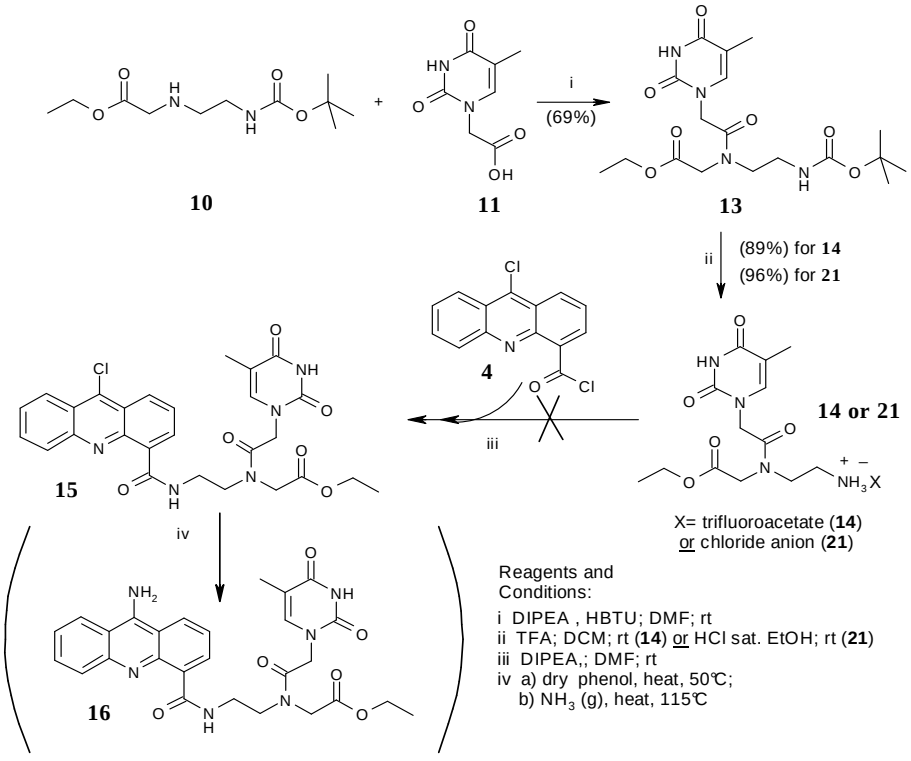

Scheme 2.14: intended **'**Denny route' to a PNA-acridine conjugate

Our initial synthetic strategy for synthesis of **16** involved attachment of the thymin-1-yl acetic acid derivative **11** to the PNA-monomer backbone **10** followed by *t*-Boc deprotection of the backbone to give **14** (or **21**) and subsequent coupling to 9-chloroacridine-4-carbonyl chloride **4** to give **15** (see **Scheme 2.14** above). Finally, the 9-chloro substituent of **15** was to be replaced by an amino group, in an identical manner to that used previously for the synthesis of 9-amino-DACA **6**, to afford the desired compound **16** (**Scheme 2.14**). Unfortunately, **Scheme 2.14** could not be completed successfully as step *iii* did not yield the hoped for conjugate **15**. The attempted steps *i*, *ii* and *iii*, outlined above, will be discussed in the following subsections.

2.7.1 Step i: generating the t-Boc-protected thyminyl-PNA-monomer 13

The first step (*i*) in this synthetic pathway involved coupling thymin-1-yl acetic acid (**11**) to the PNA monomer backbone (**10**) (see **Scheme 2.15**).

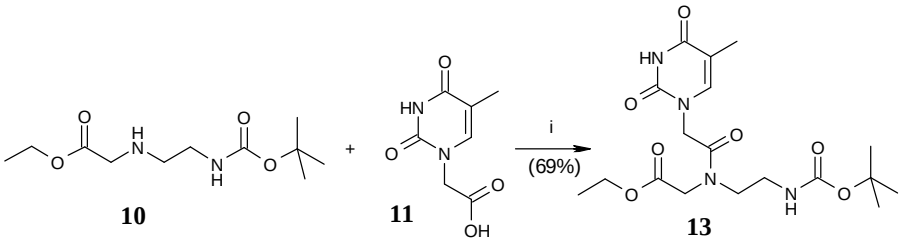

Reagents and Conditions: i DIPEA , HBTU; DMF; rt

Scheme 2.15

This conversion required treatment of **11** with 2-(1H-benzotriazol-1-yl)-1,1,3,3-tetramethyluronium hexafluorophosphate (HBTU) in the presence of an excess of di-*iso*-propylethylamine (DIPEA), according to a similar method described by Finn *et al.* [202] HBTU acted as an activator of **11**'s carboxyl function, providing it with a good leaving group and facilitating the coupling (see reaction mechanism below in **Figure 2.7**). HBTU is a peptide coupling agent belonging to the triazolols, one of two main types of activating groups used in peptide chemistry (the other group being carbodiimides). The initial triazolols (e.g. 1-Hydroxybenzotriazole or HOBt) were developed to complement the earlier developed carbodiimides by accelerating the coupling reaction and suppressing by-product formation that arose from the single use

of carbodiimides (racemisation and N-acyl urea formation).[205] A number of more recently developed triazolols, like e.g. HBTU, omit the carbodiimide step entirely.

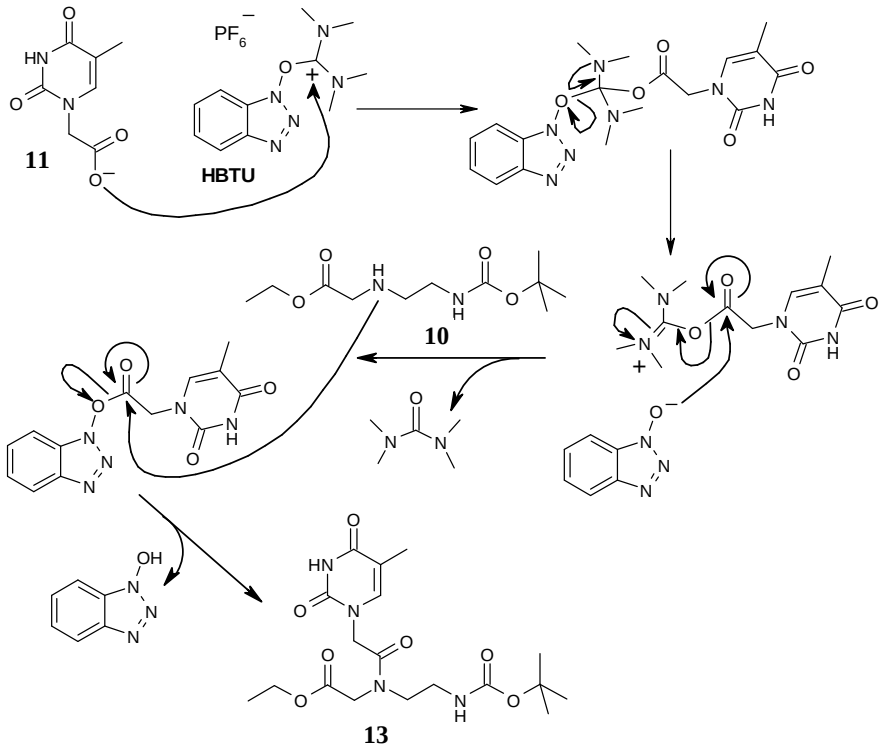

Figure 2.7: the role of HBTU in establishing the 3° amide bond in **13**

HBTU was used in **step *i*** (**Scheme 2.15**) mainly because of its established application in PNA chemistry. The resulting *t*-Boc-protected PNA monomer **13** was obtained in a 69% yield. Finn et al reported a 71% yield of **13** using a different condensing agent (TopPipU). Subsequent ^{1}H-NMR and ^{13}C-NMR analysis data were consistent to those reported in the literature [202] and confirmed the structure of **13**. The ^{1}H-NMR and ^{13}C-NMR spectra of **13** also showed the presence of two rotamers, in a 2:1 ratio, due to restricted rotation about the tertiary amide bond. 2-D ^{1}H-NMR NOESY experiments reported by Chen *et al.* [206] and Brown *et al.* [207] showed that **13 b** was the major rotational isomer (see **Figure 2.8**). They based this conclusion on the observed NOE interactions of the nucleobase linking methylene protons with different parts of the PNA backbone.

Similar NOE interactions will be discussed in more detail for one of our own PNA-acridine conjugates **53**, in subsection 2.15.1.

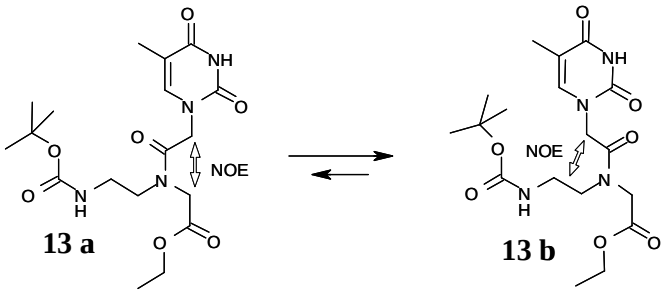

Figure 2.8: NOE interactions in the two rotational isomers of compound **13** (**a** and **b**), as described by Chen *et al.* [206] and Brown *et al.* [207]

2.7.2 Step ii: generating the salts 14 and 21 of the thyminyl-PNA-monomer.

The next step (*ii*) in the synthetic pathway involved *t*-Boc-deprotection of the PNA-monomer **13** (**Scheme 2.16** below). This was successfully accomplished by treatment of **13** with TFA, according to the method described by Breipohl *et al*. [208], and afforded the TFA-salt of the PNA-monomer (**14**) in an 89% yield. Breipohl's procedure differed from ours in that he simultaneously removed a *t*-Boc group and a *t*-Butyl group from respectively the primary amino group (as in our case) and the carboxyl group of the protected thyminyl-PNA-monomer (Breipohl reported a yield of over 100% for his crude product, in our opinion presumably due to insufficient drying).

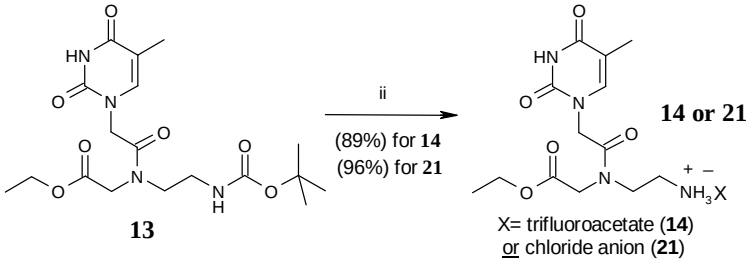

Reagents and Conditions: ii TFA; DCM; rt (**14**) or HCl sat. EtOH; rt (**21**)

Scheme 2.16

Later on in the project the *t*-Boc-deprotection of **13** was performed in HCl-saturated ethanol, yielding the PNA monomer HCl salt **21** in a 96% yield. We used the HCl-ethanol solution to guarantee the integrity of the ethyl ester group and found that the

latter procedure not only gave a slightly higher yielding white solid product **21** but as such **21** was also easier to handle and could be dried faster and easier than the brown gum of the TFA-salt **14**. Compound **14** had to be dried *in vacuo* at 50°C in a drying gun in the presence of phosphorus pentoxide. Compound **21** was dried by repeated (azeotropic) coevaporation of **21** with toluene.

^{1}H-NMR and ^{13}C-NMR analysis confirmed the structure for **14** and **21**. The *t*-Boc signal, at 1.37 ppm in compound **13,** had disappeared in **14** and **21**, indicating successful deprotection. Again, the ^{1}H-NMR and ^{13}C-NMR spectra of **14** and **21** showed the presence of two rotamers, in a 2:1 ratio, due to restricted rotation about the tertiary amide bond.

2.7.3 Step iii: attempting to link the acridine moiety 4 to the PNA-monomer 14.

Subsequently, coupling of the TFA-salt of the PNA-monomer (**14**) to the 9-chloroacridine-4-carbonyl chloride (**4**) was attempted (see **Scheme 2.17**).

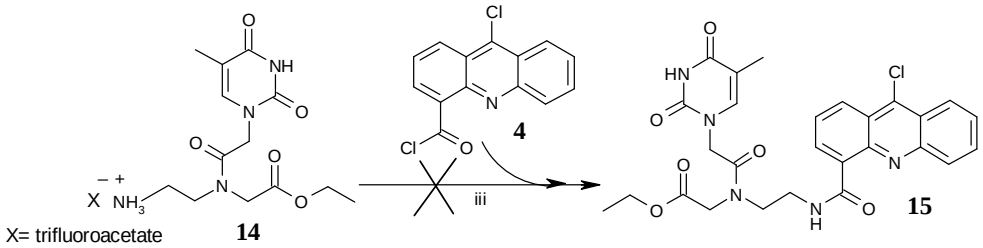

Scheme 2.17

Compound **4** was made as described earlier for the synthesis of 9-amino-DACA (**6**) (see **Scheme 2.3** in section 2.4). Hence, in step *iii* above, the free 1° amine group of **14**, after being liberated from its salt by DIPEA, was expected to nucleophilically attack the acid chloride carbonyl of **4** to yield the conjugate **15**. TLC monitoring of the reaction suggested complete conversion of the starting materials. Due to the high polarity of the product(s) it was decided to purify the potential product(s) using preparative TLC. Surprisingly, none of the expected PNA-acridine conjugate (**15**) could be identified upon NMR analysis of the collected bands. Repeated attempts to isolate and identify the product(s) by preparative TLC were unsuccessful and cumbersome. This was partially due to the longer migration time required (1.5 hours)

which caused considerable band widening of the bands on the TLC plate resulting in at least three yellow overlapping bands, slightly differing in UV activity and ranging between R_f 0.7 and the base line. Due to the overlap with neighbouring bands and low solubility of these products (and hence low peak intensity) in used polar deuterated solvents like DMSO-d_6 or CD_3OD, analysis of the afforded yellow solids by ^{1}H- and ^{13}C-NMR was unreliable and little could be concluded about the nature of the solids. Consequently, the next step *iv* (See **Scheme 2.14** earlier), generating the primary 9-amino functionality in PNA-acridine conjugate **16,** could not be attempted.

A possible interfering factor in this step *iii* could have been the tendency of the primary amine of starting material **14** to react intra-molecularly with the ethyl ester carbonyl functionality (See **Figure 2.9** below).

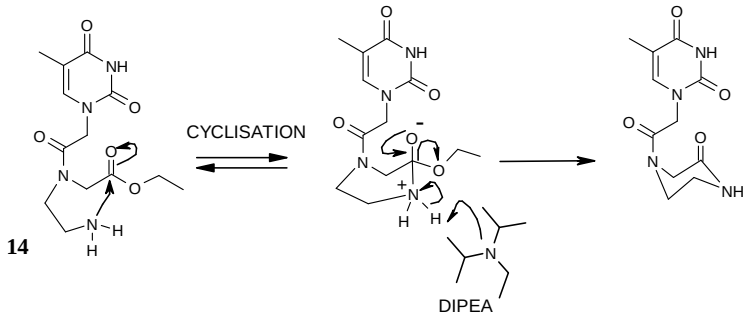

Figure 2.9: possible side-reaction in the coupling step of thyminyl-PNA-monomer **14** with acridine acid chloride **4.**

In the experiment the PNA monomer salt was deprotonated with DIPEA before the addition of the acid chloride. Although both deprotonation and addition were done at 0°C and ethoxide is a bad leaving group, the presence of an excess of DIPEA (necessary to neutralize the HCl generated by coupling of **14** with the acid chloride **4**) could have aided the ethyl ester aminolysis, presumably via deprotonation of the zwitterionic tetrahedral intermediate (See **Figure 2.9** above). Additionally, the polar solvent DMF and the 3° amido functionality (in α-position of the ethyl ester carbonyl) could also have aided the ester aminolysis, respectively via stabilisation of the zwitterionic tetrahedral intermediate and via the -I effect of the 3° amide nitrogen (increasing the ethyl ester carbonyl electrophilicity). Hence, the ethyl ester aminolysis could have resulted in the formation of a cyclic (δ-lactam) thyminyl-PNA-monomer (See **Figure 2.9** above).

Although the latter side-reaction was never thoroughly investigated it seems a more plausible explanation for the complications in step *iii* than the assumption, at the time of the experiment, that the hydrolysis-sensitive nature of the acridine acid chloride **4** and the hygroscopic nature of the PNA-monomer TFA salt **14** were, to a degree, incompatible. Although the latter 'hydrolysis' hypothesis was also unsatisfactory, as we had thoroughly dried solvent (DMF) and starting materials for the coupling step (*iii*), it led us to investigate an alternative approach in which the order was changed in which the PNA-acridine components (acridine, PNA monomer backbone and nucleobase moieties) would be linked to each other (as detailed in **Scheme 2.18** below).

2.8 Alternative PNA-acridine synthetic strategy in the 'Denny route' approach

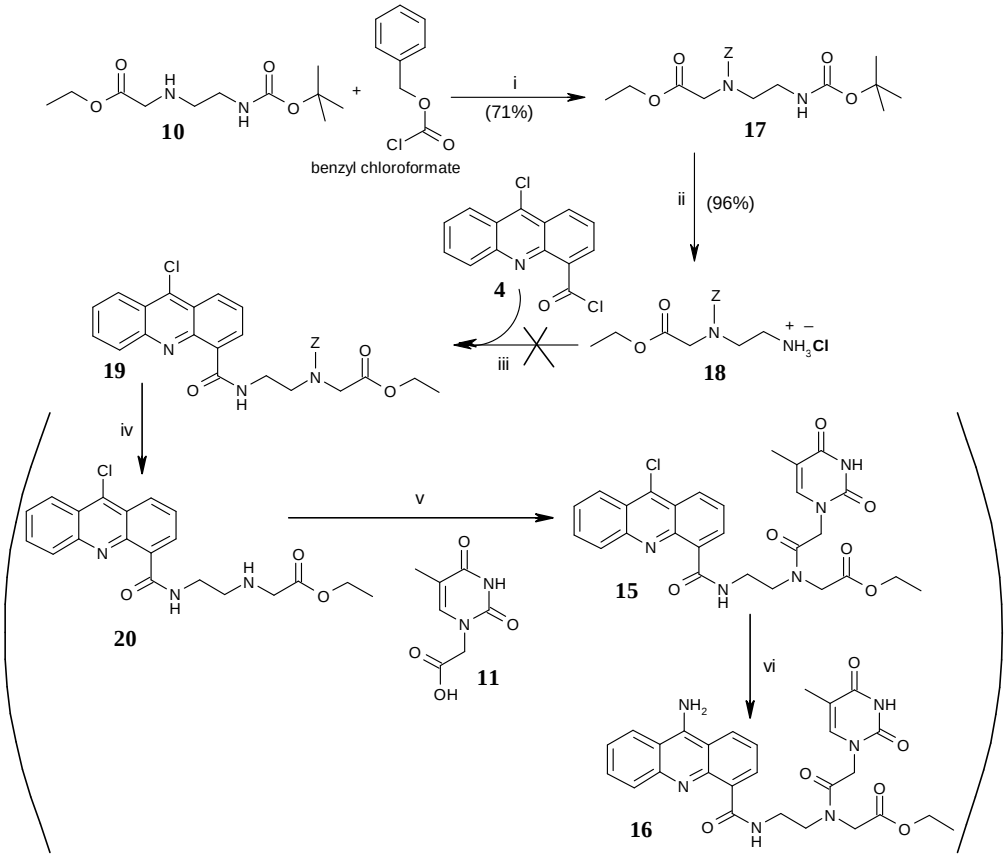

Reagents and Conditions: i 0.4 M Na_2CO_3 aq., DCM, 0℃-20°, ii HCl sat. Ethanol, rt; iii DIPEA; $CHCl_3$, rt; iv HBr in acetic acid; v HBTU, DIPEA; DMF; rt; vi a) phenol, 50℃ b) NH_3, 115℃

Scheme 2.18: Attempted alternative synthesis of a PNA-acridine conjugate

In **Scheme 2.18** above, our intention was to avoid the water-sensitive carboxamide formation step between 9-chloroacridine-4-carbonyl chloride (**4**) and the free base of

the (hygroscopic) salt of the polar nucleobase-bearing PNA monomer (**14**) (as described earlier in **Scheme 2.14**). Hence, this alternative synthetic pathway would involve coupling of the polar nucleobase moiety **11** to the PNA monomer backbone moiety, after the PNA backbone **10** had been joined to the intercalator moiety, as in **20** (see **Scheme 2.18**). Conveniently, for the coupling of the Z-protected PNA monomer backbone (**18**) to the acridine acid chloride **4**, we would be able to use chloroform as solvent instead of the more hygroscopic DMF although, admittedly, this was significant only in the light of the 'hydrolysis' hypothesis mentioned earlier as interfering with the coupling step *iii* in **Scheme 2.14** and **2.17**.

Unfortunately again, **Scheme 2.18** could not be completed successfully as step *iii* did not yield the hoped for conjugate **17**. The attempted steps outlined above will be discussed in the following subsections.

2.8.1 Step i: Z-protection of the t-Boc-protected PNA-monomer backbone 10

In the first step of **Scheme 2.18**, the secondary amine of the (*t*-Boc-protected) PNA monomer backbone **10** was protected by a benzyloxycarbonyl group via reaction of **10** with commercially available benzyl chloroformate to yield **17** (see also **Scheme 2.19** below). In our strategy, Z-protection step was necessary to avoid later reaction of the secondary amino group of **10** with the acridine's acid chloride group in **4.**

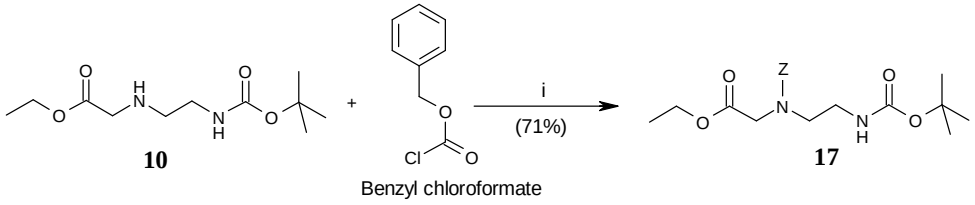

Reagents and Conditions: i 0.4 M Na_2CO_3 aq., DCM, 0℃-20℃

Scheme 2.19

The protection step was done according to a procedure described by Carbonnel *et al*. in which the secondary amine of a piperidine group was Z-protected by benzyl chloroformate.[209] We found that the procedure of Carbonnel worked well for our purposes and obtained a 71% yield for **17**. Micro-analysis and ^{1}H-NMR analysis confirmed purity and structure of **17**, and showed the presence of two rotational isomers for **17** due to restricted rotation about the tertiary amide bond, as was the case

for the PNA monomer **13** and its salts **14** and **21** (as described in **Scheme 2.14**), albeit in a ratio closer to 1:1 for **17** rather than the 2:1 ratio described earlier for the thyminyl-bearing PNA monomer intermediates **13**, **14** and **21**. This ratio difference existed presumably due to the non-polar character of the benzyl moiety for which interactions with the different functionalities of the PNA backbone were less energetically differentiated compared to the more polarised thyminyl moiety in **13**, **14** and **21.**

2.8.2 Step ii: t-Boc-deprotection of the Z-protected PNA-monomer backbone 17

In the subsequent step (*ii*), compound **17** was selectively *t*-Boc deprotected by treatment with HCl-saturated ethanol, generating the HCl salt of the Z-protected PNA monomer **18** in a 96 % yield (see **Scheme 2.20**). HCl-saturated ethanol was used here instead of the usual TFA solution because earlier use (See Boc-deprotection of **13** in **Scheme 2.16**) had shown it produced an easier to handle salt.

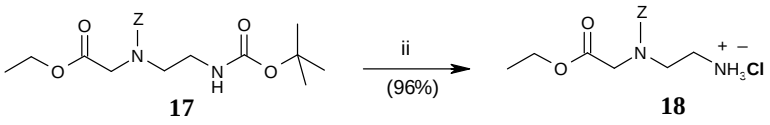

Reagents and Conditions: ii dry ethanol saturated with HCl; rt

Scheme 2.20

In the ^{1}H-NMR spectrum of **18**, absence of the *t*-Boc signal was a key feature suggesting successful deprotection. Further NMR analysis confirmed the structure of **18** and, as expected, showed the presence of two rotational isomers due to restricted rotation about the tertiary amide bond.

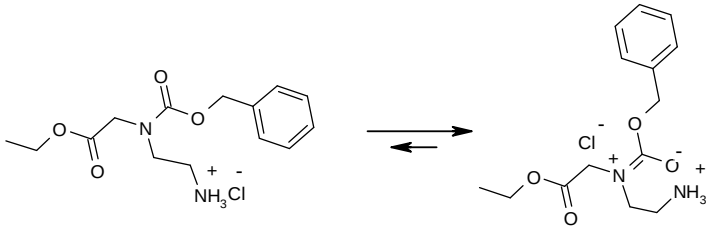

Figure 2.10: the rotameric equilibrium for **18** is possibly favoured by electrostatic interaction in an intramolecular ring conformation.

Although the rotamer ratio for the starting material **17** had been closer to 1:1, for **18** this ratio was nearer to 2:1, possibly due to a favourable electrostatic interaction of the carbamate carbonyl oxygen to the ammonia hydrogens in an intramolecular ring conformation. (See **Figure 2.10** above)

2.8.3 Step iii: linking the acridine moiety 4 to the Z-protected PNA-monomer backbone 18.

The coupling of **18** to the acid chloride functionalized intercalator moiety **4** was investigated next. In this reaction, the free 1° amine group of **18**, after being liberated from its salt by DIPEA, was expected to nucleophilically attack the acid chloride carbonyl of **4**. If successful, this would yield the desired conjugate **19** (see **Scheme 2.21** below).

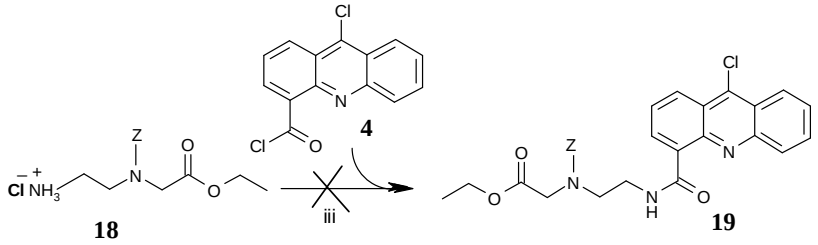

Scheme 2.21

For this coupling reaction we used chloroform as a solvent rather than DMF, used previously in **Scheme 2.17**. Assuming that hydrolysis susceptibility of the acid chloride **4** had interfered with the coupling step to the PNA monomer backbone (in **Scheme 2.17**), we reasoned that the lower hygroscopic nature of chloroform would improve the stability of the acid chloride **4** during the course of the reaction. Furthermore, since chloroform was still a reasonably polar organic solvent, we felt that the solvation of the now less polar starting materials would not be compromised too much. The carboxamide formation reaction in step *iii* was monitored by TLC which showed conversion of the starting material into a number of potential (yellow) candidate spots for compound **19**. The lower polarity of the products of this coupling reaction (compared to the products formed in the coupling step to the thyminyl-PNA-monomer discussed earlier for **Scheme 2.17**) allowed us to subject the reaction mixture

residue to flash column chromatography. However, TLC analysis of the collected fractions showed (a) consistent presence of (presumably co-eluted) polar side-product(s) in all the collected fractions. Subsequent analysis of the ^{1}H- and ^{13}C-NMR spectra of the collected fractions contaminated with the impurities, indicated they were not negligible. This was concluded from observations in the ^{1}H-NMR spectrum in which the pattern of aromatic proton signals was complex and uninterpretable in terms of number of signals and their multiplicity. In order to find out if **19** was present in the collected fractions we decided to attempt to crystallise the obtained solids in different solvents, e.g. in ethyl acetate (good solvent) / petrol ether (bad solvent), in dichloromethane and in methanol. Unfortunately, repeated crystallisation attempts resulted only in precipitation of a very fine yellow powder that failed to show a significant increase in purity of any relevant compound present, in ^{1}H-NMR analysis.
In our opinion, the complication suggested earlier for the coupling of the thyminyl-PNA-monomer **14** to the acridine acid chloride **4** (**Scheme 2.17**), i.e. intra-molecular ring closure, were occurring here as well. The Z-protected-PNA-monomer backbone would have reduced, to a degree, the polarity of the product(s) but again, the presence of excess of DIPEA to liberate the Z-protected PNA monomer **18** from its salts, prior to the addition of acridine acid chloride **4,** could have led (even at 0°C) to the same type of by-product as discussed/depicted in **Figure 2.9**.

In hindsight, admittedly, for the problematic coupling steps of the acridine acid chloride **4** with the PNA monomer moieties **14** and **18**, at the time of the experiment, the possible formation of by-products due to cyclization of the PNA monomer moiety, had been overlooked. For the coupling steps, a potentially better approach could have been to slowly add the DIPEA to a cooled mixture (0°C or lower) of both the acridine acid chloride **4** and the PNA monomer moiety **14** or **18**. This might have prevented the intra-molecular ethyl ester aminolysis, caused by the excess of DIPEA, present in our experiments to deprotonate the 1° amino group in **14** and **18,** prior to addition of the acid chloride **4**. However, as this reasoning was purely hypothetical, further experiments would need to be done to investigate whether this altered approach would lead to an improvement.
At the time of our experiments, failure to obtain the desired PNA-acridine conjugates had been attributed to a hydrolytic sensitivity of the acridine/PNA coupling step. Although this hydrolytic sensitivity needs to be taken into account in the reaction

conditions, it now seems less likely this was the main reason for failure of the coupling steps.

Finally, we concluded that, since we had spent a lot of time on this strategy and since the problems encountered did not appear to be easily surmountable, the 'Denny route' approach should be abandoned at this stage in favour of investigating other routes. Subsequently, one of the other routes towards PNA-acridine conjugates that we decided to investigate was based on the findings reported by Beal *et al*. [180], which dealt with the solid-phase synthesis of acridine-peptide conjugates. This shall be described in more detail in the following section.

2.9 The 'Beal route'

In 2000, Beal *et al*. reported the development of a strategy for the solid-phase synthesis of acridine-peptide conjugates to enable libraries of acridine-peptide to be generated.[210] It was envisaged that these would lead to the discovery of new structure-specific nucleic acid ligands. We were inspired by the fact that these conjugates bore the 9-anilinoacridine-4-carboxamide moiety, similar to our intended PNA-acridine conjugates. We will discuss Beal's synthesis of acridine-peptide conjugates, illustrated in **Scheme 2.22** below, and subsequently discuss how we utilised a similar strategy to prepare our PNA-acridine conjugates, illustrated in **Scheme 2.23**.

Beal started off, in step *i* of **Scheme 2.22**, with the conversion of the known 9-acridone-4-carboxylic acid **3** into its *iso*-propyl ester **22** via reaction of **3** with the coupling agent carbonyldiimidazole (CDI) and *iso*-propanol in tetrahydrofuran. Compound **22** was obtained in a 95% yield after work-up. The starting material 9-acridone-4-carboxylic acid **3** was synthesised by Beal, in two steps, according to Denny's method [187], in which commercially available 2-chlorobenzoic acid and anthranilic acid were conjugated, followed by a ring-closure step which generated the 9-acridone-4-carboxylic acid **3**. Reaction conditions for synthesis of **3** were similar to the ones we described earlier for the synthesis of 9-amino-DACA (**6**) in **Scheme 2.5** and step *ii* of **Scheme 2.3** (except for the use of methyl anthranilate in **Scheme 2.5** instead of anthranilic acid here). In step *ii* of **Scheme 2.22** Beal converted the *iso*-propyl ester **22** to the triazole intermediate **25** by treatment of **22** with the triazolating agent phosphoryl tristriazolide formed from phosphorus oxychloride, 1,2,4-triazole and triethylamine.

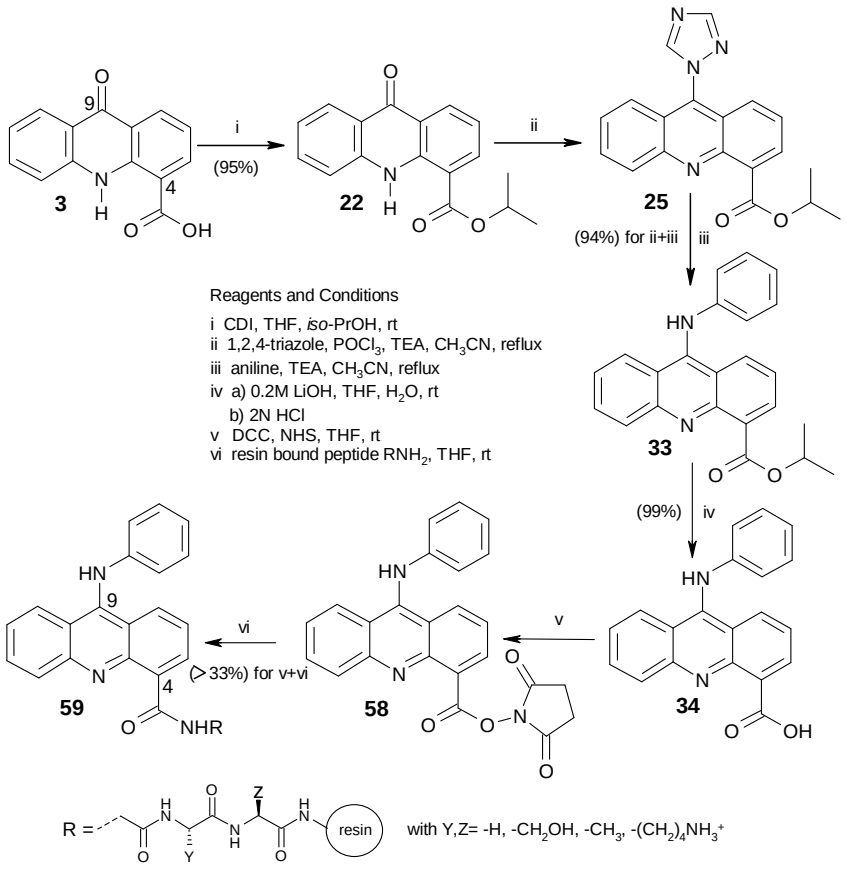

Scheme 2.22: Beal's synthesis of an acridine-peptide library.

The triazole-bearing intermediate **25** was not isolated by Beal but used directly in the following step *iii* of **Scheme 2.22**. With the triazolyl leaving group in place, treatment of **25** with aniline in acetonitrile, in the presence of triethylamine, gave the *iso*-propyl-9-anilinoacridine-4-carboxylate **33** in a 94% yield over the two steps. Subsequently, in step *iv*, **33** was treated with aqueous lithium hydroxide after which the reaction mixture was acidified with aqueous hydrochloric acid to yield the 9-anilino-acridine-4-carboxylic acid **34** in a 99% yield. In the next step *v*, the carboxylic acid group of **34** was activated as the *N*-hydroxysuccinimide (NHS) ester, by treatment of a solution of **34** and NHS, in tetrahydrofuran, with 1,3-dicyclohexylcarbodiimide (DCC). Without further characterization and after removal of dicyclohexylurea, Beal used the residue containing *N*-hydroxysuccinimidyl-9-anilinoacridine-4-carboxylate **58** in the subsequent amidation step with the free N-terminus of a solid support bound tripeptide to yield **59.** After cleavage from the solid support and work-up the (representative)

acridine-tripeptide ACR-Gly-Ala-Ala-NH_2 was obtained in a 33% yield over two steps (relative to the 9-anilino-acridine-4-carboxylic acid **34** starting material)

Hence, in summary, one of the main strategic differences between the 'Denny route' and the 'Beal route' is that, contrary to Denny's route, in Beal's protocol an amino group (anilino) is introduced at the 9-positon before the carboxamide is generated at the acridine's 4-position. In order to convert the acridine's 9-hydroxy group (in **3**) into an amine, the 4-carboxyl was protected as a hindered *iso*-propyl ester (as in **22**) after which the 9-oxo functionality could be converted into a triazol-1-yl substituent (as in **25**). The latter primed the 9-position for substitution with nitrogen (and oxygen) nucleophiles (like aniline in step *iii*).[210] Once the 9-amino (anilino) group was in place in **33**, Beal used standard peptide synthesis procedures in step *v* to activate the 4-carboxylic acid group of **34** (generated after *iso*-propyl ester deprotection in step *iv*) for carboxamide formation with the free amino terminus of an oligopeptide (step *vi*).

Beal's synthesis of the resin-bound tripeptides and cleavage from the solid support after the amidation step *vi* in the above **Scheme 2.22** will not be discussed here as, at this stage, they are not relevant to our use of Beal's strategy in preparing our own conjugates. Although Beal applied solid-phase synthesis when coupling oligopeptides to an activated 9-anilinoacridine-4-carboxylic acid we were at this stage attempting to couple a PNA monomer (as opposed to peptide oligomers in Beal's procedure) to the activated acridine acid, thereby effectively using solution phase chemistry one step further than in Beal's procedure (i.e. in the acridine's 4-carboxamide forming step).

2.10 Synthesis of PNA-acridine conjugates (via the 'Beal route')

In this section we will discuss how we used Beal's strategy in attempting to synthesise our own PNA-acridine conjugates and rationalise and compare our findings to Beal's results. Our synthetic strategies towards a PNA-acridine conjugate according an initial adaptation of Beal's protocol is outlined below (**Scheme 2.23**). Unlike in the procedure of Beal, we elected to use the methyl ester (**2** in **Scheme 2.23**) rather than the acridine acid (**3** in **Scheme 2.22**) as our starting material for all routes. The reasons for this were two-fold. Firstly, we had already made this compound (**2**) for the 'Denny route' from readily available starting materials and secondly, in our hands, we got a significantly higher yield for the synthesis of the next intermediate, *iso*-propyl ester (77%) (**22** in **Scheme 2.23**), by obtaining it via a transesterificiation of the methyl ester precursor (**2** in **Scheme 2.23**) rather than by esterification of the acid (51%) as Beal did (**3** in **Scheme 2.22**). We also decided that it would be worthwhile to investigate the potential of using a sterically more hindered *t*-butyl ester (as in **23** in **Scheme 2.23**) or even simply the methyl ester (**2** in **Scheme 2.23**) at this stage of the synthetic route, to find out if different 4-carboxyl protection groups would result in better over-all yields further down the line. In terms of the latter consideration, for the *t*-butyl ester **23** the potential advantage yield-wise was that it would potentially allow for a subsequent milder deprotection step (compared to an *iso*-propyl ester hydrolysis). For the methyl ester **2** the issue was whether it would survive the harsh conditions of the aromatic substitutions in steps *v* and *vi* of **Scheme 2.23.**

As in Beal's procedure in **Scheme 2.22**, we synthesised alkyl-9-triazolylacridine-4-carboxylate intermediates **24, 25** and **26** in order to activate them for substitution at the 9-position (conversion of oxygen-substituted heterocycles to triazoles activated them to react selectively with a number of different nitrogen and oxygen nucleophiles under mildly basic conditions [210]). Different from Beal's procedure was that we chose to use benzylamine instead of aniline to substitute the 9-triazolyl group in order to establish the acridine's 9-amino functionality. This was done to allow for later generation of a primary amino functionality through hydrogenolysis of the 9-benzylamino substituent. A detailed discussion of the individual steps of **Scheme 2.23** now follows.

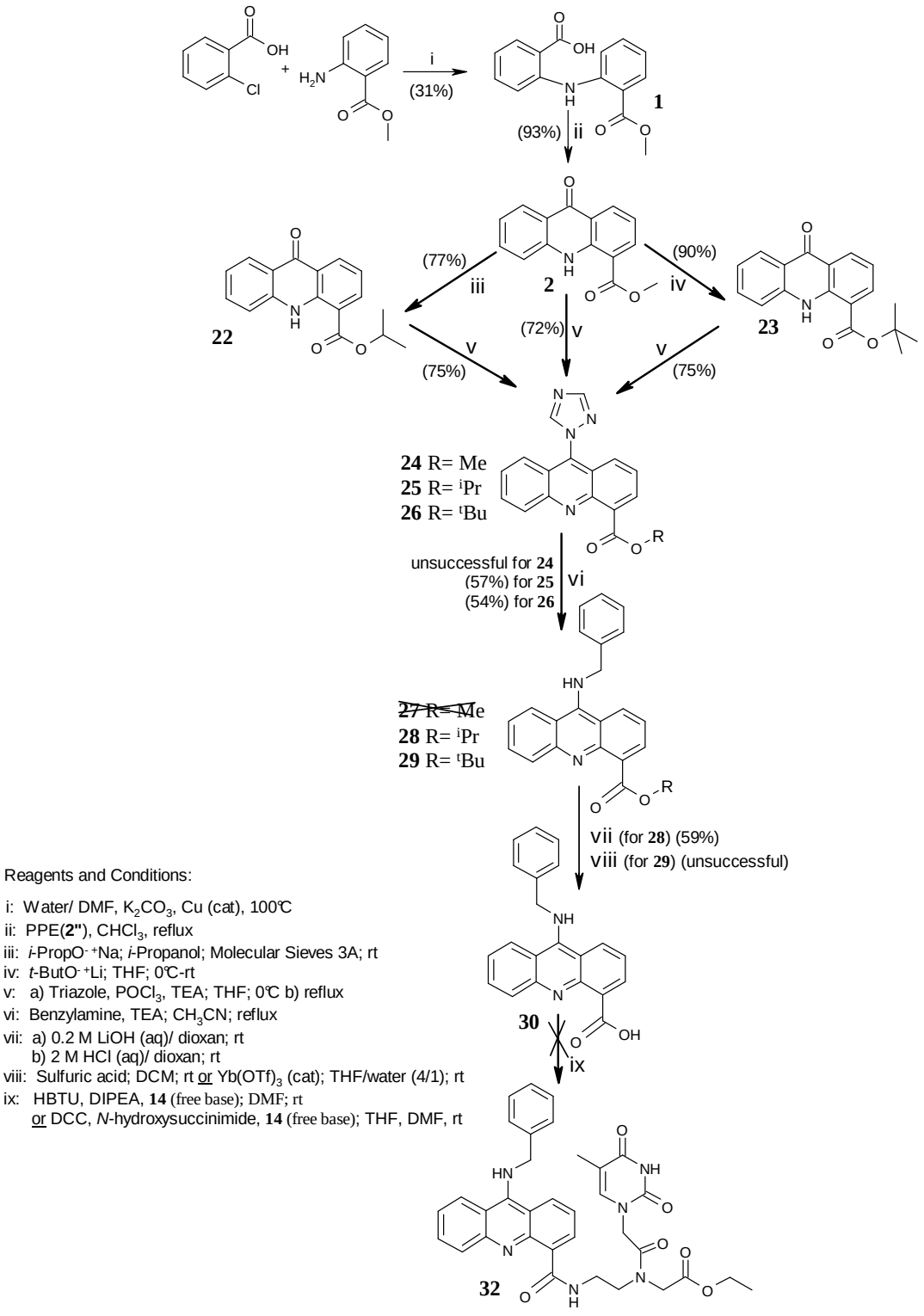

Scheme 2.23: 'Beal routes' to a PNA-acridine conjugate.

2.10.1 Steps i and ii: generating the acridine intermediate 2

Synthesis of compounds **1** and **2** was discussed in section 2.4: Synthesis of 9-amino-DACA.

2.10.2 Step iii: transesterifying the acridine methyl ester (2) into the acridine iso-propyl ester (22)

Methyl-9-oxoacridan-4-carboxylate (**2**) was transesterified according a procedure described by Roelofsen *et al*. [211] (see **Scheme 2.24** below)

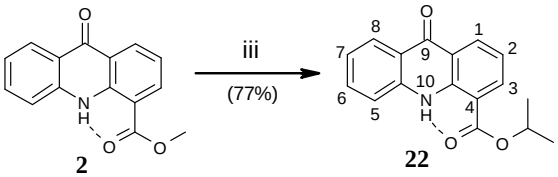

Reagents and Conditions:
iii: *i*-PropO^{-} $^{+}$Na; *i*-Propanol;Molecular Sieves 4A; rt

Scheme 2.24

This involved treatment of an *iso*-propanol solution of methyl ester **2** with sodium *iso*-propoxide, in the presence of 4Å molecular sieves (~ 0.6 g / mmol ester) to selectively absorb the released methanol, which resulted in a smooth trans-esterification which afforded **22** in a 77% yield.

Generally, the position of the equilibrium in a transesterification reaction will depend on the nature of both alcohol and ester.[212] Hence, in order to (swiftly and quantitatively) shift the equilibrium towards the *iso*-propyl ester (in step *iii* in **Scheme 2.24** above), the replacing alcohol (*iso*-propanol) was used as solvent and an equimolar amount of the more nucleophilic *iso*-propoxide was used to displace the methoxy group (in the starting material **2**) which was subsequently removed from the reaction mixture as methoxide/methanol by absorption onto the 4Å molecular sieves (inner and outer surface). Hence, the 4Å molecular sieves functioned here as a convenient alternative to the usual azeotropic removal of the unwanted alcohol to push the equilibrium towards the *iso*-propyl ester. Some *iso*-propoxide/*iso*-propanol absorption may have occurred on the outer surface of the 4Å molecular sieves as well (not within the actual beads due to the excluding 4Å pore-size) but clearly not to the extent it would interfere (on the

reaction time scale) with the activity of the *iso*-propoxide nucleophile. Regarding the latter problem, the amount of molecular sieves used seems important and should be no more than required to absorb the substituted methoxide/methanol. In the above experiment the proportion of molecular sieves used (~ 0.6 g / mmol ester) was based on a dimethylterephthalate→di-*t*-butylterephthalate transesterification in benzene/t-butanol/K^{+-}*t*-butoxide at 80°C performed by Roelofsen *et al*.[211] Although this worked reasonably well for our purpose (TLC monitoring of the reaction suggested quantitative conversion), some irreversible absorption of the product onto the sieves reduced the final yield of **22** to 77%. Hence, ideally, for different reactions, the optimal ester/sieves ratio should be determined experimentally, while the chosen pore-size should lead to selective absorption of the substituted alcohol. In addition, suitable crystals of **22** (re-crystallised from methanol) were obtained which allowed for X-ray crystal structure determination. From this structure it was apparent that H-bonding was occurring between the ring N(10)H and the carbonyl oxygen. Key bond distance and torsion angle values obtained from the crystal data experiment (see also Appendix) were: 124 pm for C(8)-O(1) (indicating a double bond and confirming the 9-oxoacridane was the crystallised tautomer for **22**) and a torsion angle of 2.8° for C(14)-C(13)-C(15)-O(3) which brought the H·····O distance in N(1)-H(1)·····O(3) to196 pm, which was within the normal H-bond distance range (see **Figure 2.11** below for X-ray structure of **22**).

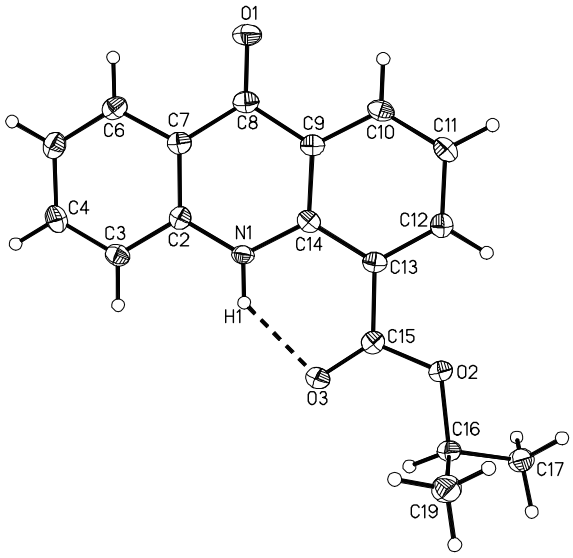

Figure 2.11: X-ray structure of *iso*-propyl-9-oxoacridan-4-carboxylate (**22**)

The intramolecular H-bonding had been suggested earlier and ^{1}H-NMR spectra analysis for relevant compounds e.g. the acridine-based methyl ester **2**, the acridine-based acid **4** and 9-amino-DACA **6**, supported this. The X-ray crystal structure for **22** now confirmed our assumption, the significance of which was that it indicated a pattern that will be further discussed at a later stage, when the acridine 4-carboxyl group requires activation towards coupling with the PNA monomer.

Key features of the ^{1}H-NMR recorded for **22** were the appearance of a doublet at δ 1.36 and a septet at δ 5.24 for the *iso*-propyl hydrogens but also the lack of the methyl group singlet at δ 4.00 which had been present in the ^{1}H-NMR spectrum of **2**. The most downfield signal at 11.71 ppm was assigned to N(10)H, its high value being attributed to the hydrogen-bonding with the carbonyl oxygen of the ester moiety.

2.10.3 Step iv: transesterifying the acridine methyl ester (2) into the acridine t-butyl ester (23)

To convert the methyl ester **2** into the *t*-butyl ester **23**, initially Roelofsen's transesterification method was applied, i.e. the use of sodium *t*-butoxide in tetrahydrofuran and in the presence of molecular sieves (4Å). However, transesterification under these conditions proved to be very slow (only partial conversion showed after 24 hours at 40°C). We found that another procedure, for the transesterification of aromatic methyl esters according to Meth-Cohn [213], enabled us to convert, at room temperature, the methyl ester **2** into the *t*-butyl ester **23,** faster and, based on TLC analysis, apparently quantitatively.

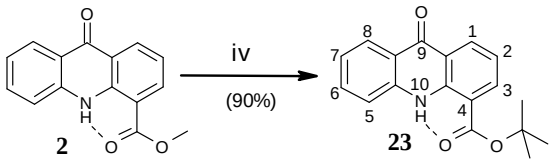

Reagents and Conditions: iv: *t*-BuO$^-$ $^+$Li; THF; 0℃-rt

Scheme 2.25

This procedure involved treatment of the methyl ester **2** with the lithium salt of *t*-butanol (see **Scheme 2.25** above). We found that the use of up to 7 equivalents of the *t*-butanolate was required to achieve complete conversion after 24 h. Subsequent work-up led to a very good 90% yield for **23**. The success of this transesterification was

attributed to the lower pK_a of methanol compared to the higher, branched alcohols resulting in the favourable equilibration and to the strong complexation of lithium salts to the ester carbonyl.[213] We can assume that the ester carbonyl oxygen-Li complexation increased the ester carbonyl carbon electrophilicity, thereby facilitating nucleophilic attack of the *t*-butoxide oxygen. The key features in the ^{1}H-NMR spectrum of **23** were the appearance of the *t*-butyl singlet at δ 1.60 (and the lack of the methyl group singlet at δ 4.00 present in the ^{1}H-NMR spectrum of **2**).

2.10.4 Step v: activating the acridine's 9-position towards subsequent substitution.

Intermediates **2, 22** and **23** were successfully substituted with a 1,2,4-triazole group at the 9-position of the acridine ring, yielding **24, 25** and **26** respectively, according to the protocol described by Beal.[210] (see **Scheme 2.26** below)

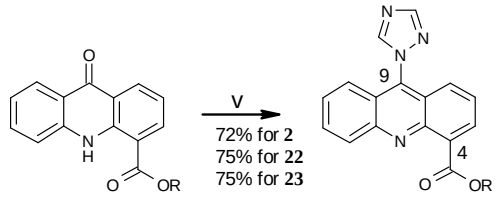

2 R=Me
22 R=^{i}Pr
23 R=^{t}Bu

24 R=Me
25 R=^{i}Pr
26 R=^{t}Bu

Reagents and Conditions: v: a) Triazole, $POCl_3$, TEA; THF; 0℃ b) reflux

Scheme 2.26

The active reagent in this substitution was the tri(1,2,4-triazol-1-yl) phosphine oxide (or phosphoryl tris-triazole) which was prepared *in situ*. Tri(1,2,4-triazol-1-yl) phosphine oxide was developed/used originally for the preparation of nucleoside 3'-phosphotriester intermediates in oligonucleotide synthesis.[214] In the latter preparations the initially formed nucleoside 3'-di(1,2,4-triazol-1-yl)-phosphomonoester (from reaction of the phosphoryl tris-triazole with the 3'-OH of a nucleoside) was treated with the appropriate alcohol(s) at room temperature to generate the nucleoside 3'-phosphotriesters. However, in our case, and as suggested by the above **Scheme 2.26,** the initially phosphorylated acridine presumably underwent substitution in the 9-position with a triazolide anion, generating the 9-triazolyl substituted acridine (see **Figure 2.12** below for our suggested reaction mechanism). Compared to the 'original' phosphotriester generating reactions, performed by Kraszewski and Stawiński (at room

temperature over a maximum of 24 hours), our reaction required reflux temperatures (~70°C) for 96 hours in order to allow, initially, the acridine's phenolic 9-OH substituent to displace a triazolyl group in the phosphoryl tris-triazole and secondly, to allow a weakly nucleophilic triazolide to substitute the generated di-triazolyl phosphomonoester in the 9-position of the acridine. Presumably, the first step was the faster one as, in the presence of excess TEA, the acridine 9-OH was deprotonated and should more easily displace a triazolyl (good leaving group) in the phosphoryl tris-triazole reagent. It is unlikely that the generated ditriazolylphosphinate anion, due to its charge, would serve again to phosphorylate the acridine in the 9-position. However, these are hypothetical assumptions and the exact reaction mechanism should be determined via further investigation.

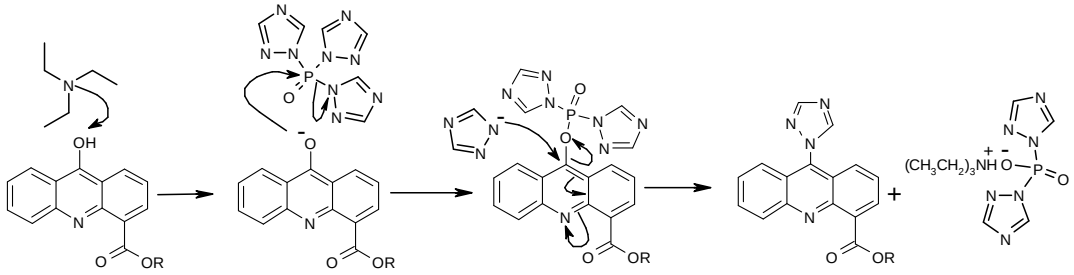

R=Me (**2**); R=^{i}Pr (**22**); R=^{t}Bu (**23**)

Figure 2.12: suggested S_NAr reaction mechanism for the triazolylation of acridine intermediates **2**, **22** and **23**.

Contrary to Beal, we isolated and characterized all three triazolyl-containing acridines **24** (72% yield), **25** (75% yield) and **26** (75% yield)**.**

^{1}H-NMR and ^{13}C-NMR analysis of compounds **24**, **25** and **26** confirmed their structures. Key features in the ^{1}H-NMR spectrum of all three compounds were the appearance of the two triazole proton singlets at δ 8.32 and 8.52 and the disappearance of the NH signal at δ 11.65.

The purpose of generating 9-triazolylated intermediates was, as mentioned earlier, to activate them for substitution at the 9-position with benzylamine, as discussed in the next step *vi*. The relatively facile substitution of the 9-triazolyl group again could be attributed to it being a good leaving group (triazolide is a weak nucleophile/base).

2.10.5 Step vi: generating the 9-benzyl amino substituted acridine esters 27, 28 and 29

Substitution of the triazolyl group in compounds **24**, **25** and **26** with benzylamine was performed according an adapted protocol of Carlson and Beal.[210] (see **Scheme 2.27** below)

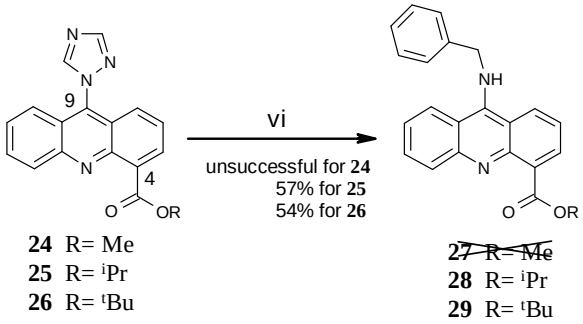

Scheme 2.27

This involved heating the triazolylated starting material and the benzylamine at reflux temperature, in the presence of triethylamine. Carlson and Beal describe the 9-triazolyl substitution of **25** with aniline. However, we chose to investigate substitution with benzylamine because we intended to remove the benzyl group in the final step (after coupling of the acridine chromophore to the PNA) by hydrogenolysis, to afford the desired PNA-acridine conjugate. For the 9-triazolyl-acridine-4-methyl ester (**24**) we expected substitution at the 9-position of the acridine ring as well as some substitution at the methyl ester carbonyl, giving the (undesired) disubstituted by-product benzylamine-9-benzylaminoacridine-4-carboxylate **27*** (See **Figure 2.13** below).

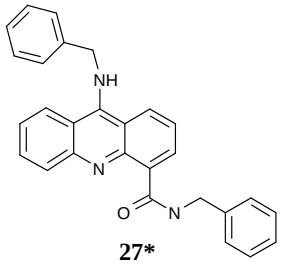

Figure 2.13: Treating the 9-triazolyl-acridine-4-methyl ester (**24**) with benzylamine mainly led to the disubstituted benzylamine-9-benzylaminoacridine-4-carboxylate **27***.

We were however hopeful that, due to some steric hindrance, the latter substitution might be minimal. However, post work-up ^{1}H-NMR analysis of columned active fractions suggested that mainly the disubstituted by-product **27*** had formed and none of the desired monosubstituted benzyl amino methyl ester **27** was observed. Although this was not unexpected we had considered this reaction worthy of investigation (even if a lower yield of the desired mono-benzylaminosubstituted **27** had been obtained) as it would have spared us from undertaking a transesterification reaction on the methyl-9-oxoacridan-4-carboxylate **2**.

With *iso*-propyl-9-triazolylacridine-4-carboxylate (**25**), we were able to selectively substitute only the 9-triazolyl substituent. This was due to the fact that the *iso*-propyl group sterically hindered the carbonyl group thereby making ester aminolysis unfavourable. The desired 9-benzylamino acridine *iso*-propyl ester **28** was afforded in a 57% yield after work-up. A similar result was also achieved with *t*-butyl-9-triazolylacridine-4-carboxylate (**26**), giving 9-benzylamino acridine *t*-butyl ester **29** in a 54% yield. Unfortunately, no reliable melting points could be taken for **28** and **29** due to the oily character of the products)

For both **28** and **29**, ^{1}H-NMR analysis showed the presence, in a 2:1 ratio, of Z- and E-isomers (due to restricted rotation about the C9-N bond) which could interconvert through a zwitterionic intermediate shown in **Figure 2.14** below. It was not determined which diastereomer was prevalent (but further 2-D NMR NOE experiments and a crystal structure could clarify this).

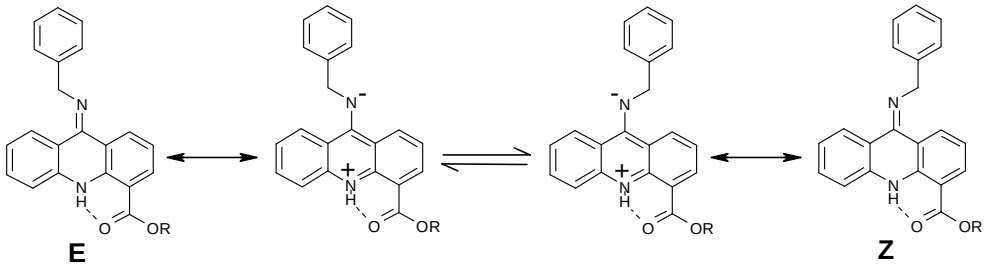

interconversion of E and Z isomers for compounds **28** (R= ^{i}Pr) and **29** (R= *t*-Bu)

Figure 2.14

2.10.6 Steps vii and viii: hydrolysis of alkyl-9-benzylaminoacridine-4-carboxylates 28 and 29

The next steps *vii* and *viii* in the 'Beal route' involved deprotection of the esters **28** and **29**. A number of different approaches were attempted in order to maximise yields (see **Scheme 2.28** below). Firstly, we explored basic hydrolysis of the *iso*-propyl ester **28** as described by Beal *et al*. (step *iv* in **Scheme 2.22** earlier).

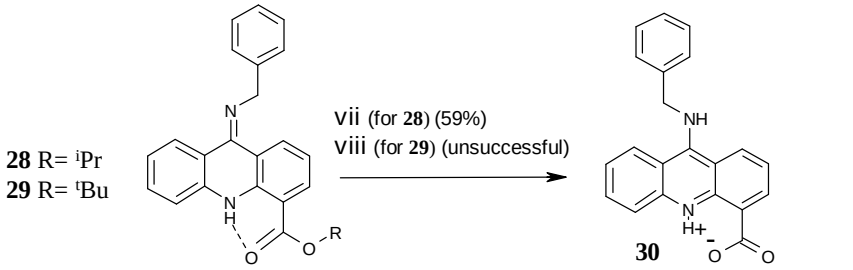

Reagents and Conditions:
vii: a) 0.2 M LiOH (aq)/ dioxan; rt b) 2 M HCl (aq)/ dioxan; rt-4℃
or NaI, $Si(CH_3)_3Cl$;CH_3CN/DCM (1/1); 90℃ (unsuccessful)
or $AlCl_3$; DCM; 0℃-rt (unsuccessful)
viii: Sulfuric acid; DCM; rt (unsuccessful) or $Yb(OTf)_3$ (cat);THF/water (4/1); rt (unsuccessful)

Scheme 2.28

Although we were successful in deprotecting the ester **28**, our work-up was different from Beal's (See **Scheme 2.22**) as our initial attempts to separate salts from product (**30**) by triturating the crude product with chloroform, as in Beal's procedure, were unsuccessful. In our alternative work-up (in which cooling of the neutral reaction mixture led to precipitation of **30**) 9-benzylaminoacridine-4-carboxylic acid (**30**) was afforded in a moderate 59 % yield. The ^{1}H and ^{13}C-NMR spectra, recorded for our obtained compound **30**, also showed the presence of Z-E isomers, but less obvious than for the *iso*-propyl ester **28**. For example, in the ^{1}H-NMR spectrum, the CH_2 signal didn't clearly split into two but was rather broad instead, which was also the case for the NH signals. A possible explanation for this would be that the C(9)-NH bond of the acid **30** has less double bond character, hence there was less impeded rotation of this bond compared to the analogous bond in the esters **28**. This could be the case because for a higher double bond character of $C(9)=NH^{+}$, the zwitterionic opposing charges would on average be (unfavourably) further apart. Hence, the more relevant canonical

structure for **30** would be as depicted in **Scheme 2.28** above (with the single C9-NH bond).

As our 59% yield for **30** was still low compared to the 99 % yield Beal *et al.* had obtained for the basic hydrolysis of their *iso*-propyl-9-anilinoacridine-4-carboxylate (**33** in **Scheme 2.22**) we wanted to explore other deprotection possibilities.

For example, following a protocol described by Olah *et al.*[215], we explored *iso*-propyl ester **(28)** cleavage via generation of the *in situ* equivalent of iodotrimethylsilane in the presence of the *iso*-propyl ester **28.** Subsequent aqueous work-up was expected to yield the free acid **30**. Olah's general reaction conditions for ester cleavage are illustrated in **Scheme 2.29** below.

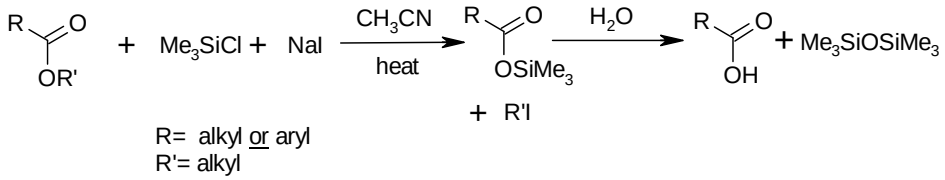

Scheme 2.29: ester cleavage reaction as reported by Olah *et al.* [215]

A similar dealkylation of alkyl esters with iodotrimethylsilane (not Olah's *in situ* equivalent) was reported earlier by Jung and Lyster.[216] However, due to a number of disadvantages linked to the preparation of iodotrimethylsilane (expensive, highly susceptible to hydrolysis, has to be prepared freshly and isolated from reaction mixture by distillation) Olah developed a more practical, cheaper way by using chlorotrimethylsilane and NaI in acetonitrile as an *in situ* equivalent for the iodotrimethylsilane.[215] Of note, Morita *et al.* reported these ester dealkylations did not occur without NaI nor was it possible to prepare iodotrimethylsilane from chlorotrimethylsilane and NaI.[217] According to Olah, initially a complex was formed between acetonitrile→trimethylsilyl and iodide driven by simultaneous and immediate precipitation of NaCl (See **Figure 2.15** below).

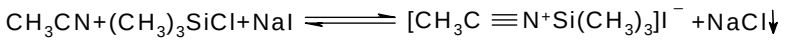

Figure 2.15: acetonitriletrimethylsilyl iodide complex formation described by Olah *et al.*[215]

Interestingly, the same complex was formed when using iodotrimethylsilane in acetonitrile. Subsequently and upon heating (to reflux temperature) a displacement/substitution of the acetonitrile by the ester carbonyl oxygen was suggested after which the associated iodide nucleophilically attacked the alkyl group (*iso*-propyl in our case) to generate an alkyliodide and the trimethylsilyl ester intermediate. In Jung's experiments with iodotrimethylsilane the latter was claimed to be the rate determining step. [216] (See **Figure 2.16** below).

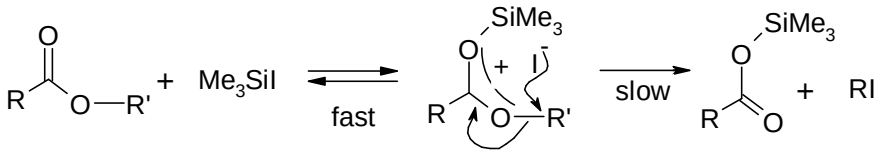

Figure 2.16: the ester dealkylation-mechanism via iodotrimethylsilane (according to Jung and Lyster [216])

Jung used DMSO or chlorinated solvents, not the acetonitrile which was assumed to be crucial in Olah's procedure in which the consequent NaCl precipitation drove the formation of the acetonitriletrimethylsilyl iodide complex.

Regarding our own experiment, in which we attempted to cleave the *iso*-propyl ester of **28**, TLC monitoring of the reaction suggested that even after sustained heating at reflux for over 72 hours little deprotection had taken place. A ^{1}H- and ^{13}C-NMR analysis of the crude reaction mixture residue suggested the *iso*-propyl ester **28** was still intact. In our opinion, the reason for this was the involvement of the ester carbonyl oxygen in H-bonding with the ring N(10)H which effectively reduced the carbonyl oxygen nucleophilicity required to displace acetonitrile in the acetonitriletrimethylsilyl iodide complex (See **Figure 2.15** earlier). Hence, it was likely no silylated ester iodide salt could form in our experiment.

Another *iso*-propyl ester cleavage attempt on **28** was inspired by Chee,[218] who had reported the selective deprotection of (aromatic and aliphatic) *iso*-propyl esters (i.e. not affecting other alkoxycarbonyl groups present) using aluminium trichloride, followed by aqueous work-up. According to Chee, "cleavage of the O-*iso*-propyl bond presumably occurred via the formation of a stable *iso*-propyl cation". We decided to explore this strategy next. Unfortunately, ^{1}H and ^{13}C-NMR analysis of the yellow precipitate afforded, after treatment of **28** with aluminium trichloride under conditions

described by Chee, showed almost exclusive presence of 9-aminoacridine-4-carboxylic acid **31** (yield 92%). Thus, both the *iso*-propyl and the benzyl protection groups had been removed in this reaction (see **Scheme 2.30** below for our suggested mechanism).

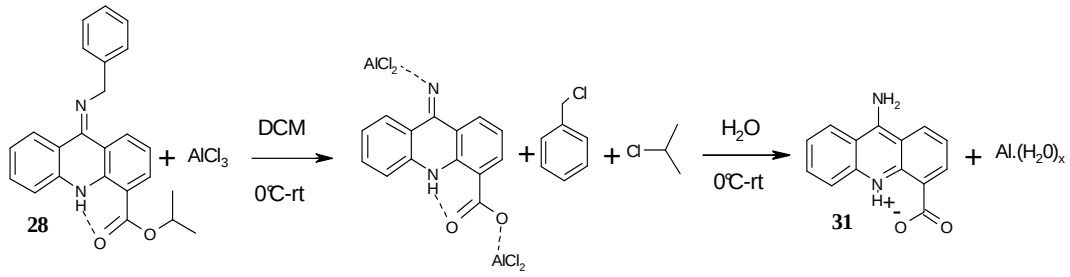

Scheme 2.30: both benzyl and *iso*-propyl protection groups were removed from **28** under selective *iso*-propyl ester deprotection conditions described by Chee *et al.* [218]

As the benzyl cation was a better leaving group than the *iso*-propyl cation, this outcome was far from unexpected. However, we believed the simple nature of this experiment had made it worth trying on a small scale.

So far our attempts to more closely match Beal's yield of 99% for the deprotection of *iso*-propyl ester **28** had been unsuccessful.

Regarding the alternative route to 9-benzylaminoacridine-4-carboxylic acid, via the *t*-butyl deprotection of ester **29,** two different approaches were attempted. Firstly, we decided to investigate a procedure selective for t-butyl ester cleavage, described by Sridhar *et al.*[219], which involved using catalytic $Yb(OTf)_3$ Lewis acid in nitromethane (solvent) under mild conditions (heating at 45°-50° C for 5 to 24 hours).

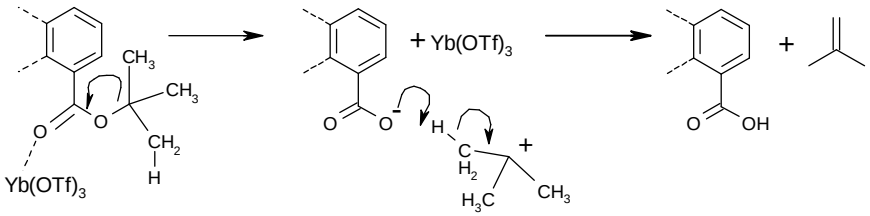

Scheme 2.31: proposed reaction mechanism for $Yb(OTf)_3$ catalysed selective *t*-butyl ester cleavage as described by Sridhar *et al.* [219]

No reaction mechanism was suggested by the author but we believe the described activation could possibly occur as follows: coordination of the carbonyl oxygen to the

$Yb(OTf)_3$ Lewis acid increases the electrophilicity of the carbonyl carbon thereby enabling the *t*-butyl cation to be released. Subsequently a proton is abstracted from the cation by a free (uncoordinated) carboxylate, thereby generating the acid product and *iso*-butene (see **Scheme 2.31** above).

Thus, a solution of **29** in nitromethane was treated with $Yb(OTf)_3$ and heated at 50°C for 18 h. Surprisingly, after work-up (and as already suspected based on TLC monitoring of the reaction) the NMR recorded on the crude product afforded showed it to be unreacted **29** (73 % recovered). In our opinion, the reason for this might (again) be competition between the acridine N(10)H and the Lewis acid for the carbonyl oxygen lone pair(s). A question one might ask is why the H-bonding here (between N(10)H and the ester carbonyl oxygen) would not also, to a degree, catalyse *t*-butyl ester cleavage. Although it wasn't investigated, we presume this probably is the case and perhaps explains why Beal, when synthesising the acridine-peptide conjugate library, chose for the less obvious *iso*-propyl ester to protect the acridine 4-carboxyl group.

A second procedure which we decided to explore (to cleave the *t*-butyl ester) was based on the work of Strazzolini *et al*. who had reported efficient cleavage of *t*-butyl esters using H_2SO_4 in dichloromethane.[220] Thus, the *t*-butyl-9-benzylaminoacridine-4-carboxylate **29** was treated accordingly and, after subsequent (partial) work-up, low resolution mass spectrometry and NMR analysis was performed on the crude product. Although both suggested that the desired carboxylic acid (**30**) may have been present, it was not in a significant amount and other unidentified products were present. Unfortunately, attempts to recrystallise **30** (or any of the other products) from the crude reaction mixture residue, using e.g. methanol, were unsuccessful. Presumably, the presence of the (acridine and benzyl) aromatic rings made it likely the latter products were sulfonated by-products, generated via aromatic electrophilic substitution in and on the concentrated sulphuric acid droplets in the (two-phase) emulsion of the sulphuric acid in dichloromethane. However, due to time constraints this was not further investigated at the time of the experiment.

Hence, based on our findings and the limited success in generating the 9-benzylamino acridine-4-carboxylic acid (**30**), we decided to abandon the *t*-butyl ester strategy for producing the desired PNA-acridine conjugates and to concentrate our efforts on the

iso-propyl route instead. After all, it had proved possible to cleave the *iso*-propyl ester group, under mildly basic conditions, to afford **30** in a moderate 59% yield.

2.10.7 Step ix: Coupling the PNA monomer 14 or 21 to the activated acridine acid 30

The coupling step was tried in two ways (see **Scheme 2.32** below).

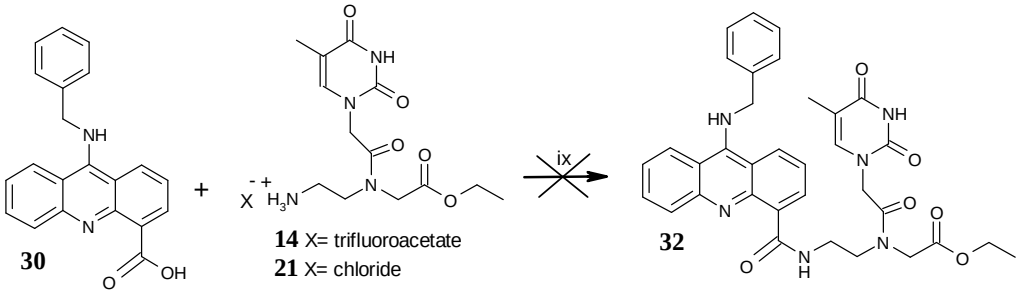

Reagents and Conditions: for **14**: HBTU, DIPEA ; DMF; rt
for **21**: DCC, *N*-hydroxysuccinimide ; THF,

Scheme 2.32

The first procedure was based on Beal's protocol (as in **Scheme 2.22**).[210] In order to couple a 9-anilinoacridine-4-carboxylic acid **30** to an oligopeptide, Beal had activated the acridine's 4-carboxyl group as the NHS ester using dicyclohexylcarbodiimide (DCC) in the presence of N-hydroxysuccinimide (NHS). Subsequently, a resin-bound oligopeptide had been added to yield the anticipated conjugate in 33% yield after cleavage from the solid support. However, a similar activation of our 9-benzylaminoacridine-4-carboxylic acid **30** with subsequent addition of the thyminyl-PNA-monomer (the free base of **21**) failed to lead to the desired PNA-acridine conjugate **32.** This was not completely unexpected because contrary to Beal's activation of his 9-anilinoacridine-4-carboxylic acid **34** (step v of **Scheme 2.22**), in our attempt to activate the acid **30** as the NHS ester, no solid dicyclohexylurea could be observed in the reaction mixture, even after stirring for 48 hours at room temperature. Subsequently, the free base of the thyminyl-PNA-monomer **21** was added to the reaction mixture. This was left stirring at room temperature for another 24 h. after which the reaction mixture was worked-up. Purification by flash column chromatography did not result in identification of the conjugate **32** in any of the collected fractions. Unclear on why DCC appeared not to be activating the carboxylic acid functionality of **30** we decided to use a different peptide coupling agent to see if

this would confirm our findings (i.e. the apparent lack of reactivity of the carboxyl group). The alternative procedure that we tried involved activation of **30** with HBTU (see **Scheme 2.33** for mechanism) rather than DCC (based on a procedure for peptide bond formation described by Schädel *et al.*[221])

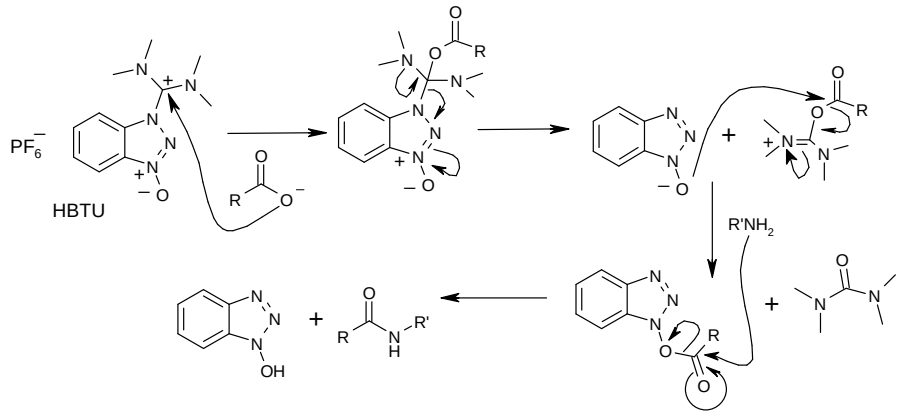

Scheme 2.33: general activation mechanism of a carboxylic acid with HBTU and subsequent peptide bond formation (Source: Li *et al.*, 2001, [222]).

Thus, a solution of **30** in DMF was treated with HBTU and DIPEA at room temperature and left stirring for 24 hours, after which the thyminyl-PNA-monomer (the free base of **14)** was added and the reaction mixture left stirring for another 24 h. After this time the reaction mixture was worked up but after purification by flash chromatography, again none of the desired conjugate **32** could be identified.

Without dismissing that successful coupling may still have been compromised by a competing cyclization side-reaction, mentioned earlier for the free base of the PNA monomer (**14** or **21**) (**Figure 2.9** p. 85), at this point it became clear that possibly the alkyl-9-benzylaminoacridine-4-carboxylate intermediate **30** was not compatible with Beal's pathway for producing 9-aminoacridine-4-carboxamides. In our opinion, the problem lay with the basicity of the heterocyclic ring nitrogen N(10) of 9-aminoacridine. We reasoned that, with a secondary amine group in the 9-position of acridine and with this amine linked to a methylene, the free electron pair of the exocyclic nitrogen in **30** only delocalised into the aromatic three-ring system of acridine. This would, in particular, increase the electron density on the heterocyclic ring nitrogen N(10) and make it more basic. This also partially accounted for the increased polarity observed on going from 9-oxo-acridans to 9-aminoacridines.

In addition to the above, the close proximity of the 4-carboxyl group of the acridine (in **30**) to the ring nitrogen N(10) increased the former's acidity and lead to the formation of a stable internal salt (zwitter ion), as depicted in **Figure 2.17** below. This made the 4-carboxyl group in **30** less susceptible to activation.

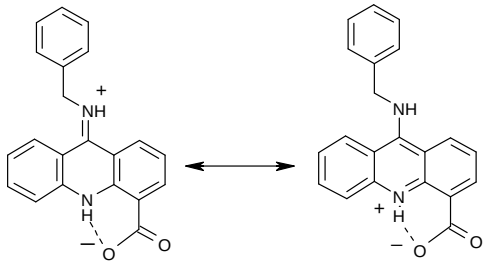

30

Figure 2.17: two canonical forms of zwitterion **30**

2.11 Investigating potential electronic effects of acridine's 9-anilino substituent on the acridine's ring nitrogen N(10) basicity.

The reasons mentioned above suggested that the exocyclic nitrogen of the 9-aminoacridine needed to be bound to a second moiety (beside the acridine system) involved in mesomeric delocalisation of the exocyclic nitrogen lone pair in order to allow for activation of the 9-aminoacridine's 4-carboxyl functionality.

We therefore decided to investigate the plausibility of this rationale by examining the ability of the analogous 9-anilinoacridine-4-carboxylic acid **34** to couple to N,N-dimethylamino ethylene diamine and then, if successful, the thyminyl-PNA-monomer (free base of **14** or **21**) to afford **35** and **36** respectively (see **Scheme 2.34** below). These were just model studies to validate our approach. Beal had used the acridine acid **34** for his couplings (see **Scheme 2.22**) which was why we considered it a worthy model to support our ideas and make sure that the thyminyl-PNA-monomer was not a barrier to the coupling. If we were to prepare our PNA-acridine conjugates via this strategy we would choose to have a mesomerically withdrawing group attached to the 9-aminoacridine function that could be removed more easily than the phenyl group after coupling to yield the free 1° amino moiety.

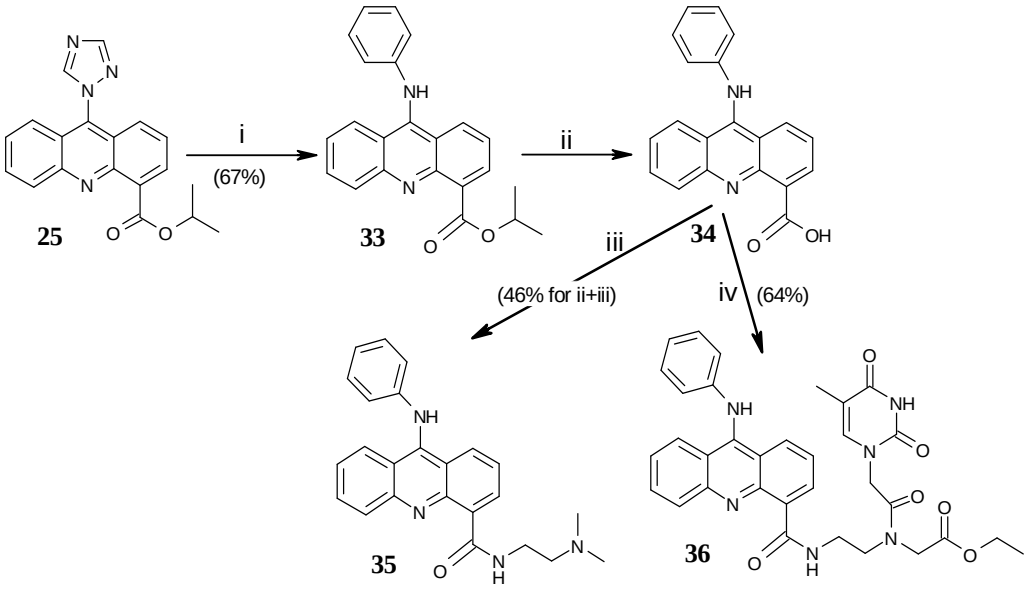

Reagents and conditions:
i: Aniline, TEA; CH_3CN; reflux
ii: 0.2 M LiOH (aq)/ THF; rt
iii: 1) DCC, *N*-hydroxysuccinimide 2) excess *N,N*-dimethylethylenediamine ; DMF, rt
iv: 1) DCC, *N*-hydroxysuccinimide 2) **14** (free base); DMF, rt

Scheme 2.34: Synthetic approach in the model study towards generation of 9-anilinoacridine-4-carboxamides **35** and **36**

The latter strategy is explained in detail later after the discussion of our model study now following and summarized in **Scheme 2.34** above.

2.11.1 Step i: generating the iso-propyl-9-anilinoacridine-4-carboxylate 33

The first step in this pathway involved substitution of the 9-triazolyl substituent of **25** with aniline, according to Carlson and Beal's protocol (see **Scheme 2.35** below).[210]

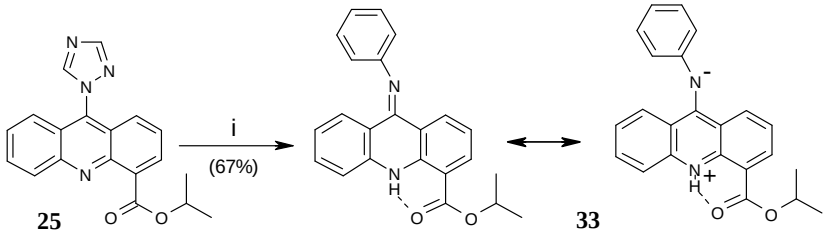

Reagents and conditions: i: Aniline, TEA; CH_3CN; reflux

Scheme 2.35

Thus, **25** was treated with aniline to yield 9-anilinoacridine *iso*-propyl ester **33** in a moderate yield (67%) after work-up. Key features of the ^{1}H-NMR spectrum for **33** were the disappearance of the triazole proton signals and appearance of the downfield signal at δ 11.0-11.4 suggesting that hydrogen bonding was now occurring between the ring N(10)H and the side-chain carbonyl oxygen. Unlike for the previous 9-benzyl analogue **28**, for **33** none of the signals in the ^{1}H-NMR and ^{13}C-NMR were 'split'. A likely explanation for this observation would be that for **33**, unlike for **28**, the Z and E isomers (about C(9)=N) interconverted rapidly on the NMR timescale. However, sterical hindrance between phenyl and acridine aromatic hydrogens made it unlikely that either the Z or E isomer were very stable. Possibly a partial negative charge was present on the exocyclic N (and partial positive charge on the ring N(10)), implying a degree of rotation for the C9-N bond fast enough, on the NMR timescale, not to generate 'split' signals.

2.11.2 Step ii: ester hydrolysis of the acridine iso-propyl ester 33.

Again, Beal's procedure [210] was followed which involved basic aqueous hydrolysis of **33** followed by acidification to neutral pH to obtain the 9-anilinoacridine-4-carboxylic acid **34** (see **Scheme 2.36** below). However, unlike Beal *et al*., during work-up we were not able to successfully separate the LiCl salt by-product from the product **34** by re-dissolving the crude reaction mixture residue, afforded after evaporation, in chloroform and filtering off the salt impurity.

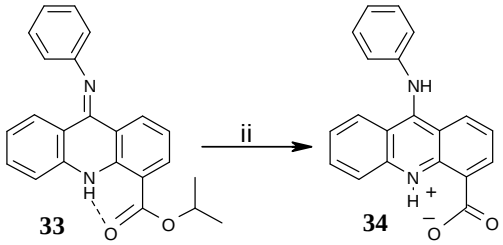

Reagents and conditions: ii: a) 0.2M LiOH (aq)/ THF; rt
b) 2.0 M HCl (aq)

Scheme 2.36

In our hands, the product **34** in the crude reaction mixture only dissolved sparingly in chloroform, even after vigorous sonication and use of other more polar solvents (e.g. methanol, ethanol). Due to these purification problems, we therefore decided to take

the crude product through to the next stage as it was. We envisaged that the presence of the LiCl salt would not hamper the subsequent reaction. NMR and mass spectrometry analysis suggested that compound **34** was present in the crude reaction mixture (ie *iso*-propyl hydrogen signals had disappeared from the NMR spectrum and a LRMS EI spectrum showed the M^+ peak for **34** at 100%)

2.11.3 Step iii: coupling N,N-dimethylethylenediamine to the acridine acid 34

Beal's peptide coupling protocol (as in steps *v* and *vi* of **Scheme 2.22**) was followed [210] in which **34** was treated with dicyclohexylcarbodiimide (DCC) and N-hydroxysuccinimide (NHS) followed by addition of excess N,N-dimethylethylenediamine (see **Scheme 2.37** below). Subsequent work-up yielded the desired product **35** in a moderate 46% yield (over steps ii + iii).

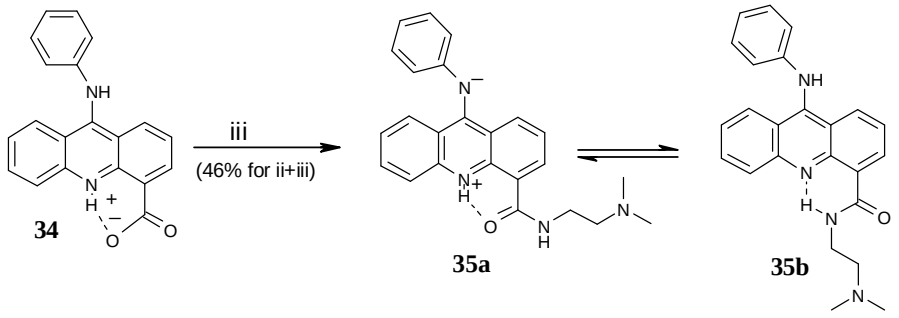

Reagents and conditions: 1) DCC, *N*-hydroxysuccinimide; DMF, rt. 2) *N,N*-dimethylethylenediamine ; DMF, rt

Scheme 2.37

As expected, and contrary to our earlier attempt to couple an amine to 9-benzylaminoacridine-4-carboxylic acid **30** (step *ix* in **Scheme 2.23**), after activating the acid **34** we did see precipitation of dicyclohexylurea side-product. This was removed by filtration before the N,N-dimethylethylenediamine was added.

^{1}H-NMR spectrum analysis for **35** suggested the presence of rotamers **35a** and **35b**. In our opinion this led to the splitting up of the two (exchangeable) proton signals, in a 4/1 ratio and to a generally broad appearance of the remaining signals in the ^{1}H-NMR spectrum for **35**. Admittedly, although providing an interpretation of the ^{1}H-NMR spectrum for **35**, the above considerations are hypothetical and need further

investigation (e.g. crystal structures and further NMR experiments, 2-D NOE and variable T, would be appropriate).

2.11.4 Step iv: coupling the PNA monomer 21 to the activated acridine acid 34.

Activation of the acid **34** was done, as in step *iii*, according to Beal's procedure, in which a solution of **34** was treated with dicyclohexylcarbodiimide (DCC) and N-hydroxysuccinimide (NHS) followed by addition of the free base of the thyminyl-PNA-monomer **21** (see **Scheme 2.38** below). Subsequent work-up yielded the desired product **36** in a 64 % yield.

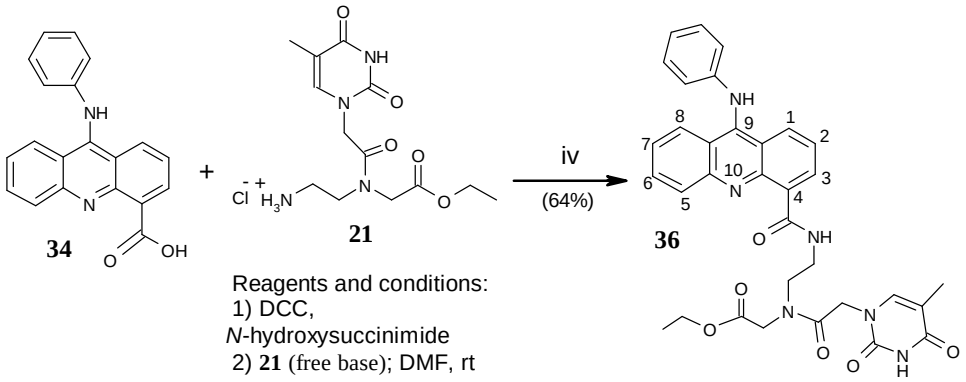

Scheme 2.38

^{1}H-NMR analysis suggested the presence of rotamers, presumably due to restricted rotation about the tertiary amide bond of the PNA moiety as this also was the case for the (*t*-Boc protected) thyminyl-PNA monomer **13** and the thyminyl-PNA monomer ammonium salts **14** and **21**. However, in **36,** restricted bond rotations could also occur about the 2° amide bond and the C(4)–(2° amide carbonyl carbon)-bond, potentially leading to 2^3 rotamers. **Figure 2.18** below shows four different rotameric isomers generated (only) by restricted amide bond rotations. The assignment of the ^{1}H-NMR signals for **36** was based on comparison of signals for homologous groups in a similar PNA-acridine conjugate (**53**) for which a number of two-dimensional NMR experiments had been done (see later in **Scheme 2.51** and subsequent discussion in subsection 2.15.1).

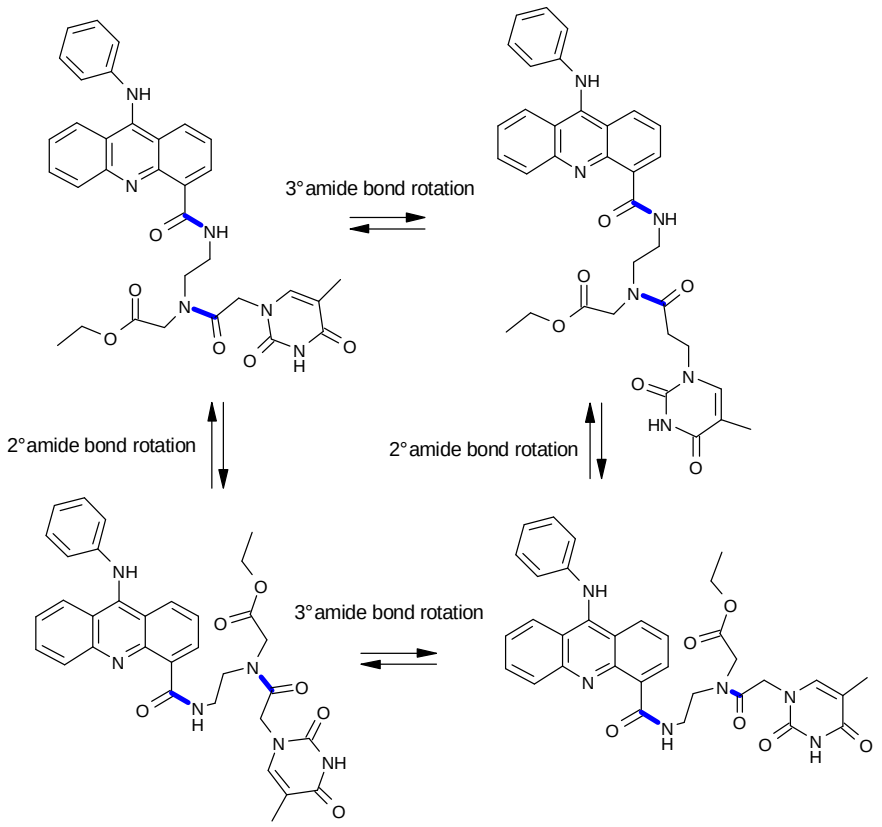

Figure 2.18: four rotameric isomers of PNA-acridine conjugate **36** in random conformations (amide bonds with restricted rotation are shown in bold)

From these 2-D experiments a more complete assignment of multiple (rotamer) signals to specific protons was possible. Thus, based on our one-dimensional ^{1}H-NMR analysis for the PNA-acridine conjugate **36** three rotameric isomers appeared to be present but little more could be said about the exact conformation of these rotamers. Most important was that we had shown in this experiment that it was possible to link the thyminyl-PNA-monomer **21** to the activated acid **34** and a potential PNA-monomer cyclization side-reaction was certainly not a barrier to the coupling step under reaction conditions applied for generating the PNA-acridine conjugate **36**.

This work on the 9-anilinoacridine models therefore verified our proposal that Beal's procedure for activation of the 4-carboxyl functionality and subsequent generation of the 4-carboxamide group worked well providing that the acridine's 9-amino free electron pair was involved in resonance delocalisation outside of the acridine system, thereby lowering the ring nitrogen's N(10) basicity. As this was not the case with a benzylamino substituent in the acridine's 9-position we decided to investigate the

potential of replacing this 9-benzylamino group with alternative 9-substituents. These substituents should allow for activation of the acridine's 4-carboxylic function but subsequently also allow generating the required primary 9-amino functionality at the end of the synthesis. We thus reasoned that if the primary 9-amino functionality could be prepared first then the 4-alkyl ester group could be hydrolysed and the generated acid could be activated followed by the peptide coupling step and 9-amino deprotection. This strategy will be discussed in detail in the following section. As the strategy uses Beal's chemistry, regarding conversions of the acridine's 4-substituent, and our own approach regarding protection of the 9-amino substituent to enable selective peptide coupling in the 4-position, it is referred to as the 'revised Beal route'.

2.12 *The 'revised Beal Route'*

Scheme 2.39 (below) shows a general outline of the 'revised Beal route' and partially recapitulates the initial 'Beal route'. It also shows the 'Beal route' compounds that were used to develop the 'revised Beal route'. So far, in the initial 'Beal route' we had come to the conclusion that the acridine ring required a 9-amino substituent, different from 9-benzylamino (as in **28** and **30** in **Scheme 2.39**), for which nitrogen's free electron pair was not only in conjugation with the aromatic acridine moiety but conjugation would extend outside of the acridine rings.

Thus for the 'revised Beal route' we decided to investigate the potential of converting/protecting the primary 9-amino substituent of the acridine ring (as in **40** and **44** in **Scheme 2.39**) to a number of urethane derivatives (by attaching benzyloxycarbonyl-, tertiary-butyloxycarbonyl- or allyloxycarbonyl-protection groups). We were hopeful that the presence of such a protected 9-amino substituent would allow for activation of the carboxyl functionality (towards a peptide coupling step) in the 4-position of the acridine ring, further down the synthetic route. It was hypothesised earlier that activation of the 4-carboxylic acid of the acridine was not occurring due to the ring N(10) basicity being too high. We had reasoned the latter was caused by unidirectional delocalisation of the lone electron pair of the exocyclic nitrogen of the 9-aminoacridine onto the ring nitrogen N10 of the acridine.

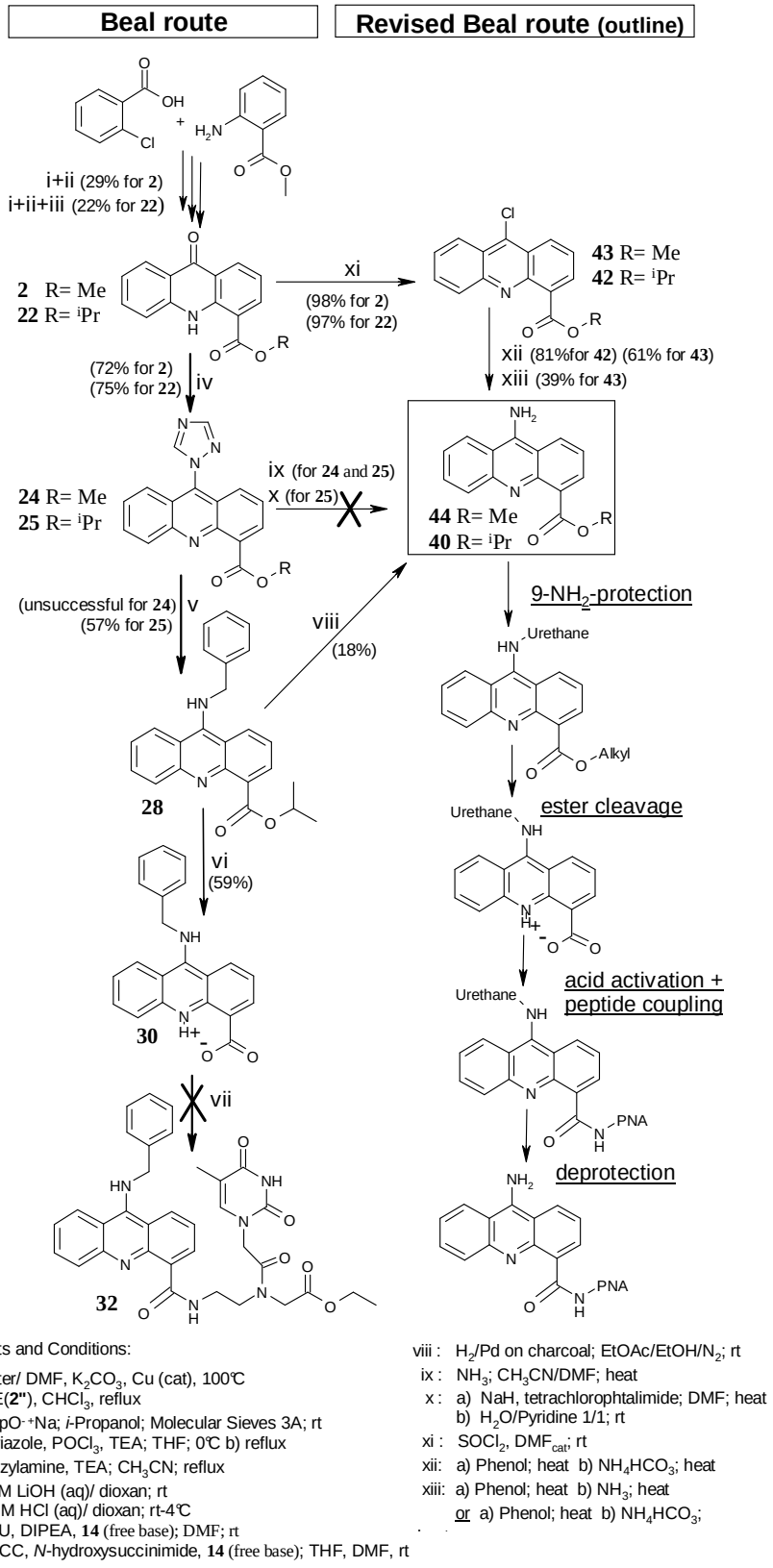

Scheme 2.39: Using 'Beal route' intermediates as precursors to alkyl-9-NH_2-acridine carboxylates **40** and **44** (boxed) in the 'revised Beal route'

In the 'revised Beal route' a urethane moiety in the acridine 9 position would serve both requirements of extended conjugation of the lone electron pair of the exocyclic nitrogen and allowing generation of the primary 9-amino substituent by deprotecting the latter at the end of the synthesis.

In order to establish urethane-based substituents we intended to establish first a primary 9-amino substituent on the acridine ring followed by the relevant 9-amino protection step. In **Scheme 2.39** above, the focus is on the use of 'Beal route' intermediates (**2**, **22**, **24**, **25** and **28**) in order to get to the alkyl-9-NH_2-acridine carboxylates **44** and **40** (boxed). Each of these reactions (*Steps viii, ix, x, xi, xii* and *xiii* in **Scheme 2.39**) will now be discussed in more detail in section **2.13** below. The subsequent steps in the 'revised Beal route' also outlined in **Scheme 2.39** and starting with the 9-NH_2-bearing intermediates **40** and **44**, will be discussed thereafter in more detail in a new section.

2.13 Synthesis of the alkyl-9-NH_2-acridine-4-carboxylates 40 and 44 in the 'revised Beal route' (as in Scheme 2.39)

2.13.1 Step viii: Hydrogenolysis of iso-propyl-9-benzylamino-4-carboxylate 28

Although the use of **28** for synthesis of **40** seemed an unnecessary detour, because the triazolylated precursor **25** (of **28**) was activated for substitution with N-nucleophiles in the 9-position and a primary amino functionality might be established directly (as in step *x* in **Scheme 2.39**), we considered this an interesting experiment as we had already synthesised **28** and wanted to investigate hydrogenolysis of the benzylamino group on **28** (see **Scheme 2.40** below).

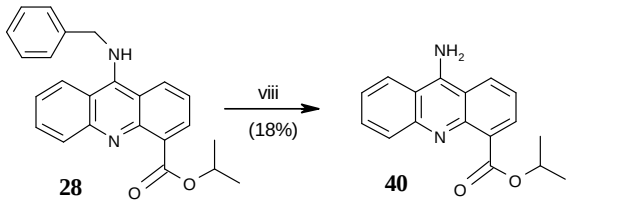

Scheme 2.40

Thus, a palladium-catalysed hydrogenolysis of the (exocyclic) NH-C bond was undertaken according a procedure described by Naylor *et al.*[223], in which **28** was subjected to a H_2 atmosphere (balloon) in the presence of the palladium catalyst.

After work-up the desired product was afforded in an 18% yield and 65 % of starting material **28** was recovered. This was not unexpected as TLC monitoring already had indicated only partial conversion of the starting material but because several by-products were appearing it was decided to proceed to work-up to determine whether and to what extent the desired product **40** had been formed. Due to time constraints and because it was more desirable to find a more direct way to establish the (1°) 9-amino functionality, it was decided not to investigate at this stage whether changes to reaction conditions (e.g. higher pressure and/or higher reaction T) would lead to better yields and/or shorter reaction times (which had been > 96 h. in this experiment).

2.13.2 Steps ix: converting the triazolyl-substituent in 24 and 25 to a primary amino group in 44 and 40 respectively.

The esters **24** and **25** had been synthesised earlier in the 'Beal route' *(Steps v* in **Scheme 2.23**) and their 9-triazolyl group primed these compounds for substitution with N-nucleophiles in the 9-position. For this reason we decided to investigate whether the triazolylated 'Beal route' intermediates **24** and **25** were susceptible to substitution with ammonia (see **Scheme 2.41** below). We chose reaction conditions based on Beal's procedure for converting the *iso*-propyl ester **25** to the 9-anilino substituted derivative **33** (see step *iii* in **Scheme 2.22**) in which Beal heated **25** to reflux in the presence of aniline. [210].

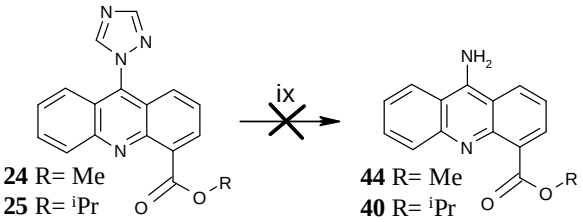

Scheme 2.41

Thus, in our experiment, anhydrous gaseous ammonia was bubbled through separate solutions of the esters **24** and **25** in acetonitrile/dimethylformamide (1/1) while heating to up to 100°C. Post work-up, the starting materials **24** and **25** were recovered in their respective experiments at 13% and 68% and for both experiments a number of unidentified by-products were observed. Identification of the latter was severely

hindered by their tendency to coelute in column chromatography and their reluctancy to recrystallise in different solvent(s) (combinations), e.g. methanol/diethyl ether, acetone/diethyl ether or chloroform/toluene. Although we did not obtain unambiguous evidence, probably some amide formation had taken place, particularly for the least sterically hindered methyl ester **24**.

Overall, we could conclude that for step *ix* (in **Scheme 2.41** above) the problem was that at the reaction temperature of around 100°C by-products started to appear before the desired substitution had taken place to any significant extent. In the earlier discussed step *vi* of the 'Beal route' (see **Scheme 2.23**), substitution of the 9-triazolyl with benzylamine had required 24 hours reaction time at reflux temperature of 81°C in acetonitrile. In step *ix* (in **Scheme 2.41** above) we had hoped that using acetonitrile/dimethylformamide (1/1), which allowed for a higher reaction temperature (100°C), would shorten necessary reaction times but this unfortunately resulted in (unidentified) by-product formation rather than faster formation of the desired products **40** or **44**.

The reason we wanted to reduce reaction times in step *ix* was to avoid the wasteful character of bubbling ammonia for 24 hours suggested in Beal's protocol to be necessary to substitute the 9-triazolyl substituent. However, because none of the desired products **40** or **44** could be identified and due to the fact the reaction set-up was cumbersome, wasteful and by-products had formed we decided no longer to consider this reaction as a potential intermediate step in the over-all pathway.

2.13.3 Step x: converting the triazolyl-substituent in 25 to an -NH_2 group in 40

Another way of substituting the triazolyl group in **25** with a primary amino group was inspired by Kamaike *et al*.[224] They reported in 1995 that the nitrotriazolyl group in 4-(3'-nitrotriazol-1'-yl)-1-β-D-ribofuranosylpyrimidine-2(1H)-one (**10'**) could be substituted with phthalimide in the presence of triethylamine, generating **11'** in **Scheme 2.42** (below). In the latter scheme subsequently the phthalimide group of **11'** was unmasked to yield the primary amino functionality in **12'**, by treatment with H_2O/pyridine for 1 hour. Inspired by these reactions we wanted to investigate if similar conversions could take place for our triazolylated starting material **25**.

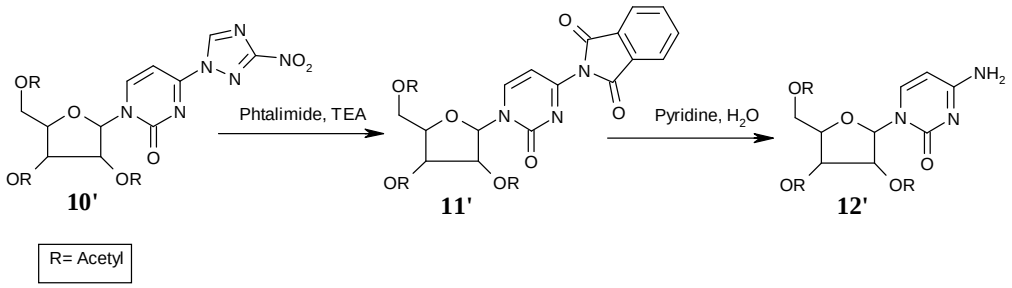

Scheme 2.42: primary amine generation via triazole substitution (according to Kamaike *et al*.)[224]

Hence, a solution of tetrachlorophthalimide in DMF was deprotonated with triethylamine and added to a solution, in DMF, of *iso*-propyl-9-(1,2,4-triazol-1-yl)acridine-4-carboxylate (**25**)(see **Scheme 2.43** below).

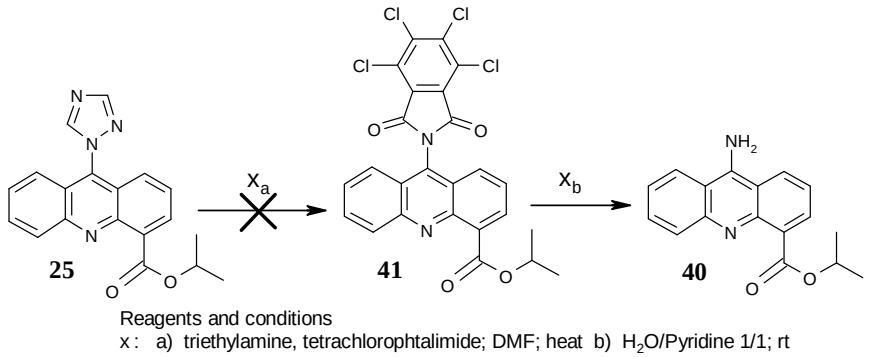

Scheme 2.43

For the conversion of Kamaike's compound **10'** to compound **11'** in the above **Scheme 2.42** Kamaike *et al.* had reported 24 hours of reaction time at room temperature. However, for step x_a (substitution of the triazolyl group in **25** with a N-3,4,5,6-tetrachlorophtaloyl group), post work-up NMR-analysis of the active (chromatography) fractions suggested only starting material **25** was present in significant amounts. This was not a surprising outcome as our triazole substituent clearly would be not as good a leaving group as the 3-nitrotriazolyl substituent in Kamaike's experiment (due to both –I and –M effects of the nitro-group). In addition, the tetrachlorophthalimide we used would be a worse nucleophile, due to the –I effect of the chloro substituents, compared to the phthalimide used by Kamaike. Admittedly, the lack of reactivity in our reaction x_a in **Scheme 2.43** above was expected, but we still considered it a worthwhile experiment as it was simple, tetrachlorophtalimide was readily available and if

successful (even in low yields), this meant the earlier prepared starting material **25** (for the unsuccessful Beal route) was still useful**.**

So far, unfortunately, attempts to generate a primary amino group in the 9-position of the acridine ring by substitution in the 9-triazolylated intermediates **24** and **25** or hydrogenolysis of the 9-benzylamino-bearing intermediate **28** had been unsuccessful. Thus, we decided to focus on earlier 'Beal route' intermediates **2** and **22** (see **Scheme 2.39**) and use some of the earlier chemistry described by Denny to activate the 9-oxo functionality of **2** and **22** towards substitution in the acridine ring 9-position. These reactions are discussed below.

2.13.4 Steps xi: converting the 9-oxo group in 2 and 22 into a 9-chloro group in 43 and 42 respectively.

Substitution of a 9-oxo-functionality (as in **2** and **22** in **Scheme 2.44** below) with a chloro-group had been demonstrated before by Denny in the synthesis of 9-NH_2-DACA (see step *v* in **Scheme 2.3**).[186] Denny had treated 9-oxoacridine-4-carboxylic acid **3** with thionyl chloride (used as solvent and reagent) to synthesise 9-chloroacridine-4-carbonyl chloride **4**. Thus, in **4** both the 9-position and the 4-carbonyl had become activated towards substitution. This had allowed Denny to subsequently generate the 4-carboxamide side-chain and the primary 9-NH_2 group in 9-NH_2-DACA (see steps *vi* and *vii* in **Scheme 2.3**).

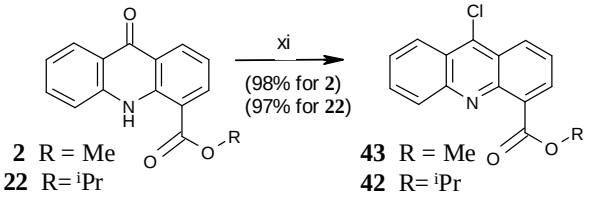

Reagents and conditions xi : $SOCl_2$, DMF_{cat}; rt

Scheme 2.44

In step *xi*, in **Scheme 2.44,** only the 9-oxo/9-hydroxy was susceptible towards conversion to the 9-chloro group and if successful this would afford the desired intermediates **42** and **43**. Thus, according to Denny's procedure, thionyl chloride was used as solvent and reagent for the substrates **2** and **22**, which afforded the respective products in high yields (98% for **43** and 97% for **42**). Key feature in the NMR-spectra

analyses of the crude reaction mixtures of compounds **42** and **43** was the lack of the high value (downfield) N(10)H signal at respectively 11.60 and 11.71 ppm due to the lack of intramolecular H-bonding in **42** and **43.** The latter would be used directly in the following 9-chloro substitution steps *xii* and *xiii* of the 'revised Beal route', without further purification.

2.13.5 Steps xii and xiii: converting the 9-chloro substituent in 42 and 43 into the 9-NH_2 substituent in 40 and 44 respectively.

In Denny's 9-NH_2-DACA (**6**) synthesis, 9-amino DACA **6** was formed from the 9-chloro-DACA (**5**) by treatment with anhydrous gaseous NH_3 in phenol at reflux (see step *vii* in **Scheme 2.3**).[186] In our revised Beal route methyl-9-aminoacridine-4-carboxylate **43** was treated accordingly (see step *xiii* in **Scheme 2.45** below)

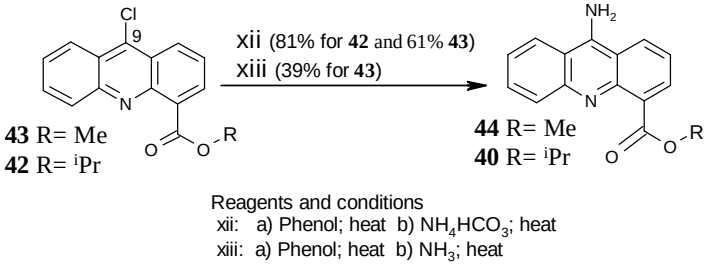

Scheme 2.45

However, as TLC monitoring suggested substantial conversion of starting material into more than one product we proceeded to work-up prior to complete conversion of the starting material **43**. Subsequent NMR analysis of (chromatography derived) active fractions containing the major product suggested it was the desired **44**, which was obtained in a modest 39% yield. Unambiguous identification of side products was complicated due to partial (chromatographic) coelution of the latter, but some 1°-amide formation (via methyl ester aminolysis) was likely to have taken place. A key feature in the ^{1}H-NMR spectrum of **44** was the reappearance of the high value (downfield) signal for the intramolecular H-bonded N(10)H at 10.95 ppm. The yield for **44** was considerably lower (39%) than for Denny's conversion of the 9-chloro group, in **5,** to a primary amino group in 9-NH_2-DACA **6** (59% yield, see step *vii* in **Scheme 2.3**). The lower yield and the longer reaction time required (2 hours compared to 20 minutes for

Denny's 9-NH_2-DACA **6**) might have been due to the absence of the 2° carboxamide functionality at the acridine's 4-position in our starting material **43** but which was present in 9-chloro-DACA **5**. This meant that in **43** no hydrogen bonding was possible involving the ring nitrogen N(10) and the carboxamide side-chain hydrogen (see **Figure 2.19** below).

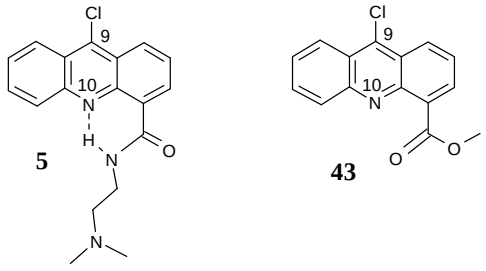

Figure 2.19: due to N10 hydrogen bonding in compound **5** the 9-chloro substituent is more susceptible to substitution than in compound **43.**

This potentially left the C(9) in **43** less susceptible to nucleophilic substitution than that in **5**, where the acridine ring nitrogen N10 carried a partial positive charge due to the intramolecular H-bonding.

In order to find a higher yielding reaction to substitute the 9-chloro group in **43** with a primary amino group, we tested a protocol designed for this purpose by Albert and Ritchie in which they used $(NH_4)_2CO_3$ instead of ammonia for the 9-chloro substitution of several multi-substituted 9-chloroacridines.[225](See also **Scheme 2.45** above) TLC monitoring suggested substantial conversion of the starting material **43** with some by-product formation (likely to be 1° amide formation in the acridine 4-position). Subsequent MS and NMR analysis confirmed presence and structure of the desired product **44**, which now was obtained in an improved but moderate 61% yield.

The *iso*-propyl-9-chloroacridine-4-carboxylate **42** was converted to the 9-NH_2-bearing product **40** according the same procedure used for conversion of **43** (above) and as described by Albert and Ritchie.[225] (See **Scheme 2.45** above) TLC monitoring suggested substantial conversion of the starting material **42** with again some by-products starting to appear. Post work-up microanalysis and NMR analysis confirmed respectively the purity and structure of the desired product **40**, which was obtained in an 81% yield.

So far, our attempts to establish a primary amino group in the acridine's 9-position had been 'most' successful via the activated alkyl-9-chloroacridine-4-carboxylate 'Beal route' intermediates **42** and **43**. The recorded yields for subsequent substitution in the 9-position with a primary 9-NH_2 group using NH_4HCO_3 (in step *xii* of the 'revised Beal route', **Scheme 2.39**) were an improvement (61% for **44** and 81% for **40**) compared to the use of NH_3 for this purpose in step *xiii* (39 % yield for **44**). Noteworthy in steps *xii* and *xiii* was that the methyl ester group in **43** had stayed largely intact after treatment with ammonia or ammonia-generating NH_4HCO_3, although formation of the carboxamide by-product probably explains the lower yields (39% and 61%) for the methyl ester **44** compared to 81% for the more robust *iso*-propyl ester **40**.
Unclear as to why the use of NH_4HCO_3 (instead of gaseous NH_3) made a difference yield-wise, one obvious physical difference between the experiments was the presence of solid NH_4HCO_3, in the phenol solution, which may have led to higher localised NH_3 activity at the solid/liquid interface. A possible reaction mechanism for these 9-chloro→9-amino substitutions with ammonia in phenol was discussed earlier in subsection 2.4.5.

Thus, having established our goal of synthesising the alkyl-9-NH_2-acridine-4-carboxylates **40** and **44** we subsequently focused our efforts on the next step in the 'revised Beal route' in **Scheme 2.39**. This will be discussed in the following section.

2.14 Carbamate NH_2-protection of alkyl-9-aminoacridine-4-carboxylates (44, 40) in the 'revised Beal route'

The next step in the 'revised Beal route' (**Scheme 2.39**) involved protection of the primary 9-amino functionality of compounds **44** and **40**. As mentioned earlier this would be accomplished by utilisation of carbamate protecting groups for the amino group in the 9-position. The reasons for using carbamate protection were fourfold: the exocyclic nitrogen's free electron pair would be involved in resonance delocalisation outside of the acridine ring system, we could choose the carbamates designed to withstand the basic hydrolysis conditions of the subsequent ester hydrolysis step in the revised Beal route, in the following step in the 'revised Beal route' the acridine's primary 9-amino group would be prevented from interfering in the peptide coupling between the activated acridine acid and the PNA and finally, the carbamate moieties

could be readily removed at the end of the synthesis thereby liberating the acridine's primary 9-amino functionality (see **Scheme 2.39**). Hence, in what follows we discuss how appropriate urethane-based 9-amino protection was established for both methyl-9-aminoacridine-4-carboxylate **44** and *iso*-propyl-9-aminoacridine-4-carboxylate **40.** However, because the *iso*-propyl ester group was established earlier by conversion of the 9-oxo-bearing methyl ester **2** into the 9-oxo-bearing *iso*-propyl ester **22** (see step *iii* in **Scheme 2.23**) but the overall yield for the 9-amino-bearing *iso*-propyl ester **40** was very similar to the overall yield for 9-amino-bearing methyl ester **44,** it was deemed the methyl ester **44** would be the most appropriate for further use because the extra synthetic step for generating the *iso*-propyl ester **40** could be omitted. Additionally, the methyl ester cleavage of **44** would take less time than the *iso*-propyl cleavage of **40** (i.e. 45 mins for **44** vs. 24 h. for **40,** in ~ 0.2 M LiOH (aq)). Originally, in the 'Beal route', the *iso*-propyl group was put in place to prevent carboxamide formation in the acridine's 4-position when substituting the 9-triazolyl substituent with an amine (as e.g. in step *iii* in **Scheme 2.22**). In the 'revised Beal route' this probably led to higher yields (in step *xii* of **Scheme 2.39**) for the 9-amino-bearing *iso*-propyl ester **40** (81%) compared to only 61% yield for the less bulky 9-amino-bearing methyl ester **44** but this advantage was balanced out by the (only) 77% yield for synthesis of the *iso*-propyl ester **22** (using the methyl ester **2** as starting material), in the first place (see step *iii* in **Scheme 2.23**).

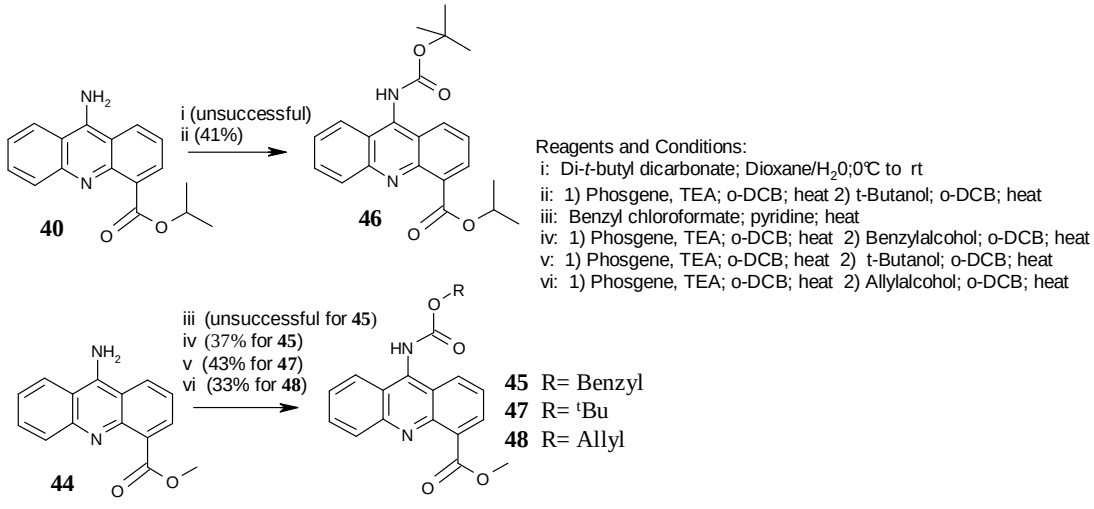

Scheme 2.46: protecting the primary amino group of the alkyl-9-aminoacridine-4-carboxylates **44** and **40**.

We chose to investigate three different carbamate protection groups for the 9-amino group of methyl ester **44** i.e. *t*-butyloxycarbonyl (*t*-Boc), benzyloxycarbonyl (Cbz) and allyloxycarbonyl (Alloc) and one for the 9-amino group of the *iso*-propyl ester **40** i.e. *t*-butyloxycarbonyl (*t*-Boc) (see **Scheme 2.46** above).

These protection groups were chosen for no other reason than that they complied with the requirements described above and we intended to compare the three different carbamate protection groups and identify the highest yielding option.

All three carbamates were stable under basic conditions.[226] This would be necessary to survive the subsequent ester cleavage in basic aqueous conditions. At the end of the synthesis we would then be able to remove the *t*-Boc and Cbz carbamate protection groups respectively under mild acidic aqueous conditions and under stronger acidic conditions, while removal of the Alloc protection group would require Pd(0) under neutral conditions.[226]

In **Scheme 2.46** above we summarize the reactions undertaken to establish the relevant carbamate protection groups. Each reaction is now discussed separately.

2.14.1 Steps i and ii: t-Boc protection of iso-propyl-9-aminoacridine-4-carboxylate (40).

According the procedure described by Finn *et al*.[202] for *t*-Boc-protection of amines (also applied earlier in step *i* in **Scheme 2.12** for protection of 3-amino-1,2-propanediol **4**), intermediate **40** was treated with di-*t*-butyl dicarboxylate in order to generate the *t*-Boc carbamate in the 9-position of the acridine (see step *i* in **Scheme 2.47** below).

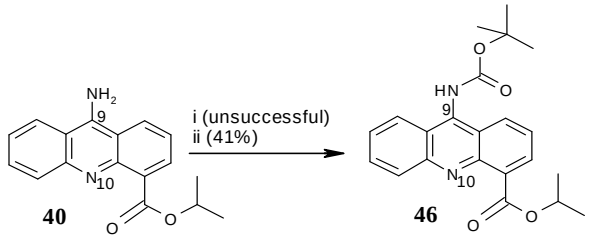

Reagents and Conditions:
i: 1) Di-*t*-butyldicarbonate; Dioxane/H_20; 0℃ to rt OR ii: 1) Phosgene, TEA; o-DCB; he at 2) t-Butanol; o-DCB; heat

Scheme 2.47

TLC monitoring of the reaction mixture suggested little conversion had taken place and subsequent post work-up ^{1}H- and ^{13}C-NMR analysis of the resulting solid suggested presence of starting material **40** only.

The likely reason for failure in this step was that di-*t*-butyl dicarboxylate was a fairly weak, sterically hindered electrophile which does not react well with sterically hindered arylamines.

Because, for **40,** we couldn't increase the nucleophilicity of the (sterically hindered) 9-amino/imino group we decided to increase the reactivity of the electrophile in order to put the 9-amino carbamate protection group in place. We envisaged this could be accomplished by using a procedure, described by Adebambo *et al.* [227], in which phosgene had reacted with the amino group of *t*-butyl (2-amino-6-chloro-9*H*-purin-9-yl)acetate (**13' in Scheme 2.48**) to form the isocyanate intermediate that subsequently reacted with benzyl alcohol to establish the Cbz protection in **14'** (80% yield) (see **Scheme 2.48**). Thus, based on Adebambo's procedure, in step *ii* (see **Scheme 2.47** above) our compound **40** was treated initially with triphosgene in order to generate the isocyanate bearing intermediate.

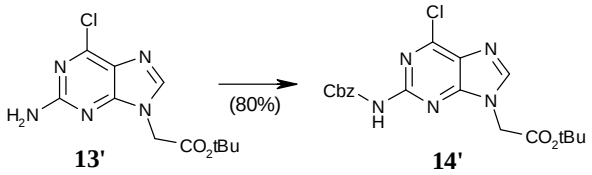

13' **14'**

Reagents and conditions: 1) triphosgene, TEA; THF; heat 2) Benzyl alcohol; heat

Scheme 2.48: Cbz carbamate protection of the primary amino group in **13'** using trisphosgene and benzyl alcohol (according to Adebambo *et al.*)[227]

TLC monitoring of this reaction suggested substantial but incomplete conversion of starting material **40** into at least 2 products. For this reason we proceeded to the next step in which the presumed isocyanate intermediate was treated with *t*-butanol to generate the carbamate protected *iso*-propyl-9-*t*-butyloxycarbonylaminoacridine-4-carboxylate (**46**). Subsequent work-up afforded the desired title compound **46** in moderate yield (0.14 g, 41 %). Key feature of the ^{1}H-NMR spectrum of **46** was the appearance of the *t*-Boc signal at 1.56 ppm. The ^{1}H-NMR analysis also showed the downfield chemical shift value δ 11.56 which was assigned to the ring N(10)*H* and indicative of a predominant 9-imino tautomer for the product **46**. The low yield (41%) was not unexpected as step *ii* in **Scheme 2.47** (above) was far from being chemoselective for the desired product but this, we found, was the price to be paid for protecting the sterically hindered 9-NH_2 group in **40**.

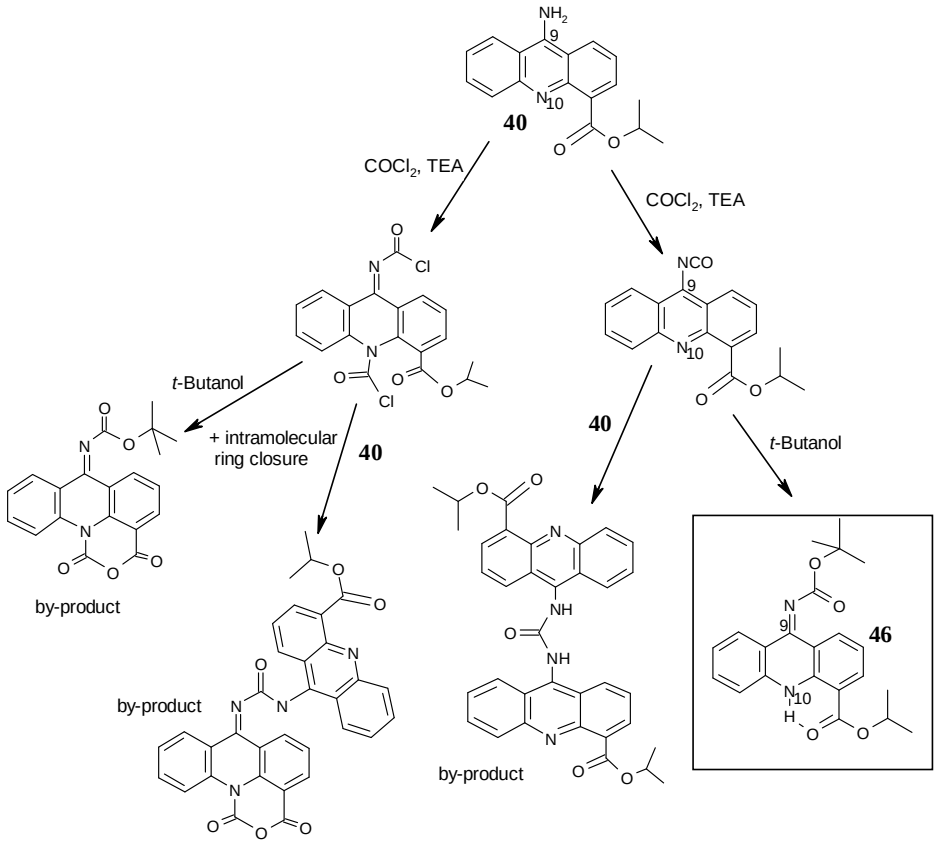

Figure 2.20: potential by-products formed during *t*-Boc protection of *iso*-propyl-9-aminoacridine-4-carboxylate (**40**), according a procedure described by Adebambo *et al.*[227]

Regarding by-product formation, besides generating a 9-NCO group, phosgene was also likely to react with the more sterically hindered but more basic ring N(10) leading to a reactive intermediate that would react further with available nucleophiles like the starting material **40** or the *t*-butanol, or even Intramolecular (See **Figure 2.20** above). The chromatographic purification during work-up had yielded a number of unidentified co-eluting impurities (to a small extent with the product **46**) that however, due to the co-elution and reluctancy to be purified via repeated recrystallisation attempts, could not unambiguously be identified as the above suggested by-products. In addition, time constraints prompted us to focus on proceeding with the intended products rather than pursuing complete purification and characterization of by-products.

2.14.2 Steps iii and iv: Cbz protection of the primary 9-amino group of 44.

Initially, in step *iii* (see **Scheme 2.49** below) we attempted to protect the 9-amino group of **44** by treating it with benzyl chloroformate, according a procedure described by Dueholm *et al*. for the NH_2-protection of cytosine.[228]

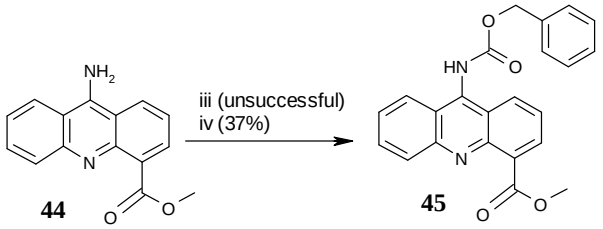

Reagents and Conditions:
iii: Benzyl chloroformate; pyridine; heat
OR
iv: 1) Phosgene, TEA; o-DCB; heat 2) Benzyl alcohol; o-DCB; heat

Scheme 2.49

TLC monitoring of the reaction suggested little conversion was taking place and this was confirmed by post work-up NMR analysis of collected fractions which suggested nothing more than starting material **44** was present (95% of **44** was recovered). The likely reason for this was similar to the one discussed earlier (in step *i* of **Scheme 2.47**) i.e. the 9-imino group of the predominant tautomer of **44** was sterically too hindered to substitute the chloride in benzyl chloroformate.

For this reason, in step *iv* (see **Scheme 2.49**) we anticipated we could successfully use the phosgene method, as reported by Adebambo *et al*.,[227] to establish the carbamate protection for the 9-amino group of **44** as this method had successfully solved the same problem for **40** in step *ii* (as discussed earlier in ***2.14.1***).

TLC monitoring of the reaction (in step *iv* of **Scheme 2.49**) suggested little change took place but based on our earlier experience it was decided to work-up the reaction mixture which did afford the title compound **45,** however contaminated with a small amount of a co-eluted impurity. Hence, crude **45** was recrystallised and this afforded the pure compound **45** as orange crystals in a very moderate 37 %. The reason for the low yield again being the low chemoselectivity for the desired product under the described reaction conditions leading to formation of several potential by-products (presumably of the sort described earlier in **Figure 2.20**). Chromatographic purification during work-up had yielded a number of co-eluting impurities that could

not unambiguously be identified as the type of by-products suggested earlier (in **Figure 2.20**) due to the co-elution and their reluctancy to be purified via repeated recrystallisation attempts. Also, time constraints prompted us to focus on proceeding with the obtained intended product.

An X-ray crystal structure was obtained for **45,** which confirmed the presumed predominance of the imino tautomer for **45** (as presumed for the starting material **44**) and in it the H-bond between the ring N(10)H and the methyl ester carbonyl oxygen. Key bond distance and torsion angle values obtained from the crystal data experiment (See appendix) were: 129 pm for C(12)-N(2) (indicating a double bond and confirming the 9-iminoacridane was the crystallised tautomer for **45**) and a torsion angle of 1.7° for C(5)-C(4)-C(14)-O(1) which brought the H·····O distance in N(1)-H(1)·····O(1) to193 pm, which was within the typical H-bond distance range (see **Figure 2.21** for the X-ray structure of **45**).

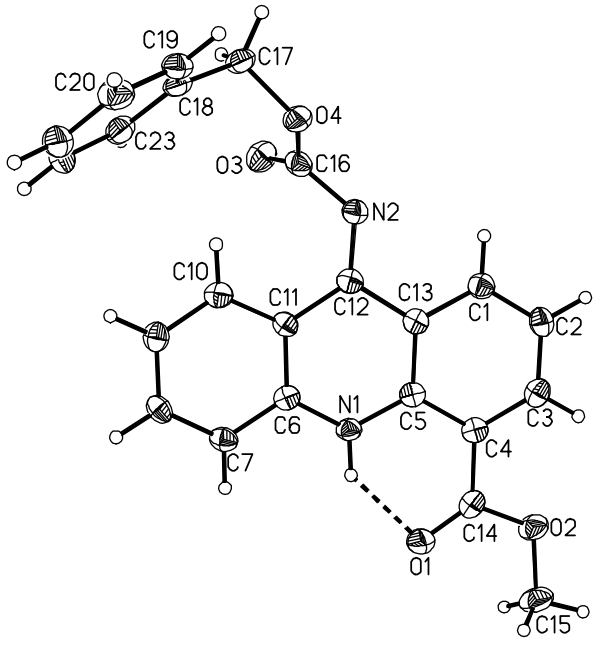

.

Figure 2.21: X-ray structure of Methyl-9-benzyloxycarbonylaminoacridine-4-carboxylate (**45**).

2.14.3 Steps v and vi: t-Boc- and Alloc-protection of the primary 9-amino group of 44.

For the *t*-Boc- and Alloc-protection of methyl-9-aminoacridine-4-carboxylate (**44**) the phosgene method according to Adebambo *et al.* was applied again [227] (see **Scheme 2.50** below).

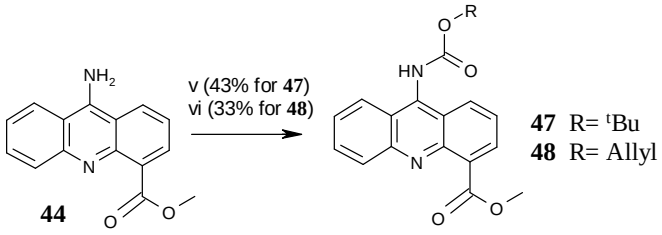

Reagents and Conditions:
v: 1) Phosgene, TEA; o-DCB; heat 2) t-Butanol; o-DCB; heat
vi: 1) Phosgene, TEA; o-DCB; heat 2) Allyl alcohol; o-DCB; heat

Scheme 2.50

The above procedure afforded the *t*-Boc protected compound **47** (step *v*) in a modest 43% yield and the Alloc-protected compound **48** (step *vi*) in a modest 33% yield. As in step earlier steps, TLC analysis in both *Steps v* and *vi* also suggested presence of a number of unidentified co-eluting by-products/impurities, which could not be identified unambiguously due to their reluctance to be resolved by column chromatography or purified by repeated crystallisation attempts.

So far, our attempts to protect the primary 9-amino group of methyl-9-aminoacridine-4-carboxylate **44** and *iso*-propyl-9-aminoacridine-4-carboxylate **40**, by converting the group into a carbamate, had succeeded although yields were moderate, presumably due to the low chemoselectivity for the intended products under the applied reaction conditions. *t*-Boc-, Alloc- and Cbz-protections of **44** (the methyl ester) were established in respective yields of 43% for **47**, 33% for **48** and 37% for **45**. *t*-Boc-protection of **40** (the *iso*-propyl ester) was established in a 41% yield for **46**. Now that the primary 9-amino functionality was appropriately protected we subsequently focused our efforts on the next steps in the 'revised Beal route' in **Scheme 2.39**. This will be discussed in the following section.

2.15 Methyl ester cleavage and subsequent acid activation of acridine intermediates 45, 47 and 48 towards coupling with a PNA monomer (as part of the 'revised Beal route').

In the revised Beal route the methyl ester group of compounds **45**, **47** and **48** now needed to be hydrolyzed to in order to free the acridine's 4-carboxylic acid group so that it could be activated to enable the peptide coupling step with a PNA. The chemistry applied to accomplish this was based on similar synthetic steps in Beal's successful approach in his development of an acridine-peptide library (see *Steps iv* and *v* in **Scheme 2.22**). In step *iv* of **Scheme 2.22** Beal had treated *iso*-propyl-9-anilinoacridine (**33** in **Scheme 2.22**) with aqueous LiOH followed by neutralisation with aqueous hydrochloric acid after which he was able to separate LiCl salts from the product 9-anilinoacridine-4-carboxylic acid (**34** in **Scheme 2.22,** 99% yield) by redissolving the solid residue (obtained after first solvent evaporation) in chloroform and filtering the suspension. Subsequently Beal activated the 9-anilinoacridine-4-carboxylic acid **34** by converting it to the N-hydroxysuccinimide (NHS) ester. The obtained crude NHS activated acid **34** was used in the following peptide coupling step with resin-bound tripeptides (see step *vi* in **Scheme 2.22**). Yield over the two steps (based on the acid **34**) was 33%. For our own compounds **45**, **47** and **48** analogous conversions as described above are summarized below in **Scheme 2.51** which are subsequently discussed in more detail and compared to Beal's results.

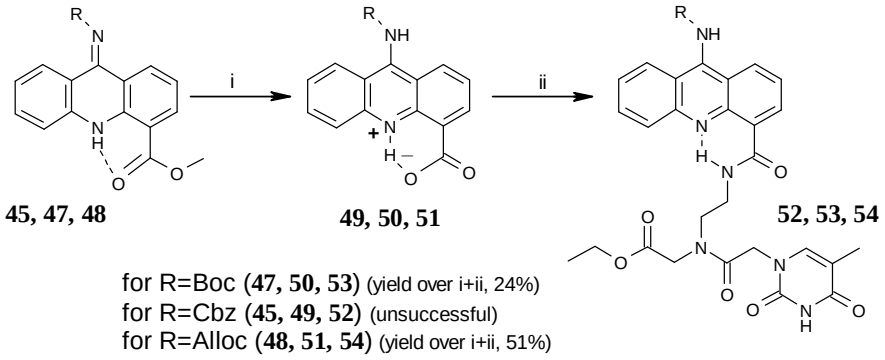

Reagents and conditions:
i: 1) Aqueous LiOH 0.2 M; THF; rt 2) Aqueous HCl 0.5 M; rt
ii: 1) DCC, N-OH succinimide; DMF; rt 2) PNA monomer **14** or **21**, TEA; DMF; rt

Scheme 2.51: Linking the thyminyl-PNA-monomer to the N-hydroxysuccinimide activated acridine acids.

2.15.1 Steps i and ii: acid generation and activation for the t-Boc-protected 9-aminoacridine intermediate 47 and subsequent linking to a PNA monomer.

To generate the acid **50** from the methyl ester **47** the latter was cleaved under basic aqueous conditions according to the procedure described by Beal (See **Scheme 2.52** below).[210] TLC monitoring suggested complete conversion of the starting material **47.**

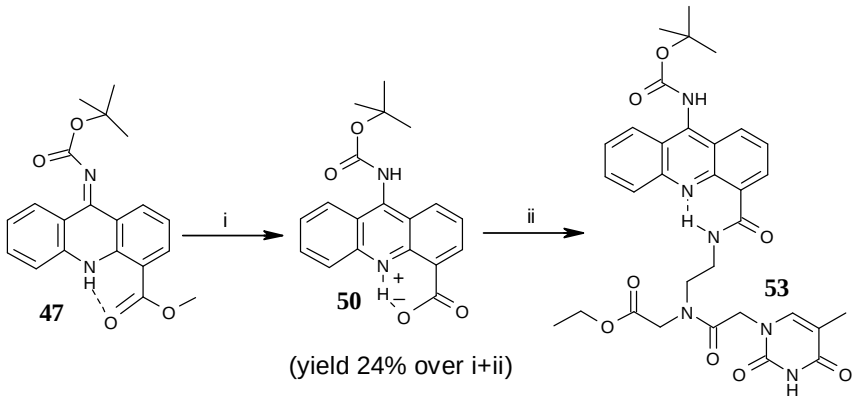

Reagents and conditions:
i: 1) Aqueous LiOH 0.2 M;THF; 0℃ to rt 2) Aqueous HCl 0.5 M; rt
ii: 1) DCC, N-OH succinimide; DMF; rt 2) PNA monomer salt **21**, TEA; DMF; rt

Scheme 2.52

In the work-up, unlike in Beal's procedure, we were not able to separate the LiCl salts from the product by redissolving the reaction residue and subsequently filtering off the solid salt residue. We therefore decided to take the crude product **50** through to the next stage as we didn't expect the LiCl salt would hamper the following reaction in step *ii* (**Scheme 2.52**).

Thus, a solution of the crude compound **50** was treated with N-hydroxysuccinimide and dicyclohexylcarbodiimide (according to Beal's procedure) after which the dicyclohexylurea by-product was removed (by filtration) and the N-(aminoethyl)-N-(thymin-1-ylacetyl) glycine ethyl ester **21** was added to generate the desired conjugate **53**. Subsequent work-up afforded the title compound **53** in a modest 24% over both *Steps i* and *ii* (based on starting material **47**)

Analysis of 1-D and 2-D NMR experiments showed rotamer presence, due to restricted rotation about the tertiary amide bond. While the presence of rotamers complicated unambiguous interpretation of the 1-D spectrum, the 2-D NMR experiments allowed for a more precise assignment of chemical shifts**.** In addition, comparison of signals

recorded in literature **[**202**]** and by ourselves, for the (unconjugated) PNA-monomer **13,** was also helpful in assigning the signals of the corresponding protons in **53**. Initially, a **ROESY** (**R**otational **O**verhauser **E**ffect **S**pectroscop**Y**) spectrum of **53** (see **Figure 2.23**) allowed us to identify the rotamer generated signals, i.e. chemical shifts connected by off-diagonal negative (red) peaks indicating chemical exchange, and it allowed us to observe NOE contacts, i.e. chemical shifts connected by off-diagonal positive (black) peaks between protons (nearby in space) of different parts of compound **53**, in different rotameric conformations. Subsequently, in order to identify the relevant rotameric conformations and to determine their relative stabilities we had to assign the NMR peaks correctly. For this, other 2-D NMR experiments, **HSQC** (**H**eteronuclear **S**ingle **Q**uantum **C**oherence, see **Figure 2.24**) and **HMBC** (**H**etero-nuclear **M**ultiple **B**ond **C**oherence, see **Figure 2.25**), were useful because direct C-H coupling (**HSQC**) and longer range coupling (2-4 bonds in **HMBC**) was recorded. Thus, a first correct assignment of a chemical shift to a (group of) proton(s) in the **HSQC** experiment subsequently allowed, in the **HMBC** experiment, to deduce assignments for nearby protons, because in the long range coupling between the initially assigned proton(s) and nearby carbons, the latter in turn each showed different (additional) couplings to other (nearby) protons. Via trial and error, assignments (for both C and H) could thus be made systematically and this lead to a better assignment of the majority of NMR peaks for both C and H. Assignments of aromatic protons and quaternary carbons were more problematic because not all ambiguities could be eliminated via this deduction method. A discussion of how the 2-D NMR experiments helped in assignment of certain NMR peaks, rotamer ratio determination and rotamer stability follows below. For this purpose a (randomly) C-atom labelled representation of the PNA-acridine conjugate **53** is depicted in **Figure 2.22** below.

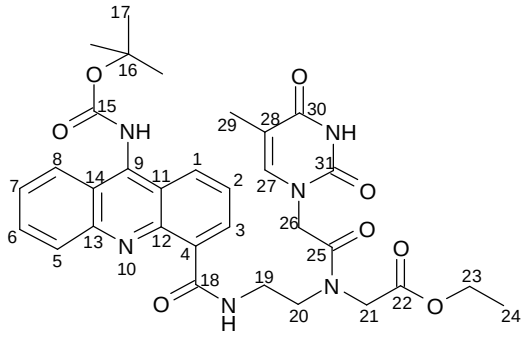

53

Figure 2.22: C-labelled representation of the PNA-acridine conjugate **53**

In the NMR spectra one of the 'split' rotamer signals was assigned to the thymine methyl protons ($C(29)H_3$ in **Figure 2.22**). In the 1-D ^{1}H-NMR spectrum the corresponding chemical shifts were at 1.10/1.69 ppm (in a 4/1 ratio). We believed this assignment to be correct because in the ROESY spectrum the two thymine methyl shifts at 1.10/1.69 ppm were connected by chemical exchange peaks and showed NOE interactions with the split signal for the thymine C(27)H at 6.07/6.83 ppm (in a 4/1 ratio) (See **Figure 2.23** below for **ROESY** spectrum).

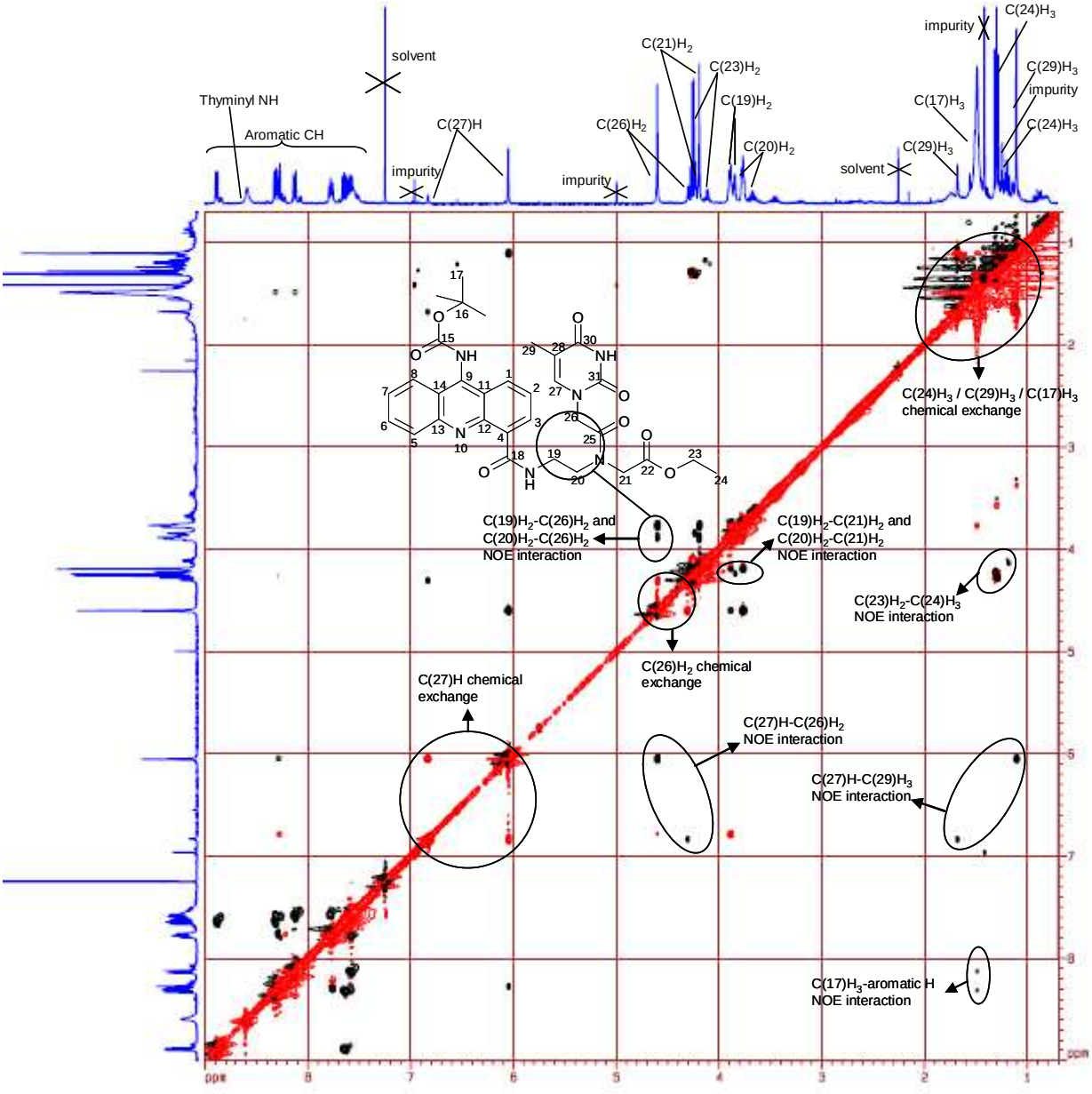

Figure 2.23: ROESY spectrum for **53** indicating chemical exchange and NOE interaction cross peaks.

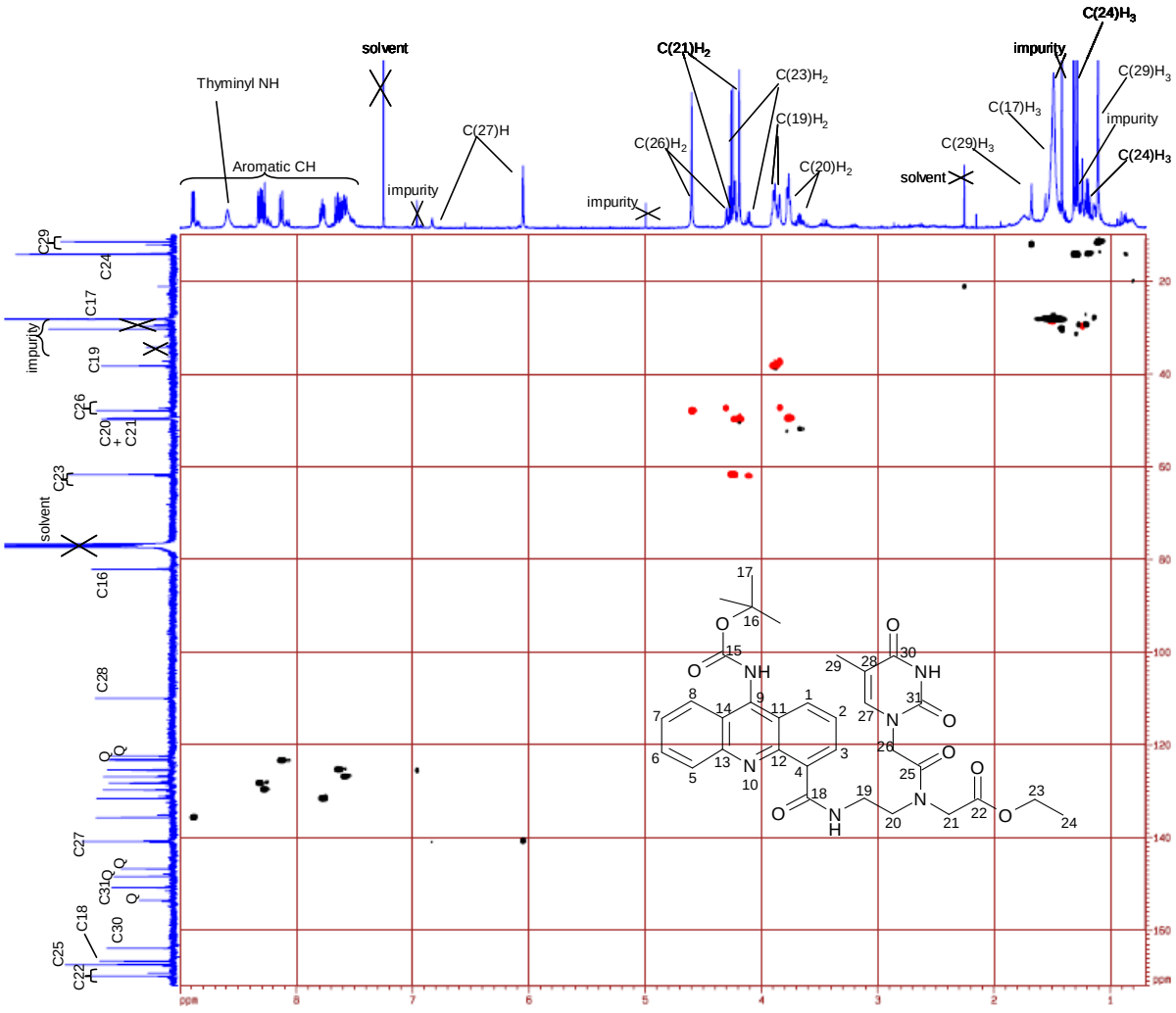

Figure 2.24: HSQC spectrum for **53** showing direct C-H coupling (the unassigned peaks between 120 and 140 ppm on the C-axis are aromatic tertiary carbons, Q=quaternary carbon)

The split thymine C(27)H signals at 6.07/6.83 ppm also were connected by chemical exchange peaks in the ROESY spectrum which proved their identical (rotameric) origin. The same observation was made for the C(26)H_2 shifts (4.31/4.61 ppm) i.e. they were connected by chemical exchange peaks in the ROESY spectrum which irrefutably proved their identical (rotameric) origin. Rotamer generated split signals were also present for the ethyl C(23)H_2 and C(24)H_3. The *t*-butyl C(17)H_3 signal at 1.49 ppm in the 1-D H-NMR spectrum was unusually broad which suggested an impeded rotation about one or more bonds of the 9-*t*-Boc-amino moiety. The ROESY experiment showed NOE interaction between the *t*-Boc signal and acridine aromatic hydrogens at 8.15 and 8.32 ppm. This suggested certain conformational preferences for the *t*-butyl

group, possibly stabilised by hydrophobic interaction forces, with non-polar parts of the acridine system and in turn this would explain the broad appearance of the *t*-butyl signal.

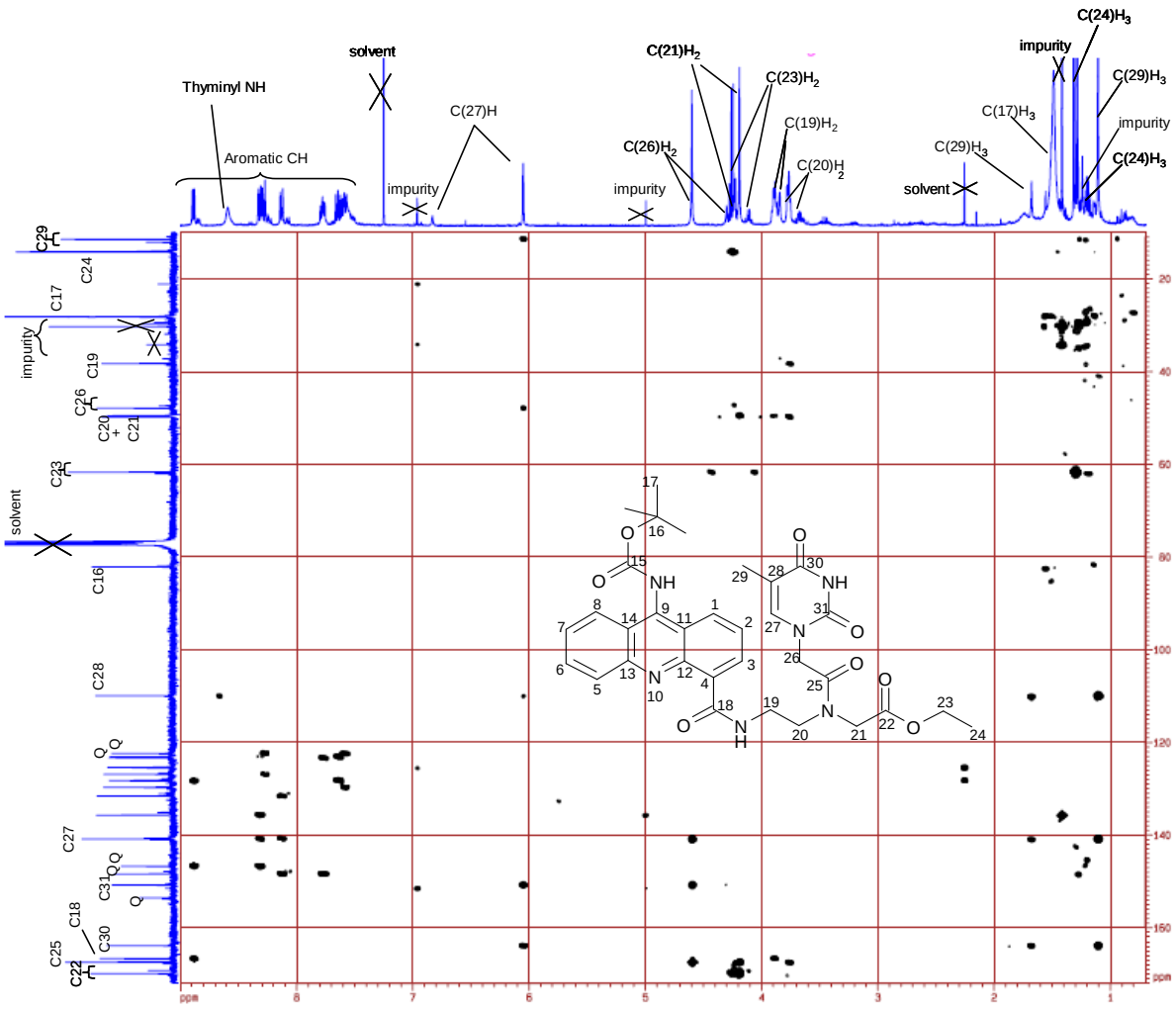

Figure 2.25: HMBC spectrum for **53** showing longer range C-H coupling (the unassigned peaks between 120 and 140 ppm on the C-axis are aromatic tertiary carbons, Q=quaternary carbon)

For C(20)H_2, at 3.68/3.77 ppm, the ROESY spectrum suggested NOE interactions with C(21)H_2 and C(26)H_2. The stronger/most stable rotamer component signal of C(20)H_2, at 3.77 ppm, showed NOE interaction with the stronger/most stable rotamer component signal of C(26)H_2 at 4.61 ppm, suggesting rotamer **53b** (see **Figure 2.26** later) was most stable. The stronger rotamer signal of C(20)H_2 also showed NOE interaction with the stronger C(21)H_2 signal at 4.18 ppm. As the distance between the latter protons did not change in either rotamer, NOE interaction should remain for the less stable rotamer,

however, the relevant cross-peaks were not observed, presumably due to the inherent lower presence of the weaker rotamer. Again, this did not contradict nor exclude rotamer presence as this was irrefutably shown by chemical exchange cross-peaks for the involved protons C(20)H_2, C(21)H_2 and C(26)H_2.

The ROESY spectrum suggested NOE interactions between the stronger rotamer signals of C(19)H_2 (at 3.90 ppm), C(21)H_2 (at 4.18 ppm) and C(26)H_2 (at 4.61 ppm). There was also NOE interaction between the weaker signal of C(19)H_2 (at 3.84 ppm) and, presumably, the weaker C(21)H_2 signal (at 4.18 ppm). The latter interaction was not entirely clear as the weaker C(21)H_2 signal overlapped (in the 1-D spectrum) with the strong signal for ethyl C(23)H_2.

For C(21)H_2, The ROESY spectrum suggested spatial interactions with C(20)H_2 and C(19)H_2 (partially discussed above). The anticipated NOE interaction (for the less stable rotamer **53a**) between the weaker C(21)H_2 signal, at 4.23 ppm, and the weaker C(26)H_2 signal, at 4.31 ppm, seemed to be present but, due to the signals being close together (and overlapping with the broad negative diagonal), this could not be observed unambiguously in the ROESY spectrum.

Additional (weak and strong) NOE interactions were observed, in the ROESY spectrum, between C(27)H_2 and C(26)H_2, and between C(27)H_2 and C(29)H_3.

The tertiary carbons of the aromatic acridine and the remaining quaternary carbons could not be assigned unambiguously. However, a DEPT spectrum in the 1-D ^{1}H-NMR experiment confirmed the presence of the expected eight major CH signals which also allowed, by elimination, to identify the remaining quaternary carbons.

Hence, analysis of the chemical exchange cross-peaks and the observed NOE interactions (in the **ROESY** spectrum) of the nucleobase-linking methylene protons with different parts of the PNA backbone suggested the existence of two major rotational isomers (**a** and **b**) for **53** present in a 4:1 ratio (see **Figure 2.26** below). The ratio was determined by comparing integral traces for the (rotamer generated) double singlet signals of the thymine –CH_3 at δ 1.10 and δ 1.69 or the thymine-CH at δ 6.07 and δ 6.83. The preferred rotameric conformation for the tertiary amide bond in **53b** was the same as the one reported for the *t*-Boc-protected thyminyl-PNA-monomer **13** by Chen *et al.* [206] and Brown *et al*., [207] albeit in a 2:1 ratio for **13**.

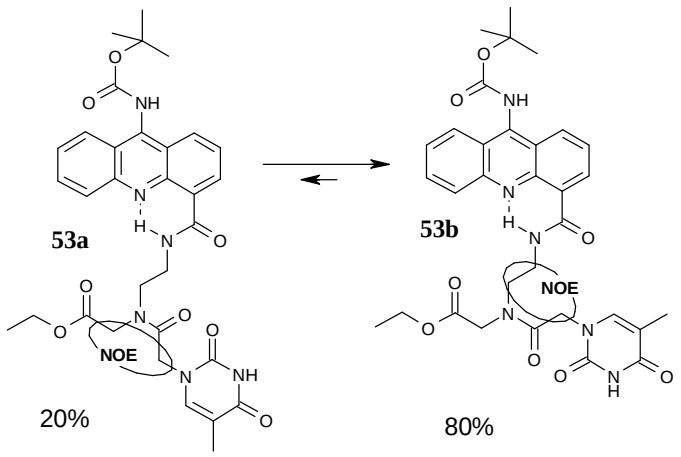

Figure 2.26: The NOE contacts in the ROESY spectrum of compound **53** allow rotational isomers **a**/**b** (generated due to restricted rotation about the 3° amide bond) to be distinguished. (Except for the latter restriction the depicted conformation is arbitrary)

2.15.2 Steps i and ii: acid generation and activation for the Cbz-protected 9-aminoacridine intermediate 45 and subsequent linking to a PNA monomer.

Reaction conditions in step *i* and *ii* (in **Scheme 2.53** below) applied here for **45** were identical to the conditions described for *t*-butyloxy protected methyl ester **47** (in **Scheme 2.52**). After the hydrolysis in step *i* the crude residue containing the acid **49** was used in step *ii*.

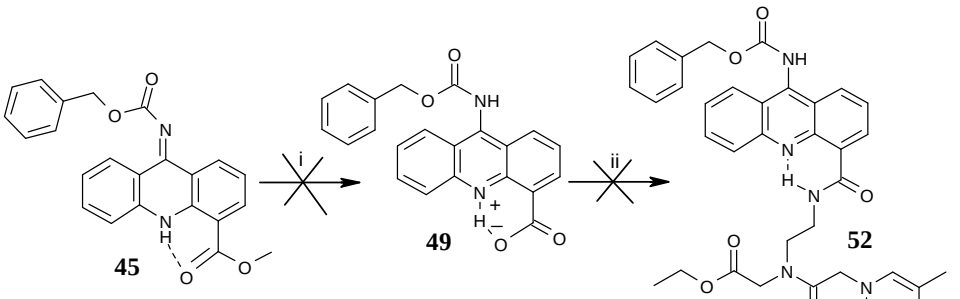

Scheme 2.53

However, acid activation of **49** had generated no observable solid dicyclohexylurea but, as this didn't necessarily exclude activation of **49** had taken place, we proceeded to the next part of step *ii* (addition of the free base of the PNA monomer salt **21**) in order to

potentially generate the desired conjugate **52**. Subsequent work-up led to the isolation of two acridine-containing products; one was unreacted acid **49** and the second remained unidentified. The latter's low solubility in NMR solvents and signal (shift) broadening did not allow proper NMR analysis. Electrospray Mass Spectrometry (ES MS) suggested that the PNA-acridine conjugate **52** was not present in the collected fractions. Unclear as to why this coupling attempt had failed, the most likely explanation was human error since the reaction had worked earlier for the *t*-Boc-protected 9-aminoacridine intermediate **47,** in subsection **2.15.1**. However, although only one unsuccessful attempt was undertaken, due to time constraints it was decided not to further investigate this problem at this point.

2.15.3 Steps i and ii: acid generation and activation for the Alloc-protected 9-aminoacridine intermediate 48 and subsequent linking to a PNA monomer.

As for **45** and **47**, the methyl ester of **48** was hydrolysed and the resulting acid **51** in the crude residue of step *i* was subsequently activated (this time solid dicyclohexylurea was observed) and coupled to the free base of the PNA monomer salt **21** in step *ii* (see **Scheme 2.54** below).

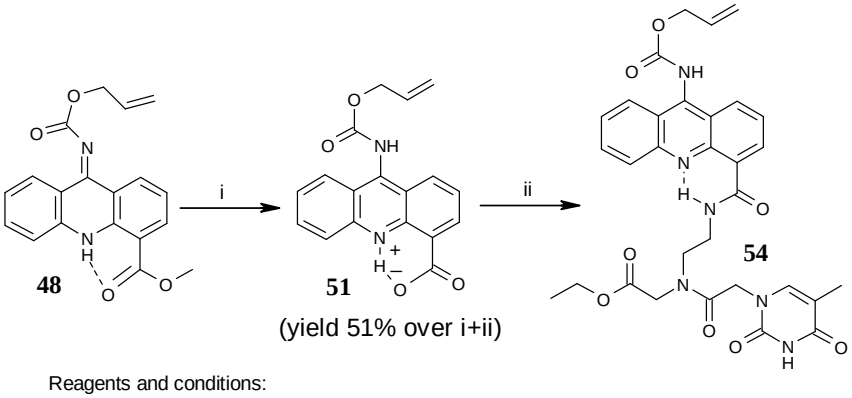

Reagents and conditions:
i: 1) Aqueous LiOH 0.2 M; THF; rt 2) Aqueous HCl 0.5 M; rt
ii: 1) DCC, N-OH succinimide; DMF; rt 2) PNA monomer salt **21**, TEA; DMF; rt

Scheme 2.54

Subsequent work-up yielded **54** in a 51% yield. **H**etero-nuclear **S**ingle **Q**uantum **C**oherence (**HSQC**) and **H**etero-nuclear **M**ultiple **B**ond **C**orrelation (**HMBC**) NMR experiments suggested rotamer presence due to restricted rotation about the tertiary amide bonds. However, limited solubility and signal broadening limited significantly the spectra analysis' value. The latter problems prevented us from obtaining a good

ROESY spectrum and for this reason we were unable to unambiguously distinguish between all rotamer generated 'split' signals. An attempt to assign chemical shifts for **54**, albeit less detailed, was undertaken nevertheless based on the recorded spectra and comparison with the existing data for the *t*-Boc protected PNA-acridine conjugate **53. 54** only differed from **53** in the type of amino carbamate protection and we reasoned that the chemical shift values for the PNA moiety of **54** and **53** should not differ too much. In particular the rotameric chemical shift values in our product **54** at δ 1.19 and δ 1.77 for thyminyl–CH_3 protons compared well with the values for **53** at δ 1.10 and δ 1.69 for thyminyl–CH_3. In the ^{1}H-NMR spectrum for **54** the integral trace for the thyminyl –CH peaks suggested a 3:1 ratio for the two (observable) rotamers. Other rotameric 'split' signals mostly appeared as multiplets due to overlap and poor resolution. Particularly the signals for the allyl protons in **54** appeared broad, which could be interpreted as for the unusual broad *t*-Boc signal in **53**, where peak broadening seemed to be caused by impeded freedom of rotation for the *t*-Boc group.

2.16 Final steps in the 'revised Beal route': deprotection of the acridine 9-amino group and the PNA C-terminus carboxyl group of PNA-acridine conjugates 53 and 54.

In summary, so far our attempts to couple the urethane protected 9-aminoacridine to the thyminyl-PNA-monomer had yielded two PNA-acridine conjugates (**53** and **54**) that subsequently needed to be de-protected. Both **53** and **54** carried a urethane protection group and had their PNA C-terminus carboxyl group protected in the form of an ethyl ester. Because there was no reason to remove either of these groups in a particular order it was arbitrarily decided for **53**, the *t*-Boc protected PNA-acridine, to first remove the *t*-Boc group. This would liberate the primary 9-amino group of the acridine **53**, after which the ethyl ester could be hydrolysed. For **54**, the Alloc protected conjugate, the ethyl ester was hydrolysed before an attempt was made to remove the Alloc group. These reactions are illustrated below in **Scheme 2.55**. Each step will now be discussed separately.

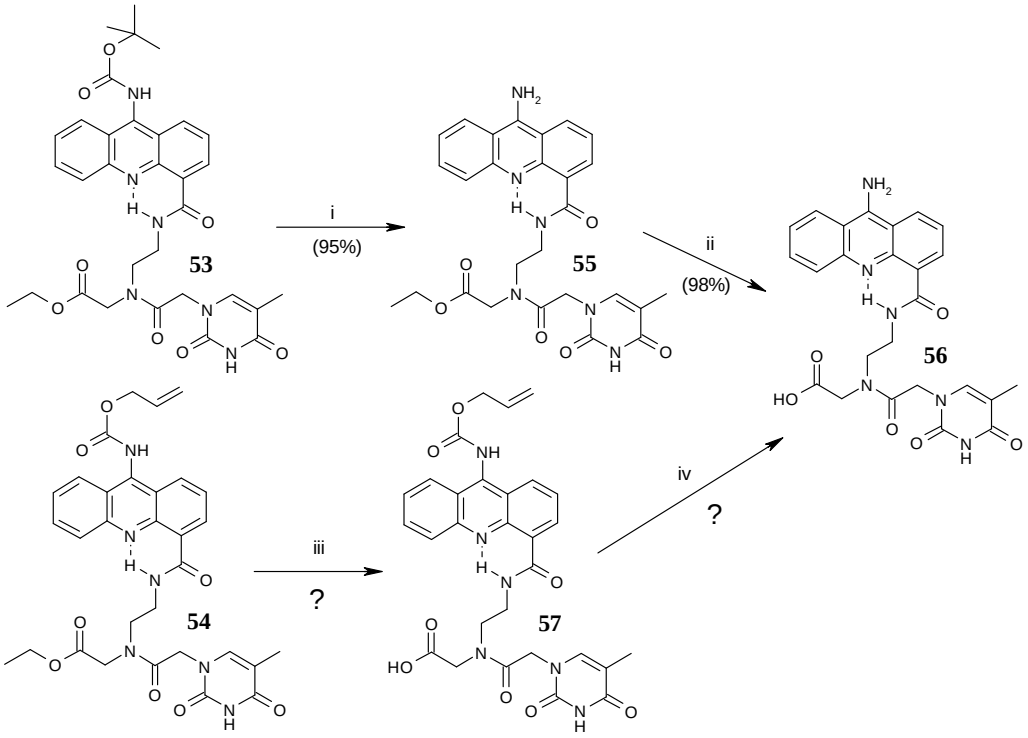

Reagents and conditions:
i: TFA; DCM; rt
ii and iii: 1) Aqueous NaOH 0.3 M; THF; rt 2) Aqueous HCl 0.1 M
iv: Tetrakis(triphenylphosphine)Palladium, Triethylammonium formate; THF/DMF; rt

Scheme 2.55: De-protecting PNA-acridine conjugates **53** and **54** (due to purification problems in steps iii and iv, yields could not be determined)

2.16.1 Step i: t-Boc deprotection of PNA-acridine conjugate 53

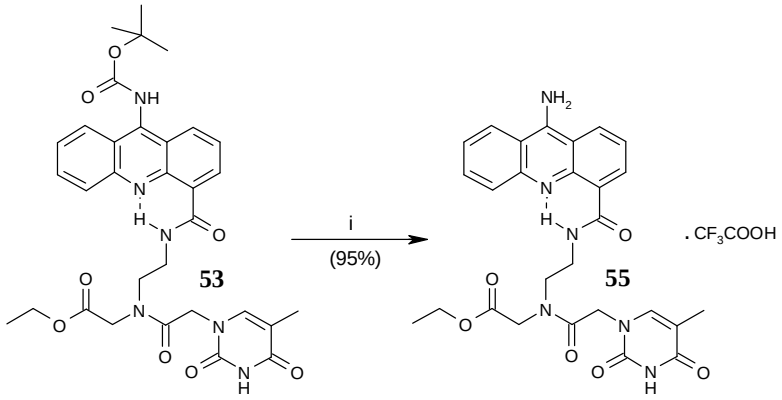

Reagents and conditions: i: TFA; DCM; rt

Scheme 2.56

In the above depicted urethane acidolysis (**Scheme 2.56**), protonation of the urethane carboxyl oxygen lead to the release of the *t*-butyl cation followed by carbon dioxide release thus generating the free 9-amino group on the middle acridine ring. Hence, **53** was treated with trifluoroacetic acid according an adapted protocol described by Englund *et al*. for the *t*-Boc-deprotection of an amino acid α-NH_2 [229], and subsequent work-up afforded the title compound **55** as a fine yellow powder (95% yield).

Analysis of the ^{1}H-NMR spectrum for **55** suggested the expected presence of two rotamers, now in a 1:1 ratio (due to restricted rotation about the tertiary amide bond) (see **Figure 2.27** below). The ratio was determined by comparing integral traces for the (rotamer generated) double singlet signals of the thymine –CH_3 at δ 1.65 and δ 1.80 or the thymine-CH at δ 7.11 and δ 7.23. A key feature in the ^{1}H-NMR spectrum of **55** was the disappearance of the *t*-Boc peak present in the ^{1}H-NMR spectrum of the starting material **53.** Assignment of peaks in the ^{1}H-NMR spectra of **55** was again aided by comparison with the spectra recorded for the starting material (the *t*-Boc protected PNA-acridine conjugate **53).**

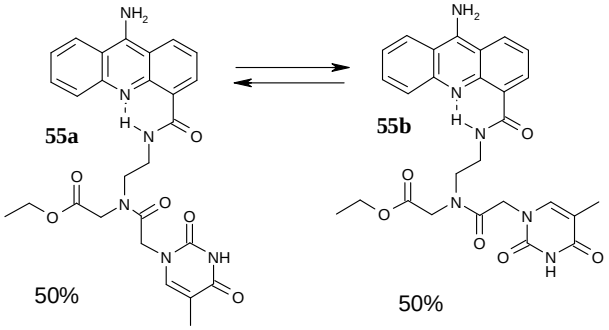

Figure 2.27: The two major rotamers **a** and **b** for PNA-acridine conjugate **55** due to restricted rotation around the tertiary amide bond (except for the latter restriction the depicted conformation is arbitrary)

55 only differed from **53** in bearing an amino carbamate protection and we reasoned that the chemical shift values for the PNA moiety of **55** and **53** should not differ too much. The different rotamer ratio, 1:1 for **55**, compared to 1:4 for **53**, at this point could only be rationalised by assuming the reduced bulkiness of the acridine moiety somehow allowed for a less impeded rotamer interconversion.

2.16.2 Step ii: C-terminus ethyl ester basic hydrolysis of PNA-acridine conjugate 55.

In step *ii*, the ethyl ester component of the TFA salt of **55** underwent aqueous basic hydrolysis after which the generated carboxylate-bearing PNA-acridine conjugate was converted to **56** via neutralisation with aqueous HCl (see **Scheme 2.57** below).

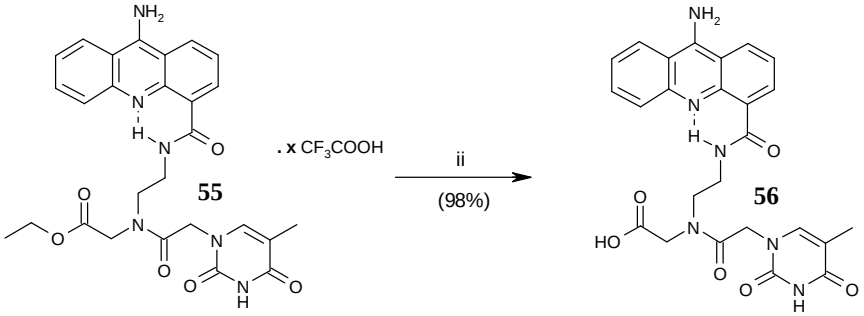

Reagents and conditions: ii: 1) Aqueous NaOH 0.3 M; THF; rt 2) Aqueous HCl 0.1 M; rt

Scheme 2.57

Subsequent work-up afforded a crude residue that contained the desired product **56** (98 % yield) and a NaCl residue. Recrystallisation attempts, e.g. using ethanol or methanol, to remove the NaCl were unfortunately not successful. The consequence of this was a low solubility of the crude precipitate in NMR solvents and only a 1D-^{1}H-NMR spectrum could be recorded as signal strength was low. Nevertheless, subsequent analysis of the ^{1}H-NMR spectrum of **56** suggested the presence of 2 rotamers in a 1:1 ratio due to restricted rotation about the tertiary amide bond (see **Figure 2.28** below).

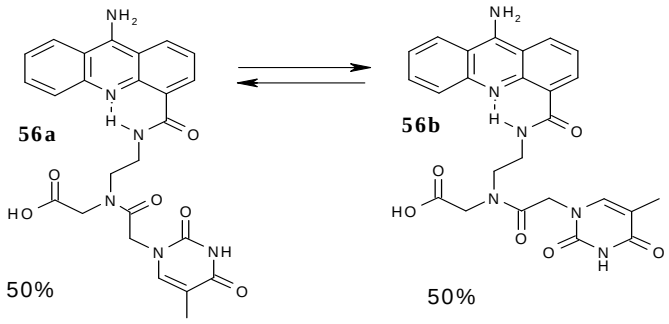

Figure 2.28: The two major rotamers **a** and **b** for PNA-acridine conjugate **56.**

The ratio was determined by comparing integral traces for the (rotamer generated) double singlet signals of the thymine $-CH_3$ at δ 1.20 and δ 1.55 or the thymine-CH at δ 6.34 and δ 6.94 in the ^{1}H-NMR spectrum of **56**.

A key feature in the ^{1}H-NMR spectrum of **56** was the disappearance of the $-CH_2CH_3$ peaks present in the ^{1}H-NMR spectrum of the starting material **55**. Analysis of the latter spectrum and comparison with the ^{1}H-NMR spectrum of **53** also (again) aided the assignment of peaks for **56**.

2.16.3 Step iii: C-terminus ethyl ester basic hydrolysis of PNA-acridine conjugate 54.

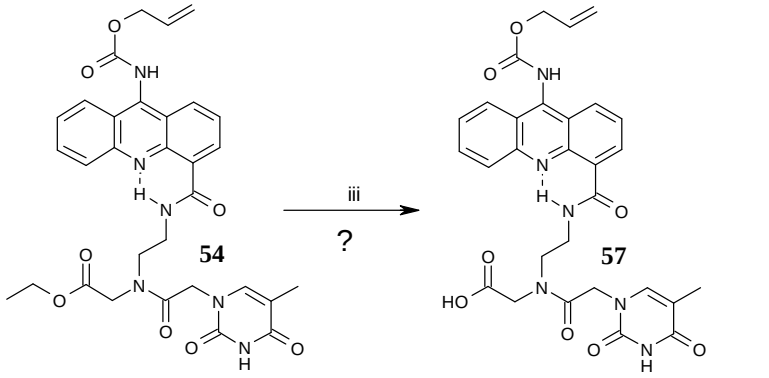

Reagents and conditions: iii: 1) Aqueous NaOH 0.3 M; THF; rt 2) Aqueous HCl 0.1 M; rt

Scheme 2.58

As for compound **55** in the former step *ii*, here in step *iii* the PNA-acridine conjugate **54** underwent aqueous basic hydrolysis after which the (intermediate) generated carboxylate-bearing PNA-acridine conjugate was converted to **57** via neutralisation with aqueous HCl. Subsequent work-up afforded a crude residue containing the product **57**, NaCl and a number of unidentified by-products. Recrystallision of the crude residue, using methanol, afforded a fine yellow powder that however still contained a substantial amount of unidentified impurities as suggested by analysis ^{1}H-NMR data for the crude yellow precipitate.

Because analysis of the latter data could not exclude presence of the desired intermediate **57**, it was decided to take the yellow precipitate through to the next step (i.e. Pd(0) catalysed Alloc cleavage in step *iv*). A subsequent successful work-up of the reaction in step *iv* could potentially still afford the desired end-product **56** via this route.

2.16.4 Step iv: Alloc-deprotection of PNA-acridine conjugate 57.

The crude residue, produced in the former step *iii* and containing the PNA-acridine conjugate **57**, was treated with catalytic amounts of tetrakis(triphenylphosphine)palladium(0) in the presence of triethylammonium formate as the allyl accepting nucleophile, according an N-alloc deprotection method successfully used by Kanda *et al*.[230] (see **Scheme 2.59** below)

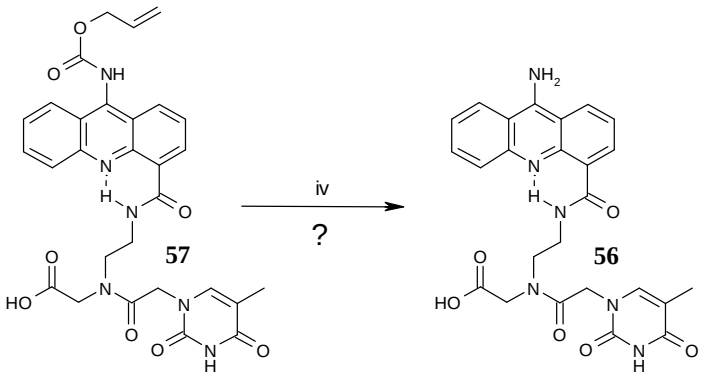

Reagents and conditions: iv: Tetrakis(triphenylphosphine)Palladium, Trieltylammonium formate; THF/DMF; rt

Scheme 2.59

In the latter procedure, the (unreactive) tetrakis(triphenylphosphine)Pd(0) was in equilibrium with (stable) tri(triphenylphosphine)Pd(0) and this in turn was in equilibrium with (reactive) di(triphenylphosphine)Pd(0).[226] The latter Pd(0) species initiated cleavage of the allylcarbamate via the formation of a Pd π–allyl complex.

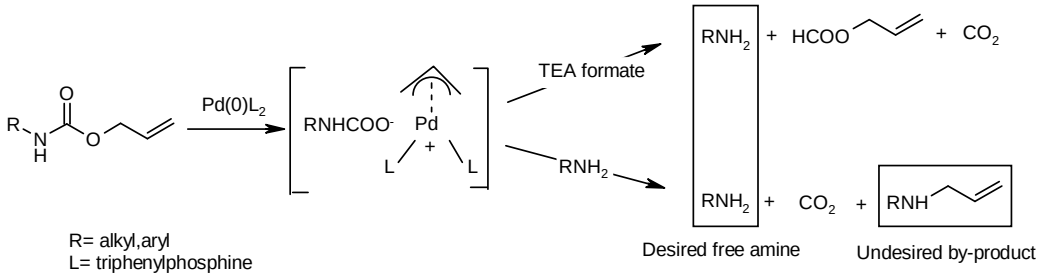

Figure 2.29: General mechanism for Pd(0) catalysed allylcarbamate cleavage using triethylammoniumformate as allyl acceptor (as suggested by Roos *et al*., 1995,[231])

Presence of nucleophilic formate (the allyl acceptor) subsequently generated the free amine **56**, CO_2 and allylformate (see **Figure 2.29** above for the reaction mechanism).[231]

In the reaction work-up a crude yellow precipitate was isolated for which ^{1}H-NMR data analysis suggested presence of the desired PNA-acridine conjugate **56** but also (a number of) undesired, unidentified by-product(s), the 9-allylamine, generated due to competition with formate for the allyl electrophile, being a likely candidate for the latter (see **Figure 2.29** above).[231]

Unfortunately, subsequent repeated attempts to re-crystallise **56** in e.g. ethanol/diethyl ether, methanol/diethyl ether and methanol/THF were not successful in significantly separating/isolating **56** from the by-product(s) and unambiguous identification of either was not possible. Due to time constraints it was decided at this point to no longer pursue the complete purification of compound **56** via this route as we had obtained a better result in doing this via steps *i* and *ii* of **Scheme 2.55**, which dealt with deprotection of the *t*-Boc, ethyl ester protected PNA-acridine **53**. Although in steps *i* and *ii* of **Scheme 2.55** we had obtained **56** with a NaCl impurity, it still allowed us to partially characterize the desired conjugate **56**.

2.17 Bioactivity of two acridine intermediates

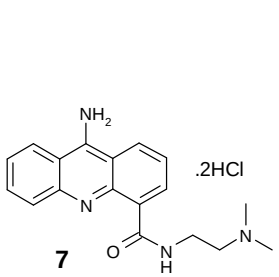

7

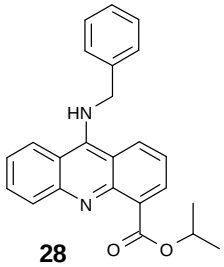

28

IC_{50}= 22 µM

IC_{50}= 100 µM

Scheme 2.60: Bioactivity of two 9-aminoacridines in an IN-activity assay. (Assay was performed by J-F Mouscadet from the Laboratoire de Biotechnologies et Pharmacologie Génétique Appliquée, CNRS UMR 8113, Ecole Normale Supérieure de Cachan, 61 av du Président Wilson, 94235 Cachan, France.)

IC_{50} values were determined for two acridine intermediates synthesised during our project (see **Scheme 2.60** above). The dihydrochloride salt of 9-amino-DACA (**7**) and *iso*-propyl-9-benzylaminoacridine-4-carboxylate (**28**) showed respective IC_{50} values of 22 µM and 100 µM in an IN-activity assay, described by Maurin *et al.*: "Full IN

activity reactions (i.e. 3'-processing + strand transfer) were performed in triplicate in 96-well plates using 0.25 pmol of labelled U5A/U5B double-stranded DNA substrate, 12 pmol of ST1/ST2 3-biotinylated target DNA and 2 pmol of integrase in buffer A [20 mM Hepes (pH 7.2), 10 mM $MgCl_2$, 25 mM NaCl, and 1 mM DTT] in a final volume of 40 mL. Radiolabelled reaction products were bound to Streptavidin-coated magnetic beads (DynaL), washed twice in buffer B (PBS buffer supplemented with 0.025% Tween 20 and 10 mg/ml BSA) and quantified on a beta radiation counter. Inhibition in the presence of drugs was expressed as the fractional product in percent of the control without drug."[232] Oligonucleotides used in the assay were purchased from Eurogentec and further purified, by Maurin *et al.*, on 18% acrylamide/urea denaturing gel (U5B: GTGTGGAAAATCTCTAGCA; U5A: 5'-ACTGCTAGAGATTT TCCACAC; ST1: AGTGAATTAGCCCTTGGTCA-biotin; ST2: 5'-TGACCA AGGGCTAATTCACT-biotin; U5B was radio labelled using T4 polynucleotide kinase for 3'-processing and strand transfer reactions).

Hence, for our compounds **7** (IC_{50}= 22 µM) and **28** (IC_{50}= 100 µM) this meant that at their respective concentrations of 22 µM and 100 µM only 50% of the radioactivity recorded for the control test (without drug) was observed. Although the tested compounds were not PNA-acridine conjugates and presented only moderate anti-IN activities, we considered this result a strong argument for the use of the 4-substituted 9-aminoacridine moiety in the development of PNA-acridine conjugates as potential HIV inhibitors.

2.18 Conclusion

When we set out a strategy to synthesise 9-aminoacridines conjugated to a PNA monomer in the acridine's 4-position we initially found inspiration in the synthetic route towards 9-amino-DACA **6**, an anti-tumour agent developed by Denny. Although we were able to apply this strategy successfully to the synthesis of 9-amino-DACA **6** and the types of chemical conversions were identical to the ones required for our purposes we were unsuccessful in the 'Denny route' towards the synthesis of the desired PNA-acridine conjugates. Due to repeated purification problems and apparent side-product formation in the latter's carboxamide formation step, we decided to investigate an alternative approach in which the order was changed in which the PNA-acridine components (acridine, PNA monomer backbone and nucleobase moieties)

would be linked to each other. Unfortunately, this alternative carboxamide formation step was also characterized by repeated purification problems and apparent side-product formation. A possible explanation for the encountered problems, when linking the acridine to the PNA moiety, could have been intra-molecular cyclization reaction involving the ethyl ester carbonyl of the PNA moiety and the primary amine of the latter and/or the hydrolytic sensitivity of the 9-chloroacridine-4-carbonyl chloride **4**. Since the problems encountered did not appear to be easily surmountable we decided to rethink our strategy to obtain the desired PNA-acridine conjugates.

Inspiration was found in Beal's reported strategy for the solid-phase synthesis of acridine-peptide conjugates to enable libraries of acridine-peptide to be generated. We were inspired by the fact that these conjugates bore the 9-anilinoacridine-4-carboxamide moiety similar to our intended PNA-acridine conjugates. The main difference with the 'Denny route' was the order in which the 9-amino and 4-carboxamide functionalities were established. We reasoned that by using Beal's synthetic strategy but establishing the acridine substituents with the amines relevant to our purpose, i.e. a 9-benzylamino and a 4-PNA substituent, this would provide us with a reproducible pathway towards the desired 9-NH_2-4-PNA-acridine conjugates. It was envisaged that once the 9-benzylamino-4-PNA-acridine conjugate had been synthesised only the 9-benzylamino substituent needed to be subjected to hydrogenolysis to establish the primary 9-amino substituent desired in our PNA-acridine conjugates. Unfortunately, before the latter step was reached, a problem arose that prevented us from establishing an acridine 4-PNA (monomer) substituent in the presence of a 9-benzylamino substituent. We also found that for the 9-anilino substituted acridine, activation of the 4-carboxyl substituent (via NHS-ester formation) and the subsequent carboxamide forming step did work, resulting in the synthesis of 9-anilino-DACA **35** and a 9-anilinoacridine-4-PNA conjugate **36**. This result inspired us to revise the 'Beal route' and led us to the development of several 9-aminoacridine intermediates in which the 9-amino group was converted into a carbamate group. The three urethane moieties established in the acridine's 9-position were the benzyloxycarbonylamino, the allyloxycarbonylamino and the *t*-butyloxycarbonylamino group. All three intermediates fulfilled the main condition to allow subsequent acridine-4-carboxyl activation, i.e. they had an electron withdrawing effect on the acridine's exocyclic nitrogen which decreased the (acridine) ring nitrogen N10 basicity. Although all three carbamate-bearing intermediates could be considered equally valuable in the synthetic

route towards the desired PNA-acridine conjugates, only the *t*-Boc-protected and the alloc protected 9-amino-4-PNA-acridine intermediates **53** and **54** were synthesised successfully. Subsequent deprotection steps for the *t*-Boc-bearing intermediate **53** (*t*-Boc and PNA monomer ethyl ester cleavage) led to the desired 9-NH_2-4-PNA-acridine conjugate **56**. Due to time constraints and purification complications for the deprotection steps of the 9-alloc-bearing intermediate **54** we were not able to characterize and determine the yield for the end product **56** via this route. Nevertheless, the complete synthetic route towards the PNA-acridine conjugate **56** (over-all yield 4%) was successfully accomplished via the 9-*t*-Boc-bearing intermediate **53** and is summarized below in **Scheme 2.63.**

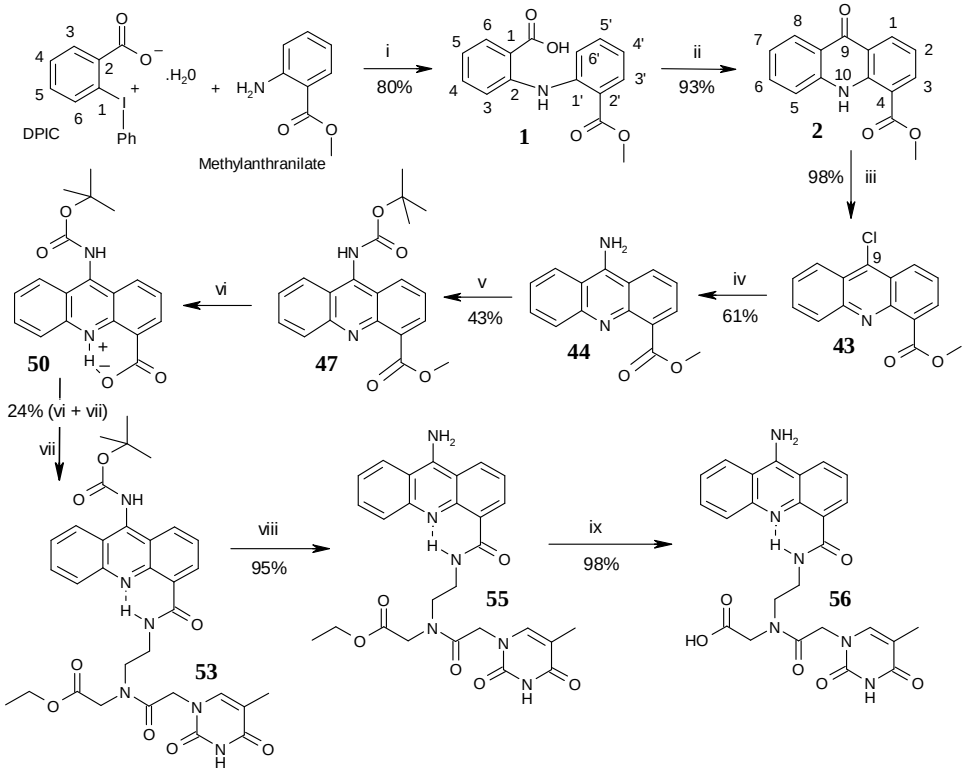

Reagents and Conditions: **i**: Cu-acetate (cat); DMF; 90℃. **ii**: PPE(**2"**); $CHCl_3$; reflux. **iii**: $SOCl_2$, DMF_{cat}; rt
iv: a) Phenol; 70℃ b) NH_4HCO_3; 120℃. **v**: a) Phosgene, TEA; o-DCB; 110℃ b) t-Butanol; o-DCB; 110℃.
vi: a) Aq. LiOH 0.2 M;THF; 0℃ to rt b) Aq. HCl 0.5 M; rt. **vii**: a) DCC, N-OH succinimide; DMF; rt
b) PNA monomer salt **21**, TEA; DMF; rt. **viii**: TFA; DCM; rt. **ix**: a) Aq. NaOH 0.3 M; THF; rt b) Aq. HCl 0.1 M; rt

Scheme 2.63: Synthetic route towards the PNA-acridine conjugate **56**.

Hence, a crucial achievement of this project was the development of the chemistry necessary to establish the acridine-PNA carboxamide link in the acridine's 4-position and this in the presence of a (carbamate protected) primary amino group in the acridine's 9-position. Although our intention to retain a primary 9-amino functionality

in our final PNA-acridine conjugates had seriously complicated our attempts to link the acridine moiety to the PNA, we had found a practical way to circumvent the associated problems by making use of 9-amino protecting carbamates. This allowed us to successfully complete the synthetic route towards the desired PNA-acridine conjugate **56** (see **Scheme 2.63** above), the chemistry of which is an important step towards the further development of PNA-acridine conjugates as potential HIV-IN inhibitors.

2.19 Future Work

Although all our compounds were prepared in solution phase, it is believed a solid-phase based strategy is the way forward in the synthesis of PNA-oligomer-Acridine conjugates. Similar to the strategy of Beal for the solid-phase synthesis of acridine-peptide libraries, PNA oligomers/polymers could be synthesised in solid-phase and subsequently peptide-linked to the acridine's NHS-activated 4-carboxyl substituent. Development of the latter (activated) acridine has been an important achievement of our project but we also believe the alternative, earlier abandoned 'Denny route', in which an acid chloride (in the acridine 4-position) would enable 4-carboxamide formation, should be re-examined. In particular, the suggested hypotheses that PNA-acridine coupling may have been compromised, by a competing cyclization side-reactions of the free base of the PNA monomer (**14** or **21**) or by hydrolytic sensitivity of the acridine acid chloride **4,** require further scrutiny as it was shown at a later stage in our project that the thyminyl-PNA-monomer (**14** or **21**) was not a barrier to the coupling step nor had (potential) hydrolytic sensitivity of **4** prevented us from making 9-NH_2-DACA via the acridine acid chloride. When investigating the latter potential problems, particular attention should be given to the prevention of intra-molecular ethyl ester aminolysis of the free base of the PNA monomer (**14** or **21**) e.g. by slow deprotonation of the latter salts, at lowered temperature and in the presence of the acridine acid chloride **4**. Extra attention should be given to rigorous drying of solvents and reagents to eliminate potential hydrolysis of the acid chloride **4**. In addition, the use of preparative reversed phase HPLC, unfortunately unavailable at the time of our experiments, would be essential to isolate the polar PNA-acridine conjugate(s) from any formed by-products (a complication we were not fully able to resolve).

Hence, providing one would be able to successfully develop the (liquid phase) 'Denny route' to PNA-acridine conjugates this would offer a useful alternative to our 'revised

Beal route' and to the envisaged subsequent (solid phase) linking of PNA to the 9-chloroacridine acid chloride **4**. With regards to the latter, any substitutions in the 9-position of the acridine could be potentially achieved after the solid phase PNA-acridine peptide linking step.

It is believed the chemistry developed so far in the 'revised Beal route' provides a solid starting point for further development of PNA(oligomer)-acridine conjugates as potential (nucleic acid sequence selective) novel inhibitors of HIV-1 integrase (IN).

Chapter 3: Experimental

3.1 General materials and methods:

Commercially available reagents and starting materials were purchased from Alfa Aesar U.K. and from Sigma Aldrich, U.K. Solvents referred to as 'dry' or 'anhydrous' were dried using standard procedures.[233] Analytical thin layer chromatography (TLC) was carried out on aluminium sheet silica gel 60 F_{254} plates (Merck). Preparative thin layer chromatography was carried out on Fisher Silica Gel Preparative TLC Plates 20 x 20 cm, 2.00 mm. thickness. Visualisation was achieved under UV light (254 nm) or by treatment with a $KMnO_4$ stain (1.5g of $KMnO_4$, 10g K_2CO_3, and 1.25mL 10% NaOH in 200mL water). All (flash) column chromatography was carried out with Fisher silica gel 60 (230-400 mesh). Acidic cation-exchange resin used was DOWEX 50W-X8(H)-100 purchased from Lancaster U.K. Infrared spectra were recorded, using a Perkin Elmer 1600 series FTIR spectrophotometer. ^{1}H-NMR and ^{13}C-NMR spectra were recorded on Bruker AC 200 and Bruker DPX 400 spectrometers. Chemical shifts were recorded in ppm, using the residual non-deuterated solvent signal as a reference. Coupling constants were quoted in Hz. Mixtures of two rotational isomers were observed for some of the products containing tertiary amide bonds. Cis-trans isomers were observed for certain 9-aminoacridines due to restricted rotation about the acridine C9-N bond. Consequently, a number of NMR signals for these products were doubled and are indicated as (max) for the major, and (min) for the minor isomer. One mixture of three rotational isomers was observed due to secondary and tertiary amide bond restricted rotation, in which case a fraction of protons was assigned to the doubled or tripled signals. Melting points were measured using an electrothermal melting point apparatus and are uncorrected. Compound crystal structures were determined from single crystal data recorded with a Bruker Nonius X8-Apex2 CCD diffractometer. Elemental analyses for C, H and N were carried out on Exeter Analytical CE440 analyser. Low and high resolution mass spectrometric analyses (CI, EI and ESI) were performed at the EPSRC National Mass Spectrometry Service Centre, University of Wales, Swansea.

3.2 Experimental procedures

2-(2-Methoxycarbonylphenylamino)-benzoic acid (1)[187]

METHOD A: via phenyliodide substitution in DPIC

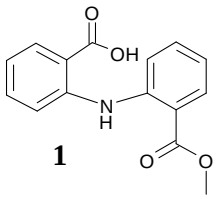

1

Methyl anthranilate (3.16 g, 20.9 mmol, 1.80 eq), DPIC (4.00 g, 11.7 mmol, 1.00 eq) and a catalytic amount of copper(II)acetate (0.08 g, 0.4 mmol, 0.04 eq) were suspended in anhydrous DMF (300 mL) and this suspension was heated with stirring at 90°C for 12 h. The solvent was removed *in vacuo* and the residue (green oil) was dissolved in ethyl acetate (150 mL). The resulting organic solution was washed with 0.1 M (aq) hydrochloric acid (150 mL) before being extracted with a 0.1 M (aq) solution of ammonia (3 x 100 mL). The combined aqueous ammonia extracts were slowly poured into a 0.1 M (aq) solution of hydrochloric acid (700 mL). The white-green precipitate afforded was isolated and washed with hot water (2 x 50 mL). The title product **1** was obtained as a green solid (2.55 g, 80%). This product showed sufficient purity to be used in a next step without further purification. mp 194-198°C (from toluene/acetone) (Lit.[187] 196-198°C); R_f 0.47 (Petroleum ether (40-60 °C) : ethyl acetate : acetic acid, 99: 99: 2); (Found: C, 66.0; H, 4.8; N, 5.0. $C_{15}H_{13}NO_4$ requires C, 66.4; H, 4.8; N, 5.2%.); ν_{max}(KBr)/cm^{-1} 3339, 2946(br), 1709, 1660, 1600, 1581, 1517, 1450, 1325, 1278, 755; δ_H(200 MHz; $CDCl_3$) 3.55 (1 H, br s, N*H*), 3.85 (3H, s, OCH_3), 6.88-7.00 (2 H, m, Ar-*H*), 7.35-7.45 (2 H, m, Ar-*H*), 7.51-7.57 (2 H, m, Ar-*H*), 8.00 (1 H, dd, *J* 7.9 and 1.7, Ar-*H*), 8.09 (1 H, dd, *J* 7.9 and 1.3, Ar-*H*), 10.85 (1 H, s, COO*H*); δ_C(50 MHz; $CDCl_3$) 52.0 (q), 117.3 (d), 118.2 (s), 118.6 (d), 119.7 (d), 120.5 (d), 131.85 (d), 132.5 (s), 132.7 (d), 133.1 (d), 134.3 (d), 143.4 (s), 145.2 (s), 167.5 (s), 182.9 (s).

METHOD B: via chloride substitution in o-Chlorobenzoic acid

Methyl anthranilate (6.15 g, 40.7 mmol, 1.80 eq), *o*-chlorobenzoic acid (3.54 g, 22.6 mmol, 1.00 eq), anhydrous potassium carbonate (1.56 g, 11.3 mmol, 1.00 eq) and a catalytic amount of copper metal powder (0.15 g, 2.4 mmol, 0.10 eq) were suspended/dissolved in a 3:1 mixture of H_2O:DMF (25 mL). This mixture was then heated at 100°C with stirring for 48 h. The solvent was removed under vacuum and the residue (green-black oil) was dissolved in ethyl acetate (125 mL). The resulting

organic solution was washed with 0.1 M (aq) hydrochloric acid (200 mL) before being extracted with a 0.1 M (aq) solution of ammonia (3 x 100 mL). The combined aqueous ammonia extracts were acidified with 2.0 M (aq) hydrochloric acid to pH 4. The precipitate was isolated and washed with hot water (150 mL) to afford the title compound **1** (1.90 g, 31%) as a green solid. This product showed sufficient purity to be used in a next step without further purification. The analysis of this product was identical to that obtained for the product yielded by method A.

Methyl-9-oxoacridan-4-carboxylate (2)[187]

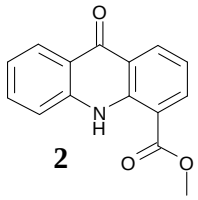

2

2-(2-Methoxycarbonylphenylamino)benzoic acid (**1**) (1.42 g, 5.23 mmol, 1.00 eq) was suspended in a mixture of tetraethyl tetrametaphosphates (**2"**) (50.00 g, 115.7 mmol, 22.10 eq) and dry chloroform (80 mL). The resulting mixture was heated under reflux with stirring until all the solids had dissolved. The solvent was then allowed to evaporate at atmospheric pressure to give a red oil which was subsequently heated on a water bath for 1.5 h. at 100°C. The oil was diluted with methanol (8 mL). Slowly, water (38 mL) was added to this solution to precipitate the crude product as a yellow solid. This was isolated by filtration, washed with a 50% aqueous solution of methanol containing 1% triethylamine (40 mL), dried and stored over P_2O_5. The title compound **2** (1.23 g, 93%) was obtained as a yellow solid. This product showed sufficient purity to be used for synthetic purposes without further purification. mp 159-162°C (from acetone/diethyl ether) (Lit.[234]172°C); R_f 0.64 (Petroleum ether (40-60 °C) : ethyl acetate : acetic acid, 99: 99: 2); (Found: C, 70.6; H, 4.2; N, 5.4. $C_{15}H_{11}NO_3$ requires C, 71.1; H, 4.4; N, 5.5%); ν_{max}(film)/cm^{-1} 3269, 2947, 1690, 1637, 1617, 1590, 1524 and 1442, 1283, 755; δ_H (200 MHz; $CDCl_3$): 3.98 (3 H, s, OC*H*$_3$), 7.18-7.40 (3 H, m, Ar-*H*), 7.58-7.69 (1 H, m, Ar-*H*), 8.41 (2 H, dd, *J* 7.5 and 1.7, Ar-*H*), 8.69 (1 H, dd, *J* 7.9 and 1.7, Ar-*H*), 11.60 (1 H, s, N*H*); δ_C (50 MHz; $CDCl_3$): 52.5 (q), 113.5 (s), 117.5 (d), 119.9 (d), 121.5 (s), 122.4 (d), 127.05 (d), 134.0 (d), 134.05 (d), 136.5 (d), 140.0 (s), 141.7 (s), 142.9 (s), 168.4 (s), 177.9 (s); LRMS m/z (EI) (%) 253 (M^+, 74), 221 (100), 193 (29), 178 (56); HRMS (EI) found 253.0731, calcd. for $C_{15}H_{11}N_1O_3$ [M^+] 253.0733.

Tetraethyl tetrametaphosphates or cyclotetraphosphoric acid ethyl esters 2" [139]

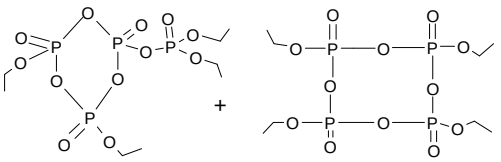

2''

Anhydrous phosphorus pentoxide (50.00 g, 176.0 mmol, 1.00 eq), chloroform (100 mL) and diethyl ether (50.0 mL, 482 mmol, 2.74 eq) were combined and heated under reflux under nitrogen with stirring for 15-30 h. The clear solution was then filtered through glass wool and the solvent removed *in vacuo*. The crude product **2"** (71.6 g, 94%) was afforded as light-yellow viscous oil, which needed no further purification for synthetic purposes. ν_{max} (film)/cm^{-1} 2990, 2941, 1479, 1446, 1397, 1373, 1310, 950-1100.

9-Oxoacridan-4-carboxylic acid (3)[187]

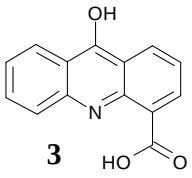

3

Compound **2** (1.10 g, 4.33 mmol, 1.00 eq) was suspended in a mixture of absolute ethanol (110 mL) and a 2 M (aq) solution of sodium hydroxide (110 mL). The resulting mixture was heated at reflux for 10 min. Then, the clear yellow solution was filtered and DOWEX cation-exchange resin (150 g) was added. The suspension was shaken for 1h. Any precipitated product was re-dissolved by the addition of a further quantity of absolute ethanol (100 mL). Subsequently, the resin was removed by filtration and washed with absolute ethanol (3 x 100 mL). Removal of the solvent *in vacuo* followed by azeotropic drying with first toluene (4 x 75 mL) then diethyl ether (4 x 75 mL), gave the title compound **3** (0.94 g, 91%) as a yellow solid. mp 322-325°C (from EtOH) (Lit.[187] 324-325 °C); R_f 0.22 (Petroleum ether (40-60 °C) : ethyl acetate : acetic acid, 99: 99: 2); ν_{max}(KBr)/cm^{-1} 3227, 2931br, 1693, 1620, 1597, 1580, 1568, 1524, 1461, 1443, 755; δ_H (200 MHz; DMSO-d_6) 7.28-7.40 (2 H, m, Ar-*H*), 7.73-7.80 (2 H, m, Ar-*H*), 8.25 (1 H, d, *J* 7.9, Ar-*H*), 8.45 (1 H, dd, *J* 7.5 and 1.7, Ar-*H*), 8.55 (1 H, dd, *J* 8.3 and 1.66, Ar-*H*), 11.95 (1H, s, O*H*), 13.95 (1H, br s, N(10)*H*); δ_C (50 MHz, DMSO-d_6): 118.4 (d), 120.0 (d), 120.6 (s), 121.2 (d), 121.3 (s), 126.4 (d), 128.1 (d), 133.8 (d), 136.0 (d), 140.4 (s), 142.2 (s), 169.9 (s), 177.2 (s); LRMS m/z (EI) (%) 239 (M^+, 84), 221 (100), 193 (60), 164 (51), 110 (50); HRMS (EI) found 239.0620, calcd. for $C_{14}H_9NO_3$ [M^+] 239.0582.

9-Chloroacridine-4-carbonyl chloride (**4**) [186]

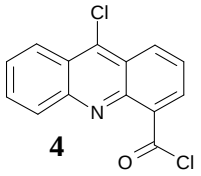

4

Compound **3** (0.35 g, 1.5 mmol, 1.00 eq) was suspended in thionyl chloride (2.20 mL, 30.0 mmol, 20.5 eq) and a catalytic amount of DMF was added (one drop). The resulting suspension was heated gently under reflux, while stirring and under nitrogen, until all the solid material had dissolved. The homogeneous solution was then left at reflux for a further 45 mins, whereupon the reaction mixture was allowed to cool to rt. The bulk of the thionyl chloride was removed *in vacuo*, whilst keeping the temperature below 40°C. The final traces of thionyl chloride were removed by re-suspending the residue in toluene (3 x 5 mL) and removing the solvent *in vacuo*. This yielded the title crude compound **4** (0.40 g, 99%) as a yellow-reddish solid. The product was used without further purification. mp 132-137°C (from $CHCl_3$ / Petroleum ether); R_f 0.32 (Petroleum ether (40-60 °C) : ethyl acetate : acetic acid, 99: 99: 2).

***N*-[2-(Dimethylamino) ethyl]-9-chloroacridine-4-carboxamide (5)**[186]

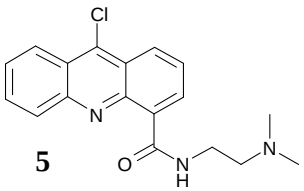

5

Crude compound **4** (0.40 g, 1.4 mmol, 1.00 eq) was dissolved in dry dichloromethane (2 mL) and the resulting solution was cooled to -5°C. Subsequently, an ice cooled solution of *N*,*N*-dimethylethylenediamine (0.63 mL, 5.7 mmol, 3.92 eq) in dry dichloromethane (4 mL) was added, whilst stirring under nitrogen. The reaction mixture was then heated to 30°C until all the solid material had disappeared and then left for a further 15 min. Subsequently, the reaction mixture was allowed to cool before being washed with a 10% (aq) solution of sodium carbonate (2 x 6 mL) followed by a saturated aqueous sodium chloride solution (6 mL). The organic layer was separated and dried over anhydrous Na_2SO_4. Filtration followed by solvent evaporation afforded a crude oil, which slowly solidified on standing. Purification was effected by flash column chromatography (dichloromethane : methanol : triethylamine, 90:10:1) to afford the title compound **5** (0.31 g, 67%) as a yellow oil which slowly solidified on standing. mp 153-158°C (from $CHCl_3$ / Petroleum ether); R_f 0.36 (dichloromethane : methanol : triethylamine, 90:10:1). δ_H (200 MHz; $CDCl_3$) 2.45 (6 H,

s, N(C*H*$_3$)$_2$), 2.72 (2 H, t, *J* 6.2, C*H*$_2$N(CH$_3$)$_2$), 3.79 (2 H, td, *J* 6.2 and *J* 5.0, CONHC*H*$_2$), 7.66-7.93 (3 H, m, Ar-*H*), 8.27 (1 H, m, Ar-*H*), 8.46 (1 H, m, Ar-*H*), 8.64 (1 H, dd, *J* 8.8 and 1.7, Ar-*H*), 9.07 (1 H, m, Ar-*H*), 11.90 (1 H, br s, CON*H*).

_N_-[2-(Dimethylamino)ethyl]-9-aminoacridine-4-carboxamide (6)[186]

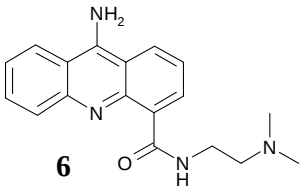

6

Compound **5** (0.19 g, 0.57 mmol, 1.00 eq) was dissolved in dry phenol (0.66 g, 7.0 mmol, 7.00 eq) and the mixture was heated slowly to 50 °C. Once this temperature had been reached, a stream of gaseous ammonia was bubbled through the solution and this was continued while the temperature of the reaction was raised slowly to 115°C. The reaction mixture was kept at this temperature for a further 20 mins. The bulk of the solvent was then removed *in vacuo* and the residue was co-evaporated with toluene (4 x 10 mL). The crude dark brown-yellow residue was purified by flash column chromatography (dichloromethane : methanol : triethylamine, 90:10:1). This gave the title compound **6** (0.12 g, 59%) as brown-yellow oil. R_f 0.18 (dichloromethane : methanol : triethylamine, 90:10:1); δ_H (200 MHz; $CDCl_3$) 2.47 (6 H, s, N(C*H*$_3$)$_2$), 2.78 (2 H, t, *J* 5.8, C*H*$_2$N(CH$_3$)$_2$), 3.80 (2 H, m, CONHC*H*$_2$), 6.50 (2 H, br s, N*H*$_2$), 7.10 (1 H, dd, *J* 7.1 and 1.7, Ar-*H*), 7.21-7.30 (1 H, m, Ar-*H*), 7.51-7.60 (1 H, m, Ar-*H*), 7.63-7.70 (1 H, m, Ar-*H*), 7.80-7.88 (2 H, m, Ar-*H*), 8.60 (1 H, dd, *J* 7.1 and 1.3, Ar-*H*), 12.38 (1 H, br s, CON*H*).

Dihydrochloride salt of _N_-[2-(dimethylamino)ethyl]-9-aminoacridine-4-carboxamide (7) [186]

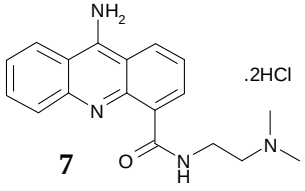

7

Compound **6** (0.09 g, 0.3 mmol, 1.00 eq) was dissolved in a hydrochloric acid saturated solution of dry methanol (50 mL) and the resulting mixture was left to stir at rt for 45 mins. Subsequently, the solvent was removed *in vacuo* and the crude material afforded was purified by recrystallisation from a 1:1 mixture of methanol : diethyl ether. The title compound **7** (0.08 g, 89%) was obtained as yellow crystals which were collected by filtration, washed with cold diethyl ether and dried *in vacuo* over phosphorus

pentoxide. mp 284-289°C (from MeOH/Diethyl ether) (Lit.[186] 292-293 °C); δ_H (200 MHz; DMSO-d_6) 2.87 (6 H, s, NH(CH_3)$_2$), 3.40 (2 H, m, CH_2NH(CH$_3$)$_2$), 3.78 (2 H, m, CONHCH_2), 7.50-7.65 (2 H, m, Ar-*H*), 7.90-8.10 (2 H, m, Ar-*H*), 8.73 (1 H, d, *J* 7.5, Ar-*H*), 8.85 (1 H, d, *J* 8.7, Ar-H), 9.05 (1 H, d, *J* 8.7, Ar-*H*), 9.85 (1 H, br s, N*H*(CH$_3$)$_2$), 10.58 (2 H, br s, C(9)NH_2), 10.90 (1 H, br s , CON*H*), 13.60 (1 H, br s, N(10)*H*); δ_C (50 MHz, DMSO-d_6) 35.3 (t), 43.1 (q), 56.2 (t), 112.1 (s), 112.9 (s), 120.0 (s), 120.3 (d), 123.2 (d), 125.3 (d), 125.6 (d), 129.8 (d), 136.6 (d), 136.9 (d), 138.8 (s), 139.0 (s), 158.7 (s), 168.2 (s); LRMS m/z (ESI) (%) 309 ([M+H]$^+$, 82), 264 (12), 155 (100), 133 (10); HRMS (ESI) found 309.1709, calcd. for $C_{18}H_{21}N_4O$ [M+H]$^+$ 309.1710.

_t_-Butoxycarbonylamino-1,2-propanediol (8)[202]

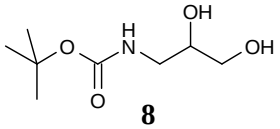

8

To a solution of 3-amino-1,2-propanediol (4.80 g, 52.8 mmol, 1.00 eq) in water (100 mL) was added dropwise at 0°C with stirring, a solution of di-*t*-butyl dicarbonate (12.12 g, 54.80 mmol, 1.04 eq) in dioxane (50 mL). The solution was warmed to rt while the pH was maintained above 10.5 by addition of (aq) 1 M NaOH. After evaporation of the solvent *in vacuo*, the remaining paste was triturated with DCM. The suspension was filtered and the organic phase was dried over anhydrous Na_2SO_4. Filtration followed by solvent evaporation *in vacuo*, yielded the title product **8** (8.21 g, 81%) as an oil which solidified (white solid) upon cooling (4°C). mp 53-57°C (Lit.[235] 55-58°C) R_f 0.49 (Ethyl acetate : methanol, 8:2); δ_H (200 MHz; $CDCl_3$) 1.42 (9 H, s, (CH_3)$_3$), 3.21 (2 H, m, NHCH_2), 3.54 (2 H, m, CH_2OH), 3.72 (1 H, m, C*H*), 4.25 (2H, br s, 2 x O*H*), 5.65 (1 H, t, N*H*).

_t_-Butoxycarbonylaminoacetaldehyde (9)[202]

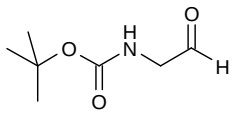

9

To a solution of the diol **8** (7.10 g, 37.0 mmol, 1.00 eq) in water (90 mL), was added sodium periodate (9.50 g, 44.4 mmol, 1.20 eq) and the solution was then left to stir for 1 h at rt. The mixture was then filtered and the aqueous filtrate extracted with dichloromethane (3 x 50 ml). The organic phase was dried over anhydrous $MgSO_4$. Filtration followed by solvent evaporation *in vacuo* afforded the

title compound **9** (4.58 g, 78%) as a colourless oil. δ_H (200 MHz; $CDCl_3$) 1.45 (9 H, s, $(CH_3)_3$), 4.08 (2 H, s, CH_2), 5.43 (1 H, br s, N*H*), 9.65 (1 H, s, C*H*O).

Ethyl *N*-(2-*t*-butoxycarbonylaminoethyl)glycinate (10)[202]

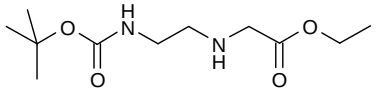

10

Glycine ethyl ester hydrochloride (8.78 g, 63.0 mmol, 2.50 eq) and $NaBH_3CN$ (1.59 g, 25.2 mmol, 1.00 eq)) were added to a solution of *t*-butoxycarbonylaminoacetaldehyde (**9**) (4.00 g, 25,2 mmol, 1.00 eq) in methanol (100 mL). The solution was stirred for 18 h at rt. Then the solvent was removed under reduced pressure and the crude residue afforded was re-dissolved in water (120 mL). The pH of the resulting aqueous solution was increased to 8 by addition of 2M (aq) sodium hydroxide. This solution was extracted with dichloromethane (3 x 100 mL) and the combined organic fractions were dried over anhydrous $MgSO_4$. Filtration followed by solvent evaporation *in vacuo* gave a crude brownish oil. This crude mixture was purified by flash column chromatography (dichloromethane : methanol, 97.5:2.5) to afford the title compound **10** (2.60 g, 42%) as a brown coloured oil. R_f 0.27 (Dichloromethane : methanol 97.5:2.5); δ_H (200 MHz; $CDCl_3$) 1.25 (3 H, t, *J* 7.0, CH_2CH_3), 1.42 (9 H, s, $(CH_3)_3$), 2.72 (2 H, t, *J* 6.0, $CH_2CH_2NHCH_2$), 3.19 (3 H, m, BocNHCH_2 and $CH_2CH_2NHCH_2$), 3.38 (2 H, s, CH_2COOEt), 4.17 (2 H, q, *J* 7.0, CH_2CH_3), 5.04 (1 H, br s, BocN*H*)

Thymin-1-yl acetic acid (11)[146]

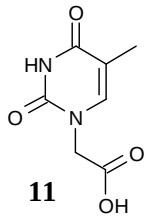

11

Thymine (1.07 g, 7.30 mmol, 1.00 eq) was added to a 5.5 M (aq) KOH solution (6 mL). To this solution was added dropwise, while stirring at 40°C, bromoacetic acid (1.77 g, 12.7 mmol, 1.74 eq). Heating was continued for a further 60 min. After cooling to room temperature, the pH of the reaction mixture was adjusted to 5.5 by addition of a concentrated HCl solution and the resulting solution was cooled to 4 °C for 2 h. The remaining precipitate was removed by filtration and the pH of the filtrate was then lowered to 2 by addition of a concentrated HCl solution. The filtrate was cooled again at 4°C for 2 h after which the crude product was collected by filtration, washed with cold water (20 mL) and dried *in vacuo* over P_2O_5. This afforded the title compound **11**

(1.254 g, 93%) as a white solid which was used in a subsequent step without further purification. mp 290-293°C (from MeOH); δ_H (200 MHz; DMSO-d_6) 1.75 (3 H, s, CH_3), 4.36 (2 H, s, CH_2), 7.49 (1 H, s, C=C*H*), 11.36 (1 H, s, COO*H*), 12.95 (1 H, br s, NH).

_N_-(2-_t_-butoxycarbonylaminoethyl)-_N_-(thymin-1-ylacetyl) glycine ethyl ester (13)[202]

Thymin-1-yl acetic acid (**11**) (0.80 g, 4.4 mmol, 1.1 eq), ethyl-N-(2-t-butoxycarbonyl-aminoethyl)glycinate (**10**) (0.98 g, 4.0 mmol, 1.0 eq) and di-*iso*-propylethylamine (2.07 mL, 11.9 mmol, 2.96 eq) were dissolved in DMF (10 mL). HBTU (1.57 g, 4.15 mmol, 1.0 eq) was then added and the resulting mixture was left to stir for 18 h at rt. Subsequently the solvent was removed *in vacuo* and the residue was re-dissolved in dichloromethane (75 mL). The organic solution was then washed, respectively, with 1M (aq) $NaHCO_3$ (3 x 50 mL), 1M (aq) $KHSO_4$ (2 x 50 mL), water (50 mL) and, finally, brine (50 mL). The organic phase was separated and dried over anhydrous $MgSO_4$. Filtration followed by solvent evaporation in vacuo afforded a crude, cream coloured foamy solid. This was purified by flash column chromatography (dichloromethane : methanol, 97:3). The title compound **13** (1.13 g, 69%) was obtained as colourless foam. R_f 0.35 (Dichloromethane : methanol, 97:3); δ_H (200 MHz; $CDCl_3$) (2 rotational isomers in a 2:1 ratio observed due to restricted rotation about the tertiary amide bond) 1.20 (max) and 1.25 (min) (3 H, t, *J* 7.2, CH_2CH_3), 1.37 (9 H, s, $(CH_3)_3$), 1.83 (3 H, s, C(5)CH_3), 3.12-3.34 (2 H, m, CH_2CH_2CON), 3.42-3.54 (2 H, m, CH_2CH_2NCO), 4.01 (max) and 4.18 (min) (2 H, s, NCH_2CO_2Et), 4.13 (max) and 4.19 (min) (2 H, q, *J* 7.2, CH_2CH_3), 4.40 (min) and 4.55 (max) (2 H, s, NCH_2CON), 5.72 (1 H, t, *J* 6.2, BocN*H*), 6.95 (max) and 7.00 (min) (1 H, s, C(6)-*H*), 9.93 (1 H, br s, CON(3)*H*CO); δ_C (50 MHz; $CDCl_3$) (2 rotational isomers observed due to restricted rotation about the tertiary amide bond) 12.0 (q), 13.7 (q), 28.0 (q), 38.3 (t), 47.5 (t), 48.3 (t), 48.7 (t), 50.06 (t), 61.3 (t), 61.9 (t), 79.03 (s), 79.47 (s), 110.3 (s), 140.7 (d), 151.0 (s), 155.8 (s), 164.3 (s), 167.1 (s), 167.5 (s), 169.1 (s), 169.3 (s).

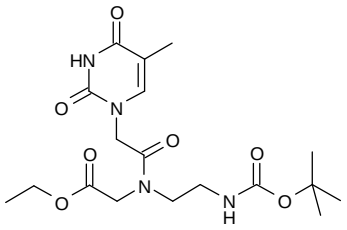

13

Trifluoroacetic acid salt of *N*-(aminoethyl)-*N*-(thymin-1-ylacetyl) glycine ethyl ester. (14)

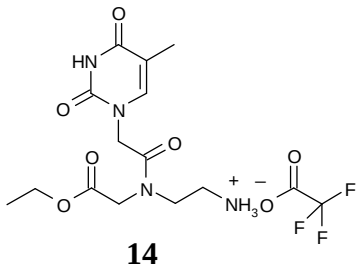

14

N-(2-*t*-butoxycarbonylaminoethyl)-*N*-(thymin-1-ylacetyl) glycine ethyl ester (**13**) (0.50 g, 1.2 mmol, 1.0 eq) and trifluoroacetic acid (10.0 mL) were dissolved in dichloromethane (30 mL). This solution was stirred at rt for 1 h. The solvent was then removed *in vacuo* and the resulting crude product **14** subsequently dried *in vacuo* in a drying pistol over P_2O_5 at 50° C. This yielded the title compound **14** (0.46 g, 89%) as a brownish gum. δ_H (200 MHz; CD_3OD) (2 rotational isomers in a 2:1 ratio observed due to restricted rotation about the tertiary amide bond) 1.16 (min) and 1.20 (max) (3 H, *J* 7.5, CH_2CH_3), 1.77 (3 H, s, $C(5)CH_3$), 3.05 (max) and 3.20 (min) (2 H, t, *J* 5.8 and 6.2, CH_2CH_2NCO), 3.60 (max) and 3.74 (min) (2 H, t, *J* 5.8 and 6.2, CH_2CH_2NCO), 4.09 (min) and 4.17 (max) (2 H, q, *J* 7.1, CH_2CH_3), 4.05 (min) and 4.27 (max) (2 H, s, NCH_2COOEt), 4.48 (max) and 4.64 (min) (2 H, s, NCH_2CON), 7.18 (max) and 7.26 (min) (1 H, s, C(6)*H*); δ_C (50 MHz; CD_3OD) (2 rotational isomers observed due to restricted rotation about the tertiary amide bond) 12.10 (q), 15.27 (q), 38.48 (t), 39.06 (t), 46.82 (t), 47,01 (t), 49.57 (t), 49.63 (t), 50.14 (t), 62.82 (t), 63.18 (t), 111.03 (s), 111.17 (s), 143.41 (d), 143.64 (d), 153.00 (s), 153.11 (s), 166.73 (s), 169.85 (s), 171.04 (s), 171.80 (s).

Attempted synthesis of ethyl 2-(*N*-(2-(9-chloroacridine-4-carboxamido)ethyl)-2-(thymin-1-yl) acetamido) acetate (15)

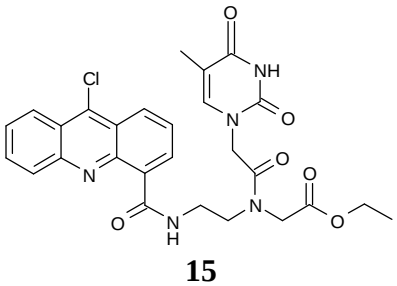

15

A solution of 9-chloroacridine-4-carbonyl chloride (**4**) (0.10 g., 0.34 mmol, 1.0 eq) in dry DMF (10 mL) was added dropwise, and under a N_2 atmosphere, to a stirred solution, at 0° C, of the trifluoroacetic acid salt of *N*-(aminoethyl)-*N*-(thymin-1-ylacetyl) glycine ethyl ester (**14**) (0.15 g., 0.34 mmol, 1.0 eq) in dry DMF (10 mL) containing excess DIPEA (0.20 mL, 1.1 mmol, 3.3 eq). The reaction mixture was allowed to warm to room temperature after which it was left to stir for 2 h. After this time, the solvent was removed *in vacuo* and the crude reaction residue obtained was subjected to purification using preparative TLC

(methanol : ethyl acetate : acetic acid, 99:99:2). Unfortunately, none of the bands yielded the title compound **15** upon analysis by ^{1}H-NMR-spectroscopy.

N-(2-*t*-butoxycarbonylaminoethyl)-N-(benzyloxycarbonyl) glycine ethyl ester (17)

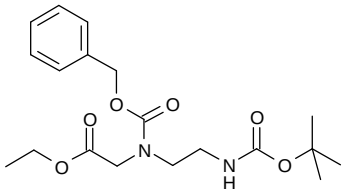

17

Ethyl-*N*-(2-*t*-butoxycarbonyl-aminoethyl)-glycinate (**10**) (0.50 g, 2.0 mmol, 1.0 eq) was dissolved in dichloromethane (75 mL) and a 0.4 M (aq) solution of sodium carbonate was added (10.1 mL, 4.06 mmol, 2.0 eq). The resulting two-phase mixture was stirred and cooled to 0°C. Subsequently, benzyl chloroformate (0.44 mL, 3.0 mmol, 1.5 eq) was added dropwise while the temperature was kept at 0°C. After the slurry had warmed up to rt it was left to stir for 2 h. at rt whereupon the organic phase was separated and the aqueous layer was extracted with dichloromethane (50 mL). The combined organic extracts were dried over anhydrous $MgSO_4$. Filtration followed by solvent evaporation *in vacuo* afforded a crude foamy white residue. This was purified by flash column chromatography (cyclohexane : ethyl acetate, 7:1). The obtained title compound **17** (0.55 g, 71%) was obtained as a colourless viscous liquid. R_f 0.21 (Cyclohexane : ethyl acetate, 7:1); (Found: C, 60.1; H, 7.3; N, 7.4. $C_{19}H_{28}O_6N_2$ requires C, 60.0; H, 7.4; N, 7.4%); ν_{max}(film)/cm^{-1} 3366, 2972, 2931, 1744, 1715, 1703 , 1520, 1511, 1494, 1469, 1458, 1365, 1241, 1199, 1173; δ_H (200 MHz; $CDCl_3$) (2 rotational isomers in a 1:1 ratio observed due to restricted rotation about the tertiary amide bond) 0.98 and 1.07 (3 H, t, *J* 7.2, CH_2CH_3), 1.20 and 1.22 (9 H, s, $(CH_3)_3$), 2.97-3.15 (2 H, m, $BocNHCH_2CH_2$), 3.20-3.31 (2 H, m, $BocNHCH_2CH_2$), 3.77 and 3.80 (2 H, s, NCH_2CO_2Et), 3.91 and 4.00 (2 H, q, *J* 7.2, CH_2CH_3), 4.91 and 4.95 (2 H, s, $PhCH_2O$), 5.10-5.25 (1 H, m, BocN*H*), 7.03-7.21 (5 H, m, Ar-*H*); δ_C (50 MHz, $CDCl_3$): (rotational isomers observed due to restricted rotation about the tertiary amide bond) 13.7 (q), 28.0 (q), 38.7 (t), 47.5 (t), 48.3 (t), 48.7 (t), 49.6 (t), 49.7 (t), 61.0 (t), 67.2 (t), 78.8 (s), 127.3 (d), 127.45 (d), 127.7 (d), 128.1 (d), 128.2 (d), 136.0 (s), 155.8 (s), 156.1 (s), 167.7 (s), 167.9 (s).

Hydrogen chloride salt of *N*-(2-aminoethyl)-*N*-(benzyloxycarbonyl) glycine ethyl ester (18)

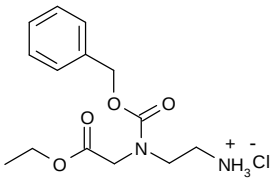

18

N-(2-*t*-Butoxycarbonylaminoethyl)-*N*-(benzyloxycarbonyl) glycine ethyl ester (**17**) (0.45 g, 1.2 mmol, 1.0 eq) was dissolved in hydrogen chloride saturated solution of absolute ethanol (50 mL). This solution was stirred at room temperature for 1 h. after which the solvent was removed *in vacuo* to yield a crude white solid. The residue was dried azeotropically by the addition of toluene (3 x 50 mL) followed by solvent removal *in vacuo* to yield the desired compound **18** (0.43 g, 96 %) as a white solid. The product showed satisfactory purity for use in subsequent experiments. Mp 184°C (dec.) (from EtOH); δ_H (200 MHz; CD_3OD) (2 rotational isomers in a 2:1 ratio observed due to restricted rotation about the tertiary amide bond) 1.17 (max) and 1.25 (min) (3H, t, *J* 7.1, CH_2CH_3), 3.10-3.26 (2H, m, CH_2CH_2NCO), 3.70 (2H, t, *J* 6.2, CH_2CH_2NCO), 4.04-4.28 (4H, m, CH_2CH_3 and NCH_2CON), 5.12 (max) and 5.29 (min) (2H, s, OCH_2Ph), 7.25 - 7.46 (5H, m, Ar-*H*); δ_C (50 MHz; CD_3OD) (2 rotational isomers observed due to restricted rotation about the tertiary amide bond) 14.8 (q), 39.8 (t), 47.5 (t), 48.1 (t), 51.1 (t), 51.5 (t), 62.9 (t), 69.2 (t), 69.3 (t), 129.1 (d), 129.6 (d), 129.9 (d), 137.7 (s), 137.8 (s), 158.0 (s), 158.3 (s), 172.4 (s), 172.5 (s).

Attempted synthesis of ethyl 2-(*N*-(2-(9-chloroacridine-4-carboxamido)ethyl)-*N*-(benzyloxycarbonyl) amino)acetate (19)

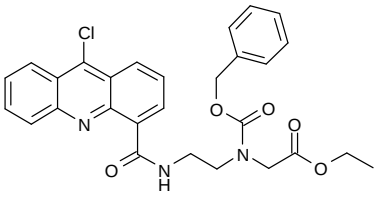

19

A solution of 9-chloroacridine-4-carbonyl chloride (**4**) (0.20 g., 0.86 mmol, 1.0 eq) in dry chloroform (15 mL) was added dropwise, and under a N_2 atmosphere, to a cooled (0°C) stirred solution of the hydrogen chloride salt of *N*-(aminoethyl)-*N*-(benzyloxycarbonyl) glycine ethyl ester (**18**) (0.28 g., 0.86 mmol, 1.00 eq) in dry chloroform (30.0 mL) containing di-*iso*-propylethylamine (0.45 mL, 2.5 mmol, 2.9 eq). The reaction mixture was allowed to warm to rt and left to stir at rt for 2 h. Subsequently, the solution was washed with a 10% aqueous solution of Na_2CO_3 (3 x 15 mL) followed by brine (20 mL). The organic

phase was separated and dried over anhydrous $MgSO_4$. After filtration, the solvent was removed *in vacuo* and the crude reaction mixture residue subjected to purification by using flash column chromatography (petroleum ether : ethyl acetate, 60:40). All the collected fractions contained (a) persistent baseline impurity(s). In order to find out if **19** was present in the collected fractions, recrystallisation of the solid (yellow) products in the active fractions was attempted, e.g. in ethyl acetate (good solvent) / petrol ether (bad solvent), in dichloromethane and in methanol. Unfortunately, the recrystallisation attempts yielded very fine yellow precipitates with persistent impurities and subsequent NMR analysis showed that in none of the precipitates the title compound **19** could be unambiguously identified.

Hydrochloric acid salt of N-(2-aminoethyl)-N-(thymin-1-ylacetyl) glycine ethyl ester (21)

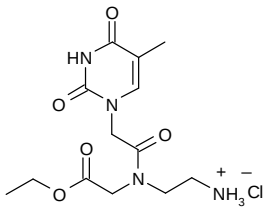

21

N-(2-*t*-butoxycarbonylaminoethyl)-*N*-(thymin-1-ylacetyl) glycine ethyl ester (**13**) (1.02g, 2.47 mmol, 1.00 eq) was dissolved in a hydrogen chloride saturated solution of absolute ethanol (75 mL). This solution was stirred at rt for 1 h. whereupon the solvent was removed *in vacuo* to yield a crude white solid. The residue was azeotropically dried by re-suspending in toluene (3 x 50 mL) followed by solvent removal *in vacuo* to yield the title compound **21** (0.83 g, 96 %) as a white solid. The product was used in subsequent reactions without further purification. mp 224°C (dec) (from MeOH); δ_H (200 MHz; CD_3OD) (2 rotational isomers in a 2:1 ratio observed due to restricted rotation about the tertiary amide bond) 1.00 (min) and 1.15 (max) (3H, t, *J* 7.1, CH_2CH_3), 1.68 (3H, s, C(5)CH_3), 3.00 (max) and 3.11 (min) (2H, t, *J* 5.4 and *J* 6.2, CH_2CH_2NCO), 3.58 (max) and 3.70 (min) (2H, t, *J* 5.4 and *J* 6.2, CH_2CH_2NCO), 4.02 (min) and 4.10 (max) (2H, q, *J* 7.1, CH_2CH_3), 4.00 (min) and 4.21 (max) (2H, s, NCH_2COOEt), 4.47 (max) and 4.65 (min) (2H, s, NCH_2CON), 7.20 (max) and 7.25 (min) (1H, s, C(6)*H*); δ_C (50 MHz; CD_3OD) (2 rotational isomers observed due to restricted rotation about the tertiary amide bond) 12.6 (q), 14.8 (q), 39.0 (t), 39.6 (t), 47.3 (t), 47.4 (t), 49.9 (t), 50.0 (t), 51.0 (t), 63.3 (t), 63.6 (t), 111.4 (s), 111.5 (s), 144.0 (d), 144.2 (d), 153.4 (s), 153.6 (s), 167.2 (s), 170.4 (s), 171.5 (s), 171.6 (s), 172.3 (s).

***Iso*-propyl-9-oxoacridan-4-carboxylate (22)**[210]

METHOD A: Via esterification of 9-oxoacridan-4-carboxylic acid (3):

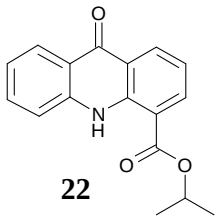

22

To a solution of 9-oxoacridan-4-carboxylic acid (**3**) (0.30g, 1.3 mmol, 1.0 eq) in THF (10 mL) was added, carbonyldiimidazole (0.42 g, 2.6 mmol, 2.0 eq) and *iso*-propyl alcohol (0.72 g, 12 mmol, 9.5 eq). This solution was stirred for 6 h. at rt. Subsequently, the solvent was removed *in vacuo* and the residue re-dissolved in dichloromethane (50 mL). The resulting organic solution was then washed with a 1 M (aq) solution of ammonium hydroxide (50 mL) followed by water (50 mL) then brine (50 mL). The organic layer was separated and dried over anhydrous $MgSO_4$. Filtration followed by solvent evaporation afforded a crude solid residue which was purified by flash column chromatography (petroleum ether (40-60°C) : ethyl acetate : acetic acid, 70:29:1). This afforded the title compound **22** (0.18 g, 51%) as a yellow solid. mp 149-150 °C (from EtOH); R_f 0.34 (petroleum ether (40-60°C) : ethyl acetate : acetic acid, 70:29:1); (Found: C, 72.3; H, 5.3; N, 5.0. $C_{17}H_{15}NO_3$ requires C, 72.6; H, 5.4; N, 5.0%); ν_{max}(film)/cm^{-1} 3264, 2981, 1687, 1638, 1620, 1599, 1523, 1441, 1277, 1176, 1146, 1101, 752, 675; δ_H (200 MHz; $CDCl_3$) 1.36 (6 H, d, *J* 6.2, CH(C*H*$_3$)$_2$), 5.24 (1 H, septet, *J* 6.2, C*H*(CH$_3$)$_2$), 7.10-7.29 (3 H, m, Ar-*H*), 7.57 (1 H, t, *J* 7.9, Ar-*H*), 8.30-8.35 (2 H, m, Ar-*H*), 8.60 (1 H, d, *J* 7.9, Ar-*H*), 11.71 (1 H, s, N*H*); δ_C (50 MHz; $CDCl_3$) 21.7 (q), 69.2 (d), 113.8 (s), 117.2 (d), 119.4 (d), 121.1 (s), 121.9 (d), 126.6 (d), 133.2 (d), 133.5 (d), 136.1 (d), 139.7 (s), 141.4 (s), 167.2 (s), 177.6 (s); LRMS m/z (EI) (%) 281 (M^+, 34), 239 (15), 221 (100), 193 (10); HRMS (ESI) found 282.1123, calcd. for $C_{17}H_{16}ON_3$ $[M+H]^+$ 282.1125.

METHOD B: Via transesterification of methyl-9-oxoacridan-4-carboxylate (2):

Sodium (0.16 g, 4.0 mmol, 1.0 eq) was dissolved in dry *iso*propanol (40 mL) and to this solution was added methyl-9-oxoacridan-4-carboxylate (**2**) (1.00 g, 3.95 mmol, 1.00 eq) and activated 4Å molecular sieves (2.4 g). The mixture was stirred gently for 5 hours at rt. After filtration followed by solvent evaporation *in vacuo*, the crude solid residue afforded was dissolved in dichloromethane (50 mL). The resulting organic solution was washed with a 0.1 M (aq) solution of hydrochloric acid (50 mL) followed by water (50 mL) then brine (50 mL). The organic layer was separated and dried over anhydrous $MgSO_4$. Filtration followed by solvent evaporation *in vacuo* afforded the title

compound **22** (0.85 g, 77 %) as a yellow solid. The analysis of this product was identical to that obtained for the product yielded by method A.

_t_-Butyl-9-oxoacridane-4-carboxylate (23)

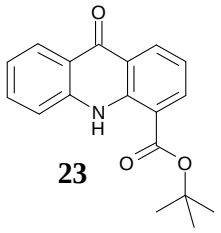
23

A solution of *t*-butanol (2.94 g, 39.7 mmol, 7.00 eq) in dry THF (50 mL) was cooled to 0°C and a 2.5 M solution of *n*-butyllithium (15.9 mL, 39.7 mmol, 7.00 eq) in hexane was added under nitrogen and whith stirring. The resulting solution was allowed to warm to rt whereupon methyl-9-oxoacridan-4-carboxylate (**2**) was added (1.44 g, 5.66 mmol, 1.00 eq). The reaction mixture was left to stir at rt, under nitrogen, for 24 h, after which the solvent was removed *in vacuo.* The crude solid residue afforded was dissolved in dichloromethane (100 mL) and the resulting organic solution was washed with water (50 mL) followed by brine (50 mL) and then dried over anhydrous $MgSO_4$. Filtration followed by solvent evaporation afforded the title compound **23** (1.50 g, 90.0 %) as a yellow solid. mp 145-148°C (from EtOH); R_f 0.63 (Petroleum ether (40-60 °C) : ethyl acetate, 50:50); ν_{max}(film)/cm^{-1}: 3268, 2976, 2912, 1683, 1639, 1618, 1600, 1523, 1442, 1294, 1255, 1166, 1138, 754, 67; δ_H (200 MHz; $CDCl_3$) 1.60 (9 H, s, C(C*H*$_3$)$_3$), 7.10-7.30 (3 H, m, Ar-*H*), 7.49-7.59 (1 H, m, Ar-*H*), 8.23 (1 H, dd, *J* 7.5 and 1.7, Ar-*H*), 8.31 (1 H, dd, *J* 8.3 and 1.7, Ar-*H*), 8.56 (1 H, dd, *J* 7.9 and 1.3, Ar-*H*), 11.76 (1 H, s, N*H*). δ_C (50 MHz. $CDCl_3$) 27.7 (q), 82.3 (s), 114.5 (s), 117.0 (d), 119.1 (d), 120.8 (s), 121.6 (d), 121.7 (s), 126.4 (d), 132.7 (d), 133.2 (d), 136.05 (d), 139.5 (s), 141.2 (s), 166.8 (s), 177.1 (s). LRMS m/z (EI) (%) 295 (M^+, 10), 239 (48), 221 (100), 193 (17), 164 (22), 139 (24); HRMS (ESI) found 296.1283, calcd. for $C_{18}H_{18}NO_3$ $(M+H)^+$ 296.1281.

Methyl-9-(1,2,4-triazol-1-yl)acridine-4-carboxylate (24)

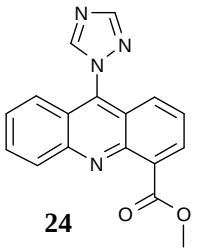
24

1,2,4-triazole (0.44 g, 6.4 mmol, 10 eq) was dissolved in dry acetonitrile (10 mL) and cooled to 0° C. To this solution was added dropwise, freshly distilled phosphorus oxychloride (0.18 mL, 1.92 mmol, 3.0 eq) followed by freshly distilled TEA (1.07 mL, 7.68 mmol, 12.0 eq) with stirring under nitrogen. This

solution was then allowed to warm to rt whereupon it was left to stir at rt for 30 mins. A solution of methyl-9-oxoacridan-4-carboxylate (**2**) (0.16 g, 0.64 mmol, 1.0 eq) in dichloromethane (3 mL) was added and the mixture was heated at reflux for 96 h. After cooling, the reaction was quenched by addition of water (0.20 mL) followed by TEA (1.10 mL) and left to stir for 10 min. Subsequently the solvent was removed *in vacuo* and the crude greenish solid residue afforded was dissolved in dichloromethane (50 mL). The resulting organic solution was washed with a saturated aqueous solution of $NaHCO_3$ (2 x 25 mL) followed by brine (50 mL). The combined aqueous layers were back-extracted with dichloromethane (50 mL). The combined organic phases were dried over anhydrous Na_2SO_4. Filtration followed by solvent evaporation afforded a crude solid residue which was purified by flash column chromatography (petroleum ether (40-60°C) : ethyl acetate : methanol 29:70:1). The title compound **24** (0.14 g, 72 %) was afforded as a green solid. mp 135 °C (dec.) (from $CHCl_3$ / Petroleum ether); R_f 0.34 (Petroleum ether (40-60°C) : ethyl acetate : methanol 29:70:1); (Found: C, 67.0; H, 3.9; N, 18.1. $C_{17}H_{12}O_2N_4$ requires C, 67.1; H, 4.0; N, 18.4%); δ_H (200 MHz; $CDCl_3$) 4.03 (3 H, s, OC*H*$_3$), 7.43-7.56 (4 H, m, Ar-*H*), 7.70 (1 H, ddd, *J* 8.8, *J* 6.2 and *J* 1.7, Ar-*H*), 8.01 (1 H, dd, *J* 6.2 and 1.7, Ar-*H*), 8.23 (1 H, d, *J* 8.8, Ar-*H*), 8.33 (1 H, s, NC*H*N), 8.59 (1 H, s, NC*H*N); δ_C (50 MHz; $CDCl_3$) 52.5 (q), 121.8 (d), 122.0 (s), 125.4 (d), 126.5 (d), 128.5 (d), 130.3 (d), 130.8 (d), 131.2 (d), 132.0 (s), 137.3 (s), 145.8 (s), 146.3 (d), 149.3 (s), 153.1 (d), 167.6 (s), 170.9 (s); LRMS m/z (EI) (%) 304 (M^+,46), 273 (27), 246 (94), 83 (54), 69 (85), 55 (70), 43 (100).

Iso-propyl-9-(1,2,4-triazol-1-yl)acridine-4-carboxylate (25)

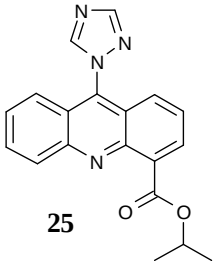

25

1,2,4-triazole (0.44 g, 6.4 mmol, 10 eq) was dissolved in dry acetonitrile (10 mL) and the resulting solution was cooled to 0° C. To this solution was added dropwise, freshly distilled phosphorus oxychloride (0.18 mL, 1.9 mmol, 3.0 eq) followed by freshly distilled TEA (1.07 mL, 7.68 mmol, 12 eq) with stirring under nitrogen. The resulting mixture was warmed to rt before being left to stir for 30 min. at rt. A solution of *iso*-propyl-9-oxoacridan-4-carboxylate (**22**) (0.18 g, 0.64 mmol, 1.0 eq) in dichloromethane (3 mL) was added and the mixture was heated at reflux for 96 h. After cooling, the reaction was quenched by

addition of water (0.20 mL) followed by TEA (1.10 mL) and left to stir for 10 min. Subsequently the solvent was removed *in vacuo* and the crude greenish solid residue afforded was dissolved in dichloromethane (50 mL). The resulting organic solution was washed with a saturated aqueous solution of $NaHCO_3$ (2 x 25 mL) followed by brine (50 mL). The combined aqueous layers were back extracted with dichloromethane (50 mL). The combined organic phases were dried over anhydrous Na_2SO_4. Filtration followed by solvent evaporation afforded a crude solid residue which was purified by flash column chromatography (petrol ether (40-60°C) : ethyl acetate : methanol 32:65:3). This afforded the title compound **25** (0.16 g, 75%) as a dark green solid. mp 149-153°C (from CH_2Cl_2 / Petroleum ether); R_f 0.28 (Petroleum ether (40-60 °C) : ethyl acetate : methanol, 32:65:3); ν_{max}(KBr)/cm^{-1} 3086, 2979, 1720, 1556, 1524, 1503, 1440, 1422, 1304, 750, 694, 675, 662; δ_H (200 MHz; $CDCl_3$) 1.44 (6 H, d, *J* 6.2, $CH(CH_3)_2$), 5.47 (1 H, septet, *J* 6.2, $CH(CH_3)_2$), 7.40-7.57 (4 H, m, Ar-*H*), 7.73-7.81 (1 H, m, Ar-*H*), 7.99 (1 H, dd, *J* 5.8 and 2.5, Ar-*H*), 8.26 (1 H, d, *J* 8.0, Ar-*H*), 8.35 (1 H, s, NC*H*N), 8.48 (1 H, s, NC*H*N); δ_C (50 MHz; $CDCl_3$) 21.5 (q), 68.8 (d), 121.5 (d), 124.5 (d), 126.4 (d), 127.7 (s), 128.2 (d), 128.5 (s), 130.0 (d), 130.1 (d), 130.4 (d), 132.8 (s), 136.8 (s), 145.7 (s), 145.9 (d), 149.1 (s), 152.9 (d), 166.7 (s); LRMS m/z (EI) (%) 332 (M^+, 12), 273 (14), 246 (78), 86 (53), 69 (72), 43 (100); HRMS (ESI) found 333.1345, calcd. for $C_{19}H_{17}O_2N_4$ $[M+H]^+$ 333.1346.

_t_-Butyl-9-(1,2,4-triazol-1-yl)acridine-4-carboxylate (26)

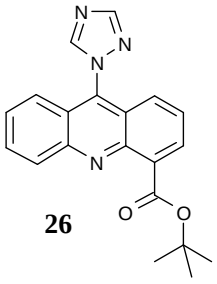
26

1,2,4-triazole (2.37 g, 34.4 mmol, 10 eq) was dissolved in dry acetonitrile (50 mL) and cooled to 0° C. To this solution was added dropwise, freshly distilled phosphorus oxychloride (0.95 mL, 10 mmol, 3.0 eq) followed by freshly distilled TEA (5.67 mL, 40.7 mmol, 12 eq) with stirring under nitrogen. The resulting mixture was warmed to rt before being left to stir for 30 min. at rt. A solution of *t*-butyl-9-oxoacridane-4-carboxylate (**23**) (0.98 g, 3.3 mmol, 1.0 eq) in dichloromethane (15 mL) was added and the resulting mixture was heated at reflux for 96 h. After cooling, the reaction was quenched by addition of water (1.10 mL) followed by TEA (5.67 mL) and left to stir for 10 min. Subsequently the solvent was removed *in vacuo* and the greenish solid residue was dissolved in dichloromethane

(250 mL). The resulting organic solution was washed with a saturated aqueous solution of $NaHCO_3$ (2 x 125 mL) followed by brine (250 mL). The combined aqueous layers were back extracted with dichloromethane (150 mL). The combined organic phases were dried over anhydrous Na_2SO_4. Filtration followed by solvent evaporation afforded a crude solid residue which was purified by flash column chromatography (petroleum ether (40-60°C) : ethyl acetate : methanol, 33.5:65.0:1.5). This afforded the title compound **26** (0.86 g, 75%) as a dark green solid. mp 143-147°C (from $CHCl_3$ / Petroleum ether); R_f 0.26 (petroleum ether (40-60°C) : ethyl acetate : methanol, 33.5:65.0:1.5); δ_H (200 MHz; $CDCl_3$) 1.66 (9 H, s, C(C*H*$_3$)$_3$), 7.36-7.51 (4 H, m, Ar-*H*), 7.68-7.76 (1 H, m, Ar-*H*), 7.88 (1 H, dd, *J* 4.9 and 3.3, Ar-*H*), 8.21 (1 H, d, *J* 8.8, Ar-*H*), 8.32 (1 H, s, NC*H*N), 8.52 (1 H, s, NC*H*N); δ_C (50 MHz, $CDCl_3$): 28.1 (q), 82.2 (s), 121.7 (d), 121.8 (s), 121.9 (s), 124.2 (d), 126.7 (d), 128.3 (d), 129.4 (d), 130.2 (d), 130.5 (d), 134.2 (s), 136.9 (s), 145.8 (s), 146.2 (d), 149.1 (s), 153.0 (d), 166.9 (s); LRMS m/z (EI) (%) 346 (M^+, 8), 246 (100), 192 (24), 179 (16), 57 (48); HRMS (ESI) found 347.1501, calcd. for $C_{20}H_{19}O_2N_4$ $[M+H]^+$ 347.1503.

Attempted preparation of methyl-9-benzylaminoacridine-4-carboxylate (27) (led to benzylamine-9-benzylaminoacridine-4-carboxylate **27*** instead)

Methyl-9-(1,2,4-triazol-1-yl)acridine-4-carboxylate (**24**) (0.14 g, 0.41 mmol, 1.0 eq) was dissolved in dry acetonitrile (10 mL). To this solution was added dry benzylamine (0.45 mL, 4.1 mmol, 10 eq) followed by dry TEA (0.90 mL, 6.4 mmol, 16 eq). The reaction mixture was heated to reflux, with stirring under a nitrogen atmosphere, and left at this temperature for 24 h. Subsequently, the reaction mixture was allowed to cool and the solvent was removed *in vacuo*. A crude solid residue was afforded which was purified by flash column chromatography (ethyl acetate : petrol ether : triethylamine, 60:39:1). ^{1}H-NMR analysis of active fractions suggested exclusive presence of the undesired benzyl-9-benzylaminoacridine-4-carboxamide by-product **27*** (^{1}H-NMR data for **27*** are reported below)

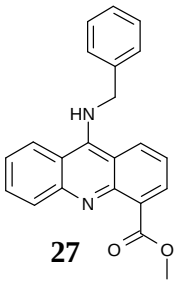

27

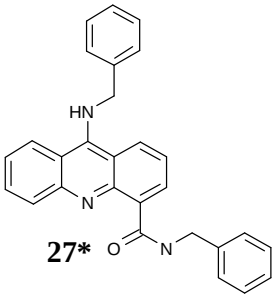

27*

δ_H (200 MHz; DMSO-d_6) 4.81 (2H, d, *J* 4.0, CH_2), 5.15 (2H, d, *J* 8.4, CH_2), 7.18-7.61 (12H, m, Ar-*H*), 7.71-7.89 (3H, m, Ar-*H*), 8.29-8.74 (2H, m, Ar-*H*), 12.71 (1H, t, *J* 8.4, N*H*)

Iso-propyl-9-benzylaminoacridine-4-carboxylate (28)

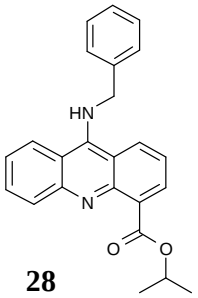

28

*I*so-propyl-9-(1,2,4-triazol-1-yl)acridine-4-carboxylate (**25**) (0.32 g, 0.95 mmol, 1.0 eq) was dissolved in dry acetonitrile (20 mL). To this solution was added dry benzylamine (1.04 mL, 9.53 mmol, 10 eq) followed by dry TEA (2.08 mL, 15.0 mmol, 16 eq). The reaction mixture was heated to reflux, with stirring under a nitrogen atmosphere, and left at this temperature for 24 h. Subsequently, the reaction mixture was allowed to cool and the solvent was removed *in vacuo*. A crude solid residue was afforded which was purified by flash column chromatography (petroleum ether (40-60°C) : diethyl ether : ethanol : triethylamine, 80:15:4:1). The title compound **28** (0.20 g, 57%) was obtained as a yellow oily solid. R_f 0.28 (petroleum ether (40-60°C) : diethyl ether : ethanol : triethylamine, 80:15:4:1); ν_{max}(film)/cm^{-1}: 3309, 3062, 3028, 2979, 2960, 2933, 2872, 1682, 1647, 1609, 1578, 1515, 1494, 1446, 1270, 1188, 1150, 1088, 775, 750, 725, 700; δ_H (200 MHz; $CDCl_3$) (cis-trans isomers observed in a 2:1 ratio due to restricted rotation about the C9-N bond) 1.37 (6 H, d, *J* 6.2, CH(C*H*$_3$)$_2$), 5.10 (min) and 5.15 (max) (2 H, s, C*H*$_2$Ph), 5.25 (1 H, septet, *J* 6.2, C*H*(CH$_3$)$_2$), 6.88-7.50 (9 H, m, Ar-*H*), 7.84-7.99 (1 H, m, Ar-*H*), 8.08-8.15 (1 H, m, Ar-*H*), 8.28-8.57 (1 H, m, Ar-*H*), 10.91 (max) and 11.13 (min) (1 H, s, N(10)*H*); δ_C (50 MHz; $CDCl_3$) (cis-trans isomers observed due to restricted rotation about the C9-N bond) 22.13 (q), 56.95 (t), 68.94 (d), 112.40 (s), 113.19 (s), 115.85 (d), 117.31 (d), 117.45 (d), 117.90 (s), 119.92 (d), 120.26 (d), 122.50 (d), 125.56 (d), 125.83 (d), 126.16 (d), 126.62 (d), 127.10 (d), 127.60 (d), 127.78 (d), 128.29 (d), 128.37 (d), 128.56 (d), 129.26 (d), 130.54 (d), 131.10 (d), 132.61 (d), 133.41 (d), 135.03 (d), 137.72 (s), 140.91 (s), 141.02 (s), 142.40 (s), 143.96 (s), 153.88 (s), 167.90 (s), 168.07 (s); LRMS m/z (EI) (%) 370 (M^+, 21), 327 (16), 283 (5), 205 (19), 177 (20), 91 (51), 43 (100); HRMS (ESI) found 371.1756, calcd. for $C_{24}H_{23}O_2N_2$ $[M+H]^+$ 371.1754.

_t_-Butyl-9-benzylaminoacridine-4-carboxylate (29)

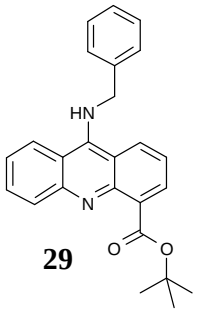

29

t-Butyl-9-(1,2,4-triazol-1-yl)acridine-4-carboxylate (**26**) (1.21 g, 3.39 mmol, 1.00 eq) was dissolved in dry acetonitrile (50 mL). To this solution was added dry benzylamine (3.62 mL, 33.2 mmol, 9.78 eq) followed by dry TEA (6.92 mL, 49.8 mmol, 14.7 eq). The resulting mixture was stirred under nitrogen and heated at reflux for 24 h. Subsequently, the reaction mixture was allowed to cool down and the solvent was removed *in vacuo*. This afforded a crude yellow oily residue which was purified by flash column chromatography (petroleum ether (40-60°C) : ethyl acetate : triethylamine 90:9:1). The title compound **29** (0.63 g, 54%) was obtained as slowly solidifying yellow oil. R_f 0.27 (petroleum ether (40-60°C) : ethyl acetate : triethylamine 90:9:1); ν_{max}(film)/cm^{-1} 3313, 3052, 3018, 2973, 2960, 2924, 1683, 1645, 1608, 1578, 1521, 1494, 1449, 1284, 1256, 1170, 1138, 759, 747, 735, 700; δ_H (200 MHz; $CDCl_3$) (cis-trans isomers observed in a 2:1 ratio due to restricted rotation about the C9-N bond) 1.55 (9H, s, C(C*H*$_3$)$_3$), 5.04 (min) and 5 .09 (max) (2H, s, C*H*$_2$Ph), 6.90-7.45 (9 H, m, Ar-*H*), 7.84-7.99 (1 H, m, Ar-*H*), 8.18-8.28 (1 H, m, Ar-*H*), 8.40-8.50 (1 H, m, Ar-*H*), 10.87 (max) and 11.11 (min) (1 H, s, N(10)*H*); δ_C (50 MHz; $CDCl_3$) (cis-trans isomers observed due to restricted rotation about the C9-N bond) 28.1(q), 56.6 (t), 81.7 (s), 82.0 (s), 113.0 (s), 113.7 (s), 115.5 (d), 116.9 (d), 117.5 (s), 119.4 (d), 119.8 (d), 122.0 (s), 124.0 (s), 125.2 (d), 125.8 (d), 126.2 (d), 126.8 (d), 127.2 (d), 127.8 (d), 128.1 (d), 128.2 (d), 128.3(d), 128.4 (d), 128.9 (d), 129.5 (d), 130.1 (d), 130.5 (d), 130.6 (d), 132.0 (d), 132.8 (d), 133.2 (d), 134.4 (d), 136.0 (s), 137.4 (s), 139.2 (s), 140.6 (s), 142.1 (s), 143.6 (s), 153.5 (s), 153.7 (s), 167.4 (s), 167.6 (s); LRMS m/z (EI) (%) 384 (M^+, 30), 327 (100), 282 (61), 279 (11), 177 (78); HRMS (ESI) found 385.1913, calcd. for $C_{25}H_{25}O_2N_2$ $[M+H]^+$ 385.1911.

9-benzylaminoacridine-4-carboxylic acid (30)

METHOD A: Via hydrolysis of *iso*-propyl-9-benzylaminoacridine-4-carboxylate (28) under basic aqueous conditions:

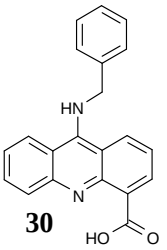

30

A solution of *iso*-propyl-9-benzylaminoacridine-4-carboxylate (**28**) (0.050 g, 0.14 mmol, 1.0 eq) in dioxane (2mL) and a 0.6 M

aqueous lithium hydroxide solution (1.0 mL, 0.60 mmol, 4.3 eq) were combined with stirring at rt for 24 h. Subsequently, the reaction mixture was neutralised with 2.0 M HCl and cooled to 4 °C for 24 hours, after which a yellow solid had precipitated. The solid was filtered off and washed with cold water (0°C) (20.0 mL) followed by diethyl ether (20.0 mL) and dried *in vacuo* over P_2O_5. This afforded the product **30** (0.028 g, 59 %) as a yellow solid that was used in a subsequent step without further purification. mp 236°C (dec) (from MeOH). δ_H (200 MHz; DMSO-d_6) (cis-trans isomers observed in a 2:1 ratio due to restricted rotation about the C9-N bond) 5.45 (min) and 5.51 (max) (2 H, s, CH_2Ph), 7.46-7.80 (7 H, m, Ar-*H*), 7.88-8.10 (2 H, m, Ar-*H*), 8.39-8.91 (3 H, m, Ar-*H*), 11.69 (max) and 11.90 (min) (1 H, s, CH_2NH), 13.71 (1 H, br s, COO*H*); δ_C (50 MHz; DMSO-d_6) (cis-trans isomers observed due to restricted rotation about the C9-N bond) 51.0 (t), 111.7 (s), 113.0 (s), 113.4 (s), 118.2 (d) , 119.6 (d), 120.2 (s), 120.9 (d), 121.0 (d), 121.7 (d), 122.0 (s), 123.1 (d), 123.4 (d), 125.6 (d), 126.0 (d), 126.7 (d), 127.5 (d), 128.0 (d), 128.8 (d), 133.4 (d), 134.0 (d), 135.7 (d), 136.1 (d), 137.9 (s), 140.1 (s), 141.2 (s), 141.8 (s), 143.1 (s), 156.3 (s), 167.9 (s), 172.0 (s), 177.0 (s), 201.3 (s); LRMS m/z (ESI) (%) 327 ($[M-H]^-$, 3), 238 (8), 77 (4), 75 (100); HRMS (ESI) found 327.1140, calcd. for $C_{21}H_{15}O_2N_2$ $[M-H]^-$ 327.1139.

METHOD B: Attempted preparation of 9-benzylaminoacridine-4-carboxylic acid (30) via ester cleavage of *iso*-propyl-9-benzylaminoacridine-4-carboxylate (28) with iodotrimethylsilane.

Iso-propyl-9-benzylaminoacridine-4-carboxylate (**28**) (0.050 g, 0.14 mmol, 1.0 eq) and sodium iodide (0.040 g, 0.26 mmol, 2.0 eq) were dissolved in acetonitrile (4 mL). To this solution was added, with stirring and under nitrogen, trimethylsilyl chloride (0.03 mL, 0.3 mmol, 2 eq). The reaction mixture was then heated at 85°C for 72 hours, with stirring under nitrogen atmosphere, whereupon the mixture was cooled to rt and the reaction was quenched by addition of water (3.5 mL). The reaction mixture was left to stir at rt for 30 mins whereupon the solvent was removed in *vacuo* and the crude residue analysed by NMR. This analysis showed little or no deprotection had taken place.

METHOD C: Attempted preparation of 9-benzylaminoacridine-4-carboxylic acid (30) via ester cleavage of *iso*-propyl-9-benzylaminoacridine-4-carboxylate (28) with $AlCl_3$.

To a cooled solution (0°C) of $AlCl_3$ (0.22 g, 1.6 mmol, 4.0 eq) in dry DCM (2 mL) was added dropwise a solution of *iso*-propyl-9-benzylaminoacridine-4-carboxylate (**28**) (0.15 g, 0.41 mmol, 1.0 eq) in dry DCM (1 mL). The reaction mixture was stirred for 1 h at rt and then poured into an ice-slurry (15 mL) whereupon the resulting suspension was filtered and the separated yellow solid washed with water (15 mL) followed by diethyl ether (15mL) and dried *in vacuo* over phosphorus pentoxide. NMR analysis of the yellow precipitate suggested almost exclusive presence of 9-aminoacridine-4-carboxylic acid **31** (0.09 g, 92 %), not the expected 9-benzylamino acridine-4-carboxylic acid **30**.

METHOD D: Attempted preparation of 9-benzylaminoacridine-4-carboxylic acid (30) via selective ester cleavage of *t*-butyl-9-benzylaminoacridine-4-carboxylate (29) with $Yb(OTf)_3$

t-Butyl-9-benzylaminoacridine-4-carboxylate (**29**) (0.20 g, 0.58 mmol, 1.0 eq) was dissolved in nitro methane (3 mL) and to the resulting solution was added 0.02 g (5 mol%) of $Yb(OTf)_3$. The resulting reaction mixture was stirred for 18 hours at 50°C. Subsequently, the solvent was removed *in vacuo* and the crude solid residue was taken up in dioxane and filtered through a Celite pad. The filtrate was cooled (4°C) for 24 h whereupon a yellow precipitate was separated by filtration and washed with water (10 mL) followed by diethyl ether (10 mL) and dried *in vacuo* over P_2O_5. NMR analysis of the yellow solid revealed almost exclusive presence of the starting material **29**.

METHOD E: Attempted preparation of 9-benzylaminoacridine-4-carboxylic acid (30) via acid ester hydrolysis of *t*-butyl-9-benzylaminoacridine-4-carboxylate (29) with sulphuric acid

A solution of *t*-butyl-9-benzylaminoacridine-4-carboxylate (**29**) (0.070 g, 0.18 mmol, 1.0 eq) in dichloromethane (5 mL) was added dropwise into a cooled (0° C), stirred emulsion of concentrated sulphuric acid (0.005 mL, 0.2 mmol, 1 eq) in dichloromethane (5 mL). The resulting mixture was stirred for six hours at room temperature. Solvents were removed *in vacuo* and the crude solid yellow residue was re-suspended in water (5 mL) and stirred for 5 mins. Subsequently, the yellow solid

was separated by filtration, washed with diethyl ether (5 mL) and dried *in vacuo* over P_2O_5. MS and NMR analysis of the yellow solid did however suggest very little of the expected 9-benzylaminoacridine-4-carboxylic acid (**30**) was present besides a number of unidentified by-products.

Attempted preparation of Ethyl 2-(*N*-(2-(9-benzylaminoacridine-4-carboxamido) ethyl)-2-(thymin-1-yl)acetamido)acetate (32)

METHOD A: Via acid activation of 9-benzylaminoacridine-4-carboxylic acid (30) with dicyclohexylcarbodiimide and N-hydroxysuccinimide:

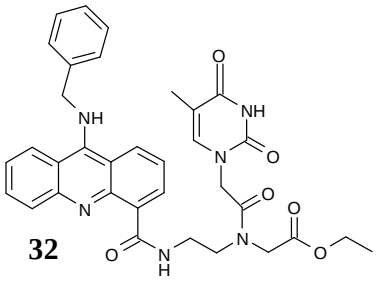

32

To a solution of 9-benzylaminoacridine-4-carboxylic acid (**30**) (0.16 g, 0.49 mmol, 1.0 eq) and N-hydroxysuccinimide (0.070 g, 0.62 mmol, 1.2 eq) in DMF (5 mL) was added, slowly, dicyclohexylcarbodiimide (0.21 g, 0.62 mmol, 1.2 eq) in DMF (5 mL) and the resulting mixture was stirred for 48 h. at rt. To this mixture was then added a solution of the hydrochloric acid salt of N-(aminoethyl)-N-(thymin-1-ylacetyl) glycine ethyl ester (**21**) (0.22 g, 0.62 mmol, 1.2 eq) and TEA (172 µL, 1.24 mmol, 2.5 eq) in dimethylformamide (5 mL) and this was stirred for 24 h. at rt. Subsequently, the solvent was removed *in vacuo* and the crude solid residue was purified by flash column chromatography (petroleum ether : ethyl acetate : methanol : triethylamine, 40:45:14:1). Unfortunately, neither MS nor NMR analysis confirmed presence of the potential conjugate **32** in any of the collected fractions.

METHOD B: Via acid activation of 9-benzylaminoacridine-4-carboxylic acid (30) with O-Benzotriazole-N,N,N',N'-tetramethyl-uronium-hexafluoro-phosphate (HBTU):

To a solution of 9-Benzylaminoacridine-4-carboxylic acid (**30**) (0.070 g, 0.20 mmol, 1.0 eq) in dimethylformamide (3 mL) was added HBTU (0.080 g, 0.20 mmol, 1.0 eq) and DIPEA (0.10 mL, 0.55 mmol, 2.7 eq). The resulting mixture was stirred for 24 h. at rt. whereupon a solution of the trifluoroacetic acid salt of N-(aminoethyl)-N-(thymin-1-ylacetyl) glycine ethyl ester (0.22 g, 0.62 mmol, 1.2 eq) **14** and TEA (172 µL, 1.24 mmol, 2.5 eq) in DMF (5 mL) was added. The resulting mixture was stirred for another

24 h. at rt. Subsequently, the reaction was quenched with a 5% (aq) solution of NH_4Cl (1 mL) and left to stir at rt for 10 mins. The solvent was removed *in vacuo* and the crude reaction residue was purified by flash column chromatography (petroleum ether : ethyl acetate : methanol : triethylamine, 40:45:14:1). Unfortunately, neither MS nor NMR analysis confirmed presence of the potential conjugate **32** in any of the collected fractions.

Iso-propyl-9-anilinoacridine-4-carboxylate (33)[210]

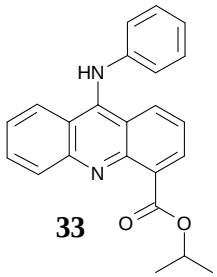

33

To a solution of *I*so-propyl-9-(1,2,4-triazol-1-yl)acridine-4-carboxylate (**25**) (0.32 g, 0.95 mmol, 1.0 eq) in dry acetonitrile (20 mL) was added dry aniline (0.87 mL, 9.5 mmol, 10 eq) and dry TEA (2.1 mL, 14 mmol, 15 eq). The resulting mixture was heated at reflux while stirring and under nitrogen for 24 h. Subsequently, the reaction mixture was allowed to cool down and the solvent was removed *in vacuo*. This afforded a solid residue which was purified by flash column chromatography (petroleum ether (40-60°C) : ethyl acetate : triethylamine, 95:4:1). The title compound **33** (0.23 g, 67 %) was obtained as an orange-red solid. mp 135-137°C (from dichloromethane/petrol ether); R_f 0.26 (Petroleum ether (40-60°C) : ethyl acetate : triethylamine, 95:4:1); (Found: C, 77.2; H, 5.8; N, 7.5. $C_{23}H_{20}N_2O_2$ requires C, 77.5; H, 5.7; N, 7.8%); ν_{max}(film)/cm^{-1}: 3285, 3067, 2980, 2938, 1680, 1612, 1587, 1519, 1478, 1446, 1276, 1141, 1104, 776, 750, 696; δ_H (200 MHz; $CDCl_3$) 1.33 (6 H, d, *J* 6.2, CH(C*H*$_3$)$_2$), 5.22 (1 H, septet, *J* 6.2, C*H*(CH$_3$)$_2$), 6.48-6.66 (1 H, m, Ar-*H*), 6.78 (2 H, d, *J* 8.3, Ar-*H*), 6.92 (1 H, t, *J* 7.5, Ar-*H*), 7.05 (2 H, t, *J* 7.1, Ar-*H*), 7.28 (4 H, t, *J* 7.5, Ar-*H*), 8.09 (1 H, s, Ar-*H*), 8.60 (1 H, s, Ar-*H*), 11.20 (1 H, br s, N(10)*H*); δ_C (50 MHz; $CDCl_3$) 21.4 (q), 68.4 (d), 112.4 (s), 116.9 (d), 117.7 (d), 119.0 (s), 120.1 (d), 121.3 (d), 124.8 (d), 127.7 (d), 128.5 (d), 129.2 (d), 130.8 (d), 133.1 (s), 133.4 (d), 139.5 (s), 140.8 (s), 150.4 (s), 152.9 (s), 167.2 (s); LRMS m/z (ESI) (%) 357 ($[M+H]^+$, 100), 60 (2); HRMS (ESI) found 357.1602, calcd. for $C_{23}H_{21}O_2N_2$ $[M+H]^+$ 357.1598.

9-anilinoacridine-4-carboxylic acid (34)[210]

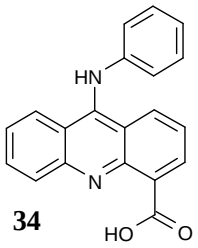

34

To a solution of *iso*-propyl-9-anilinoacridine-4-carboxylate (**33**) (0.21 g, 0.58 mmol, 1.0 eq) in tetrahydrofuran (4 mL) was added a 1.0 M (aq) lithium hydroxide solution (1.00 mL, 1.00 mmol, 1.7 eq). The resulting mixture was stirred at rt for 48 h whereupon the reaction mixture was quenched by addition of a 2.0 M (aq) HCl solution until a neutral pH was reached. Subsequently, solvents were removed *in vacuo* and the crude orange solid residue containing the 9-anilinoacridine-4-carboxylic acid (**34**) and LiCl was not purified further for use in the subsequent (activation) step. R_f 0.32 (Petroleum ether (40-60 °C) : ethyl acetate : methanol : triethylamine, 40:40:19:1); ν_{max}(KBr)/cm^{-1} 3416br, 1622, 1587, 1568, 1552, 1525, 1452, 1432, 1400, 1356, 1273, 1156; δ_H (200 MHz; CD_3OD) 7.30-7.53 (7 H, m, Ar-*H*), 7.78-7.92 (2 H, m, Ar-*H*), 8.01 (1 H, d, *J* 9.1, Ar-*H*), 8.35 (1 H, dd, *J* 8.7 and 1.2, Ar-*H*), 8.60 (1 H, dd, *J* 7.5 and 1.2, Ar-*H*); δ_C (50 MHz; CD_3OD) 115.2 (s), 115.8 (s), 119.0 (s), 121.5 (d), 124.4 (d), 126.3 (d), 126.4 (d), 127.3 (d), 130.0 (d), 131.9 (d), 132.8 (d), 137.9 (d), 140.8 (d), 141.1 (s), 141.9 (s), 142.0 (s), 158.2 (s), 171.0 (s); LRMS m/z (EI) (%) 314 (M^+, 100), 270 (61), 246 (27), 176 (8).

***N*-[2-(dimethylamino)ethyl]-9-anilinoacridine-4-carboxamide (35)**

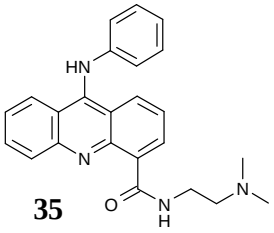

35

To a solution of 9-anilinoacridine-4-carboxylic acid (**34**) (0.14 g, 0.43 mmol, 1.0 eq) and N-hydroxysuccinimide (0.10 g, 0.87 mmol, 2.0 eq), in dimethylformamide (5 mL), was added slowly dicyclohexylcarbodiimide (0.18 g, 0.54 mmol, 1.2 eq) in dimethylformamide (3 mL). The resulting mixture was stirred for 24 h. at rt. whereupon the dicyclohexylurea by-product was removed by filtration. To the filtrate was subsequently added an excess of N,N-dimethylethylenediamine (5.00 mL, 45.0 mmol, 105 eq) and the resulting mixture was stirred for another 24 h. at rt. After removing the solvent *in vacuo* the reaction mixture residue was purified by flash column chromatography (ethyl acetate : methanol : triethylamine, 90:9:1). This afforded the title compound **35** (0.08 g, 46 %) as a yellow-orange oily solid. Unfortunately, the oily solid character of **35** prevented us from taking a reliable mp. R_f 0.29 (ethyl acetate : methanol : triethylamine, 90:9:1); ν_{max} (film)/cm^{-}

[1]: 3262, 3166, 3059, 2975, 2945, 2860, 2821, 2774, 1773, 1698, 1640, 1620, 1600, 1587, 1558, 1525, 1496, 1471, 1438, 1417, 1360, 1293, 1272, 1252; δ_H (200 MHz; DMSO-d_6) (rotational isomers observed in a 4:1 ratio due to restricted rotation about C(4)–CONH) 2.45 (6 H, s, N(C*H*$_3$)$_2$), 2.69 (2 H, m, C*H*$_2$N(CH$_3$)$_2$), 3.79 (2 H, m, CONHC*H*$_2$), 6.86 (1 H, m, Ar-*H*), 6.91-7.10 (2 H, m, Ar-*H*), 7.21-7.32 (2 H, m, Ar-*H*), 7.45-7.63 (2 H, m, Ar-*H*), 7.85-7.98 (1 H, m, Ar-*H*), 8.15-8.31 (2 H, m, Ar-*H*), 8.42 (1 H, d, *J* 8.7, Ar-*H*), 8.74 (1 H, d, *J* 6.6, Ar-H), 8.88 (min) and 9.60 (max) (1H, s, CON*H*), 11.90 (min) and 12.16 (max) (1H, s, N(10)*H*); δ_C (50 MHz, DMSO-d_6): 37.9 (t), 45.9 (q), 65.8 (t), 118.7 (d), 119.8 (s), 120.7 (s), 122.3 (d), 124.0 (d), 125.5 (d), 125.7 (d), 129.2 (d), 130.1 (d), 130.6 (s), 132.3 (d), 134.0 (d), 135.1 (d), 146.2 (s), 147.8 (s), 147.9 (s), 149.0 (s), 165.6 (s); LRMS m/z (ESI) (%) 385 ([M+H]$^+$, 100), 193 (3); HRMS (ESI) found 385.2023, calcd. for $C_{24}H_{25}O_1N_4$ [M+H]$^+$ 385.2022.

Ethyl 2-(*N*-(2-(9-anilinoacridine-4-carboxamido)ethyl)-2-(thymin-1-yl)acetamido) acetate (36)

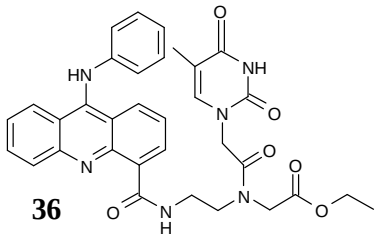

36

To a solution of 9-anilinoacridine-4-carboxylic acid (**34**) (0.18 g, 0.58 mmol, 1.0 eq) and N-hydroxysuccinimide (0.13 g, 1.2 mmol, 2.0 eq) in dimethylformamide (5 mL) was added slowly dicyclohexylcarbodiimide (0.24 g, 0.72 mmol, 1.2 eq) in dimethylformamide (3 mL). The resulting mixture was stirred for 24 h. at rt, whereupon the dicyclohexylurea by-product was removed by filtration. To the filtrate was added a solution of the hydrochloric acid salt of the thyminyl-PNA-monomer **21** (0.25 g, 0.72 mmol, 1.2 eq) and triethylamine (0.20 mL, 1.4 mmol, 2.5 eq) in dimethylformamide (5 mL). The resulting mixture was stirred for another 24 h. at rt. Subsequently, the solvent was removed *in vacuo* and the reaction residue was purified by flash column chromatography (petroleum ether : ethyl acetate : methanol : triethylamine, 50:50:4:1) as the eluent. This afforded the title compound **36** (0.23 g, 64.4 %) as a yellow oily solid. Unfortunately, the oily solid character of **36** prevented us from taking a reliable mp. R_f 0.35 (petroleum ether : ethyl acetate : methanol : triethylamine, 50:50:4:1); ν_{max}(KBr)/cm^{-1} 3185, 3052, 2981, 2946, 1744, 1689, 1674, 1641, 1619, 1602, 1560, 1525, 1494, 1473, 1442, 1435, 1424, 1363, 1334, 1299, 1262,

1212, 1190, 1166, 1150, 1096, 1036, 1021, 962, 760; δ_H (400 MHz; DMSO-d_6) (rotational isomers observed in a 6:3:1 or 9:1 ratio due to restricted rotation about the tertiary and secondary amide bond) 1.18 (0.3 H) and 1.20 (2.7 H) (3 H, t, *J* 7.1, CH_2CH_3), 1.24 (1.8 H) and 1.54 (0.3 H) and 1.68 (0.9 H) (3 H, s, $CHCCH_3$), 3.45-3.59 (0.4 H) and 3.60-3.73 (1.2 H) and 3.73-3.85 (2.4 H) (4 H, m, CH_2CH_2NCO), 4.10 (0.2 H) and 4.12 (1.8 H) (2H, q, *J* 7.1, CH_2CH_3), 4.21 (1.2 H) and 4.39 (0.2 H) and 4.46 (0.2 H) and 4.51 (0.6 H) and 4.73 (1.8 H) (4 H, s, NCH_2COOEt and NCH_2CON), 6.52-7.04 (4 H, m, Ar-*H* and $CHCCH_3$), 7.14-7.36 (3 H, m, Ar-*H*), 7.40-7.57 (2 H, m, Ar-*H*), 7.78-8.08 (1 H, m, Ar-*H*), 8.15 and 8.28 (1 H, d, J 8.60, Ar-*H*), 8.31-8.38 (1 H, m, Ar-*H*), 8.62-8.70 (1 H, m, Ar-*H*), 9.50 and 9.54 (1 H, br s, N*H*), 11.28 and 11.36 (1 H, br s, N*H*), 11.70-11.92 (1 H, br s, N*H*); δ_C (100 MHz; DMSO-d_6) (rotational isomers observed in a 6:3:1 ratio due to restricted rotation about the tertiary and secondary amide bond)11.4 (q), 11.7 (q), 11.8 (q), 14.0 (q), 30.4 (q), 37.6 (t), 46.5 (t), 47.7 (t), 47.8 (t), 48.4 (t), 60.6 (t), 107.8 (d), 108.1 (d), 117.8 (d), 117.9 (d), 119.0 (s), 119.8 (s), 121.4 (d), 121.5 (d), 121.7 (d), 123.1 (d), 124.3 (d), 124.7 (d), 128.3 (s), 128.5 (d), 128.7 (d), 129.2 (d), 129.5 (d), 129.7 (d), 131.0 (d), 131.3 (d), 131.8 (d), 134.2 (d), 134.5 (d), 141.35 (d), 141.8 (d), 141.9 (d), 145.1 (s), 145.3 (s), 146.75 (s), 147.1 (s),148.1 (s), 150.8 (s), 150.9 (s), 164.1 (s), 164.3 (s), 165.7 (s), 167.3 (s), 169.0 (s), 169.5 (s), 177.2 (s); LRMS m/z (ESI) (%) 609 ($[M+H]^+$, 100), 105 (10); HRMS (ESI) found 609.2450, calcd. for $C_{33}H_{33}O_6N_6$ $[M+H]^+$ 609.2456.

***Iso*-propyl-9-aminoacridine-4-carboxylate (40)**

METHOD A: Via 9-chloro substitution in *iso*-propyl-9-chloroacridine-4-carboxylate (42) using NH_4HCO_3

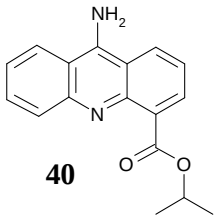

40

Iso-propyl-9-chloroacridine-4-carboxylate (**42**) (0.30 g, 1.0 mmol, 1.0 eq) was dissolved in phenol (1.50 g, 15.9 mmol, 16 eq) at 70°C. To the resulting solution was then added NH_4HCO_3 (0.16 g, 2.0 mmol, 2.0 eq) whereupon the temperature was increased to 120° C and maintained for 2 h. with stirring. Subsequently, the reaction mixture was cooled down to rt and phenol was removed *in vacuo* by co-evaporation with toluene. The reaction residue was purified by flash column chromatography (petroleum ether (40-60°C) : ethyl acetate : methanol : triethylamine, 45:45:10:1). This afforded the title compound **40** (0.24 g, 81%) as

slowly solidifying green-yellow oil. mp 198°C (dec) (from $CHCl_3$/petroleum ether); R_f 0.12 (Petroleum ether (40-60°C) : ethyl acetate : methanol : triethylamine, 45:45:10:1); (Found: C, 72.5; H, 5.6; N, 9.7. $C_{17}H_{16}N_2O_2$ requires C, 72.8; H, 5.7; N, 10.0%); ν_{max} (film)/cm^{-1} 3305, 3280, 2980, 2927, 1682, 1613, 1558, 1523, 1465, 1448, 1373, 1269, 776, 749, 713; δ_H (200 MHz; $CDCl_3$) 1.37 (6 H, d, *J* 6.4, $CH(CH_3)_2$), 5.21 (1 H, septet, *J* 6.4, $CH(CH_3)_2$), 6.98-7.12 (3 H, m, Ar-*H*), 7.36-7.44 (1 H, m, Ar-*H*), 7.99 (1 H, dd, *J* 8.3 and *J* 1.7, Ar-*H*), 8.15 (1 H, d, *J* 7.5 and *J* 1.7, Ar-*H*), 8.49 (1 H, d, *J* 7.9 and *J* 1.7, Ar-*H*), 11.15 (1 H, br s, N(10)*H*); δ_C (50 MHz; $CDCl_3$) 21.70 (q), 68.81 (d), 113.05 (s), 117.18 (d), 118.50 (s), 119.08 (d), 120.26 (s), 121.72 (d), 124.31 (d), 131.19 (d), 131.70 (d), 134.30 (d), 137.55 (s), 140.48 (s), 161.33 (s), 167.40 (s); LRMS m/z (EI) (%) 280 ($[M]^+$, 21), 252 (13), 238 (10), 221 (17), 220 (100), 192 (35), 166 (12), 165 (21), 164 (25); HRMS m/z (EI) found 280.1209, calcd. for $C_{17}H_{16}N_2O_2$ $[M]^+$ 280.1206.

METHOD B: Preparation of *iso*-propyl-9-aminoacridine-4-carboxylate (40) via hydrogenolysis of *iso*-propyl-9-benzylaminoacridine-4-carboxylate (28)

Iso-propyl-9-benzylaminoacridine-4-carboxylate (**28**) (0.86 g, 2.3 mmol, 1.0 eq) was dissolved in ethyl acetate/ethanol 1/1 (50mL) after which palladium (10% on charcoal) was added (0.08 g). The resulting suspension was left stirring at rt for 96 h. under a hydrogen atmosphere. Subsequently, the suspension was filtered through a Celite pad (5 cm in height) and the filtrate solvents removed *in vacuo*. The resulting crude reaction residue was subjected to flash column chromatography (petroleum ether : ethyl acetate : triethylamine, 90:9:1). This afforded the title compound **40** as a green-yellow solid in a very moderate 18% (0.12 g) yield. The analysis of this product was identical to that obtained for the product yielded by method A. 65% of the starting material (**28**) was recovered.

METHOD C: Attempted preparation of 40 via substitution of the 9-triazole substituent in *iso*-propyl-9-(1,2,4-triazol-1-yl)acridine-4-carboxylate (25) with ammonia.

Iso-propyl-9-(1,2,4-triazol-1-yl)acridine-4-carboxylate (**25**) (0.050 g, 0.15 mmol, 1.0 eq) was dissolved in acetonitrile/dimethylformamide 1/1 (15 mL) whereupon ammonia was bubbled through the solution while the temperature was increased from rt up to 100° C. Bubbling ammonia was maintained for another 3 h. at 100°C. Subsequently, the reaction mixture was cooled to rt, solvents were removed *in vacuo* and the resulting

reaction residue was subjected to flash column chromatography (ethyl acetate : petrol ether: triethylamine, 60:40:1). NMR analysis of active, columned fractions showed the presence of starting material (**25**) (68% of **25** was recovered) and at least two more unidentified compounds.

METHOD D: Attempted preparation of 40 via substitution of the 9-triazole substituent in *iso*-propyl-9-(1,2,4-triazol-1-yl)acridine-4-carboxylate (25) with 3,4,5,6-tetrachlorophthalimide followed by unmasking of the N-3,4,5,6-tetrachlorophthaloyl group.

Triethylamine (0.50 mL, 3.6 mmol, 5.0 eq) and tetrachlorophthalimide (0.24 g, 0.83 mmol, 1.1 eq) were dissolved in dimethylformamide (5 mL) whereupon this mixture was added to a solution of *iso*-propyl-9-(1,2,4-triazol-1-yl)acridine-4-carboxylate (**25**) (0.24 g, 0.72 mmol, 1.0 eq) in dimethylformamide (6 mL). The resulting solution was stirred for 24 hours at room temperature under a nitrogen atmosphere, after which time the reaction mixture was heated to 80° C for another 24 hours, with stirring under nitrogen. Subsequently, the solvent was removed *in vacuo* and the crude reaction residue was subjected to flash column chromatography (ethyl acetate : petrol ether : triethylamine, 50:50:1). NMR analysis of collected fractions suggested mainly presence of the starting material (**25**). None of the expected intermediate tetrachlorophthalimide (**41**) could be identified.

***Iso*-propyl-9-chloroacridine-4-carboxylate (42)**

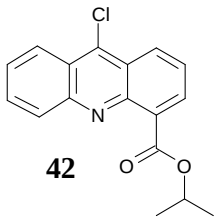

42

Iso-propyl-9-oxoacridan-4-carboxylate (**22**) (2.81 g, 10.0 mmol, 1.00 eq) was suspended in excess thionyl chloride (25 mL) and a catalytic amount of dimethylformamide was added (one drop). The resulting suspension was heated gently at reflux, while stirring and under nitrogen, until all solid material was dissolved. The homogeneous solution was then left at reflux temperature for 45 minutes, whereupon the reaction mixture was allowed to cool to room temperature. Subsequently, the remaining thionyl chloride was removed *in vacuo* whilst keeping the temperature below 40°C. The last traces of thionyl chloride were removed by resuspending the residue in toluene (3 x 15 mL) and removing the solvent *in vacuo* to yield the title compound **42** (2.91 g, 97%) as an orange solid. The product was used

without further purification in a subsequent step. mp 152-154°C (from $CHCl_3$ / Petroleum ether); R_f 0.66 (Petroleum ether (40-60 °C) : ethyl acetate : triethylamine, 50:50:1); δ_H (200 MHz; $CDCl_3$) 1.41 (6 H, d, *J* 6.2, $CH(CH_3)_2$), 5.35 (1 H, septet, *J* 6.2, $CH(CH_3)_2$), 7.59-7.69 (3 H, m, Ar-*H*), 8.21-8.27 (1 H, m, Ar-*H*), 8.40 (2 H, dd, *J* 7.5 and 1.7, Ar-*H*), 8.70 (1 H, dd, *J* 8.3 and 1.2, Ar-*H*); δ_C (50 MHz; $CDCl_3$) 21.77 (q), 69.12 (d), 123.80 (s), 124.00 (s), 124.22 (d), 125.62 (d), 127.26 (d), 127.38 (d), 129.80 (d), 130.72 (d), 130.98 (d), 132.40 (s), 141.90 (s), 145.00 (s), 148.23 (s), 167.11 (s).

Methyl-9-chloroacridine-4-carboxylate (43)

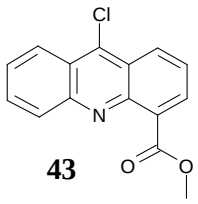

43

Methyl-9-oxoacridan-4-carboxylate (**2**) (2.53 g, 10.0 mmol, 1.00 eq) was suspended in excess thionyl chloride (25 mL) and a catalytic amount of dimethylformamide was added (one drop). The resulting suspension was heated gently at reflux, while stirring and under nitrogen, until all solid material had dissolved. The homogeneous solution was then left at reflux for 45 minutes, whereupon the reaction mixture was allowed to cool to room temperature. Subsequently, the remaining thionyl chloride was removed *in vacuo* whilst keeping the temperature below 40°C. The last traces of thionyl chloride were removed by resuspending the residue in toluene (3 x 15 mL) and removing the solvent *in vacuo* to yield the title compound **43** (2.66 g, 98 %) as an orange-red solid. The product was used without further purification in a subsequent step. mp 154-158°C (from $CHCl_3$ / Petroleum ether); R_f 0.61 (Petroleum ether (40-60 °C) : ethyl acetate : triethylamine, 50:50:1); δ_H (200 MHz; $CDCl_3$) 4.22 (3 H, s, CH_3), 7.90-8.04 (2 H, m, Ar-*H*), 8.25 (1 H, t, *J* 7.5, Ar-*H*), 8.60 (1 H, d, *J* 8.7, Ar-*H*), 8.74 (1 H, d, *J* 7.1, Ar-*H*), 8.85 (1 H, d, *J* 8.3, Ar-*H*), 9.27 (1 H, d, *J* 8.7, Ar-*H*); δ_C (50 MHz; $CDCl_3$) 54.4 (q), 122.5 (s), 122.7 (d), 124.5 (s), 124.8 (s), 125.6 (d), 128.0 (s), 128.3 (d), 130.2 (d), 130.5 (d), 136.8 (s), 138.5 (d), 140.2 (d), 154.4 (s), 165.2 (s).

Methyl-9-aminoacridine-4-carboxylate (44)

METHOD A: Via 9-chloro substitution in methyl-9-chloroacridine-4-carboxylate (43) using NH_4HCO_3

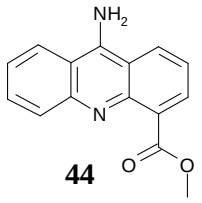

44

Methyl-9-chloroacridine-4-carboxylate (**43**) (0.27 g, 1.0 mmol, 1.0 eq) was dissolved in phenol (1.50 g, 15.9 mmol, 16 eq) at 70°C and to this solution was then added NH_4HCO_3 (0.16 g, 2.0 mmol, 2.0 eq) whereupon the temperature was increased to 120°C and maintained for 2h. with stirring. Subsequently, the reaction mixture was cooled down to rt and and phenol was removed *in vacuo* by co-evaporation with toluene. The crude reaction residue was purified by flash column chromatography (petroleum ether (40-60°C) : ethyl acetate : methanol : triethylamine, 45:45:10:1). This afforded the title compound **44** (0.16 g, 61%) as a greenish yellow solid. mp 205-209°C (from MeOH); R_f 0.13 (Petroleum ether (40-60°C) : ethyl acetate : methanol : triethylamine, 45:45:10:1); ν_{max} (film)/cm^{-1} 3293, 3285, 2952, 2913, 1693, 1614, 1556, 1524, 1488, 1448, 1271, 776, 747, 713; δ_H (200 MHz; $CDCl_3$) 3.88 (3 H, s, C*H*$_3$), 6.95-7.12 (3 H, m, Ar-*H*), 7.33-7.43 (1 H, m, Ar-*H*), 7.99 (1 H, d, *J* 8.3, Ar-*H*), 8.11 (1 H, dd, *J* 7.5 and *J* 1.7, Ar-*H*), 8.45 (1 H, dd, *J* 8.3 and *J* 1.2, Ar-*H*), 10.95 (1 H, br s, N(10)*H*); δ_C (50 MHz; $CDCl_3$) 52.4 (q), 112.7 (s), 117.5 (d), 118.9 (s), 119.5 (d), 120.6 (s), 122.1 (d), 124.6 (d), 131.7 (d), 132.1 (d), 134.6 (d), 137.8 (s), 140.8 (s), 161.6 (s), 168.6 (s); LRMS m/z (ESI) (%) 253 ($[M+H]^+$, 100), 74 (5); HRMS (ESI) found 253.0976, calcd. for $C_{15}H_{13}N_2O_2$ $[M+H]^+$ 253.0972.

METHOD B: Via 9-chloro substitution in methyl-9-chloroacridine-4-carboxylate (43) using NH_3

Methyl-9-chloroacridine-4-carboxylate (**43**) (0.050 g, 0.18 mmol, 1.0 eq) was dissolved in dry phenol and the mixture was heated slowly to 115 °C during which time, above 50 °C , a stream of gaseous ammonia was bubbled through the solution and continued for 2 hours 115 °C. Subsequently, the solvent was removed *in vacuo* by co-evaporation with toluene and the crude reaction residue was purified by flash column chromatography (petroleum ether (40-60°C) : ethyl acetate : methanol : triethylamine, 45:45:10:1). This afforded the title compound **44** (0.02 g, 39%) as a greenish yellow solid. The analysis of this product was identical to that obtained for the product yielded by method A.

METHOD C: Attempted preparation of 44 via substitution of the 9-triazole substituent in methyl-9-(1,2,4-triazol-1-yl)acridine-4-carboxylate (24) with ammonia.

Methyl-9-(1,2,4-triazol-1-yl)acridine-4-carboxylate (**24**) (0.050 g, 0.15 mmol, 1.0 eq) was dissolved in acetonitrile/dimethylformamide 1/1 (15 mL) whereupon ammonia was bubbled through the solution while the temperature was increased from rt up to 100° C over a period of one hour. Bubbling ammonia was maintained for another 3 h. at 100°C. Subsequently, the reaction mixture was cooled to rt, solvents were removed *in vacuo* and the resulting reaction residue was subjected to flash column chromatography (ethyl acetate : dioxane : triethylamine, 80:20:1). NMR analysis of active, columed fractions suggested the presence of starting material (**24**) (13% of **24** was recovered) and at least two more unidentified compounds.

Methyl-9-benzyloxycarbonylaminoacridine-4-carboxylate (45)

METHOD A: Via treatment of methyl-9-aminoacridine-4-carboxylate (44) with phosgene followed by benzyl alcohol.

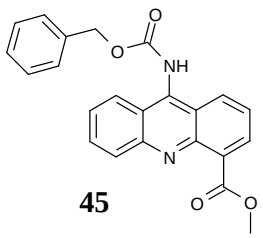

45

Methyl-9-aminoacridine-4-carboxylate (**44**) (1.50 g, 5.95 mmol, 1.0 eq) was dissolved in dichlorobenzene (75 mL) and to this mixture was added, successively, triethylamine (2.48 mL, 17.8 mmol, 3.0 eq) and triphosgene (0.88 g, 8.9 mmol, 1.2 eq). The resulting solution was heated to 110°C and kept at this temperature for 2 h., with stirring under nitrogen. Subsequently, benzyl alcohol (1.82 mL, 17.8 mmol, 3.0 eq) was added and the reaction mixture was heated at 110°C for another 3 h. After this time the reaction mixture was cooled down to rt and the solvent was removed *in vacuo*. This afforded a crude orange-red oily reaction residue which was separated by flash column chromatography (petroleum ether (40-60°C) : ethyl acetate : triethylamine, 50:50:1). This afforded the title compound **45** (0.85 g., 37 %) as slowly solidifying orange oil. mp 131-133°C (from chloroform / petrol ether); R_f 0.33 (Petroleum ether (40-60°C) : ethyl acetate : triethylamine, 50:50:1); (Found: C, 71.0; H, 4.4; N, 7.1. $C_{23}H_{18}N_2O_4$ requires C, 71.5; H, 4.7; N, 7.2%); ν_{max}(film)/cm^{-1} 3270, 3053, 3035, 3030, 2975, 2952, 1692, 1675, 1614, 1597, 1525, 1494, 1447, 1289, 1270, 780, 750, 698; δ_H (200 MHz; $CDCl_3$) 3.79 (3 H, s, C*H*$_3$), 5.28 (2 H, s, C*H*$_2$), 6.90-7.02 (2 H, m, Ar-*H*), 7.16 (1 H, d, *J* 8.3, Ar-*H*),

7.32-7.39 (3 H, m, Ar-*H*), 7.42-7.50 (3 H, m, Ar-*H*), 7.87 (1 H, d, *J* 8.3, Ar-*H*), 8.17 (1 H, dd, *J* 7.5 and *J* 1.7, Ar-*H*), 8.33 (1 H, dd, *J* 7.9 and *J* 1.7, Ar-*H*), 11.42 (1 H, s, N(10)*H*); δ_C (50 MHz; $CDCl_3$) 52.3 (q), 67.6 (t), 112.7 (s), 116.9 (s), 117.5 (d), 119.1 (s), 119.8 (d), 122.2 (d), 127.0 (d), 128.1 (d), 128.4 (d), 129.0 (d), 133.0 (d), 133.6 (d), 135.5 (d), 136.0 (s), 138.5 (s), 140.3 (s), 153.9 (s), 163.2 (s), 168.0 (s); LRMS m/z (ESI) (%) 387 ($[M+H]^+$, 100), 238 (6), 91 (3), 60 (3); HRMS (ESI) found 387.1340, calcd. for $C_{23}H_{19}N_2O_4$ $[M+H]^+$ 387.1339.

METHOD B: Attempted preparation of methyl-9-benzyloxycarbonylamino acridine-4-carboxylate (45) via reaction of methyl-9-aminoacridine-4-carboxylate (44) with benzyl chloroformate

Methyl-9-aminoacridine-4-carboxylate (**44**) (0.17 g, 0.67 mmol, 1.0 eq) was dissolved in pyridine (5 mL) and to this mixture was added, dropwise, a solution of benzyl chloroformate (0.24 mL, 1.7 mmol, 2.5 eq) in pyridine (1 mL), with stirring under nitrogen. The resulting solution was stirred for 24 h. at rt, whereupon the temperature was raised first to 50°C for 8 hours, then to 80° C for another 16 hours. Subsequently, the reaction mixture was cooled to rt and water (1 mL) was added to quench the reaction. The solvent was removed *in vacuo* and the crude reaction residue was subjected to flash column chromatography (ethyl acetate : petroleum ether : methanol : triethylamine, 45:45:10:1). Unfortunately, subsequent NMR analysis of collected fractions suggested mainly presence of starting material.

***Iso*-propyl-9-*t*-butyloxycarbonylaminoacridine-4-carboxylate (46)**

METHOD A: Via treatment of *iso*-propyl-9-aminoacridine-4-carboxylate (40) with phosgene followed by *t*-butanol

Iso-propyl-9-aminoacridine-4-carboxylate (**40**) (0.24 g, 0.86 mmol, 1.0 eq) was dissolved in dichlorobenzene (12 mL) and to this mixture was added, successively, triethylamine (0.36 mL, 2.6 mmol, 3.0 eq) and triphosgene (0.13 g, 1.3 mmol, 1.5 eq). The resulting solution was then heated to 110°C, which was maintained for 2 h, with stirring under nitrogen. Subsequently, *t*-butanol (0.24 mL, 2.6 mmol, 3.0 eq) was added and the reaction mixture was heated at 110°C for another 3 h. After this time the

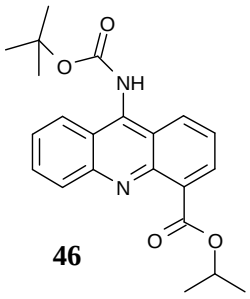

46

reaction mixture was cooled down and the solvent removed *in vacuo* to leave a crude yellow oily residue which was separated by flash column chromatography (petroleum ether (40-60°C) : ethyl acetate : triethylamine, 50:50:1). This afforded the title compound **46** (0.14 g, 41 %) as yellow oil; R_f 0.35 (Petroleum ether (40-60°C) : ethyl acetate : triethylamine, 50:50:1); ν_{max}(film)/cm^{-1}: 3269, 3066, 2979, 2933, 1717, 1688, 1615, 1598, 1524, 1465, 1448, 1366, 1271, 1166, 1135, 1105, 780, 750, 682; δ_H (200 MHz; $CDCl_3$) 1.37 (6 H, d, *J* 6.4, CH(C*H*$_3$)$_2$), 1.56 (9 H, s, C(C*H*$_3$)$_3$), 5.22 (1 H, septet, *J* 6.4, C*H*(CH$_3$)$_2$), 6.98-7.22 (2 H, m, Ar-*H*), 7.29-7.37 (1 H, m, Ar-*H*), 7.42-7.50 (1 H, m, Ar-*H*), 8.09 (1 H, dd, *J* 8.3 and *J* 1.2, Ar-*H*), 8.22 (1 H, dd, *J* 7.9 and *J* 1.7, Ar-*H*), 8.45 (1 H, dd, *J* 8.3 and *J* 1.2, Ar-*H*) 11.56 (1H, br s, N(10)*H*); δ_C (50 MHz; $CDCl_3$) 21.4 (q), 27.7 (q), 68.8 (d), 80.3 (s), 112.9 (s), 117.0 (d), 119.1 (d), 121.4 (d), 126.9 (d), 130.0 (s), 132.0 (s), 132.3 (d), 133.3 (d), 134.9 (d), 138.3 (s), 140.4 (s), 152.3 (s), 162.3 (s), 167.0 (s); LRMS m/z (ESI) (%) 381 ([M+H]$^+$, 100), 325 (55), 265 (42), 239 (23); HRMS (ESI) found 381.1810, calcd. for $C_{22}H_{25}N_2O_4$ [M+H]$^+$ 381.1809.

METHOD B: Attempted preparation of *iso*-propyl-9-*t*-butyloxycarbonylamino acridine-4-carboxylate (46) via reaction of *iso*-propyl-9-aminoacridine-4-carboxylate (40) with di-*t*-butyl dicarboxylate.

Iso-propyl-9-aminoacridine-4-carboxylate (**40**) (0.060 g, 0.21 mmol, 1.0 eq) was dissolved in dioxane/H_2O 2/1 (15 mL) and cooled to 0°C, whereupon di-*t*-butyl dicarboxylate (0.070 g, 0.32 mmol, 1.5 eq) was added to the reaction mixture. The resulting solution was allowed to warm up to rt while the pH was kept above 11 with a 1.0 M (aq) sodium hydroxide solution. Solvents were removed *in vacuo* after which the residue was triturated with dichloromethane. The suspension was filtered and the organic phase was dried over anhydrous $MgSO_4$. Filtration followed by solvent evaporation *in vacuo* yielded a green solid residue. Unfortunately, subsequent NMR analysis of the afforded solid showed exclusively starting material **40**.

Methyl-9-*t*-butyloxycarbonylaminoacridine-4-carboxylate (47)

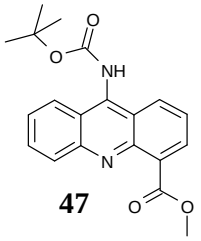

47

To a solution of methyl-9-aminoacridine-4-carboxylate (**44**) (1.24 g, 4.91 mmol, 1.0 eq) in dichlorobenzene (50 mL) was added,

successively, triethylamine (2.05 mL, 14.7 mmol, 3.0 eq) and triphosgene (0.73 g, 7.4 mmol, 1.5 eq) whereupon the resulting solution was heated to 110°C and kept at this temperature for 2 h. with stirring under nitrogen. Subsequently, *t*-butyl alcohol (1.39 mL, 14.7 mmol, 3.0 eq) was added and the reaction mixture was heated at 110°C for another 2 h. After this time the reaction mixture was cooled and the solvent removed *in vacuo* to leave an orange oily residue which was separated by flash column chromatography (petroleum ether (40-60°C) : ethyl acetate : triethylamine, 50:50:1). This afforded the title compound **47** (0.78 g, 43.0 %) as slowly solidifying orange oil. mp 107-111°C (from $CHCl_3$ / Petroleum ether); R_f 0.28 (Petroleum ether (40-60°C) : ethyl acetate : triethylamine, 50:50:1); ν_{max}(film)/cm^{-1} 3275, 2998, 2975, 2925, 2905, 1690, 1677, 1615, 1599, 1524, 1448, 1285, 1272, 780, 750, 684; δ_H (200 MHz; $CDCl_3$) 1.58 (9 H, s, C(C*H*$_3$)$_3$), 3.92 (3 H, s, C*H*$_3$), 7.00-7.22 (3 H, m, Ar-*H*), 7.40-7.52 (1 H, m, Ar-*H*), 8.09 (1 H, d, *J* 8.3, Ar-*H*), 8.20 (1 H, d, *J* 7.5, Ar-*H*), 8.47 (1 H, d, *J* 7.9, Ar-*H*) 11.44 (1 H, br s, N(10)*H*); δ_C (50 MHz; $CDCl_3$) 28.2 (q), 52.3 (q), 80.8 (s), 112.7 (s), 117.4 (d), 119.6 (d), 121.7 (s), 121.9 (d), 127.4 (d), 129.0 (s), 132.8 (d), 133.9 (d), 135.4 (d), 138.7 (s), 140.7 (s), 152.6 (s), 162.7 (s), 168.3 (s); LRMS m/z (ESI) (%) 353 ([M+H]$^+$, 100); HRMS (ESI) found 353.1492, calcd. for $C_{20}H_{21}N_2O_4$ [M+H]$^+$ 353.1496.

Methyl-9-allyloxycarbonylaminoacridine-4-carboxylate (48)

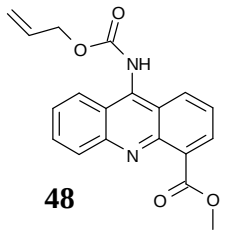

48

To a solution of methyl-9-aminoacridine-4-carboxylate (**44**) (0.45 g, 1.8 mmol, 1.0 eq) in dichlorobenzene (25 mL) was added, successively, triethylamine (0.75 mL, 5.3 mmol, 3.0 eq) and triphosgene (0.27 g, 2.7 mmol, 1.5 eq) whereupon the resulting solution was heated to 110°C and kept at this temperature for 2 h. with stirring under nitrogen. Subsequently, allyl alcohol (0.37 mL, 5.3 mmol, 3.0 eq) was added and the reaction mixture was heated at 110°C for another 2 hours. After this time the reaction mixture was cooled and the solvent removed *in vacuo* to leave an orange oily residue which was separated by flash column chromatography (petroleum ether (40-60°C) : ethyl acetate : triethylamine, 50:50:1). This afforded the title compound **48** (0.20 g, 33 %) as slowly solidifying yellow oil. mp 110-113°C (from $CHCl_3$ / Petroleum ether); R_f 0.22 (Petroleum ether (40-60°C) : ethyl acetate : triethylamine, 50:50:1); ν_{max} (film)/cm^{-1}:

3271, 2939, 2913, 1693, 1674, 1628, 1615, 1598, 1524, 1465, 1448, 1366, 1290, 1266, 780, 750, 666; δ_H (200 MHz; $CDCl_3$) 3.95 (3 H, s, C*H*$_3$), 4.78 (2 H, dt, *J* 5.8 and *J* 1.2, C*H*$_2$), 5.23 (1 H, dq, *J* 10.4 and *J* 1.2, =CH*H*), 5.37 (1 H, dq, *J* 17.0 and *J* 1.2, =C*H*H), 6.01 (1 H, ddt , *J* 17.0, *J* 10.4 and *J* 5.8, CH_2=C*H*), 7.04-7.32 (3 H, m, Ar-*H*), 7.49-7.59 (1 H, m, Ar-*H*), 8.03 (1 H, d, *J* 7.9, Ar-*H*), 8.29 (1 H, dd, *J* 7.5 and *J* 1.7 , Ar-*H*), 8.48 (1 H, dd, *J* 7.9 and *J* 1.7, Ar-*H*), 11.63 (1 H, br s, N(10)*H*); δ_C (50 MHz; $CDCl_3$) 52.8 (q), 67.0 (t), 113.2 (s), 117.4 (s), 118.0 (d), 119.1 (t), 119.8 (s), 120.3 (d), 122.2 (s), 122.8 (d), 127.6 (d), 132.8 (d), 133.5 (d), 134.3 (d), 136.1 (d), 139.2 (s), 141.0 (s), 163.7 (s), 168.8 (s); LRMS m/z (EI) (%) 336 (M^+, 40), 278 (73), 253 (84), 221 (100), 193 (66); HRMS (ESI) found 337.1183, calcd. for $C_{19}H_{17}N_2O_4$ $[M+H]^+$ 337.1183.

9-benzyloxycarbonylaminoacridine-4-carboxylic acid (49)

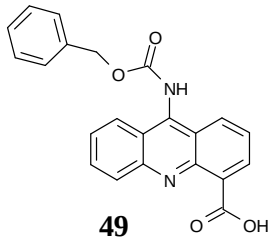

49

To a cooled solution (0°C) of methyl-9-benzyloxy carbonylaminoacridine-4-carboxylate (**45**) (0.58 g, 1.5 mmol, 1.0 eq) in THF (5 mL) was added a cooled (0°C) 0.6 M (aq) LiOH solution (3.50 mL, 2.10 mmol, 1.4 eq) and the resulting solution was kept at 0°C for 45 minutes, with stirring, whereupon the mixture was allowed to warm to rt. Subsequently, the reaction was quenched by addition of 0.5 M (aq) HCl solution until neutral pH was reached. The solvents were removed *in vacuo* and the crude reaction residue (a yellow solid) containing the title compound **49** and LiCl was used without further purification in a subsequent activation step. R_f 0.40 (Petroleum ether (40-60 °C) : ethyl acetate : methanol : triethylamine, 40:40:20:1)

9-*t*-butyloxycarbonylaminoacridine-4-carboxylic acid (50)

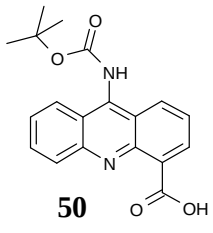

50

To a cooled solution (0°C) of methyl-9-*t*-butyloxycarbonyl aminoacridine-4-carboxylate (**47**) (0.060 g, 0.17 mmol, 1.0 eq) in tetrahydrofuran (1.5 mL) was added a cooled (0°C) 1.2 M (aq) LiOH solution (0.28 mL, 0.34 mmol, 2.0 eq) and the resulting solution was kept at 0°C for 45 minutes, with stirring, whereupon the mixture was allowed to warm to rt. Subsequently, the reaction was quenched by addition of 0.5 M (aq) HCl solution until neutral pH was reached. The solvents were

removed *in vacuo* and the crude reaction residue (a yellow solid) containing the title compound **50** and LiCl was used without further purification in a subsequent activation step. R_f 0.35 (Petroleum ether (40-60 °C) : ethyl acetate : methanol : triethylamine, 40:40:20:1)

9-allyloxycarbonylaminoacridine-4-carboxylic acid (51)

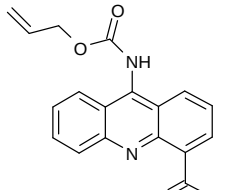

51

To a cooled (0°C) solution of methyl-9-allyloxycarbonyl aminoacridine-4-carboxylate (**48**) (0.23 g, 0.67 mmol, 1.0 eq) in tetrahydrofuran (2.4 mL) was added a cooled (0°C) 0.6 M (aq) LiOH solution (1.2 mL, 0.72 mmol, 1.1 eq) and the resulting solution was kept at 0°C for 45 minutes, with stirring, whereupon the mixture was allowed to warm to rt. Subsequently, the reaction was quenched by addition of 0.5 M (aq) HCl solution until neutral pH was reached. The solvents were removed *in vacuo* and the crude reaction residue (a yellow solid) containing the title compound **51** and LiCl was used without further purification in a subsequent activation step. R_f 0.37 (Petroleum ether (40-60 °C) : ethyl acetate : methanol : triethylamine, 40:40:20:1); δ_H (200 MHz; DMSO-d_6) 4.70 (2 H, d, *J* 5.4, CH_2), 5.26 (1 H, dd, *J* 10.4 and *J* 1.2, =CH*H*), 5.38 (1 H, dd, *J* 17.0 and *J* 1.2, =C*H*H), 6.02 (1 H, ddt , *J* 17.0, *J* 10.4 and *J* 5.4, CH_2=C*H*), 7.60-7.76 (2 H, m, Ar-*H*), 7.91-8.02 (1 H, m, Ar-*H*), 8.10-8.26 (2 H, m, Ar-*H*), 8.32-8.48 (1 H, m, Ar-*H*), 8.65 (1 H, dd, *J* 7.1 and *J* 1.2 Ar-*H*), 13.88 (1 H, br s, COO*H*); δ_C (50 MHz; DMSO-d_6) 65.7 (t), 117.8 (d), 118.5 (t), 121.4 (d), 123.1 (s), 124.7 (s), 125.1 (d), 125.5 (s), 125.9 (d), 130.0 (d), 133.0 (d), 133.3 (d), 133.8 (s), 134.7 (s), 136.3 (d), 144.9 (s), 156.0 (s), 167.0 (s).

Attempted preparation of ethyl 2-(*N*-(2-(9-(benzyloxycarbonylamino)acridine-4-carboxamido)ethyl)-2-(thymin-1-yl)acetamido)acetate (52)

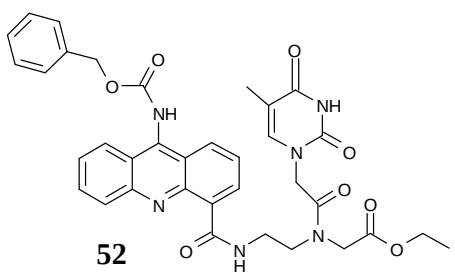

52

A solution of 9-benzyloxycarbonyl aminoacridine-4-carboxylic acid (**49**) (0.56 g, 1.5 mmol, 1.0 eq), N-hydroxysuccinimide (0.42 g, 3.6 mmol, 2.4 eq), and dicyclohexylcarbodiimide (0.72 g, 2.2 mmol,

1.4 eq) in DMF (40 mL) was stirred for 48 h. at rt. Subsequently, a solution of the hydrochloric acid salt of N-(aminoethyl)-N-(thymin-1-ylacetyl) glycine ethyl ester **21** (0.77 g, 1.9 mmol, 1.2 eq) and triethylamine (520 µL, 3.75 mmol, 2.5 eq) in DMF (10 mL) was added and the resulting solution was stirred for another 24 h. at rt. After removing the solvent *in vacuo*, the reaction residue was purified by flash column chromatography (ethyl acetate : methanol : triethylamine, 90:10:1). Unfortunately, neither MS nor NMR-analysis of the collected fractions could confirm the desired product **52** was present in significant amounts.

Ethyl 2-(*N*-(2-(9-(*t*-butoxycarbonylamino)acridine-4-carboxamido)ethyl)-2-(thymin-1-yl)acetamido)acetate (53)

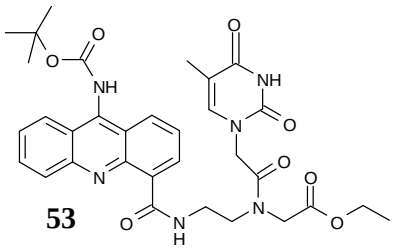

53

A solution of 9-*t*-butyloxycarbonylaminoacridine-4-carboxylic acid (**50**) (0.060 g, 0.17 mmol, 1.0 eq), N-hydroxysuccinimide (0.050 g, 0.43 mmol, 2.4 eq), and dicyclohexylcarbodiimide (0.090 g, 0.26 mmol, 1.4 eq) in DMF (3 mL) was stirred for 48 h. at rt. Subsequently, the dicyclohexylurea by-product was separated by filtration and to the filtrate was added a solution of the hydrochloric acid salt of N-(aminoethyl)-N-(thymin-1-ylacetyl) glycine ethyl ester **21** (0.070 g, 0.19 mmol, 1.0 eq) and triethylamine (0.050 mL, 0.34 mmol, 1.9 eq) in DMF (3 mL). The resulting solution was stirred for another 24 h. at rt. After removing the solvent *in vacuo*, the reaction residue was purified by flash column chromatography (petroleum ether : ethyl acetate : methanol : triethylamine, 45:45:10:1). This afforded the title compound **53** (0.025 g, 24%) as a yellow-orange oily solid. No reliable mp could be taken due to the oily nature of **53**; R_f 0.21 (petroleum ether : ethyl acetate : methanol : triethylamine, 45:45:10:1); ν_{max} (film)/cm^{-1} : 3288, 3182, 2952, 2930, 1739, 1700, 1660, 1623, 1563, 1526, 1470, 1370, 1340, 1231, 1208, 1158, 1113, 1047, 1022, 896; δ_H (400 MHz; $CDCl_3$) (2 rotational isomers observed in a 4:1 ratio due to restricted rotation about the tertiary amide bond) 1.20 (min) and 1.30 (max) (3 H, t, *J* 7.1, CH_2CH_3), 1.10 (max) and 1.69 (min) (3 H, s, $CHCCH_3$), 1.49 (9 H, br s, $C(CH_3)_3$), 1.74 (1 H, br s, NH), 3.68 (min) and 3.77 (max) (2 H, t, *J* 5.3, CH_2CH_2NCO), 3.84 (min) and 3.90 (max) (2 H, m, CH_2CH_2NCO), 4.18 (max) and 4.23 (min) (2 H, s, NCH_2COOEt), 4.11 (min) and 4.26 (max) (2 H, q, *J* 7.1, CH_2CH_3), 4.31 (min) and 4.61 (max) (2 H, s, NCH_2CON), 6.07

(max) and 6.83 (min) (1 H, s, C*H*CCH$_3$), 7.55-7.62 (1 H, m, Ar-*H*), 7.59 (1 H, br s, N*H*), 7.65 (1 H, m, Ar-*H*), 7.78 (1 H, m, Ar-*H*), 8.08 (min) and 8.13 (max) (1 H, d, *J* 8.5, Ar-*H*), 8.29 (1 H, d, *J* 8.8, Ar-*H*), 8.32 (1 H, dd, *J* 8.8 and 1.5, Ar-*H*), 8.60 (1H, br s, N*H*), 8.85 (min) and 8.89 (max) (1H, dd, *J* 7.1 and 1.2, Ar-*H*). 11.68 (max) and 11.75 (min) (1H, br t, *J*, CON*H*(CH$_2$)$_2$); δ_C (100 MHz; CDCl$_3$) (rotational isomers observed due to restricted rotation about the tertiary amide bond) 11.5 and 12.1 (CHC*C*H$_3$), 14.0 and 14.2 (CH$_2$*C*H$_3$), 28.2 (C(*C*H$_3$)$_3$), 38.3 (NH*C*H$_2$CH$_2$), 47.5 and 47.9 (N*C*H$_2$CON), 49.5 (NHCH$_2$*C*H$_2$), 49.8 (N*C*H$_2$COO), 61.7 and 62.0 (*C*H$_2$CH$_3$), 82.0 and 82.1 (*C*(CH$_3$)$_3$), 110.0 (CH*C*CH$_3$), 122.4 (s), 123.1 (s), 123.3 (d), 125.5 (d), 126.9 (d), 128.2 (d), 129.7 (d), 131.6 (d), 135.0 (s), 135.7 (d), 140.8 and 141.0 (*C*HCCH$_3$), 146.8 (s), 148.3 (s), 150.9 (CONH*C*ON), 153.5 (s), 163.9 (*C*ONHCON), 166.6 (*C*ONHCH$_2$CH$_2$), 167.4 (NCH$_2$*C*ON), 169.2 and 169.9 (NCH$_2$*C*OO); LRMS m/z (ESI) (%) 633 ([M+H]$^+$, 100), 322 (8), 242 (36), 74 (68); HRMS (ESI) found 633.2667, calcd. for $C_{32}H_{37}N_6O_8$ [M+H]$^+$ 633.2668.

Ethyl 2-(*N*-(2-(9-(allyloxycarbonylamino)acridine-4-carboxamido)ethyl)-2-(thymin-1-yl)acetamido)acetate (54)

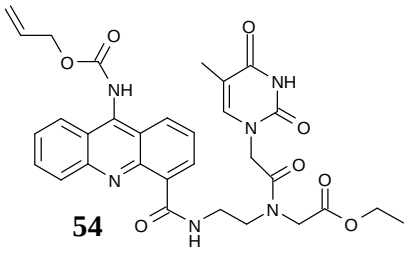

54

A solution of 9-allyloxycarbonylaminoacridine-4-carboxylic acid (**51**) (0.10 g, 0.30 mmol, 1.0 eq), N-hydroxysuccinimide (0.070 g, 0.60 mmol, 2.0 eq), and dicyclohexylcarbodiimide (0.13 g, 0.38 mmol, 1.2 eq) in DMF (5 mL) was stirred for 48 h. at rt. Subsequently, the dicyclohexylurea by-product was separated by filtration and to the filtrate was added a solution of the hydrochloric acid salt of N-(aminoethyl)-N-(thymin-1-ylacetyl) glycine ethyl ester **21** (0.13 g, 0.38 mmol, 1.2 eq) and triethylamine (0.13 mL, 0.94 mmol, 3.1 eq) in DMF (5 mL). The resulting solution was stirred for another 24 h. at rt. After removing the solvent *in vacuo*, the reaction mixture residue was purified by flash column chromatography (petrol ether : ethyl acetate : methanol : triethylamine, 50:50:5:1). This afforded the title compound **54** (0.095 g, 51 %) as a yellow-orange oily solid. No reliable mp could be taken due to oily nature of compound **54**; R_f 0.29 (petrol ether : ethyl acetate : methanol : triethylamine, 50:50:5:1); ν_{max} (film)/cm^{-1} : 3198, 3061, 3019, 2952, 2929, 1737, 1709, 1684, 1673, 1649, 1621, 1561, 1524, 1468, 1375, 1356, 1246,

1216, 1160, 1117, 1098, 1046, 756, 666; δ_H (400 MHz; DMSO-d_6) (rotational isomers present in a 3:1 ratio due to restricted rotation about the tertiary amide bond) 1.11-1.22 (3 H, m, CH_2CH_3), 1.19 (max) and 1.77 (min) (3 H, s, $CHCCH_3$), 3.60-3.81 (4 H, m, CH_2CH_2NCO), 4.05-4.42 (4 H, m, CH_2CH_3 + NCH_2COOEt), 4.50-4.75 (4 H, m, NCH_2CON + $CH_2CH{=}CH_2$), 5.20-5.34 (2 H, m, $CH{=}CH_2$), 5.91-6.10 (1 H, m, $CH{=}CH_2$), 6.53 (max) and 6.98 (min) (1 H, s, $CHCCH_3$), 7.66-7.80 (2 H, m, Ar-*H*), 7.89-7.95 (1 H, m, Ar-*H*), 8.15-8.24 (1 H, m, Ar-*H*), 8.32-8.46 (2 H, m, Ar-*H*), 8.68-8.75 (1 H, m, Ar-*H*), 11.20-11.45 (1 H, m, $CONH(CH_2)_2$); δ_C (100 MHz; DMSO-d_6) (rotational isomers present due to restricted rotation about the tertiary amide bond) 11.4 (q), 13.9 (q), 14.0 (q), 37.69 (t), 47.8 (t), 47.6 (t), 48.4 (t), 60.6 (t), 65.5 (t), 107.9 (s), 117.6 (s), 122.2 (s), 122.8 (s), 124.1 (d), 125.3 (s), 126.7 (d), 128.2 (s), 128.4 (d), 128.8 (s), 128.9 (s), 129 3 (d), 131.6 (d), 133.1 (d), 134.6 (d), 137.3 (s), 141.3 (s), 141.7 (d), 146.1 (s), 147.8 (s), 150.8 (s), 154.3 (s), 164.1 (s), 165.5 (s), 167.4 (s), 169.5 (s); LRMS m/z (ESI) (%) 617 ($[M+H]^+$, 100), 102 (48), 60 (78); HRMS (ESI) found 617.2350, calcd. for $C_{31}H_{33}O_8N_6$ $[M+H]^+$ 617.2354.

Trifluoroacetic acid salt of ethyl 2-(*N*-(2-(9-aminoacridine-4-carboxamido)ethyl)-2-(thymin-1-yl)acetamido)acetate (55)

To a solution of ethyl 2-(*N*-(2-(9-(*t*-butoxycarbonylamino)acridine-4-carboxamido) ethyl)-2-(thymin-1-yl)acetamido) acetate (**53**) (0.020 g, 0.030 mmol, 1.0 eq) in dichloromethane (1 mL) was added excess TFA 99% (1.00 mL). The resulting mixture was left stirring for 45 mins at rt and subsequently the solvent and excess TFA were removed *in vacuo.* This afforded the title compound **55** (0.02 g, 95%) as a very fine yellow powder which was used without purification in a subsequent step. mp 253°C (dec) (from MeOH); δ_H (400 MHz; CD_3OD) (rotational isomers present in a 1:1 ratio due to restricted rotation about the tertiary amide bond) 1.25-1.35 (3 H, m, CH_2CH_3), 1.65 and 1.80 (3 H, s, $CHCCH_3$), 3.62-3.88 (4 H, m, CH_2CH_2NCO), 4.20-4.30 (2 H, m, CH_2CH_3), 4.25 and 4.42 (2 H, s, NCH_2COOEt), 4.50 and 4.81 (2 H, s, NCH_2CON), 7.11 and 7.23 (1 H, s, $CHCCH_3$), 7.58-7.71 (2 H, m, Ar-*H*), 7.90-8.05 (2 H, m, Ar-*H*), 8.25 (0.5 H, d, *J* 7.3, Ar-*H*), 8.46-

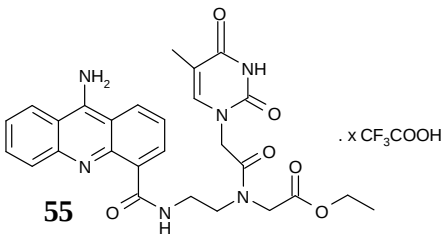

55

8.54 (1.5 H, m, Ar-*H*), 8.69 (1 H, d, *J* 8.5, Ar-*H*); LRMS m/z (ESI) (%) 533 ($[M+H]^+$, 100), 102 (45); HRMS (ESI) found 533.2146, calcd. for $C_{27}H_{29}O_6N_6$ $[M+H]^+$ 533.2143.

2-(*N*-(2-(9-aminoacridine-4-carboxamido)ethyl)-2-(thymin-1-yl)acetamido)acetic acid (56)

METHOD A: Via aqueous basic hydrolysis of the ethyl ester 55

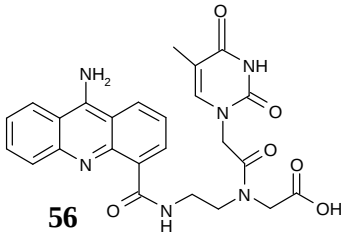

56

A solution of the trifluoroacetic acid salt of ethyl 2-(*N*-(2-(9-aminoacridine-4-carboxamido)ethyl)-2-(thymin-1-yl)acetamido) acetate (**55**) (0.020 g, 0.030 mmol, 1.0 eq) in 1.2 M (aq) sodium hydroxide / tetrahydrofuran (0.1 mL / 0.3 mL) was stirred at rt for 4 h. Subsequently, the reaction mixture was quenched with a 0.1 M (aq) HCl solution (1.2 mL) until neutral pH was reached. The solvents were removed *in vacuo* which afforded a crude yellow precipitate containing the title compound **56** (0.015 g, 98%) and NaCl (0.005 g). δ_H (400 MHz; DMSO-d_6) (rotational isomers present in a 1:1 ratio due to restricted rotation about the tertiary amide bond) 1.20 and 1.55 (3 H, s, CHCCH_3), 3.58-3.90 (4 H, m, CH_2CH_2NCO), 3.98 and 4.11 (2 H, s, NCH_2COOEt), 4.50 and 4.68 (2 H, s, NCH_2CON), 6.34 and 6.94 (1 H, s, C*H*CCH$_3$), 7.11-7.44 (3 H, m, Ar-*H*), 7.30 (1 H, m, Ar-*H*), 8.06 (1 H, m, Ar-*H*), 8.35 and 8.42 (1 H, br s, N*H*), 8.48 (1 H, m, Ar-*H*), 8.64 (1 H, m, Ar-*H*), 11.16 and 11.21 (1 H, s, COO*H*), 12.28 and 12.40 (2 H, br s, NH_2), 13.00 (1 H, br s , CON*H*CH$_2$); LRMS m/z (ESI) (%) 505.2 ($[M+H]^+$, 100), 81.0 (44), 59.2 (31); HRMS (ESI) found 505.1829, calcd. for $C_{25}H_{25}O_6$ N_6 $[M+H]^+$ 505.1830.

METHOD B: Attempted preparation of 56 via Palladium catalyzed allyloxycarbonyl deprotection of compound 57

To a solution of 2-(*N*-(2-(9-(allyloxycarbonylamino)acridine-4-carboxamido)ethyl)-2-(thymin-1-yl)acetamido)acetic acid (**57**) (0.070 g, 0.15 mmol, 1.0 eq) in 1/1 tetrahydrofuran/dimethylformamide (10 mL) was added tetrakis(triphenylphosphine) palladium(0) catalyst (0.020 g, 0.020 mmol, 0.12 eq) and triethylammonium formate (0.050 mL, 0.30 mmol, 2.0 eq). This mixture was stirred overnight at rt after which a yellow precipitate had formed. Subsequently this solid was separated by filtration, washed with DCM and recrystallisation was attempted in several solvent systems e.g.

ethanol/ diethyl ether, methanol/diethyl ether and methanol/THF. Unfortunatly, the resulting yellow solid still contained a number of unidentified impurities besides an undetermined amount of the title compound **56** (according to LR and HR mass spectrometry analysis).

2-(*N*-(2-(9-(allyloxycarbonylamino)acridine-4-carboxamido)ethyl)-2-(thymin-1-yl)acetamido)acetic acid (57)

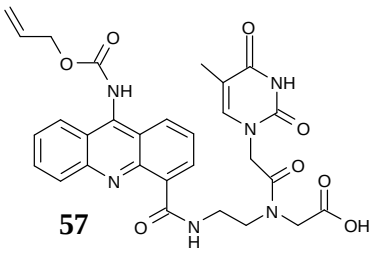

57

A solution of Ethyl 2-(*N*-(2-(9-(allyloxy carbonylamino)acridine-4-carboxamido) ethyl)-2-(thymin-1-yl)acetamido) acetate (**54**) (0.090 g, 0.15 mmol, 1.0 eq) in aqueous sodium hydroxide 1.2 M / tetrahydrofuran (1.5 mL / 4.5 mL) was stirred at rt for 4 h. Subsequently, the reaction mixture was neutralised with a 0.4 M (aq) HCl (4.5 mL) solution until a neutral pH was reached. The solvents were removed *in vacuo*, affording a crude yellow precipitate containing the product **57** that was used in a subsequent step without further purification.

References

1 Key facts about HIV/AIDS at http://www3.niaid.nih.gov/topics/HIVAIDS/

2 UNAIDS AIDS epidemic update December **2007**, UNAIDS/07.27E / JC1322E (English original, December 2007)

3 Haseltine, W. A., FASEB J., **1991**, 5, 2349-2360.

4 Perelson, A. S.; Neumann, A. U.; Markowitz, M.; Leonard, J. M.; Ho, D. D., *Science*, **1996**, 271, 1582-1586.

5 Aids Info: A service of the U.S. Department of Health and Human Services available at: http://www.aidsinfo.nih.gov

6 Patel, I. H.; Zhang, X.; Nieforth, K.; Salgo, M. and Buss, N., *Clin. Pharmacokinet.*, **2005**, 44, 175-186.

7 Davison, D.; Medinas, R.; Mosier, S. and Greenberg, M., Targeting HIV Entry: 3rd International Workshop. December 7-9, **2007**. Washington, DC. Abstract 18A.

8 Biswas, P.; Tambussi, G. and Lazzarin, A., *Expert Opin. Pharmacother.* **2007**, 8, 923-993.

9 Harris, K. S.; Brabant, W.; Styrchak, S.; Gall, A. and Diafuku, R., *Antiviral Res.*, **2005**, 67, 1-9.

10 De Clercq, E., *Antiviral Res.*, **1998**, 38, 153-179.

11 Das, K.; Clark, A. D.; Lewi, P. J.; Heeres, J.; de Jonge, M. R.; Koymans, L. M. H.; Vinkers, H. M.; Daeyaert, F.; Ludovici, D. W.; Kukla, M. J.; De Corte, B.; Kavash, R. W.; Ho, C. Y.; Ye, H.; Lichtenstein, M. A.; Andries, K.; Pauwels, R.; de Béthune, M.-P.; Boyer, P. L.; Clark, P.; Hughes, S. H.; Janssen, P. A. J.; Arnold, E., *J. Med. Chem.*, **2004**, 47, 2550-2560.

12 Hsiou, Y.; Das, K.; Ding, J.; Clark, A. D.; Kleim, J.-P.; Rösner, M.; Winkler, I.; Riess, G.; Hughes, S. H.; Arnold, E., *J. Mol. Biol.* **1998**, 284, 313-323.

13 Das, K.; Ding, J.; Hsiou, Y.; Clark, A. D.; Moereels, H.; Koymans, L.; Andries, K.; Pauwels, R.; Janssen, P. A. J.; Boyer, P. L.; Clark, P.; Smith, R. H.; Kroeger Smith, M. B.; Michejda, C. J.; Hughes, S. H.; Arnold, E., *J. Mol. Biol.* **1996**, 264, 1085-1100.

14 Goebel, F.; Yakovlev, A.; Pozniak, A. L.; Vinogradova, E.; Boogaerts, G.; Hoetelmans, R.; de Béthune, M.-P. P.; Peeters, M. and Woodfall, B., *AIDS*, **2006**, 20, 1721-1726.

15 Kohl, N. E.; Emini, E. A.; Schleif, W. A.; Davis, L. J.; Heimbach, J. C.; Dixon, R. A. F., Scolnick, E. M. and Sigal, I. S., *Proc. Natl. Acad. Sci. USA*, **1988**, 85, 4686-4690.

16 Brik, A.; Wong, C.H., *Org. Biomol. Chem.*, **2003**, 1, 5-14.

17 Suguna, K; Padlan, E. A.; Smith, C. W.; Carlson, W. D. and Davies, D. R., *Proc. Natl. Acad. Sci. USA*, **1987**, 84, 7009-7013.

18 Turner, S. R., *Current Medicinal Chemistry - Anti-Infective Agents*, **2002**, 1, 141-162(22).

19 Zeldin, R. K. and Petruschke, R. A., *J. Antimicrobial Chemother.*, **2004**, 53, 4-9.

20 Walker, M. A.; Johnson, T.; Naidu, B. N.; Banville, J.; Remillard, Ro.; Plamondon, S.; Martel, A.; Li, C.; Torri, A.; Samanta, H.; Lin, Z.; Dicker, I.; Krystal, M. and Meanwell, N.A., *Bioorg. Med. Chem. Lett.*, **2007**, 17, 4886-4890.

21 12th Conf. Retroviruses Opportunistic Infect., **2005**, Abstract 159.

22 United States Department of Health and Human Services (**2004**). "A Guide to Primary Care for People With HIV/AIDS, 2004 Edition"

23 Attacking AIDS with a 'Cocktail' Therapy, U.S. Food and Drug Administration Consumer magazine, July-August **1999**

24 De Clerq, E., *Nature Res. Drug Discovery*, **2007**, 6, 1001-1018.

25 Diaz, L.; Destefano, J. J., *Abstract General Meeting of the American Society of Microbiology*, May 17-21 **1998**, 98, 493 (abstract no.T-16).

26 Watson, J. D.; Baker, T. A.; Bell, S. P.; Gann, A.; Levine, M. and Losick, R., *Molecular Biology of the Gene (5th ed. ed.)*, **2004**, Peason Benjamin Cummings (Cold Spring Harbor Laboratory Press). ISBN 080534635X.

27 Witrouw, M.; Van Maele, B.; Vercammen, J.; Hantson, A.; Engelborghs, Y.; De Clercq, E.; Pannecouque, C. and Debyser, Z., *Current Drug Metabolism*, **2004**, 5, 291-304.

28 Hazuda, D. J.; Young, S. D.; Guare, J. P.; Anthony, N. J.; Gomez, R. P.; Wai, J. S.; Vacca, J. P.; Handt, L.; Motzel, S. L.; Klein, H. J.; Dornadula, G.; Danovich, R. M.; Witmer, M. V.; Wilson, K. A. A.; Tussey, L.; Schleif, W. A.; Gabryelski, L. S.; Jin, L.; Miller, M. D.; Casimiro, D. R.; Emini, E. A. and Shiver, J. W., *Science*, **2004**, 305, 528-532.

29 Dejesus, E.; Berger, D.; Markowitz, M.; Cohen, C.; Hawkins, T.; Ruane, P.; Elion, R.; Farthing, C.; Cheng, A.; Kearney, B. and 183-0101 Study Team In: Program and

abstracts of the 13th Conference on Retroviruses and Opportunistic Infections; February 5-8, **2006**; Denver, Colo. Abstract 160LB.

30 Johnson, A. A.; Marchand, C. and Pommier, Y., *Curr. Top. Med. Chem.*, **2004**, 4, 1059-1077.

31 Melek, M.; Jones, J. M.; O'Dea, M. H.; Pais, G., Burke,T. R. Jr.; Pommier, Y.; Neamati, N. and Gellert, M., *Proc. Natl. Acad. Sci. USA*, **2002**, 99, 134-137.

32 Schröder, A. R. W.; Shinn, P.; Chen, H.; Berry, C.; Ecker, J. R. and Bushman, F., *Cell*, **2002**, 110, 521-529.

33 Espeseth, A. S.; Felock, P.; Wolfe, A.; Witmer, M.; Grobler, J.; Anthony, N.; Egbertson, M.; Melamed, J. Y.; Young, S.; Hamill, T.; Cole, J. L. and Hazuda, D. J., *Proc. Natl. Acad. Sci. USA*, **2000**, 97, 11244-11249.

34 Marchand, C.; Johnson, A. A.; Semenova, E. and Pommier, Y., *Drug Discovery Today: Disease Mechanisms*, **2006**, 3, 253-260.

35 Dyda, F.; Hickman, A. B.; Jenkins, T.; Engelman, A.; Craigie R. and Davies, D. R., *Science*, **1994**, 266, 1981-1986.

36 Heuer, T. S. and Brown, P. O., *Biochemistry*, **1998**, 37, 6667-6678.

37 Leavitt, A. D.; Shiue, L. and Vaarmus, H. E., *J. Biol. Chem.*, **1993**, 268, 2113-2119.

38 Eijkelenboom, A. P.; van den Ent, F. M.; Vos, A.; Doreleijers, J. F.; Hard, K.; Tullius, T. D.; Plasterk, R. H.; Kaptein, R. and Boelens, R., *Current Biology*, **1997**, 7, 739-746.

39 Katzman, M. and Sudol, M., *Journal of Virology*, **1995**, 69, 5687-5696.

40 Lee, S. P., Xiao, J.; Knutson, J. R.; Lewis, M. S. and Han, M. K., *Biochemistry*, **1997**, 36, 173-180.

41 Greenwald, J.; Le, V.; Butler, S. L.; Bushman, F. D. and Choe, S., *Biochemistry*, **1999**, 38, 8892-8898.

42 Drelich, M.; Wilhelm, R. and Mous, J., *Virology*, **1992**, 188, 459-468.

43 Engelman, A. and Craigie, R.; *Journal of Virology*, **1992**, 66, 6361-6169.

44 Kulkosky, J.; Jones, K. S.; Katz, R. A.; Mack, J. P. and Skalka, A. M., *Molecular and Cellular Biology*, **1992**, 12, 2331-2338.

45 van Gent, D. C.; Oude Groeninger, A. A. M. and Plasterk, R. H., *Proc. Natl. Acad. Sci. USA*, **1992**, 89, 9598-9602.

46 Chiu, T. K. and Davies, D. R., *Curr. Top. Med. Chem.*, **2004**, 4, 965-977.

47 Steitz, T. A., *Nature*, **1998**, 391, 231-232.

48 Yang, W. and Steitz, T. A., *Structure*, **1995**, 3, 131-134.

49 Steitz, T. A., *J. Biol. Chem*, **1999**, 274, 17395-17398.

50 Chen, I.-J.; Neamati, N. and MacKerrel, A. D., *Curr. Drug. Targ.*, **2002**, 2, 217-234.

51 Goldgur, Y.; Dyda, F.; Hickman, A.B.; Jenkins, T. M.; Craigie, R. and Davies, D.R., *Proc. Natl. Acad. Sci. USA*, **1998**, 95, 9150-9154.

52 Engelman, A.; Hickman, A. B. and Craigie, R., *Journal of Virology*, **1994**, 68:5911-5917.

53 Gerton, J. L.; Ohgi, S.; Olsen, M.; DeRisi, J. and Brown, P. O., *Journal of Virology*, **1998**, 72, 5046-5055.

54 Shibagaki, Y. and Chow, S. A., *J. Biol. Chem.*, **1997**, 272, 8361-8369.

55 Lodi, P. J.; Ernst, J. A.; Kuszewski, J.; Hickman, A. B.; Engelman, A.; Craigie, R.; Clore, G. M. and Gronenborn, A. M., *Biochemistry*, **1995**, 34, 9826-9833.

56 Khan, E.; Mack, J. P. G.; Katz, R. A.; Kulkosky, J. and Skalka, A. M., *Nucleic Acids Research*, **1991**, 19, 851-860.

57 Vink, C.; Oude Groeninger, A. A. M. and Plasterk, R. H. A., *Nucleic Acids Research*, **1993**, 21, 1419-1425.

58 Woerner, A. M.; Klutch, M.; Levin, J. G. and Marcus-Sekura, C. J., *AIDS Research and Human retroviruses*, **1992**, 8, 297-304.

59 Woerner, A. M. and Marcus-Sekura, C. J., *Nucleic Acids Research*, **1993**, 21, 3507-3511.

60 Jenkins, T. M.; Engelman, A.; Ghirlando, R. and Craigie, R., *J. Biol. Chem.*, **1996**, 271, 7712-7718.

61 Andrake, M. D. and Skalka A. M., *J. Biol. Chem.*, **1996**, 271, 19633-19636.

62 Puras Lutzke, R. A.; Vink, C. and Plasterk, R. H., *Nucleic Acids Research*, **1994**, 22, 4125-4131.

63 Puras Lutzke, R. A. and Plasterk, R. H., *Journal of Virology*, **1998**, 72, 4841-4848.

64 Esposito, D. and Craigie, R., *The EMBO journal*, **1998**, 17, 5832-5843.

65 Zeinalipour-Loizidou, E.; Nicolaou, C.; Nicolaides, A. and Kostrikis, L. G., *Current HIV Research*, **2007**, 5, 365-388.

66 De Luca, L.; Pedretti, A.; Vistoli, G.; Barreca, M. L.; Villa, L.; Monforte, P. and Chimirri, A., *Biochem. Biophys. Res. Comm.*, **2003**, 310, 1083-1088.

67 Guiot, E.; Carayon, K.; Delelis, O.; Simon, F.; Tauc, P.; Zubin, E.; Gottikh, M.; Mouscadet, J. F.; Brochon, J. C. and Deprez, E., *J. Biol. Chem.*, **2006**, 281, 22707-22719.

68 HIV Sequence Compendium **2002**, Kuiken, C.; Foley, B.; Freed, E.; Hahn, B.; Marx, P.; McCutchan, F.; Mellors, J.; Wolinsky, S. and Korber, B., editors. Published by Theoretical Biology and Biophysics Group, Los Alamos National Laboratory, LA-UR number 03-3564.

69 Sherman, P. A. and Fyfe, J. A., *Proc. Natl. Acad. Sci. USA*, **1990**, 87, 5119-5123.

70 Asante-Appiah, E. and Skalka, A. M., *J. Biol. Chem.*, **1997**, 272, 16196-16205.

71 Pemberton, I. K.; Buckle, M. and Buc, H., *J. Biol. Chem.*, **1996**, 271, 1498-1506.

72 Vink, C.;Yeheskiely, E.; van der Marel, G. A.; van Boom, J. H. and Plasterk, R. H. A., *Nucleic Acids Research*, **1991**, 19, 6691-6698.

73 Bukrinsky, M., *Mol. Med.*, **2004**, 10, 1-5.

74 Busschots, K.; Vercammen, J.; Emiliani, S.; Benarous, R.; Engelborghs, Y.; Christ, F. and Debyser, Z., *J Biol Chem*, **2005**, 280, 17841-17847.

75 Cherepanov, P.; Maertens, G.; Proost, P.; Devreese, B.; Van Beeumen, J.; Engelborghs, Y.; De Clercq, E. and Debyser, Z., *J Biol Chem*, **2003**, 278, 372-381.

76 Pommier, Y.; Pilon, A. A.; Bajaj, K.; Mazumder, A. and Neamati, N., *Antiviral Chemistry and Chemotherapy*, **1997**, 8, 463-483.

77 Savarino, A., *Expert Opin. Invest. Drugs*, **2006**, 15, 1507-1522.

78 Sioud, M. and Drlica, K., *Proc. Natl. Acad .Sci. USA*, **1991**, 88, 7303-7307.

79 Neamati, N., *Expert. Opin. Ther. Patents*, **2002**, 12, 709-724.

80 Cushman, M. and Sherman, P., *Biochem. Biophys. Res. Comm.*, **1992**, 185, 85-90.

81 Di Santo, R.; Costi, R.; Artico, M.; Tramontano, E.; La Colla, P. and Pani, A., *Pure Appl. Chem.*, **2003**, 75, 195-206.

82 Field, A. K., *Curr. Opin. Mol. Ther.*, **1999**, 1, 323-331.

83 Mazumder, A.; Neamati, N.; Ojwang, J. O.; Sunder, S.; Rando, R. F. and Pommier, Y., *Biochemistry*, **1996**, 35, 13762-13771.

84 Cherepanov, P.; Este, J. A.; Rando, R. F.; Ojwang, O. J.; Reekmans, G.; Steinfeld, R.; David, G.; De Clercq, E. and Debyser, Z., *Molecular Pharmacology*, **1997**, 52, 771-780.

85 Lafemina, R. L.; Graham, P. L.; Legrow, K.; Hastings, J. C.; Wolfe, A.; Young, S. D.; Emini, E. A. and Hazuda, D. J., *Antimicrob. Agents Chemother.*, **1995**, 39, 320-324.

86 Mazumder, A.; Raghavan, K.; Weinstein, J.; Kohn, K. W. and Pommier, Y., *Biochem. Pharmacol*., **1995**, 49, 1165-1170.

87 Robinson, W. E. Jr; Reinecke, M. G.; Abdel-Malek, S.; Jia, Q. and Chow, S. A., *Proc. Natl. Acad. Sci. USA*, **1996**, 93, 6326-6331.

88 Singh, S. B.; Pelaez, F.; Haduza, D. J. and Lingham, R. B., *Drugs Fut*., **2005**, 30, 277-299.

89 Savarino, A.; Comito, G.; Vidotto, V.; Vieta, I.; Biglino, A. and Pugliese, A., 2nd meeting of the European Confederation of Medical Mycology, Brussels, **1995**.

90 Singh, S. B.; Zink, D. L.; Goetz, M. A.; Dombrowski, A. W.; Polishook, J. D. and Hazuda, D. L., *Tetrahedron Lett.*, **1998**, 39, 2243-2246.

91 Vesonder, R. F.; Tjarks, L. W.; Rohwedder, W. K.; Burmeister, H. R. and Laugal, J. A., *J. Antibiot.*, **1979**, 32, 759-761.

92 Merck&Co, Inc.: US5759842 (**1998**).

93 Mousnier, A.; Leh, H.; Bonnenfant, S.; Mouscadet, J. F. and Dargemont, C., 2nd International AIDS Society Conference on HIV Pathogenesis and Treatment, Paris, France (July **2003**) (Abstract 532).

94 Goldgur, Y.; Craigie, R., Cohen, G. H.; Fujiwara, T.; Yoshinaga, T.; Fujishita, J.; Sugimoto, H.; Endo, T.; Murai, H. and Davies. D. R., *Proc. Natl. Acad. Sci. USA*, **1999**, 96, 13040-13043.

95 Pais, G. C. G.; Zhang, X.; Marchand, C.; Neamati, A.; Cowansage, K.; Svarovskaia, E. S.; Pathak, V. K.; Tang, Y.; Nicklaus, M.; Pommier, Y. and Burke, T. R., *J. Med. Chem*., **2002**, 45, 3184-3194.

96 Cox Rosemond, M. J.; St. John-Williams, L.; Yamaguchi, T.; Fujishita, T. and Walsh, J. S., *Chem. Biol. Interact.*, **2004**, 147, 129.

97 Witvrouw, M.; Fikkert, V.; Van Remoortel, B.; Van Maele, B.; De Clercq, E. and Debyser, Z., 11th Conference on Retrovirus and Opportunistic Infections, San Francisco, USA, **2004** (abstract 632).

98 Hazuda, D.J.; Felock, P.; Witmer, M.; Wolfe, A.; Stillmock, K.; Grobler, J.A.; Espeseth, A.; Gabryelski, L.; Schlelf, W.; Blau, C. and Miller, M.D., *Science*, **2000**, 287**,** 646-650.

99 Grobler, J. A.; Stillmock, K.; Hu, B.; Witmer, M.; Felock, P.; Espeseth, A. S.; Wolfe, A.; Egbertson, M.; Bourgeois, M.; Melamed, J.; Wai, J. S.; Young, S.; Vacca, J. and Hazuda, D. J., *Proc. Natl. Acad. Sci. USA*, **2002**, 99, 6661-6666.

100 Marchand, C.; Johnson, A. A.; Karki, R. G.; Pais, G. C. G.; Zhang, X. C.; Cowansage, K.; Patel, T. A.; Nicklaus, M. C.; Burke, T. R. and Pommier, Y., *Mol. Pharmacol*., **2003**, 64, 600-609.

101 Zhuang, L.; Wai, J. S.; Embrey, M. W.; Fisher, T. E.; Egbertson, M. S.; Payne, L. S.; Guare, J. P.; Vacca, J. P.; Hazuda, D. J.; Felock, P. J.; Wolfe, A. L.; Stillmock, K. A.; Witmer, M. V.; Moyer, G.; Schleif, W. A.; Gabryelski, L. J.; Leonard, Y. M.; Lynch, J. J.; Michelson, S. R. and Young S. D., *J. Med. Chem*., **2003**, 46, 453-456.

102 American Chemical Society, 228th National Meeting (Part XIII), Technical Achievements in Organic Synthesis, Philadelphia, USA, Rotella DPIDdb Meeting Report, 14th September **2004**.

103 Little, S.; Drusano, G.; Schooley, R.; Haas, D.; Kumar, P.; Hammer, S.; McMahon, D.; Squires, K.; Asfour, R.; Richman, D.; Chen, J.; Saah, A.; Leavitt, R.; Hazuda, D.; Nguyen, B.-Y. and Protocol 004 Study Team in: Program and abstracts of the 12th Conference on Retroviruses and Opportunistic Infections; February 22-25, **2005**; Boston, Mass. Abstract 161

104 Sato, M.; Motomura, T.; Aramaki, H.; Matsuda, T.; Yamashita, M.; Ito, Y.; Kawakami, H.; Matsuzaki, Y.; Watanabe, W.; Yamataka, K.; Ikeda, S.; Kodama, E.; Matsuoka, M. and Shinkai, H., *J. Med. Chem.*, **2006**, 49, 1506-1508.

105 Morales-Ramirez, J. O.; Teppler, H.; Kovacs, C.; Steigbigel, R. T.; Cooper, D.; Liporace, R. L.; Schwartz, R.; Wenning, L.; Zhao, J.; Gilde, L.; Isaacs, R. D.; Nguyen B.-Y. and Protocol 004 Team. In: Program and abstracts of the 10th European AIDS Conference; November 17-20, **2005**; Dublin, Ireland. Abstract LBPS1/6.

106 Matsuzaki, Y.; Watanabe, W.; Yamataka, K.; Sato, M.; Enya, S.; Kano, M.; Kodama, E.; Matsuoka, M. and Ikeda, S. in: Program and abstracts of the 13th Conference on Retroviruses and Opportunistic Infections; February 5-8, **2006**; Denver, Colo. Abstract 508.

107 Garvey, E. P.; Johns, B. A.; Gartland, M. J.; Foster, S. A.; Miller, W. H.; Ferris, R. G.; Hazen, R. J.; Underwood, M. R.; Boros, E. E.; Thompson, J. B.; Weatherhead, J. G.; Koble, C. S.; Allen, S. H.; Schaller, L. T.; Sherrill, R. G.; Yoshinaga, T.; Kobayashi, M.; Wakasa-Morimoto, C.; Miki, S.; Nakahara, K.; Noshi, T.; Sato, A. and Fujiwara, T., *Antimicrob. Agents Chemother.*, **2008**, 52, 901-908.

108 Pommier, Y.; Johnson, A. A. and Marchand, C., *Nat. Rev. Drug Discov*., **2005**, 4, 236-248.

109 Pannecouque, C.; Pluymers, W.; Van Maele, B.; Tetz, V.; Cherepanov, P.; De Clercq, E.; Witvrouw, M. and Debyser, Z., *Current Biology*, **2002**, 12, 1169-1177.

110 Al-Mawsawi, L. Q.; Fikkert, V.; Dayam, R.; Witvrouw, M.; Burke, T. R.; Borchers, C. H. and Neamati, N., *Proc. Natl. Acad. Sci. USA*, **2006**, 103, 10080-10085.

111 Puras Lutzke, R. A.; Eppens, N. A.; Weber, P. A.; Houghten, R. A. and Plasterk, R. H. A., *Proc. Natl. Acad. Sci. USA*, **1995**, 92, 11456-11460.

112 Maroun, R. G.; Gayet, S.; Benleulmi, M. S.; Porumb, H.; Zargarian, L.; Merad, H.; Leh, H.; Mouscadet, J.-F.; Troalen, F. and Fermandijan, S., *Biochemistry*, **2001**, 40, 13840-13848.

113 Singh, S. B.; Jayasuriya, H.; Salituro, G.M .; Zink, D. L.; Shafiee, A.; Heimbuch, B.; Silverman, K. C.; Lingham, R. B.; Genilloud, O.; Teran, A.; Villela, D.; Felock, P. and Hazuda, D., *Journal of Natural Products*, **2001**, 64, 874-882.

114 Singh, S. B.; Herath, K.; Guan, Z.; Zink, D. L.; Dombrowski, A. W.; Polishook, J. D.; Silverman, K. C.; Lingham, R. B.; Felock, P. J. and Hazuda, D. J., *Organic Letters*, **2002**, 4, 1431-1434.

115 Yi, J.; Arthur, J. W.; Dunbrack, R. L. and Skalka, A. M., *Journal of Biological Chemistry*, **2000**, 275, 38739-38748.

116 Mansharamani, M.; Graham, D. R. M., Monie, D.; Lee, K. K.; Hildreth, J. E. K.; Siliciano, J. F. and Wilson, K. L., *Journal of Virology*, **2003**, 77, 13084-13092.

117 Van Maele, B.; Busschots, K.; Vandekerckhove, L.; Christ, F. and Debyser, Z., *Trends Biochem. Sci.*, **2006**, 31, 98-105.

118 Hayouka, Z.; Rosenbluh, J.; Levin, A.; Loya, S.; Lebendiker, M.; Veprintsev, D.; Kotler, M.; Hizi, A.; Loyter, A. and Friedler, A., *Proc. Natl. Acad. Sci. USA*, **2007**, 104, 8316-8321.

119 Gallay, P.; Swingler, S.; Song, S.; Bushman, S. and Trono, P., *Cell*, **1995**, 83, 569-576.

120 Voet, D. and Voet, J., *'Biochemistry'*, 2nd. edn., **1995**.

121 Engelman, A.; Englund, G.; Orenstein, J. M.; Martin, M. A. and Craigie, R., *Journal of Virology*, **1995**, 69, 2729-2736.

122 Hehl, E. A.; Joshi, P.; Kalpana, G. V. and Prasad, V. R., *Journal of Virology*, **2004**, 78, 5056-5067.

123 Gleenberg, I. O.; Avidan, O.; Goldgur, Y.; Herschhorn, A. and Hizi, A., *J. Biol. Chem.*, **2005**, 280, 21987-21996.

124 Wakelin, L. P. G. and Waring, M. J., *Comp. Med. Chem.*, **1990**, 2, 703-704.

125 Li, H. J. and Crothers, D. M., *J. Mol. Biol.*, **1969**, 39, 461-477.

126 Bresloff, J. L. and Crothers, D. M., *J. Mol. Biol.*, **1975**, 95, 103-123.

127 Fox, K. R. and Waring, M. J., *Nucleic Acids Res.*, **1987**, 15, 491-507.

128 Nelson, H. C. M.; Finch, J. T.; Luisi, B. F. and Klug, A., *Nature*, **1987**, 330, 221-226.

129 Neidle, S. and Abraham, Z., *Crit. Rev. Biochem.*, **1984**, 17, 73-121.

130 Gale, E. F.; Cundliffe, E.; Reynolds, P. E.; Richmond, M. H. and Waring, M. J., *'The Molecular Basis of Antibiotic Action'*, 2nd edn., **1981**, 258.

131 Denny, W., *Current Medicinal Chemistry*, **2002**, 9: 1655-1665.

132 Liaw, Y.-C.; Gao, Y.-G.; Robinson, H.; van der Marel, G. A.; van Boom, J. H. and Wang, A. H.-J., *Biochemistry*, **1989**, 28, 9913-9918.

133 Li, L. H.; Kuentzel, S. L.; Murch, L. L.; Pschigoda, L. M. and Krueger, W. C., *Cancer Res.*, **1979**, 39, 4816-4822.

134 Fox, K. R. and Waring, M. J., *Biochim. Biophys. Acta*, **1984**, 802, 162-168.

135 Collier, D. A.; Neidle, S. and Brown, J. R., *Biochem. Pharmacol.* **1984**, 33, 2877-2880.

136 Williams, L. D.; Egli, M.; Qi, G.; Gao, Q.; Bash, P.; van der Marel, G. A.; van Boom, J. H.; Rich, A. and Frederick, C. A., *Proc. Nat. Acad. Sci. USA*, **1990**, 87, 2225-2229.

137 Fox, K. R. and Waring, M. J., *Biochemistry*, **1986**, 25, 4349-4356.

138 Searle, M.S.; Hall, J.G.; Denny, W. A. and Wakelin, L. P.G., *Biochemistry*, **1988**, 27, 4340-4349.

139 Pollman, W. and Schramm, G., *Biochim. Biophys. Acta*, **1964**, 80, 1-7.

140 Wakelin, L. P.; Atwell, G. J.; Rewcastle, G. W. and Denny, W. A., *J. Med. Chem.*, **1987**, 30, 855-61.

141 Todd, A. K.; Adams, A.; Thorpe, J. H.; Denny, W. A.; Wakelin, L. P. G. and Cardin, C. J., *J. Med. Chem.*, **1999**, 42, 536-540.

142 Crenshaw, J. M.; Graves, D. E. and Denny, W. A., *Biochemistry*, **1995**, 34, 13682-13687.

143 Adams, A.; Guss, J. M.; Collyer, C. A.; Denny, W. A. and Wakelin, L. P. G., *Biochemistry*, **1999**, 38, 9221-9233.

144 Ray, A. and Nordén, B., *The FASEB Journal*, **2000**, 14, 1041-1060.

145 Nielsen, P. E., *Curr. Opin. Biotechnol.*, **1999**, 10**,** 71-75.

146 Kosinkyna, L.; Wang, W. and Liang, T. C., *Tetrahedron Lett.*, **1994**, 35, 5173-5176.

147 Uhlmann, E.; Peyman, A.; Breipohl, G. and Will, D. W., *Angew. Chem. Int. Ed.*, **1998**, 37, 2796-2823.

148 Nielsen, P.E., *Pure Appl. Chem*., **1998**, 70, 105-110.

149 Tomac, S.; Sarkar, M.; Ratilainen, T.; Wittung, P.; Nielsen, P. E.; Nordén, B. and Graeslund, A., *J. Am. Chem. Soc.*, **1996**, 118, 5544-5552.

150 Shakeel, S.; Karim, S. and Ali, A., *J. Chem. Technol. Biotechnol*, **2006**, 81, 892-899.

151 Knudsen, H. and Nielsen, P. E., *Nucleic Acids Res*., **1996**, 24, 494-500.

152 Nielsen, P. E.; Egholm, M.; Berg, R. H. and Buchardt, O., *Science*, **1991**, 254, 1497-1500.

153 Nielsen, P. E. and Egholm, M., *Curr. Iss. Molec. Biol.*, **1999**, 1, 89-104.

154 Kim, S. K.; Nielsen, P. E.; Egholm, M.; Buchardt, O.; Berg, R. H. and Nordén, B., *J. Am. Chem. Soc*., **1993**, 115, 6477-6481.

155 Betts, L.; Josey, J. A.; Veal, J. M. and Jordan, S. R., *Science*, **1995**, 270, 1838-1841.

156 Nielsen, P. E., *Curr. Opin. Struct. Biol*., **1999**, 9, 353-357.

157 Nielsen, P. E.; Egholm, M.; Berg, R. H. and Buchardt, O. in: *Antisense Research and Application*, Crook, S. and Lebleu, B. (eds.), **1993**, 363-373.

158 Lohse, J.; Dahl, O. and Nielsen, P. E., *Proc. Natl. Acad. Sci USA*, **1999**, 96, 11804-11808.

159 Rapireddy, S.; He, G.; Roy, S.; Armitage, B. and Ly, D., *J. Am. Chem. Soc*., **2007**, 129, 15596-15600.

160 Dragulescu-Andrasi, A.; Rapireddy, S.; Frezza, B. M.; Gayathri, C.; Gil, R. R. and Ly, D. H., *J. Am. Chem. Soc*., **2006**, 128, 10258-10267.

161 Cram, D. J., *Science*, **1988**, 240, 760-767.

162 Kool, E. T., *Chem. Rev.*, **1997**, 97, 1473-1487.

163 Bentin, T.; Nielsen, P. E., *J. Am. Chem. Soc.*, **2003**, 125, 6378-6379.

164 Shiraishi, T.; Bendifallah, N. and Nielsen, P. E., *Bioconj. Chem.* **2006**, 17, 189-194.

165 Simmons, C. G.; Pitts, A. E.; Mayfield, L. D.; Shay, J. W. and Corey, D. R., *Bioorg. Med. Chem. Lett*., **1997**, 7, 3001-3007.

166 Hamilton, S. E.; Simmons, C. G.; Kathiriya, I. S. and Corey, D. R., *Chem. Biol*., **1999**, 6, 343-351.

167 Demidov, V.; Frank-Kamenetskii, M. D.; Egholm, M.; Buchardt, O. and Nielsen, P. E., *Nucleic Acids Res*., **1993**, 21, 2103-2107.

168 Lansdorp, P. M.; Verwoerd, N. P.; van de Rijke, F. M.; Dragowska, V.; Little, M. T.; Dirks, R. W.; Raap, A. L. and Tanke, H. J., *Hum. Mol. Genet.*, **1996**, 5, 685-691.

169 Denny, W. A. in: *Small Molecule DNA and RNA Binders* (Demeunynck, M.; Bailly, C.; Wilson, W.D., Eds.), **2003**, 482-502.

170 Šebestík, J.; Hlaváček, J. and Stibor, I., *Current Protein and Peptide Science*, **2007**, 8, 471-483.

171 Bauer, K., *Chem. Ber*., **1950**, 83, 10-14.

172 Allen, C. F. H. and McKee, G. H. W., *Organic Syntheses*, **1943**, 2, 15-17.

173 Rudas, M.; Nyerges, M.; Töke, L.; Pete, B. and Groundwater, P. W., *Tetrahedron Lett.*, **1999**, 40, 7003-7006.

174 Albert, A. and Ritchie, B., *Organic Syntheses*, **1955**, 3, 53-55.

175 Dupre, D. J. and Robinson, F. A., *J. Chem. Soc*., **1945**, 549-551.

176 Robidoux, S.; Guo, Y. and Damha, M. J., *Tetrahedron Lett*., **1995**, 36, 6651-6654.

177 Katritzky, A. R.; Lewis, J.; Musumarra, G. and Ogretir, C., *Chim. Ind. (Milan)*, **1976**, 58, 381-383.

178 Alarcon, K.; Demeunynck, M.; Lhomme, J.; Carrez, D. and Croisy, A., *Bioorg. Med. Chem*., **2001**, 9, 1901-1910.

179 Pinskaya, M.; Romanova, E.; Volkov, E.; Deprez, E.; Leh, H.; Brochon, J.-C.; Mouscadet, J.-F. and Gottikh, M., *Biochemistry*, **2004**, 43, 8735-8743.

180 Carlson, C. B. and Beal, P. A., *Bioorg. Med. Chem. Lett.*, **2000**, 10, 1979-1982.

181 Korth, C.; May, B. C. H; Cohen, F. E. and Prusiner, S. B., *Proc. Natl. Acad. Sci. USA*, **2001**, 98, 9836-9841.

182 May, B. C. H.; Fafarman, A. T.; Hong, S. B.; Rogers, M.; Deady, L. W.; Prusiner, S. B. and Cohen, F. E., *Proc. Natl. Acad. Sci. USA*, **2003**, 100, 3416-3421.

183 Anderson, M. O.; Sherrill, J.; Madrid, P. B.; Liou, A. P.; Weisman, J. L.; DeRisi, J. L. and Guy, R. K., *Bioorg. Med. Chem.*, **2006**, 14, 334-343.

184 Denny, W. A. and Wakelin, L. P. G., *Cancer Res.*, **1986**, 46, 1717-1721.

185 Bailly, C.; Denny, W. A.; Mellor, L. E.; Wakelin, L. P. G. and Waring, M. J., *Biochemistry*, **1992**, 31, 3514-3524.

186 Atwell, G. J.; Cain, B. F.; Baguley, B. C.; Finlay, G. J. and Denny, W. A., *J. Med. Chem.*, **1984**, 27, 1481-1485.

187 Rewcastle, G. W. and Denny, W. A., *Synthesis*, **1985**, 220-223.

188 Scherrer, R. A. and Beatty, H. R., *J. Org. Chem.*, **1980**, 45, 2127-2131.

189 Beringer, F. M. and Falk, R. A., *J. Chem. Soc.*, **1964**, 4442-4451.

190 Docampo Palacios, M. L. and Pellón Comdom R. F., *Synth. Commun.*, **2003**, 33, 1771-1775.

191 Bunnett, J. F. and Zahler, R. E., *Chem. Rev.*, **1951**, 49, 273.

192 Weston, P. E. and Adkins, H., *J. Amer. Chem. Soc.*, **1928**, 50, 859.

193 Goldberg, I., *Chem. Ber.*, **1906**, 39, 1691.

194 Rosenmund, K. W., Luxat, K. and Tiedemann, W., *Chem. Ber.*, **1923**, 56, 1950.

195 Goldberg, A. A., *J. Chem. Soc.*, **1952**, 4368.

196 Gagan, J. M. F., *The chemistry of heterocyclic compounds*, **1973**, 9, 162-163.

197 Cramer, F. and Hettler, H., *Chem. Ber.*, **1958**, 91, 1181.

198 Raulins, N. R., *The chemistry of heterocyclic compounds*, **1973**, 9, 72-73.

199 Magidson, O. Y. and Grigorovskii, A. M., *Chem. Ber.*, **1933**, 66, 866.

200 Adcock, B., *The chemistry of heterocyclic compounds*, **1973**, 9, 119.

201 Banks, C. K., *J. Amer. Chem. Soc.*, **1944**, 66, 1127.

202 Finn, P. J.; Gibson, N. J.; Fallon, R.; Hamilton, A. and Brown, T., *Nucleic Acid Res.*, **1996**, 24, 3357-3363.

203 G. J. Buist and C. A. Bunton, *J. Chem. Soc.*, **1959**, 743-747.

204 Ganguly, S.; Kundu K. K., *Can. J. Chem.*, **1994**, 72, 1120-1126.

205 Han, S-Y. and Kim, Y-A., *Tetrahedron*, **2004**, 60, 2447-2467.

206 Chen, S.-M.; Mohan, V.; Kiely, J. S.; Griffith, M. C. and Griffey, R. H., *Tetrahedron Lett.*, **1994**, 35, 5105-5108.

207 Brown, S. C.; Thomson, S. A.; Veal, J. M. and Davis, D. G., *Science*, **1994**, 265, 777-780.

208 Breipohl, G.; Will, D. W.; Peyman, A. and Uhlmann, E., *Tetrahedron*, **1997**, 53, 14671-14686.

209 Carbonnel, S. and Troin, Y., *Heterocycles*, **2002**, 57, 1807-1830.

210 Carlson, C. B. and Beal, P. A., *Org. Lett.*, **2000**, 2, 1465-1468.

211 Roelofsen, D. P.; Hagendoorn, J. A. and van Bekkum H., *Chem. Ind*, **1966**, 1622-1623.

212 Otera, J., *Chem. Rev*., **1993**, 93, 1449-1470.

213 Meth-Cohn, O., *J. Chem. Soc., Chem. Commun*., **1986**, 695-697.

214 Kraszewski, A. and Stawiński, J. *Tetrahedron Lett*., **1980**, 21, 2935-2936.

215 Olah, G. A.; Narang, S. C.; Balaram Gupta, B. G. and Malhotra, R., *J. Org. Chem.*, **1979**, 44, 1247-1251.

216 Jung, M. E. and Lyster, M. A., *J. Am. Chem. Soc.*, **1977**, 99, 968-969.

217 Morita, T.; Okamoto, Y. and Sakurai, H., *J.C.S. Chem. Comm.*, **1978**, 20, 874-875.

218 Chee, G. L., *Synlett*, **2001**, 1593-1595.

219 Sridhar, P. R.; Sinha, S. and Chandrasekaran, S., *Indian J. Chem*., **2002**, 41B, 157-160.

220 Strazzolini, P.; Misuri, M. and Polese, P., *Tetrahedron Lett.*, **2005**, 46, 2075-2078.

221 Schädel, U.; Sansone, F.; Casnati, A. and Ungaro, R., *Tetrahedron*, **2005**, 61, 1149-1154.

222 Li, P. and Xu, J. C., *J. Chem. Soc. Perkin Trans. 2*, **2001**, 113-120.

223 Naylor, A.; Howarth, N. and Malpass, J. R., *Tetrahedron*, **1993**, 49, 451-468.

224 Kamaike, K.; Takahashi, M.; Utsugi, K.; Tomizuka, K.; Ishido, Y., *Tetrahedron Lett*., **1995**, 36, 91-94.

225 Albert, A. and Ritchie, B., *Org. Synth*., **1942**, 22, 5.

226 Clayden, J.; Greeves, N.; Warren, S. and Wothers, P., *'Organic Chemistry'*, 4th ed., **2004**.

227 Adebambo, K. F.; Zanoli, S.; Thomas, M. G.; Cancio, R.; Howarth, N. M. and Maga, G., *Chemmedchem*, **2007**, 2, 1405-1409.

228 Dueholm, K. L.; Egholm, M.; Behrens, C.; Christensen, L.; Hansen, H. F.; Vulpius, T.; Petersen, K. H.; Berg, R. H.; Nielsen, P. E. and Buchardt, O., *J. Org. Chem.*, **1994,** 59, 5767-5773.

229 Englund, E. A.; Gopi, H. N. and Appella, D. H., *Org. Lett.*, **2004**, 6, 213-215.

230 Kanda, Y.; Arai, H.; Ashizawa, T.; Morimoto, M. and Kasai, M., *J. Med. Chem*., **1992**, 35, 2781-2786.

231 Roos, E. C.; Bernabé, P.; Hiemstra, H. and Speckamp, W. N., *J. Org. Chem*. **1995**, 60, 1733-1740.

232 Maurin, C.; Bailly, F.; Mbemba, G.; Mouscadet, J.-F. and Cotelle. P., *Bioorg. Med. Chem.*, **2006**, 14, 2978-2984.

233 Leonard, J.; Lygo, B. and Procter, G., *Advanced Practical Organic Chemistry*, 2nd Edition, **1991**, Nelson Thornes, Cheltenham, UK.

234 Ullmann, F., *Liebigs Ann. Chem.*, **1907**, 355, 355.

235 Wolf, E; Kennedy, I. A.; Himmeldirk, K. and Spenser, I. D., *Can. J. Chem.*, **1997**, 75, 942-948.

Appendix

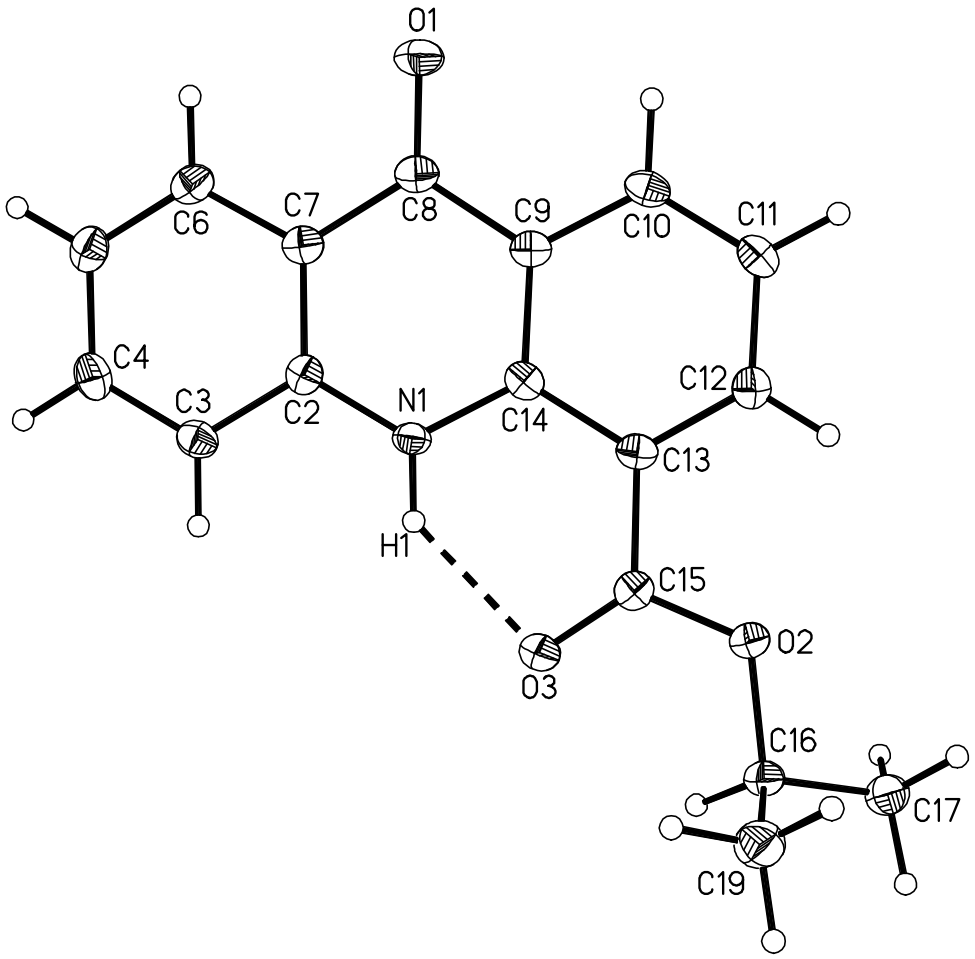

Table 1. Crystal data and structure refinement for *iso*-propyl-9-aminoacridan-4-carboxylate (**22**).

Identification code	twin5	
Empirical formula	C17 H15 N O3	
Formula weight	281.30	
Temperature	100(2) K	
Wavelength	0.71073 Å	
Crystal system	Triclinic	
Space group	P-1	
Unit cell dimensions	a = 7.9450(10) Å	α= 77.264(2)°.
	b = 8.4506(11) Å	β= 88.763(4)°.
	c = 11.1255(12) Å	γ = 67.982(4)°.

Volume	673.91(14) $Å^3$
Z	2
Density (calculated)	1.386 Mg/m^3
Absorption coefficient	0.096 mm^{-1}
F(000)	296
Crystal size	0.38 x 0.24 x 0.06 mm^3
Theta range for data collection	2.67 to 30.57°.
Index ranges	-11<=h<=11, -11<=k<=12, 0<=l<=15
Reflections collected	25508
Independent reflections	3964 [R(int) = 0.0346]
Completeness to theta = 25.00°	98.8 %
Absorption correction	Semi-empirical from equivalents
Max. and min. transmission	0.9943 and 0.8977
Refinement method	Full-matrix least-squares on F^2
Data / restraints / parameters	3964 / 1 / 200
Goodness-of-fit on F^2	0.944
Final R indices [I>2sigma(I)]	R1 = 0.0440, wR2 = 0.1055
R indices (all data)	R1 = 0.0774, wR2 = 0.1175
Largest diff. peak and hole	0.440 and -0.227 $e.Å^{-3}$

Table 2. Bond lengths [Å] and angles [°] for *iso*-propyl-9-aminoacridan-4-carboxylate (**22**).

N(1)-C(14)	1.3696(15)
N(1)-C(2)	1.3772(15)
N(1)-H(1)	0.890(11)
O(1)-C(8)	1.2368(14)
C(2)-C(7)	1.4025(16)
C(2)-C(3)	1.4046(16)
O(2)-C(15)	1.3338(14)
O(2)-C(16)	1.4697(14)
C(3)-C(4)	1.3757(17)
C(3)-H(3)	0.9500
O(3)-C(15)	1.2200(14)
C(4)-C(5)	1.3997(17)
C(4)-H(4)	0.9500
C(5)-C(6)	1.3719(17)
C(5)-H(5)	0.9500
C(6)-C(7)	1.4054(16)

C(6)-H(6)	0.9500
C(7)-C(8)	1.4625(16)
C(8)-C(9)	1.4745(16)
C(9)-C(10)	1.3961(16)
C(9)-C(14)	1.4082(16)
C(10)-C(11)	1.3769(17)
C(10)-H(10)	0.9500
C(11)-C(12)	1.3922(16)
C(11)-H(11)	0.9500
C(12)-C(13)	1.3865(16)
C(12)-H(12)	0.9500
C(13)-C(14)	1.4261(16)
C(13)-C(15)	1.4827(16)
C(16)-C(17)	1.5063(18)
C(16)-C(19)	1.5102(17)
C(16)-H(16)	0.973(12)
C(17)-H(17A)	0.9800
C(17)-H(17B)	0.9800
C(17)-H(17C)	0.9800
C(19)-H(19A)	0.9800
C(19)-H(19B)	0.9800
C(19)-H(19C)	0.9800

C(14)-N(1)-C(2)	122.80(10)
C(14)-N(1)-H(1)	115.6(8)
C(2)-N(1)-H(1)	121.6(8)
N(1)-C(2)-C(7)	120.36(11)
N(1)-C(2)-C(3)	119.78(11)
C(7)-C(2)-C(3)	119.86(11)
C(15)-O(2)-C(16)	118.89(9)
C(4)-C(3)-C(2)	119.86(11)
C(4)-C(3)-H(3)	120.1
C(2)-C(3)-H(3)	120.1
C(3)-C(4)-C(5)	120.77(12)
C(3)-C(4)-H(4)	119.6
C(5)-C(4)-H(4)	119.6
C(6)-C(5)-C(4)	119.55(12)
C(6)-C(5)-H(5)	120.2

C(4)-C(5)-H(5)	120.2
C(5)-C(6)-C(7)	121.09(11)
C(5)-C(6)-H(6)	119.5
C(7)-C(6)-H(6)	119.5
C(2)-C(7)-C(6)	118.85(11)
C(2)-C(7)-C(8)	120.46(11)
C(6)-C(7)-C(8)	120.69(11)
O(1)-C(8)-C(7)	122.39(11)
O(1)-C(8)-C(9)	121.83(11)
C(7)-C(8)-C(9)	115.77(10)
C(10)-C(9)-C(14)	119.73(11)
C(10)-C(9)-C(8)	119.69(10)
C(14)-C(9)-C(8)	120.58(11)
C(11)-C(10)-C(9)	121.30(11)
C(11)-C(10)-H(10)	119.4
C(9)-C(10)-H(10)	119.4
C(10)-C(11)-C(12)	119.13(11)
C(10)-C(11)-H(11)	120.4
C(12)-C(11)-H(11)	120.4
C(13)-C(12)-C(11)	121.89(11)
C(13)-C(12)-H(12)	119.1
C(11)-C(12)-H(12)	119.1
C(12)-C(13)-C(14)	118.82(11)
C(12)-C(13)-C(15)	120.30(11)
C(14)-C(13)-C(15)	120.88(10)
N(1)-C(14)-C(9)	119.84(11)
N(1)-C(14)-C(13)	121.04(10)
C(9)-C(14)-C(13)	119.13(11)
O(3)-C(15)-O(2)	123.66(11)
O(3)-C(15)-C(13)	124.73(11)
O(2)-C(15)-C(13)	111.61(10)
O(2)-C(16)-C(17)	104.84(9)
O(2)-C(16)-C(19)	108.33(10)
C(17)-C(16)-C(19)	113.64(10)
O(2)-C(16)-H(16)	107.2(7)
C(17)-C(16)-H(16)	110.6(8)
C(19)-C(16)-H(16)	111.8(7)
C(16)-C(17)-H(17A)	109.5

C(16)-C(17)-H(17B)	109.5
H(17A)-C(17)-H(17B)	109.5
C(16)-C(17)-H(17C)	109.5
H(17A)-C(17)-H(17C)	109.5
H(17B)-C(17)-H(17C)	109.5
C(16)-C(19)-H(19A)	109.5
C(16)-C(19)-H(19B)	109.5
H(19A)-C(19)-H(19B)	109.5
C(16)-C(19)-H(19C)	109.5
H(19A)-C(19)-H(19C)	109.5
H(19B)-C(19)-H(19C)	109.5

Symmetry transformations used to generate equivalent atoms:

Table 3. Torsion angles [°] for *iso*-propyl-9-aminoacridan-4-carboxylate (**22**).

C(14)-N(1)-C(2)-C(7)	-4.44(18)
C(14)-N(1)-C(2)-C(3)	175.45(10)
N(1)-C(2)-C(3)-C(4)	179.42(11)
C(7)-C(2)-C(3)-C(4)	-0.70(17)
C(2)-C(3)-C(4)-C(5)	-0.44(19)
C(3)-C(4)-C(5)-C(6)	0.78(19)
C(4)-C(5)-C(6)-C(7)	0.01(18)
N(1)-C(2)-C(7)-C(6)	-178.66(11)
C(3)-C(2)-C(7)-C(6)	1.45(17)
N(1)-C(2)-C(7)-C(8)	1.55(17)
C(3)-C(2)-C(7)-C(8)	-178.34(10)
C(5)-C(6)-C(7)-C(2)	-1.12(18)
C(5)-C(6)-C(7)-C(8)	178.68(11)
C(2)-C(7)-C(8)-O(1)	-178.27(11)
C(6)-C(7)-C(8)-O(1)	1.94(18)
C(2)-C(7)-C(8)-C(9)	2.38(16)
C(6)-C(7)-C(8)-C(9)	-177.41(11)
O(1)-C(8)-C(9)-C(10)	-3.06(18)
C(7)-C(8)-C(9)-C(10)	176.30(10)
O(1)-C(8)-C(9)-C(14)	176.87(11)
C(7)-C(8)-C(9)-C(14)	-3.77(17)

C(14)-C(9)-C(10)-C(11)	-0.94(18)
C(8)-C(9)-C(10)-C(11)	178.99(11)
C(9)-C(10)-C(11)-C(12)	0.63(18)
C(10)-C(11)-C(12)-C(13)	-0.38(18)
C(11)-C(12)-C(13)-C(14)	0.43(17)
C(11)-C(12)-C(13)-C(15)	-179.90(11)
C(2)-N(1)-C(14)-C(9)	2.99(17)
C(2)-N(1)-C(14)-C(13)	-176.80(11)
C(10)-C(9)-C(14)-N(1)	-178.81(10)
C(8)-C(9)-C(14)-N(1)	1.26(17)
C(10)-C(9)-C(14)-C(13)	0.98(17)
C(8)-C(9)-C(14)-C(13)	-178.95(10)
C(12)-C(13)-C(14)-N(1)	179.07(10)
C(15)-C(13)-C(14)-N(1)	-0.60(17)
C(12)-C(13)-C(14)-C(9)	-0.72(17)
C(15)-C(13)-C(14)-C(9)	179.61(10)
C(16)-O(2)-C(15)-O(3)	0.30(17)
C(16)-O(2)-C(15)-C(13)	-179.55(9)
C(12)-C(13)-C(15)-O(3)	-176.87(11)
C(14)-C(13)-C(15)-O(3)	2.79(19)
C(12)-C(13)-C(15)-O(2)	2.97(16)
C(14)-C(13)-C(15)-O(2)	-177.36(10)
C(15)-O(2)-C(16)-C(17)	148.05(10)
C(15)-O(2)-C(16)-C(19)	-90.30(12)

Symmetry transformations used to generate equivalent atoms:

Table 4. Hydrogen bonds for *iso*-propyl-9-aminoacridan-4-carboxylate (**22**) [Å and °].

D-H...A	d(D-H)	d(H...A)	d(D...A)	<(DHA)
N(1)-H(1)...O(3)	0.890(11)	1.957(12)	2.6791(13)	137.2(11)

Symmetry transformations used to generate equivalent atoms:

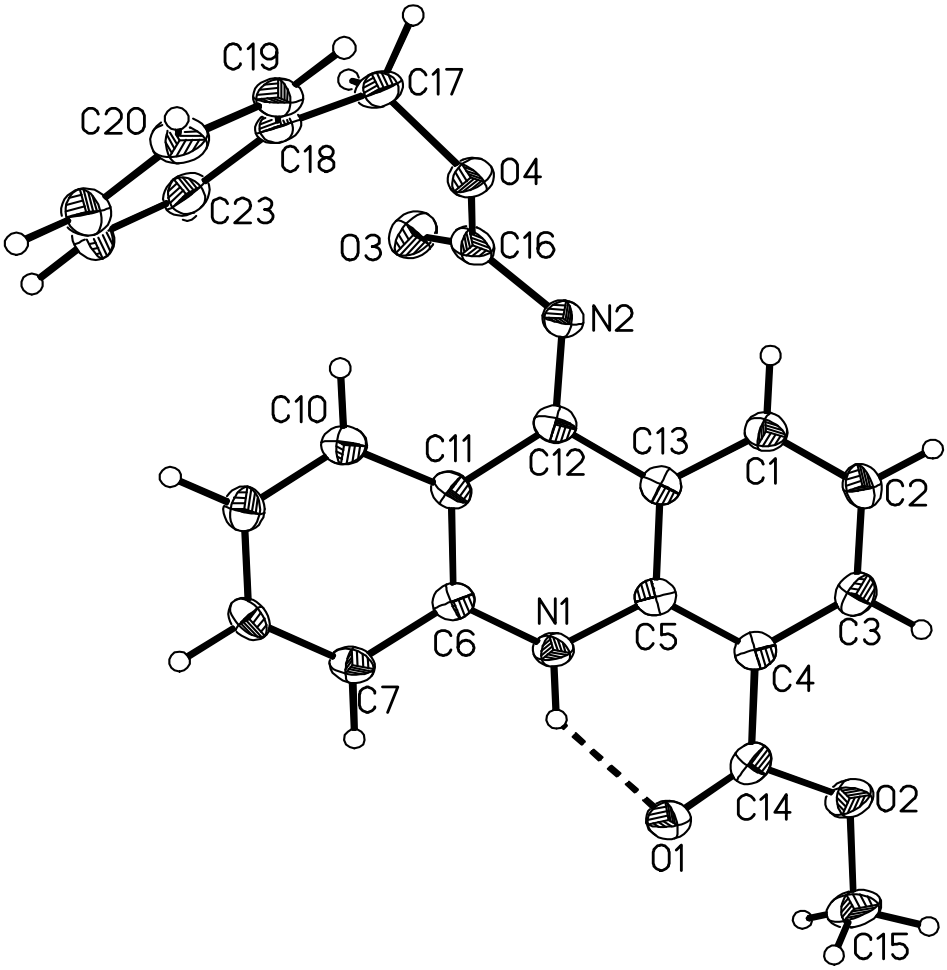

Table 1. Crystal data and structure refinement for methyl-9-benzyloxycarbonylaminoacridine-4-carboxylate (**45**).

Identification code	x81821_0m
Empirical formula	C23 H18 N2 O4
Formula weight	386.39
Temperature	100(2) K
Wavelength	0.71073 Å
Crystal system	Monoclinic
Space group	P2(1)/n

Unit cell dimensions	a = 9.528(2) Å	α= 90°.
	b = 8.325(2) Å	β= 100.896(8)°.
	c = 23.478(6) Å	γ = 90°.
Volume	1828.7(8) $Å^3$	
Z	4	
Density (calculated)	1.403 Mg/m^3	
Absorption coefficient	0.097 mm^{-1}	
F(000)	808	
Crystal size	0.62 x 0.18 x 0.04 mm^3	
Theta range for data collection	2.50 to 30.10°.	
Index ranges	-13<=h<=13, -10<=k<=11, -33<=l<=33	
Reflections collected	36840	
Independent reflections	5356 [R(int) = 0.1126]	
Completeness to theta = 25.00°	99.9 %	
Absorption correction	Semi-empirical from equivalents	
Max. and min. transmission	0.9961 and 0.7106	
Refinement method	Full-matrix least-squares on F^2	
Data / restraints / parameters	5356 / 0 / 267	
Goodness-of-fit on F^2	1.009	
Final R indices [I>2sigma(I)]	R1 = 0.0643, wR2 = 0.1249	
R indices (all data)	R1 = 0.1640, wR2 = 0.1563	
Largest diff. peak and hole	0.251 and -0.345 $e.Å^{-3}$	

Table 2. Bond lengths [Å] and angles [°] for methyl-9-benzyloxycarbonylaminoacridine-4-carboxylate (**45**).

N(1)-C(5)	1.368(3)
N(1)-C(6)	1.376(3)
N(1)-H(1N)	0.90(2)
N(2)-C(12)	1.292(3)
N(2)-C(16)	1.381(3)
O(1)-C(14)	1.215(3)
O(2)-C(14)	1.343(3)
O(2)-C(15)	1.450(3)
O(3)-C(16)	1.212(3)
O(4)-C(16)	1.351(3)
O(4)-C(17)	1.462(3)
C(1)-C(2)	1.376(3)

C(1)-C(13)	1.397(3)
C(1)-H(1)	0.9500
C(2)-C(3)	1.382(3)
C(2)-H(2)	0.9500
C(3)-C(4)	1.387(3)
C(3)-H(3)	0.9500
C(4)-C(5)	1.424(3)
C(4)-C(14)	1.471(3)
C(5)-C(13)	1.411(3)
C(6)-C(11)	1.405(3)
C(6)-C(7)	1.407(3)
C(7)-C(8)	1.367(3)
C(7)-H(7)	0.9500
C(8)-C(9)	1.391(3)
C(8)-H(8)	0.9500
C(9)-C(10)	1.371(3)
C(9)-H(9)	0.9500
C(10)-C(11)	1.409(3)
C(10)-H(10)	0.9500
C(11)-C(12)	1.462(3)
C(12)-C(13)	1.468(3)
C(15)-H(15A)	0.9800
C(15)-H(15B)	0.9800
C(15)-H(15C)	0.9800
C(17)-C(18)	1.501(3)
C(17)-H(17A)	0.9900
C(17)-H(17B)	0.9900
C(18)-C(19)	1.390(3)
C(18)-C(23)	1.393(3)
C(19)-C(20)	1.394(3)
C(19)-H(19)	0.9500
C(20)-C(21)	1.372(3)
C(20)-H(20)	0.9500
C(21)-C(22)	1.386(3)
C(21)-H(21)	0.9500
C(22)-C(23)	1.384(3)
C(22)-H(22)	0.9500
C(23)-H(23)	0.9500

C(5)-N(1)-C(6)	122.81(18)
C(5)-N(1)-H(1N)	114.6(15)
C(6)-N(1)-H(1N)	122.6(15)
C(12)-N(2)-C(16)	126.38(19)
C(14)-O(2)-C(15)	115.87(18)
C(16)-O(4)-C(17)	117.78(18)
C(2)-C(1)-C(13)	121.0(2)
C(2)-C(1)-H(1)	119.5
C(13)-C(1)-H(1)	119.5
C(1)-C(2)-C(3)	120.0(2)
C(1)-C(2)-H(2)	120.0
C(3)-C(2)-H(2)	120.0
C(2)-C(3)-C(4)	121.5(2)
C(2)-C(3)-H(3)	119.3
C(4)-C(3)-H(3)	119.3
C(3)-C(4)-C(5)	118.85(19)
C(3)-C(4)-C(14)	120.8(2)
C(5)-C(4)-C(14)	120.39(19)
N(1)-C(5)-C(13)	119.33(19)
N(1)-C(5)-C(4)	121.28(18)
C(13)-C(5)-C(4)	119.38(19)
N(1)-C(6)-C(11)	120.85(19)
N(1)-C(6)-C(7)	118.83(18)
C(11)-C(6)-C(7)	120.32(19)
C(8)-C(7)-C(6)	119.91(19)
C(8)-C(7)-H(7)	120.0
C(6)-C(7)-H(7)	120.0
C(7)-C(8)-C(9)	120.7(2)
C(7)-C(8)-H(8)	119.6
C(9)-C(8)-H(8)	119.6
C(10)-C(9)-C(8)	119.7(2)
C(10)-C(9)-H(9)	120.1
C(8)-C(9)-H(9)	120.1
C(9)-C(10)-C(11)	121.6(2)
C(9)-C(10)-H(10)	119.2
C(11)-C(10)-H(10)	119.2
C(6)-C(11)-C(10)	117.61(19)

C(6)-C(11)-C(12)	119.00(19)
C(10)-C(11)-C(12)	123.35(18)
N(2)-C(12)-C(11)	127.5(2)
N(2)-C(12)-C(13)	116.36(19)
C(11)-C(12)-C(13)	116.12(18)
C(1)-C(13)-C(5)	119.30(19)
C(1)-C(13)-C(12)	120.33(18)
C(5)-C(13)-C(12)	120.27(19)
O(1)-C(14)-O(2)	122.1(2)
O(1)-C(14)-C(4)	125.4(2)
O(2)-C(14)-C(4)	112.47(19)
O(2)-C(15)-H(15A)	109.5
O(2)-C(15)-H(15B)	109.5
H(15A)-C(15)-H(15B)	109.5
O(2)-C(15)-H(15C)	109.5
H(15A)-C(15)-H(15C)	109.5
H(15B)-C(15)-H(15C)	109.5
O(3)-C(16)-O(4)	125.0(2)
O(3)-C(16)-N(2)	125.5(2)
O(4)-C(16)-N(2)	109.13(19)
O(4)-C(17)-C(18)	108.35(17)
O(4)-C(17)-H(17A)	110.0
C(18)-C(17)-H(17A)	110.0
O(4)-C(17)-H(17B)	110.0
C(18)-C(17)-H(17B)	110.0
H(17A)-C(17)-H(17B)	108.4
C(19)-C(18)-C(23)	119.2(2)
C(19)-C(18)-C(17)	120.5(2)
C(23)-C(18)-C(17)	120.2(2)
C(18)-C(19)-C(20)	120.3(2)
C(18)-C(19)-H(19)	119.8
C(20)-C(19)-H(19)	119.8
C(21)-C(20)-C(19)	120.2(2)
C(21)-C(20)-H(20)	119.9
C(19)-C(20)-H(20)	119.9
C(20)-C(21)-C(22)	119.8(2)
C(20)-C(21)-H(21)	120.1
C(22)-C(21)-H(21)	120.1

C(23)-C(22)-C(21)	120.7(2)
C(23)-C(22)-H(22)	119.7
C(21)-C(22)-H(22)	119.7
C(22)-C(23)-C(18)	119.9(2)
C(22)-C(23)-H(23)	120.0
C(18)-C(23)-H(23)	120.0

Symmetry transformations used to generate equivalent atoms:

Table 3. Torsion angles [°] for methyl-9-benzyloxycarbonylaminoacridine-4-carboxylate (**45**).

C(13)-C(1)-C(2)-C(3)	0.5(3)
C(1)-C(2)-C(3)-C(4)	-0.4(3)
C(2)-C(3)-C(4)-C(5)	-0.5(3)
C(2)-C(3)-C(4)-C(14)	-179.9(2)
C(6)-N(1)-C(5)-C(13)	-4.5(3)
C(6)-N(1)-C(5)-C(4)	176.21(19)
C(3)-C(4)-C(5)-N(1)	-179.39(19)
C(14)-C(4)-C(5)-N(1)	0.1(3)
C(3)-C(4)-C(5)-C(13)	1.3(3)
C(14)-C(4)-C(5)-C(13)	-179.23(19)
C(5)-N(1)-C(6)-C(11)	3.6(3)
C(5)-N(1)-C(6)-C(7)	-176.28(19)
N(1)-C(6)-C(7)-C(8)	178.75(19)
C(11)-C(6)-C(7)-C(8)	-1.1(3)
C(6)-C(7)-C(8)-C(9)	-2.4(3)
C(7)-C(8)-C(9)-C(10)	3.4(3)
C(8)-C(9)-C(10)-C(11)	-0.8(3)
N(1)-C(6)-C(11)-C(10)	-176.27(19)
C(7)-C(6)-C(11)-C(10)	3.6(3)
N(1)-C(6)-C(11)-C(12)	6.1(3)
C(7)-C(6)-C(11)-C(12)	-174.00(19)
C(9)-C(10)-C(11)-C(6)	-2.7(3)
C(9)-C(10)-C(11)-C(12)	174.8(2)
C(16)-N(2)-C(12)-C(11)	-11.6(4)
C(16)-N(2)-C(12)-C(13)	167.3(2)
C(6)-C(11)-C(12)-N(2)	164.9(2)

C(10)-C(11)-C(12)-N(2)	-12.6(3)
C(6)-C(11)-C(12)-C(13)	-14.0(3)
C(10)-C(11)-C(12)-C(13)	168.52(19)
C(2)-C(1)-C(13)-C(5)	0.3(3)
C(2)-C(1)-C(13)-C(12)	-175.9(2)
N(1)-C(5)-C(13)-C(1)	179.44(19)
C(4)-C(5)-C(13)-C(1)	-1.3(3)
N(1)-C(5)-C(13)-C(12)	-4.4(3)
C(4)-C(5)-C(13)-C(12)	174.95(19)
N(2)-C(12)-C(13)-C(1)	10.4(3)
C(11)-C(12)-C(13)-C(1)	-170.55(19)
N(2)-C(12)-C(13)-C(5)	-165.76(19)
C(11)-C(12)-C(13)-C(5)	13.3(3)
C(15)-O(2)-C(14)-O(1)	-5.1(3)
C(15)-O(2)-C(14)-C(4)	174.94(18)
C(3)-C(4)-C(14)-O(1)	177.8(2)
C(5)-C(4)-C(14)-O(1)	-1.7(3)
C(3)-C(4)-C(14)-O(2)	-2.2(3)
C(5)-C(4)-C(14)-O(2)	178.31(18)
C(17)-O(4)-C(16)-O(3)	5.5(3)
C(17)-O(4)-C(16)-N(2)	179.05(16)
C(12)-N(2)-C(16)-O(3)	-71.5(3)
C(12)-N(2)-C(16)-O(4)	115.0(2)
C(16)-O(4)-C(17)-C(18)	102.3(2)
O(4)-C(17)-C(18)-C(19)	88.7(2)
O(4)-C(17)-C(18)-C(23)	-87.6(2)
C(23)-C(18)-C(19)-C(20)	-0.1(3)
C(17)-C(18)-C(19)-C(20)	-176.4(2)
C(18)-C(19)-C(20)-C(21)	0.8(3)
C(19)-C(20)-C(21)-C(22)	-0.7(3)
C(20)-C(21)-C(22)-C(23)	-0.1(3)
C(21)-C(22)-C(23)-C(18)	0.8(3)
C(19)-C(18)-C(23)-C(22)	-0.7(3)
C(17)-C(18)-C(23)-C(22)	175.6(2)

Symmetry transformations used to generate equivalent atoms:

Table 4. Hydrogen bonds for methyl-9-benzyloxycarbonylaminoacridine-4-carboxylate (**45**). [Å and °].

D-H...A	d(D-H)	d(H...A)	d(D...A)	<(DHA)
N(1)-H(1N)...O(1)	0.90(2)	1.93(2)	2.670(2)	138(2)

Symmetry transformations used to generate equivalent atoms: